



A11106 039730

REFERENCE

NBSIR 81-1655

NIST
PUBLICATIONS

ESTIMATED UNCERTAINTY OF CALIBRATIONS OF FREESTANDING PRISMATIC LIQUEFIED NATURAL GAS CARGO TANKS

J. D. Siegwarth
J. F. LaBrecque

Thermophysical Properties Division
National Engineering Laboratory
National Bureau of Standards
U.S. Department of Commerce
Boulder, Colorado 80303

January 1982

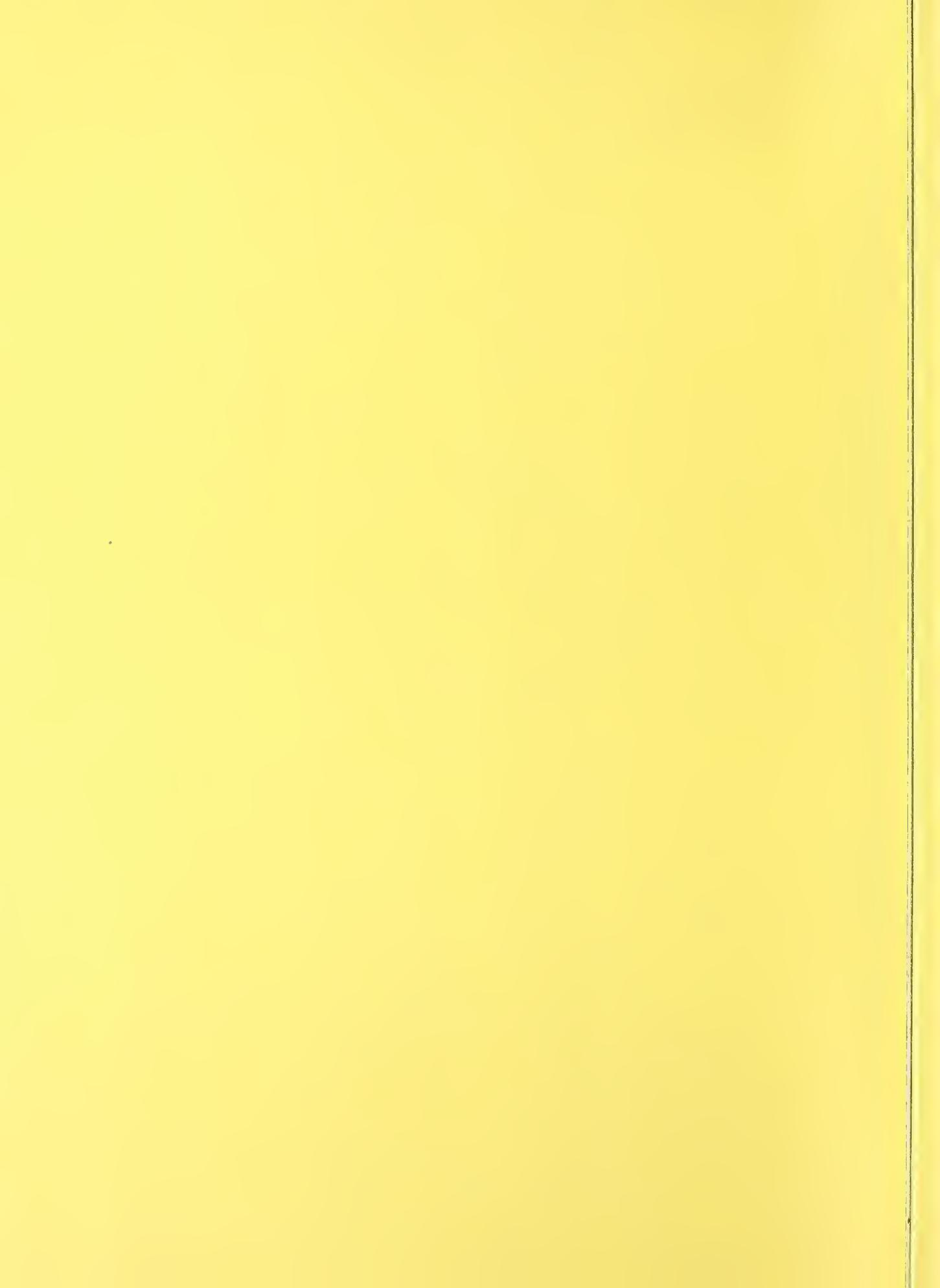
Supported by
LNG Custody Transfer Measurements Supervisory Committee
and the Maritime Administration



QC
100
-456
81-1655
1982

DEPARTMENT OF COMMERCE, Malcolm Baldrige, Secretary

NATIONAL BUREAU OF STANDARDS, Ernest Ambler, Director



NBSIR 81-1655

ESTIMATED UNCERTAINTY OF CALIBRATIONS OF FREESTANDING PRISMATIC LIQUEFIED NATURAL GAS CARGO TANKS

J. D. Siegwarth
J. F. LaBrecque

National Bureau of Standards
U.S. Department of Commerce
Boulder, Colorado 80303

January 1982

Supported by
LNG Custody Transfer Measurements Supervisory Committee
and the Maritime Administration

Contents

	Page
1. Introduction.	1
2. Description of the Tanks.	2
3. The Photogrammetric Calibration Method.	9
4. Accuracy of the Photogrammetric Calibration Method as Applied to the Freestanding Prismatic Tanks.	11
5. Accuracy of Tanks in Service.	14
6. References.	17

Appendix A - Accuracy and Precision of Photogrammetric Dimensioning of Freestanding Prismatic Cargo Tanks
by J. F. LaBrecque, C. L. Carroll, and J. D. Siegwarth

Appendix B - Uncertainty in Tank Volume Determination Introduced by the Calculation Method
by J. F. LaBrecque

Appendix C - Uncertainties Due to Temperature Effects
by J. D. Siegwarth and J. F. LaBrecque

Appendix D - A Laser-Based Calibration of Tank #3 on the Tanker El Paso Columbia
by W. C. Haight, F. Scire, R. G. Hartsock, and R. J. Hocken

Appendix E - Deformation Measurements on Freestanding LNG Cargo Tanks
by W. C. Haight, B. Borchardt, R. G. Hartsock, R. C. Veale, and R. J. Hocken

Appendix F - Hydrostatic Deformation of Freestanding LNG Cargo Tanks
by W. C. Haight, F. Scire, R. G. Hartsock, and R. J. Hocken

Appendix G - Deadwood Survey Data El Paso Columbia, Hull 2266, Tank 3
by W. C. Haight, R. G. Hartsock, and R. J. Hocken

Appendix H - Bottom Surveys of Freestanding LNG Cargo Tanks
by W. C. Haight, F. Scire, R. G. Hartsock, C. Johnson, and R. J. Hocken

Estimated Uncertainty of Calibrations of Freestanding
Prismatic Liquefied Natural Gas Cargo Tanks

J. D. Siegwarth and J. F. LaBrecque
Thermophysical Properties Division
Center for Chemical Engineering
National Engineering Laboratory
National Bureau of Standards
Boulder, Colorado 80303

The accuracy of the tank calibrated by the photogrammetric technique was examined during the calibration of fifteen freestanding prismatic LNG transport tanks. This examination indicated that the calibration accuracy of the tanks calibrated in the storage position was better than $\pm 0.1\%$. Additional factors influencing the accuracy of the calibration of the tanks, such as the effects of installing the tanks into the ship and loading the ships with LNG, were examined in the course of this work and the results are reported here. The various measurements used by various NBS personnel to analyze the calibration accuracy are detailed in the eight Appendices included in this report.

Key words: calibration accuracy; laser calibration; LNG ship tanks; photogrammetry; volume calibration.

Estimated Uncertainty of Calibrations
of Freestanding Prismatic Liquefied Natural Gas Cargo Tanks

J. D. Siegwarth and J. F. LaBrecque

1. Introduction.

The National Bureau of Standards has done preliminary studies [1] to establish an upper limit for the tank volume uncertainty of a spherical transport tank calibrated by photogrammetry [2,3]. The Maritime Administration of the Department of Commerce and the LNG Custody Transfer Measurements Supervisory Committee [4] have provided funds both to test the accuracy of the present state of the art of tank calibration and to develop new methods of calibrating tanks that are suitable for industrial use. This additional support has made possible an expanded study of the calibration uncertainties of freestanding prismatic LNG transport tanks. The objectives of this work are two fold. The first objective is to make more extensive measurements to provide an independent verification of the uncertainty of the photogrammetric method of determining spatial coordinates of points on the surface of the tanks. The second objective is to provide an upper limit for the uncertainty of the calibration of these particular tanks. This latter objective contains the first, but additional factors must be considered. As in the case of the spherical tanks, the photogrammetric survey is done before the tanks are transported to and installed in the ship. In addition, the photogrammetry is done with the tank empty. Effects of lifting, installing, cooling, and loading the tanks should be included in the calibration uncertainty.

In this work, we have examined by independent measurements and calculations the photogrammetric calibration method and effects on the tank volume of events following the tank calibration. The photogrammetric calibration has been analyzed for each of the tanks using length standards. The NBS has tested the calibration of one tank by a completely independent volume determination method. The laser plane method developed by NBS for the conformation of the volume tables of membrane tanks [5] was modified and used on the exterior of the tank.

The method of volume calculations has also been tested for accuracy by independent calculations using the photogrammetrically determined coordinate data for points on the tank surface. The dimensions of the aluminum in the tank walls and internal structure were measured for one tank to obtain an estimate of the error induced when using the blueprint dimensions in the correcting for volume taken by the tank walls and structure.

The same tank dimensioned by laser planes was also dimensioned while filled with the maximum amount of water during the hydrostatic tests. A distortion study was done based on these results.

In other measurements, the tank bottoms were resurveyed after the tanks were installed to determine whether the tank support blocks were properly shimmed so that the constructed bottom contour of the tank was retained.

Finally, two of the early tanks were surveyed, both before and after they were lifted into place aboard the ship, to investigate the effects the lifting might have on the tank volume calibration.

The methods used and the results obtained from the various measurements by NBS are detailed in the reports contained in the appendices. The authors of the various appendices identify those who did that particular part of the project. An estimate of just the uncertainty of the photogrammetric survey technique as applied to this particular calibration problem is provided.

2. Description of the Tanks.

Each ship contains five tanks similar to the tank shown in figure 1. Counting from the bow, the third and fourth tanks are identical; the second tank is nearly the same in capacity as tanks three and four but the sides taper slightly towards the bow. Tank five is shorter and tapered slightly toward the stern. Tank one is again shorter and heavily tapered towards the bow. The outer walls of the tanks are flat planes, eight in all. The bottoms and tops are horizontal planes; the ends are vertical planes. The sides are composed of two planes each. The top most plane is vertical and connects to the bottom via a chine plane that slopes in toward the center line of the tank at the bottom. This narrowing of the bottom provides clearance for the curved corners between the sides and bottom of the hull. The larger of the tanks have widths and lengths of about 36 m; all have heights of about 23 m, and are constructed of rectangular plates of 5083 aluminum varying in thickness from approximately 1.5 to 3 cm. These plates are edge welded to form panels. These panels are



Figure 1. Exterior view of a completed tank waiting to be loaded aboard the ship.

preassembled complete with the vertical stiffening channels and horizontal girders. The panels are lifted by crane, fitted into place and welded. The tanks are divided internally into four quadrants by vertical walls. The fore to aft wall is liquid tight. The port to starboard wall or swash bulkhead is not liquid tight. The external and internal walls of the tank are heavily braced internally first by vertical 23 cm wide L shaped ribs at roughly 2/3 m intervals. These ribs in turn are attached to seven wide flanged horizontal girders at intervals from the bottom to the top of the tank. Stiffening ribs are also welded to the top plates inside and I-beam girders brace the floor panels at the same intervals as the ribs on the walls. These in turn are welded to heavy girders in both the floor and ceiling. Numerous triangular braces are fit between the various stiffening girders. Figures 2 and 3 are photographs of this internal structure. The corners between the planes composing the tank surface are radiused. The radius is approximately 30.5 cm on the inside. The volume of the aluminum comprising the tank amounts to between one and two percent of the total volume of the tank. Figure 4 is a diagram of the tank showing the interior structure.

The tanks, after the assembly is complete or nearly complete, are transported from the assembly area to a hydrotest stand. The tanks are transported by four crawler tractors, one under each corner lifting the tank by means of lifting brackets. The tank is hydrotested by filling it a little more than half full with water. The tank is then pressurized with air to 0.14 bar (2 psi). After hydrotesting, the tank is transported again by the crawlers to the storage area and placed on three rows of concrete pillars. The photogrammetric calibration usually takes place while the tanks are in this storage area. One tank of each ship set has been calibrated while on the hydrotest stand. Only the sides of the tanks are actually dimensioned photogrammetrically. The top and bottom of the tanks are profiled using conventional theodolite techniques. These surveys supply the top and bottom data used in the tank table calculation. This bottom survey is used to shim the surfaces of the support blocks on the ship located in the bottom of the tank socket so the tank is uniformly supported. The tank and contents are supported completely on these blocks.

The ship is brought to the tank construction site to load the tanks. The tanks are moved up one at a time via the crawlers, then lifted, swung out over the ship and lowered into the insulated tank socket by a 1.36×10^6 kg (1500 ton) capacity crane. Figure 5 shows a tank being lifted aboard the ship.



Figure 2. Interior photograph showing ceiling and upper wall structure of a tank.



Figure 3. Interior photograph showing the floor and chine surfaces of a tank.

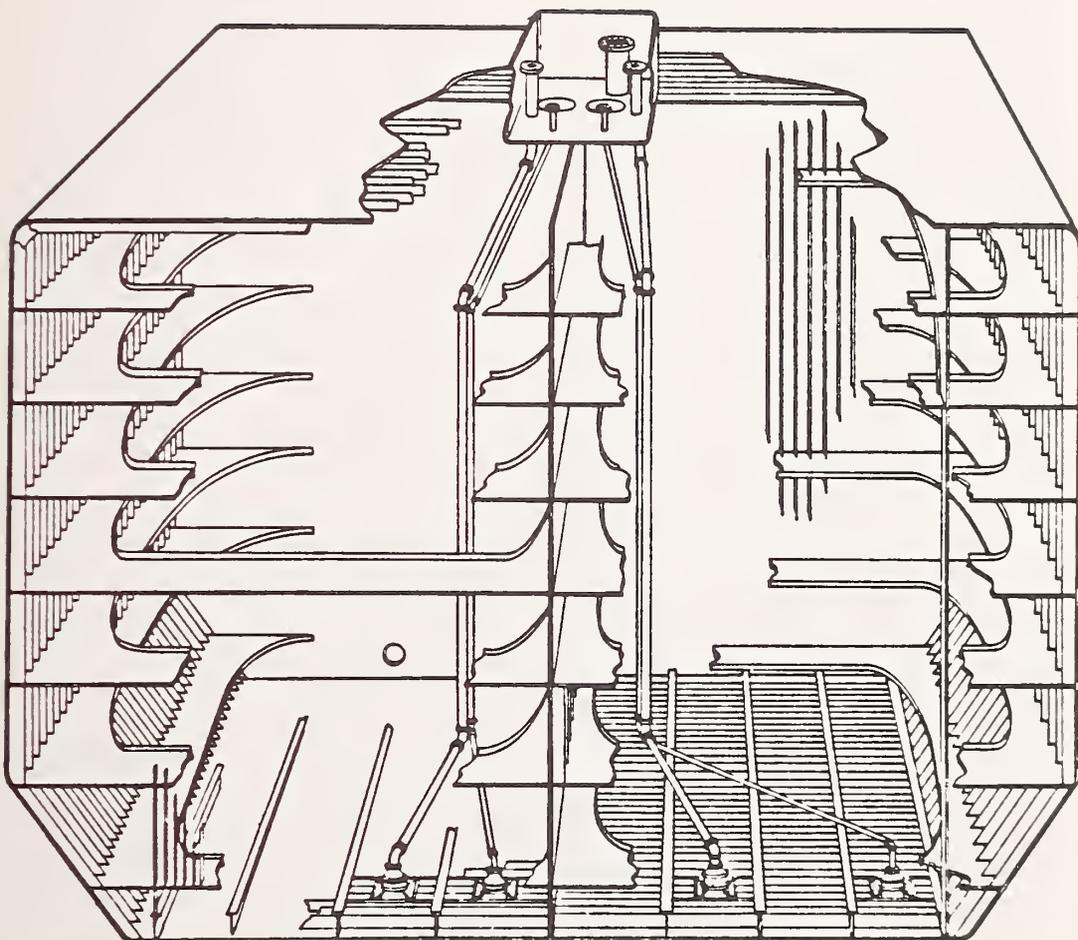


Figure 4. Cutaway drawing of two quadrants of a cargo tank showing the internal bracing configuration.



Figure 5. Tank #5 being loaded on the Columbia. From the time the tank left the crawlers until it was in place on the ship, slightly over an hour had elapsed.

The tank is connected to a horizontal lifting beam of the crane by a large number of cables supported by interconnected hydraulic cylinders such that the tank load is equally supported on all the cables. Insulation is placed over the top of the tank; then the deck section covering of the tank socket is replaced. The walls of the tank are then accessible only from the inside of the tank.

3. The Photogrammetric Calibration Method

The photogrammetric process is employed to determine x,y,z coordinates of a number of points distributed over the surface, in this case the outside surface, of the tank. These points are, physically, 19 mm diameter white dots placed on a black background or 19 mm diameter white balls placed on the tank prior to photography. The white dots and background are either painted on the tank wall or are printed on adhesive-backed paper and placed on the tank wall. The white balls are offset a known distance from the walls. The number and placement pattern are quite flexible and generally chosen to give sufficient detail of any wall variations with the minimum number of targets. The x,y,z coordinates of the points on the tank can be in any arbitrary coordinate system. This coordinate system is later translated and rotated such that the z axis is perpendicular to the gravitational plane when the tank is on the ship and the x axis is parallel to the center of the ship in the gravitational plane; hence, the y axis is transverse to the ship and in the gravitational plane.

The photogrammetric method of determining the coordinates of the tank surfaces is closely related to the method of determining the coordinates of the tank surfaces is closely related to the method of using a theodolite to locate identifiable points on the surface by measuring vertical angles to the points from horizontal and horizontal angles from a baseline of known length at both ends of the baseline. The axes of the theodolite determined coordinate system might be the horizontal baseline, the gravitational field direction and the axis perpendicular to both. One such theodolite set-up or station can be related to the next by repeating measurements of some of the targets located from the adjacent stations. The theodolite must be aimed twice at each point to be located: once from each end of the baseline, or one aimed from each end of the baseline if two theodolites are used.

In the photogrammetric method, the eyepiece of the theodolite is replaced by a camera employing a very flat photographic plate. A photograph of the complete surface from each of the two ends of the baseline contains the same

information as all the theodolite readings since all the point images off the optical axis are recorded in each photograph. The angle data from a theodolite aimed at a point is contained in the position of the photographic image of the point. The x,y coordinates of these photographic images can be measured to + 3 micrometers. Sufficient photographic image data are acquired such that not only x,y,z coordinates of each target spot can be calculated but also the camera positions and orientations, a lens correction and an uncertainty for the coordinate position. In practice, the calibrated base line used with the theodolite can be replaced by a few known target spacings on the tank surfaces. Although many of the details of the stereo-triangulation methods used by the photogrammetric consultants are proprietary, the general approach here is explained in references [2] and [3].

4. Accuracy of the Photogrammetric Calibration Method as Applied to the Freestanding Prismatic Tanks

The accuracy of calibration of the tanks has been independently estimated from a number of measurements made by NBS personnel. The various measurements and the results are described in detail in Appendices A through H.

The method used to verify the accuracy and precision of the photogrammetrically determined coordinates of designated points on the tank exterior walls is described in Appendix A, and the results are presented for all fifteen tanks of the three ship sets.

In Appendix B, gaging tables, calculated at NBS using the photogrammetrically determined coordinate data, and gaging tables, calculated by the photogrammetrist from the same data, are compared in order to examine the computational method. The computational method and results for all fifteen tanks are also given. The results are for the total volumes of the tank to the outside surfaces.

The photogrammetric measurements are made on the tank under conditions assumed nearly isothermal and at ambient conditions. The tank volume is then mathematically sized at the normal operating condition using the thermal expansion coefficient for 5083 Aluminum [7]. Possible errors introduced by lack of isothermal conditions, uncertainty of the expansion coefficient and incorrect determination of temperature are discussed in Appendix C.

Tables A, B, and C give summaries of the estimated maximum errors of the volume determined by the photogrammetric method. Details are in the first three Appendices. Tables A through C are for the Savannah, the Cove Point, and the Columbia, respectively.

The random errors are represented by 95% confidence limits for the random error source in question. While the errors due to volume calibration, scale factor, and target spacing are considered random, the thermal expansion coefficient error is systematic, but unknown; the limits for this error are based on the bounds for the thermal expansion coefficient [6]. All errors are given in percent. In the tables a plus sign signifies an overestimate and a minus sign an underestimate.

TABLE I: Error Summary (percent) for the Savannah Tanks

Tank	Volume Calculation	Random Uncertainty			Limits of Systematic Error for			Scale bias + systematic and random error
		Target spacing	Scale factor	RMS total	Thermal coef.	Scale bias		
1	+ .01	+ .014	+ .01	+ .020	+ .03	-.04	-.04 + .050	
2	+ .01	+ .014	+ .01	+ .020	+ .03	-.06	-.06 + .050	
3	+ .01	.00	+ .01	+ .014	+ .03	.00	0 + .044	
4	+ .01	.00	+ .01	+ .014	+ .03	-.03	-.03 + .044	
5	+ .01	.00	+ .01	+ .014	+ .03	-.03	-.03 + .044	

TABLE II: Error Summary (percent) for the Cove Point Tanks

Tank	Volume Calculation	Random Uncertainty			Limits of Systematic Error for			Scale bias + systematic and random error
		Target spacing	Scale factor	RMS total	Thermal coef.	Scale bias		
1	+ .01	+ .014	+ .015	+ .023	+ .03	.00	.00 + .053	
2	+ .01	+ .014	+ .009	+ .019	+ .03	.00	.00 + .049	
3	+ .01	.014	+ .005	+ .018	+ .03	-.02	-.02 + .048	
4	+ .01	.014	+ .011	+ .020	+ .03	.01	.01 + .050	
5	+ .01	.014	+ .007	+ .019	+ .03	.00	.00 + .049	

TABLE III: Error Summary (percent) for the Columbia Tanks

Tank	Volume Calculation	Random Uncertainty			Limits of Systematic Error for		Systematic and random error limit
		Target spacing	Scale factor	RMS total	Thermal coef.		
1	+ .01	+ .014	+ .025	+ .03	+ .03	+ .06	
2	+ .01	+ .014	+ .025	+ .03	+ .03	+ .06	
3	+ .01	.014	+ .025	+ .03	+ .03	+ .06	
4	+ .01	.014	+ .025	+ .03	+ .03	+ .06	
5	+ .01	.014	+ .025	+ .03	+ .03	+ .06	

The second column in the tables gives the estimate of the random uncertainty in the volume introduced by the computational method. The third column gives an estimate of the random uncertainty introduced when the number of identifiable points or targets on the tank used for the photogrammetric survey is reduced to half those used on tanks 3, 4, and 5 of the Savannah. The fourth column gives the random uncertainty associated with the magnitude of the scale factor required to convert coordinate number data to true lengths as determined from the NBS tape results. Column five gives the rms sum of these random errors.

A systematic error results from the uncertainty in the coefficient of thermal contraction for the aluminum tank cooled to operating temperature. The estimated limits of this error are given in column six. The seventh column of Tables I and II give the systematic error in the tank volume resulting from systematic errors in the photogrammetric scale factor, which is discussed Appendix A. Detectable scale factor systematic errors were observed only for some of the calibrations of the tanks of the Savannah and Cove Point. No scale factor systematic error was discernable for the tanks of the Columbia, so that column has been deleted. The scale-factor systematic error can be eliminated by applying a multiplying factor to the gage table volumes.

The last column of the three tables shows a combined value of the uncertainty of the tank calibration for each tank.

Some photogrammetrically-determined numbers were used in this error estimate in combination with some independent measurements. A gaging table for tank 3 of the Columbia was calculated by NBS personnel using a completely independent measurement method. This method consisted of erecting a laser plane defined solid exterior to the tank wall, then measuring the offset from the laser-defined planes to the walls at a large number of points. The spatial relationship of the planes was measured using tapes and theodolites. The method was adapted from a tank volume measurement method used internally on membrane-type LNG tanks [5]. The results of the measurements of tank 3 of the Columbia are given in Appendix D. These results agree with the photogrammetrically-determined gaging tables and agree in total volume at 22.445 m height to 0.7 m³ or 0.003%. The largest difference is 3.0 m³ in the region of 15 m height.

5. Accuracy of Tanks in Service

The results of the last section are consistent with the tanks being calibrated within the accuracy claimed by the photogrammetrist. The tanks, however, are constructed and calibrated on shore and while empty. The procedures of loading the tanks aboard ship, or the hydrostatic loading of the cargo could change the volume of the tank. Furthermore, the volumes discussed in the previous section were external; so that the volume of aluminum in the walls and internal framing must be subtracted from the external volume to obtain the actual liquid volume. This deadwood correction is 1.3% for the smallest tank (tank 1) and ranges down to 0.9% for the largest tank. The distortion of the tank caused by lifting it into the ship, the hydrostatic distortion and the deadwood have been studied by NBS personnel to determine what errors may be introduced into the gaging tables.

To test for lifting distortion, flatness surveys as described in Appendix E were done on the top and bottom surfaces of tanks 4 and 5 of the Savannah. The tanks were surveyed in the storage yard and then immediately after being placed in the ship. The root mean square differences of the surveyed points from a fitted plane were calculated for each survey. Appendix E argues that, as there was no significant change in the rms values of any of the before and after surveys, there could not be significant change in tank volume. Also, it was assumed that since the top and bottom of the tank, which would be most affected by the move, did not distort, then the walls did not distort either.

The hydrostatic pressure on the bottom of the tank when filled with LNG is about 1 bar. Since the tanks were hydrostatically tested by filling them half-full of water, it was possible for NBS personnel to measure hydrostatic deformation of the tank. Flatness measurements were made on the walls of tank 3 of the Columbia both with and without water in the tank. The results of these measurements are given in Appendix F. The rms differences of the surveyed points from a fitted plane were calculated and compared for the survey done before the hydrostatic test and for the survey made during the test. As no significant differences were detected for the rms values, it was inferred that no significant volume change had occurred.

The tank volume comparisons given in Appendix B are for the outside dimensions of the tank. To obtain the liquid volume, the volume of aluminum in the walls and internal structure must be calculated as a function of height. The deadwood volume at height h must be subtracted from the external tank volume at height h to get the liquid volume at this height. The photogrammetric contractor determined deadwood volume as a function of height from drawings of the tanks and the nominal dimensions of the various plates. In measurements made by

NBS on tank 3 of the Columbia, it was found that the deadwood dimensions are generally slightly larger than nominal. For this tank, the larger dimensions decrease the total liquid volume by about 8 m^3 or 0.03%. The measurements are reported in Appendix G.

In Appendix H, the survey effort and the results obtained for the tank bottom surveys of the 10 tanks of the first two ships are presented. The desired measurement accuracy was not achieved with these measurements because the shipyard continued work during the measurements, which caused both constant movement and permanent changes of the list and trim. The flatness surveys of the four tank quadrants could not be satisfactorily correlated by the water tube measurements. The flatness surveys by quadrant did suggest however that little bottom distortion had resulted from placing the tanks. The motions of the ship during the surveys also precluded accurate measurement of the orientation of the tank with respect to the draft marks. The third ship was not completed because the gas trials of the Savannah showed the insulation system used was unsatisfactory for LNG service.

Because of the central location of the gage in these tanks, the volume error is not a strong function of list or trim. For example, a 5 cm list adds an error of $\pm 3 \text{ m}^3$ to the volume of the largest tanks, the sign depending on whether the list is to starboard (positive) or to port. The attempt to measure the tank and gage orientations with respect to the draft marks was done when the ships were essentially complete. This measurement could be repeated anytime in the future when the ship tanks are brought up to air during the periodic inspections. This could best be done in a non-floating drydock. The measurements might also be done with the ship afloat in a quiet body of water when no other work is being done either on the ship or nearby.

Of the three sources of error considered in the section - lifting distortion, hydrostatic distortion, and errors in deadwood specification - only errors in the deadwood corrections are seen to be significant. For the lifting and hydrostatic distortions, no bounds have been calculated for how much change in volume could have occurred without having been detected by the methods of measurement used. The study by NBS on tank 3 of the Columbia showed the deadwood volume to be 2.9% larger than the deadwood volume calculated from the tank's nominal dimensions.

The uncertainty of this 2.9% value has been calculated to be approximately $\pm 0.2\%$. While it is not possible to predict what the error in the deadwood volume due to oversized dimensions would be for the remaining fourteen tanks, the material from which the other tanks were constructed is likely to be similar in sizing to the material for this tank, and it is not expected that this deadwood volume error would exceed 5%.

In conclusion, the NBS verification of the photogrammetric method of determining the external tank volumes found the uncertainty of this method to be within $\pm 0.1\%$ of total volume. This includes the errors in the use of the temperature coefficient to calculate the volume at operating temperature and in the deadwood calculation, but not the errors in the bottom survey or the effects of lifting, installing, and loading the tanks. The deadwood calculation error is expected to be within $\pm 0.04\%$ for the largest tank and within $\pm 0.06\%$ for the smallest. We have no good estimate of the bottom survey error. We have no indication of any distortion due to hydrostatic loading or to moving the tanks, and no estimate of how much volume change could have occurred without being detected by the techniques used in this study.

6. References

- [1] Jackson, R.H.F., R.S. Collier, S. Haber, R.V. Tryon, et al. 1979. Custody Transfer Systems for LNG Ships: Tank Survey Techniques and Sounding Tables. NBSIR 79-1751

- [2] Brown, D.C., 1958. A Solution to the General Problem of Multiple Station Analytical Stereoangulation. Air Force Missile Test Center Report No. 58-8, Patrick AFB, Florida

- [3] Kenefick, J.F., 1971. Ultra-Precise Analytics. Photogrammetric Engineering Vol. 37, p. 1167.

- [4] The members of the LNG Custody Transfer Measurements Supervisory Committee are Ivan W. Schmitt, Chairman, El Paso Marine Company; Bland Osborn, Columbia LNG Corporation; Howard S. Joiner, Consolidated Systems LNG Company; and Ed Crenshaw, Southern Energy Company

- [5] Hocken, R.J. and Haight, W.C., 1978; "Multiple Redundancy in the Measurement of Large Structures", Annals of the International Institution of Production Engineering Research (CIRP), Volume 27, p. 1.

- [6] Brown, D.C., Application of Close-Range Photogrammetry to Structures in Orbit, Vol. 1 and 2, GSI Technical Report #20-012. Available from Geodetic Services incorporated, 1511 South River View Drive, Melbourne, Florida 32901.

- [7] Mann, D. B., Editor, 1977. LNG Materials and Fluids. Thermophysical Properties Division, National Bureau of Standards, Boulder, Colorado.

Appendix A

Accuracy and Precision of the
Photogrammetric Dimensioning of
Freestanding Prismatic Cargo Tanks

By

J. F. LaBrecque, C. L. Carroll, and J. D. Siegwarth

Contents for Appendix A

	Page
1. Test Method	A-1
2. Tape Installation	A-2
3. Tape Calibration	A-3
4. Results of the Photogrammetric Calibration Tests	A-5
4.1 El Paso Savannah Tape Results	A-5
4.2 El Paso Cove Point Tape Results	A-16
4.2a Tape Descriptions and Locations	A-16
4.2b Method of Analyzing Tape Data	A-22
4.2c Results of Analysis	A-23
4.3 El Paso Columbia Tape Results	A-29
4.3a Tape Descriptions and Locations	A-29
4.3b Method of Analyzing Tape Data	A-32
4.3c Results of Analysis	A-33
5. Tape Data Summary and Comments	A-41
6. References	A-44

Accuracy and Precision of the Photogrammetric Dimensioning of Freestanding Prismatic Cargo Tanks

J. F. LaBrecque, C. L. Carroll and J. D. Siegwarth

1. Test Method

Since the resolution of the photogrammetric survey method can be as high as 1 part in 100,000, even for large objects, confirmation of the accuracy of the method is difficult. The most straightforward method is to measure the spacing between pairs of reference targets with sufficient accuracy so that the measured distances and the distances calculated from the photogrammetrically determined target coordinates can be compared. The first test by NBS of the photogrammetric method was done during the survey of a 36-1/2 meter diameter spherical tank.

Because of the high accuracy required in the spherical tank calibration, measuring the distance between pairs of the photogrammetric targets on the tank walls was not sufficient. Accurate taping was precluded because of the curved walls. Even if some tank wall target spacings could be accurately measured, wall temperature changes and gradients would probably alter the distances a measurable amount between the taping and the photography.

To provide some measured target spacings for the spherical tanks, reference targets of similar optical quality to the photogrammetric targets were placed on each end of a number of approximately 4 m long aluminum rods. These rods attached to the tank wall by suction cups were placed at various locations on the accessible, i.e. the lower, portion of the tank wall. These lengths were made as long as they could be and still be handled and transported. The only place greater reference target spacings were possible was tapes with targets hung along the central tower. The tower locations, however, were already occupied by the photogrammetrists calibration tapes. The comparison of the NBS measured and the photogrammetrically measured target spacings on the calibration rods gave values for the random uncertainty in reasonable agreement with the uncertainty predicted by the photogrammetrist. Unfortunately, these test rods give only limited information on bias errors, since to test the resolution, the separation of the NBS reference targets should be as large as the major dimensions of the tank.

The rectangular geometry of the free standing prismatic tanks made reference target spacings approaching the tank dimensions realizable. Surveyor's tapes could be hung parallel to the vertical sides and ends of the tank and aligned horizontal tapes could be supported along the straight sides. Since the calibrations of all fifteen tanks were tested, a much larger amount of length data was obtainable with no great increase in hardware over that used in the spherical tank test.

These tapes became the NBS length standards by clamping targets, again having properties similar to those used by the photogrammetrist, directly to them. The position of a target edge was referenced to the scribe mark, either by scribing the tape at the reference edge of the target for new positions or by measuring to 0.1 mm with a metric scale the location of the target placed within a few centimeters of an existing scribe line. The distance from the reference edge of the target to the target center was measured in the laboratory. This distance was around 3.2 or 4.5 cm depending on type of target.

Since the photography on these tanks was to be done in the open air under varying weather conditions, we chose iron-36% nickel alloy tapes to minimize thermal effects. The thermal expansion coefficient of this material is assumed to be 0.4×10^{-6} cm/cm°C [1] and since the maximum difference between the temperature of the photography and the tape calibration at NBS is about 7°C, the maximum temperature correction never exceeded 3 ppm. These tapes are unruled making it impossible to determine target separations by examining the tape.

2. Tape Installation

Sufficient time elapsed between tanks, and a sufficient number of tank calibrations were tested, to allow comparison of results and modifications to the techniques as the work progressed. The vertical tapes were hung from the top of the tank, allowed to slide through aluminum foil guides at the bottom of the tank and tensioned by 5 kg weights hung on the bottom end. We found on the first tank that the targets, consisting of a 19 mm diameter white spot on an 87 mm square black aluminum plate, could only be placed near the top and bottom ends because of the frequent wind in the area. The tapes were immune to all but the strongest winds with targets only at the ends. The tapes were pulled up from the bottom on the first two tanks but lowered from the top on all subsequent tanks. No other changes in the vertical tape installation were effected over the course of the work.

On the first four tanks, a horizontal tape was placed near ground level in a catenary suspension between two roller supports with one end fixed and the other tensioned by a 10 kg weight attached to the tape end via a string through a pulley. One target was placed on each short horizontal section between the end of the tape and support roller. This tape was discontinued because wind and moisture were probably affecting the target spacing. Horizontal tapes were placed on most of the subsequent tanks by supporting the tapes on aligned brackets with about 3 m separations. The brackets were first aligned by visual sighting, then later by laser beam. At first, the tapes were placed on edge with the vertical tape targets clamped on. The targets had to be placed near support brackets. The tape was free to slide over the supports but fixed at one end and tensioned by a 5 kg weight attached to the other via a string and pulley. Later, the tapes were laid flat with 19 mm diameter white balls attached to black anodized aluminum plates clamped to the tape. These balls present a circular cross section from any angle above the plane of the tape. On a few of the later tanks, horizontal tapes were passed under the tank, supported at 3 m intervals, with ball targets at each end. These tape installations differed from the other tapes in that no one photographic plate contained images of targets on more than one end of the tape. These were time consuming to apply and often construction work on the tank prevented their installation.

The positions of the targets relative to the scribe marks on the tape were measured before and again after photography. Only in two instances had the target moved. In those cases the clamp screws were loosened by the wind rattling the target against the tank wall.

During the photography, the air temperature was monitored to determine tape temperature.

3. Tape Calibration

The tape calibration consisted of measuring the separations between the scribe marks on the tapes. The tapes were sent to NBS at Gaithersburg, Maryland, for calibration. All distances between the scribe lines were determined at 20 degrees Celsius on a horizontal flat surface with 5 and 10 kilograms tension applied. An interferometric laser system was used with the measuring leg of the interferometer designed and built by NBS. It consists of a three wheel dolly carrying a corner cube for the laser and a 10 power micrometer microscope for viewing the scribe lines. The dolly travels over the tapes on a 61 m bench that slightly sags between its 1.22 m points of support, but

straight and flat enough for the laser beam. A spirit level and adjustable support for the dolly's third wheel corrects the plumb of the microscope. Ten vial scale divisions produces 0.0076 millimeter change in length. The level vial is so sensitive that any on-scale reading of the vial is acceptable. But if the level is not adjusted for on-scale reading, as much as 0.1 millimeter error has been noted.

The pooled standard deviation of the difference between repeated measurements of the scribe mark spacings was 0.0129 millimeters with 28 degrees of freedom. The maximum difference being 0.042 millimeters.

From the lengths determined for the two tensions applied during the tape calibration at NBS, the tape lengths at Mobile were computed. The effective tension of a tape hanging vertically is one-half the weight of the tape ribbon of the desired interval, plus the weight of all objects that hung below the interval. The tapes weigh 0.027 kg/m, the targets weigh 0.071 kg, and the eye-bolts and attachments weigh 0.040 kg.

Adding up the weights, the effective tension is about 5.5 kg, and a 1/2 kg change for the tapes produces about 0.05 mm change in length. The uncertainty of the calibration of the tapes is about 0.03 mm, and using these tapes at Mobile the uncertainty in the distance between targets should be less than 0.3 mm which includes the error of positioning the targets. The calibration report and data has been included at the end of this Appendix.

4. Results of the Photogrammetric Calibration Tests

The tape results were analyzed and reported as each ship set was completed. These results are presented in this section in the same way.

4.1 El Paso Savannah Tape Results

a. Tape Descriptions and Locations

Each calibration tape used on the Savannah tanks had two or three reference targets attached. The positions of these reference targets, as determined by the survey, are contained in the coordinate data supplied to NBS by the photogrammetrist. Three targets on a tape represent three distances, but only two distances can be considered independent. The largest and smallest of the three distances are used. If targets 1 and 2 on a tape had photogrammetric coordinates (x_1, y_1, z_1) and (x_2, y_2, z_2) , then the distances between them as determined from the coordinate data, assuming an orthogonal coordinate system, is

$$d_{12} = \left[(x_1 - x_2)^2 + (y_1 - y_2)^2 + (z_1 - z_2)^2 \right]^{1/2}.$$

The temperature of the air near some of the calibration tapes was measured during the course of the photography and the target separations in table I are determined at the average of these temperatures. The values d_{NBS} are the reference target spacings determined by NBS. The target separations determined by the photogrammetric survey, d_p , appear in the next to the last column of table I.

The invar calibration tapes are labeled #1 through #5 in table I. The targets are in the same positions for tanks 3 and 4 for all but tape #3, but have been moved for tank 5. For tanks 3 and 4, tape #1 was placed vertically on the bow end and tapes #2 and #4 were placed vertically on the stern. Tape #3 was placed vertically on the port side of tank 3 and the starboard side of tank 4. These tapes were all hung about 5 meters from the corners of the tanks. Tape #5, installed horizontally along the length of the tanks, hung in a catenary between two pulleys about 30 meters apart. Because wind was stirring this tape during the survey, this measurement may be less accurate than the vertical tape measurements.

For the photogrammetric survey of tank 5, tape #1 was installed horizontally across the stern end and supported at intervals so that no sag correction was needed. Tapes #3, #4, and #5 were positioned as on tank 4, and tape #2 was hung on the bow end.

TABLE I. Comparison of NBS Determined Target Spacings and Photogrammetrically Measured Target Spacings on the Tanks of the El Paso Savannah.

Tape # and Location	NBS Length (m)	Photogrammetric Length (m)	d - d (mm)
	NBS	P	
Tank #3 Temperature, 21.3°C 11-8-77			
1 For. Vert.	1.7127 20.6311		
2 Aft Vert.	1.2626 21.0533	1.2625 21.0535	-0.1 +0.2
3 Port Vert.	16.6249	16.6247	-0.2
4 Aft Vert.	2.6416 20.8542	2.6416 20.8548	0 +0.6
5 Port Horiz.	31.9933		
Tank #4 Temperature, 17.8°C 11-7-77			
1 For. Vert.	1.7127 20.6311	1.7135 20.6303	+0.8 -0.8
2 Aft Vert.	1.2626 21.0533	1.2629 21.0514	+0.3 -1.9
3 Stbd. Vert.	16.5769	16.5764	-0.5
4 Aft Vert.	2.6416 20.8542	2.6424	+0.8
5 Stbd. Horiz.	31.9932	31.9909	-2.3
Tank #5 Temperature, 12.0°C 1-5-78			
1 Aft Horiz.	20.6309	20.6278	-3.1
2 For. Vert.	1.2684 20.5906	1.2678 20.5893	-0.6 -1.3
3 Aft Vert.	16.6249	16.6233	-1.5
4 Aft Vert.	2.6307 20.1892	2.6310 20.1867	+0.3 -2.5
5 Stbd. Horiz.	23.1234	23.1224	-1.0
Tank #2 Temperature, 21.0°C 4-6-78			
1 For. Vert.	20.6311 0.4453	20.6266 0.4455	-4.5 +0.2
2 Aft Vert.	21.0533 0.4681	21.0485 0.4680	-4.8 -0.1
3 Stbd. Vert.	16.5770	16.5742	-2.8
4 Aft Vert.	20.8545 0.6656	20.8500 0.6655	-4.5 -0.1
5 Stbd. Horiz	31.9933		

TABLE I. (Continued)

Tape # and Location		NBS Length (m) d_{NBS}	Photogrammetric Length (m) d_{P}	$d_{\text{P}} - d_{\text{NBS}}$ (mm)
Tank #1		Temperature, 19.1°C 4-22-78		
1	For. Vert.	1.7507	1.7504	-0.3
		18.8578	18.8538	-4.0
2	Aft Vert.	1.3070	1.3070	0
		20.6193	20.6174	-1.9
3	Stbd. Vert.	15.9697	15.9678	-1.9
4	Aft Horiz.	2.6045	2.6047	-0.2
		20.8172	20.8148	-2.4

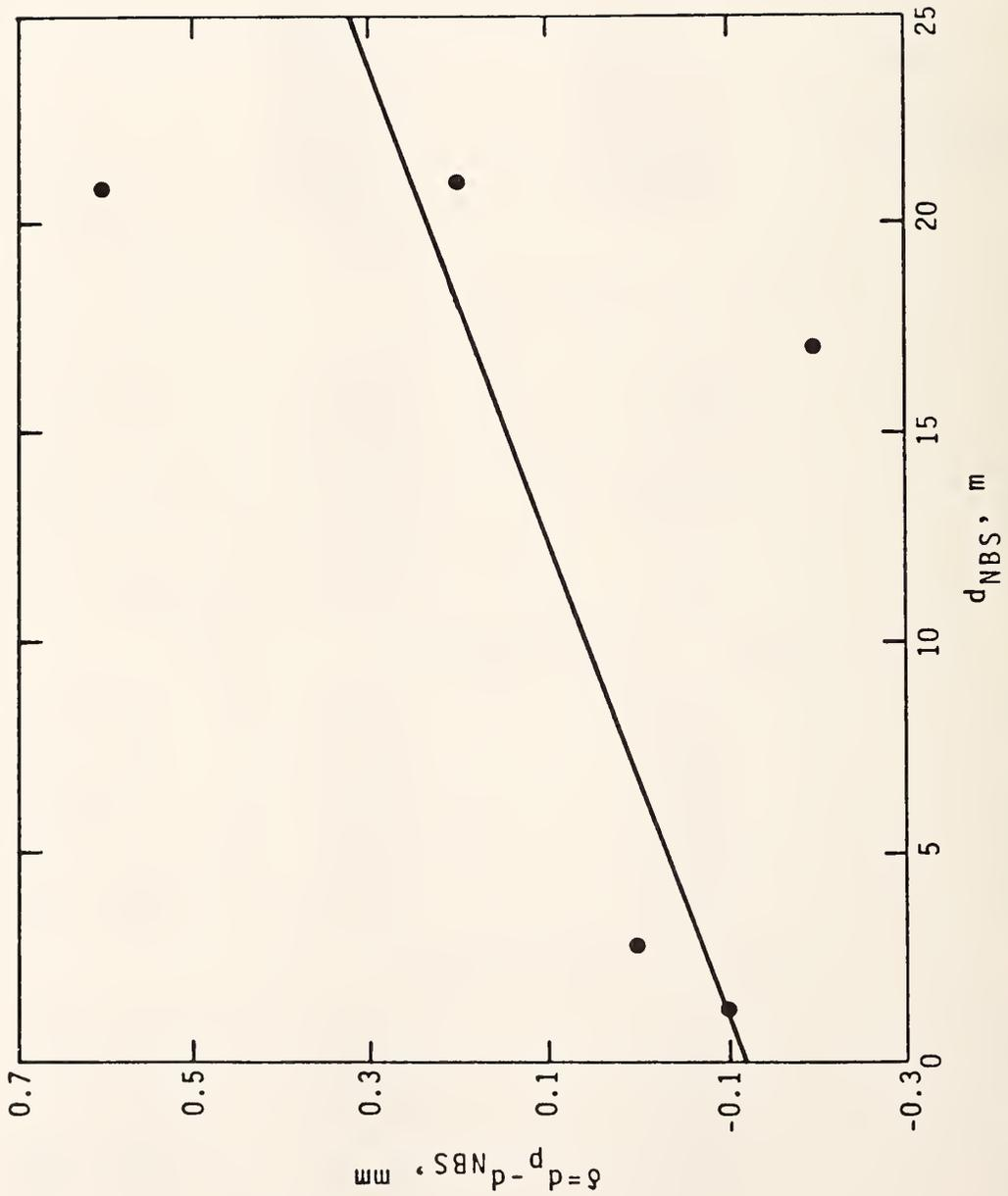


Figure 1. Deviation δ of photogrammetrically determined test tape lengths from NBS determined lengths, d_{NBS} , versus d_{NBS} for Tank 3 of the Savannah.

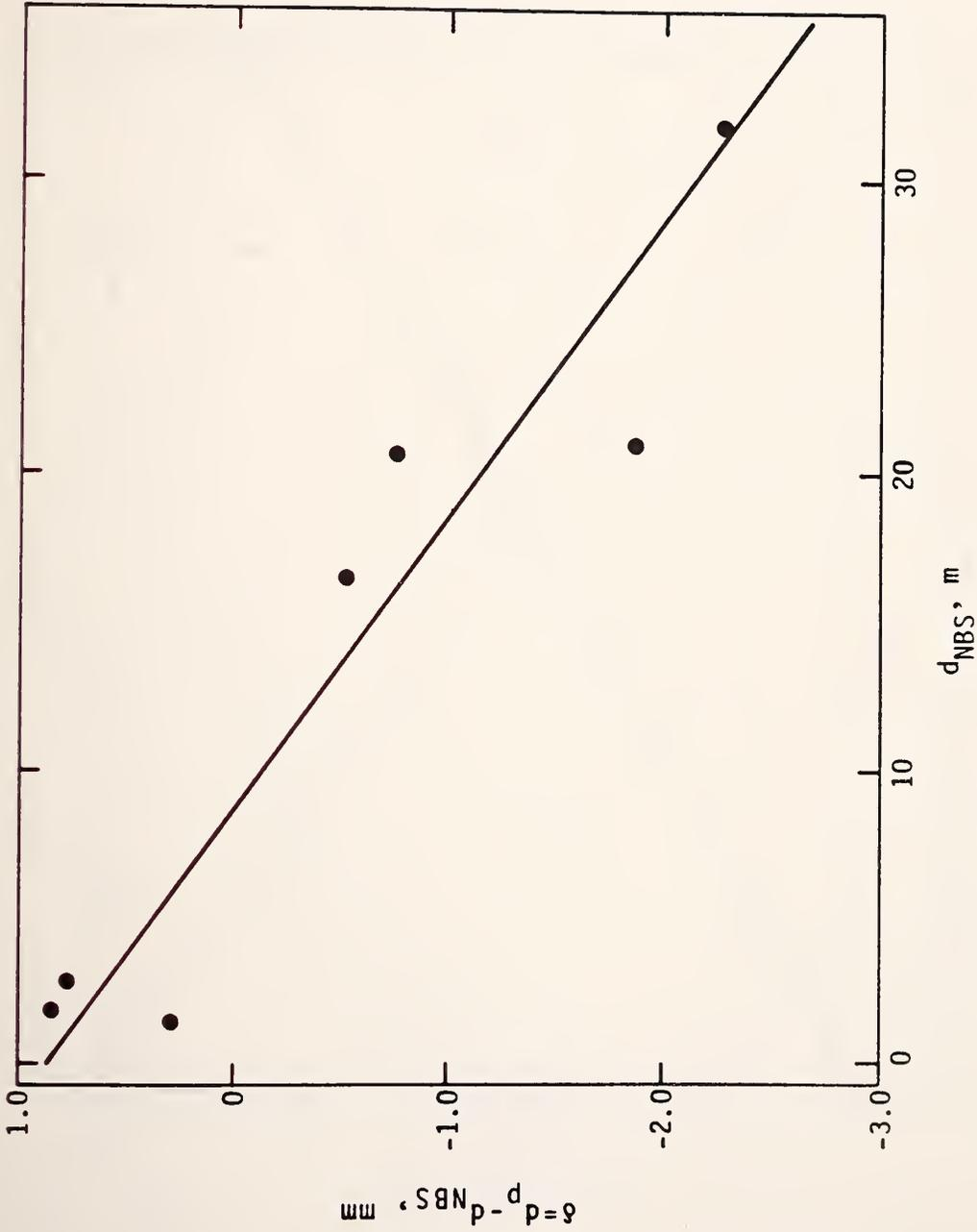


Figure 2. Deviation δ of photogrammetrically determined test tape length from NBS determined lengths d_{NBS} versus d_{NBS} for Tank 4 of the Savannah.

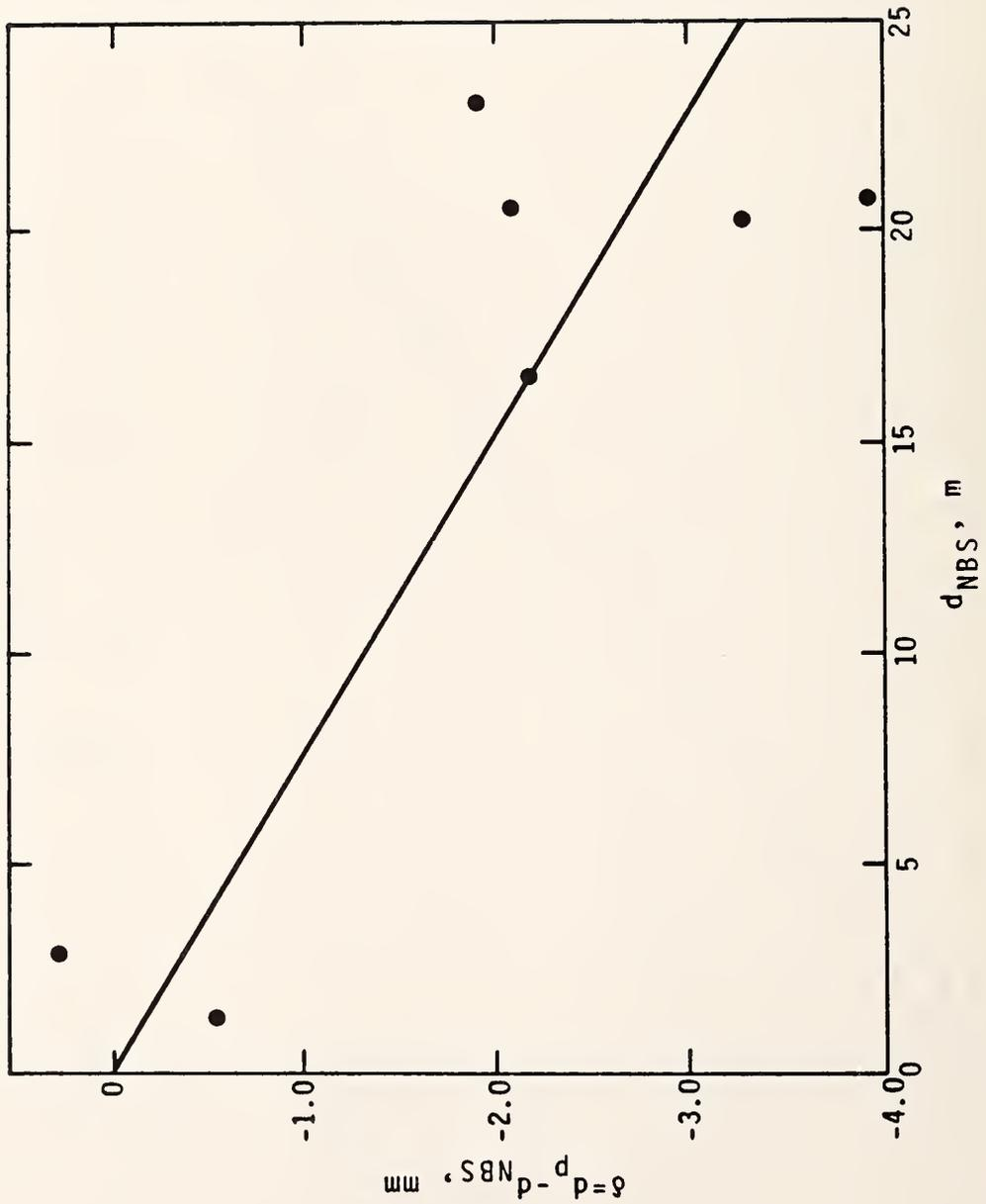


Figure 3. Deviation δ of photogrammetrically determined test tape lengths from NBS determined lengths, d_{NBS} versus d_{NBS} for Tank 4 of the Savannah.

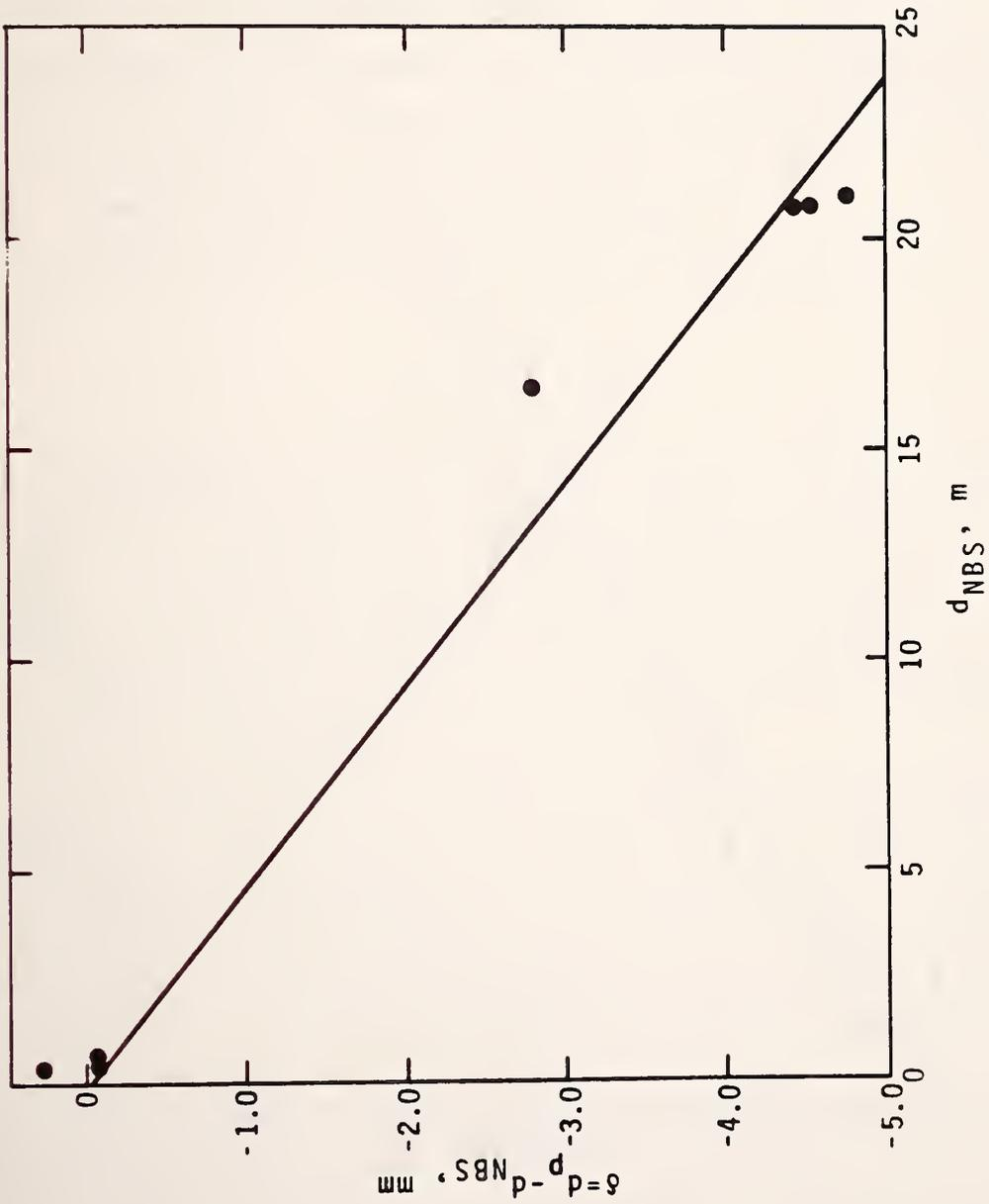


Figure 4. Deviation δ of photogrammetrically determined test tape lengths from NBS determined lengths, d_{NBS} , versus d_{NBS} for tank 2 of the Savannah.

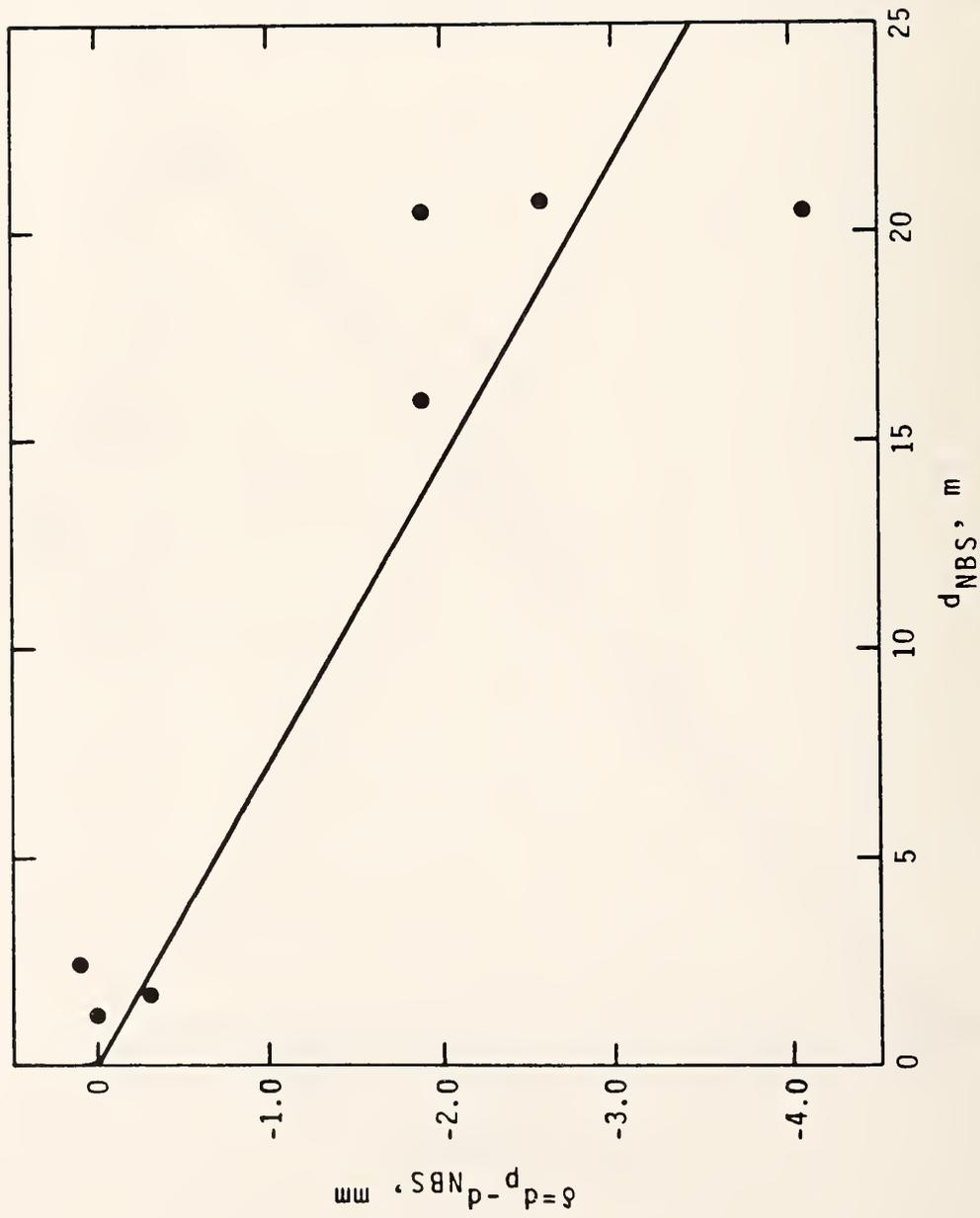


Figure 5. Deviation δ of photogrammetrically determined test tape lengths from NBS determined lengths, d_{NBS} , versus d_{NBS} for Tank 1 of the Savannah.

On tank 2, tape #2 and #4 were placed on the aft end of the tank with tape #4 near the port and #2 near the starboard corner. Tape #3 was placed near the forward corner on the starboard side and #1 was placed near the port corner of the forward end of the tank. Tape #5 was placed along the starboard side.

On tank 1, the placements were: tape #3 near the aft corner of the starboard side, tape #2 on the aft end near the port corner, tape #1 on the forward end near the starboard corner and tape #4 horizontally across the aft end of the tank. Tape #5 was not placed on the tank since the tank lifting brackets were still attached and in the way.

b. Method of Analyzing Tape Data and Results

The data in Table I for each tank were fit by the equation:

$$\delta = c + s \cdot d_{NBS}$$

where $\delta = d_p - d_{NBS}$, c represents a constant error in all values of δ , and s represents a scaling error. The above equation was fit by least squares for each tank and the results are shown in figures 1 through 5. A non-zero value for c means the targets used as the reference are offset. Tank 4 shows a value of c of 0.8 mm which is statistically significant at the 1% level. The values of c on the other four tanks are not statistically different from zero.

The first column of table II gives the observed values of s with a 95% confidence interval for each of the five tanks. The second column gives the estimated standard deviation of δ for each tank.

In the last column of table II, volume bias with 95% confidence intervals are given for the percentage error in the tank volume because of the scale error. The largest of these is the 0.06% underestimate on tank 2.

Since no intermediate target spacings were checked by tapes, it must be assumed that s does represent a scale error. Only tank 3 shows a value for s small enough to be statistically insignificant. All the observed values of s for the remaining tanks are negative, and all are comparable in magnitude except for tank 2 which has an observed value of s about twice the magnitude of the others. The photogrammetric consultant uses six 15 1/4 meter lengths to determine the scale factor for each tank survey. If we assume that the standard deviation for the

Table II

<u>Tank</u>	<u>s value with 95% C.I.*</u>	<u>Standard deviation for length measurements</u>	<u>d.f.</u>	<u>Volume Bias with 95% C.I.</u>
1	-13.4 \pm 3.2 (10^{-5})	0.72 mm	6	-0.04% \pm 0.01%
2	-21.1 \pm 3.1 (10^{-5})	0.36 mm	6	-0.06% \pm 0.01%
3	1.1 \pm 3.6 (10^{-5})	0.28 mm	4	0.00% \pm 0.01%
4	-9.8 \pm 3.6 (10^{-5})	0.43 mm	5	-0.03% \pm 0.01%
5	-9.2 \pm 2.7 (10^{-5})	0.82 mm	6	-0.03% \pm 0.01%

*confidence intervals based on overall observed standard deviations of 0.58 mm with 27 degrees of freedom.

measurement of such lengths to be 1 mm--which is conservative based on our information from the photogrammetric consultant--the standard deviation for the scale factor would be 2.7×10^{-5} . For 99% of the time, we should then expect values of s in the interval $\pm 6.9 \times 10^{-5}$. The values observed for s for tanks 1, 2, 4, and 5 fall outside this interval.

NBS estimates a standard deviation for the tape lengths of 0.3 mm. This includes all errors of laboratory length measurement, catenary correction, temperature correction, and errors in positioning the targets with respect to the tape markings. The photogrammetric consultant gives standard deviations for these lengths from 0.4 mm to 0.8 mm. The combined overall standard deviation from all tanks has a value of 0.58 mm (27 degrees of freedom) which is in good agreement with these values.

4.2 El Paso Cove Point Tape Results

4.2a Tape Descriptions and Locations

Each calibration tape used on the Cove Point tanks had two or more targets attached. The positions of these targets, as determined by the survey, are contained in the coordinate data supplied to NBS by the photogrammetrist. The n targets on a tape represent only $n-1$ independent distances. An end target on a tape was chosen as target 1 and the distances to the other targets were determined from this target. If targets 1 and i on a tape had photogrammetric coordinates (x_1, y_1, z_1) and (x_i, y_i, z_i) , then the distances between them as determined from the coordinate data, assuming an orthogonal coordinate system, is

$$d_i = \left\{ (x_i - x_1)^2 + (y_i - y_1)^2 + (z_i - z_1)^2 \right\}^{1/2}$$

The temperature of the air near some of the calibration tapes was measured during the course of the photography and the target separations in table II are determined at the temperature of the photogrammetric survey. The values d_{NBS} are the target spacings determined by NBS. The target separations determined by the photogrammetric survey, d_p , appear in the next to the last column of table II.

The invar calibration tapes are labeled #1 through #8 in table II. On tank 3, the vertical tapes #1, #2, and #3 were placed near the port corner of the forward end of the tank, near the port corner of the aft end of the tank and on the starboard side near the forward end of the tank respectively. Tape #4 with six targets was placed on edge horizontally across the forward end of the tank and supported at 3 m intervals on aligned brackets. Tape #5 was similarly mounted along the port side again with six targets. Tape #7 was mounted crosswise under the tank with two ball targets on each end. The tape was laid flat on aligned wire hangers placed at 3 m intervals. Tape Nos. 6 and 8 were similarly mounted but ran diagonally under the tank. Tape #8 extended from the after starboard corner to the forward port corner. The targets on one end of tape #6 which laid on the opposite diagonal was obscured by something and no photogrammetric length was obtained.

On tank 4, the vertical tapes #1, #2 and #3 were placed on the forward end of the tank near the port corner, aft near the port corner, and on the starboard side near the forward corner respectively. Tape #4 was placed horizontally on the forward end with five targets and #5 was placed horizontally on the starboard side with seven targets. The mounting and support methods were the same as for these tapes on tank 3.

Tapes #2 and #3 were placed at the same locations on tank 5 as on tank 4. Tape #1 was placed on the forward end of the tank near the starboard corner. Tapes #4 and #5 were placed in the same positions as on tank 4 with six targets each. Tapes #6 and #8 were installed diagonally underneath the tank with the forward ends near the centerline of the tank and the after ends near the starboard and port corners respectively. Two ball targets were attached at each end. The horizontal tape installations were the same as those for tanks 3 and 4 but the supports were aligned for the first time by means of laser beam. Tape #7 was installed horizontally along the port side of the tanks and mounted with five ball targets. This tape was, for the first time, installed flat rather than on edge and ball targets were used because this tape was located on the side adjoining tank 4.

For the photography on tank 2, tape #1 was mounted horizontally on the forward end of the tank. This tape was mounted flat with some new 3/4" diameter ball targets on 2.5 by 6.4 mm plates. Again, the supports were aligned by a laser beam. Tapes #2, #3, and #4 were placed vertically toward the starboard side of the forward end, on the port side toward the aft end of the tanks and on the aft end near the port corner respectively.

On tank 1, tapes #1, #2, and #3 were placed vertically on the aft of the tank toward the port corner, on the forward end of the tank near the starboard quarter, and on the port side of the tank toward the aft end respectively. No other tapes were installed.

The number of tapes installed and the positions they are placed is dictated not only by the information desired, but also by the location of the tanks, the tank construction work underway at the time, and the installation time available.

The difference in the NBS determined and the photogrammetrically determined target spacings shown in Table III were generally less than 2 mm with a few exceptions. The exceptions involve one target on each of two tapes and perhaps tape #5 on tank 4 completely. The single target position errors on tape #1 of tank 4 and tape #7 of tank 5 cannot be attributed definitely to either the photogrammetric length determination or the NBS length determination; though, in the case of the tape #1 target position error, the photogrammetric uncertainty in the vertical direction given by the photogrammetrist is twice that of the other targets on vertical tapes suggesting the possibility that the error is in the photogrammetry. For tape #7, no such clue exists. These two data were not used in the analysis. Tape #5 on tank 4 (see Table III) shows length errors that increase with length to 6 mm for the longest length indicating a scale factor error. Such an error is not indicated by any other tape on that tank, however. If the tape was under tensioned, this result could be obtained. Though the 5 kg tensioning weight does not elongate the tape more than about 3 mm for the entire length, sag between supports could account for the additional decrease in the photogrammetrically determined length as the weight is decreased below 5 kg. The weight was placed on the tape, but if the tape hung up on something on the weight end thus reducing the tape tension, the tape may not have been stretched the amount assumed in the NBS length determination. Laboratory tests showed that the required tape sag to account for the observed shortening is slight enough that it could have gone unnoticed during the photography. Since this apparent scale factor error showed up in only one of the 11 horizontal tapes used on these five tanks, a slacked tape seems the more likely cause of error rather than a horizontal scale error in the photogrammetry on one side of the tank.

Two of the diagonal tapes beneath the tank, tape #8 on tank 3 and tape #6 on tank 5, showed errors of nearly 1 cm and 9 cm respectively in the original photogrammetric target coordinate data. The four targets, two on each end of the tape, should lie on a straight line. An examination of the coordinate data of both tapes showed that one target location on one end of each tape was well off a line through the remaining three targets. An examination of the detailed photogrammetric data showed that in both cases, the location of the target was determined

TABLE III. Comparison of NBS Determined Target Spacings and Photogrammetrically Measured Target Spacings on the Tanks of the El Paso Cove Point.

Tape # and Location		NBS Length (m) d_{NBS}	Photogrammetric Length (m) d_P	$d_P - d_{NBS}$ (mm)
Tank #3		Temperature, 26.8°C 8-17-78		
1	For. Vert.	1.7188	1.7182	-0.6
		20.5985	20.5969	-1.6
2	Aft Vert.	1.2673	1.2674	+0.1
		20.5812	20.5801	-1.1
3	Port Vert.	0.5826	Target center out	
		16.0113	16.0105	-0.8
4	For. Horiz.	2.6679	Target obscured	
		13.0921	13.0906	-1.5
		16.0220	16.0210	-1.0
		20.2112	20.2095	-1.7
		20.8869	20.8851	-1.7
5	Port Horiz.	5.9795	5.9798	+0.3
		Target not recorded	7.0734	
		12.0630	12.0626	-0.4
		19.7401	19.7388	-1.3
		Target not recorded	20.4795	
		25.7966	25.7953	-1.3
		31.9756	31.9736	-2.0
6	Diag. Horiz.	.3278	Target obscured	
		38.9965	" "	
		39.1896	" "	
7	Trans. Horiz.	0.1989	0.1985	-0.4
		30.1526	30.1493	-3.3
		30.4457	30.4428	-2.9
8	Diag. Horiz.	0.1690	0.1690	0
		39.6625	39.6599	-2.6
		39.8910	39.8887	-2.3
Tank #4		Temperature, 26°C 9-15-78		
1	For. Vert.	1.7256	1.7252	-0.4
		20.6195	20.6144	-5.1
2	Aft Vert.	1.2304	1.2301	-0.3
		20.9810	20.9808	-0.2
3	Stbd. Vert.	0.5672	0.5673	+0.1
		16.6537	16.6532	-0.5
4	For. Horiz.	2.6532	2.6537	+0.5
		13.0551	13.0562	+1.1
		15.9874	15.9890	+1.6
		20.8413	20.8430	+1.7
5	Stbd. Horiz.	6.0658	6.0645	-1.3
		7.0668	7.0650	-1.8
		12.1546	12.1521	-2.5
		19.7142	19.7108	-3.4
		25.7845	25.7800	-4.5
		32.0028	31.9968	-6.0

TABLE III. (continued)

Tape # and Location		NBS Length (m) d_{NBS}	Photogrammetric Length (m) d_p	$d_p - d_{NBS}$ (mm)
Tank #5		Temperature, 24°C 10-12-78		
1	For. Vert.	1.7407	1.7410	+0.3
		20.1578	20.1580	+0.2
2	Aft Vert.	1.3327	1.3331	+0.4
		21.1277	21.1271	-0.6
3	Stbd. Vert.	0.5746	0.5747	+0.1
		16.6067	16.6077	+1.0
4	For. Horiz.	2.6450	2.6449	-0.1
		13.0582	13.0581	-0.1
		15.9717	15.9714	-0.3
		20.1938	20.1933	-0.5
		20.8499	20.8498	-0.1
5	Stbd. Horiz.	5.9948	5.9949	+0.1
		7.0890	7.0894	+0.4
		12.0673	12.0679	+0.6
		19.7514	19.7523	+0.9
		23.0463	23.0469	+0.6
6	Diag. Horiz.	0.3263	0.3264	+0.1
		29.2902	29.2919	+1.7
		29.6015	29.6033	+1.9
7	Port Horiz.	6.0835	6.0836	+0.1
		12.0287	12.0192	-9.5
		21.2385	21.2358	-2.8
		24.1893	24.1913	+2.0
8	Diag. Horiz.	0.1652	0.1652	0
		29.5943	29.5933	-1.0
		29.8706	29.8719	+1.3
Tank #2		Temperature, 18.5°C 11-20-79		
1	For. Horiz.	1.7128	1.7139	+1.1
		8.9399	8.9405	+0.6
		14.0045	14.0052	+0.7
		20.1844	20.1844	0
		20.6216	20.6222	+0.6
2	For. Vert.	1.2420	1.2424	+0.4
		20.5848	20.5849	+0.1
		21.0513	21.0517	+0.4
3	Port Vert.	0.5550	0.5547	-0.3
		16.5642	16.5645	+0.3
4	Aft Vert.	0.6678	0.6674	-0.4
		20.8501	20.8516	+1.5

TABLE III. (continued)

Tape # and Location		NBS Length (m) d_{NBS}	Photogrammetric Length (m) d_{P}	$d_{\text{P}} - d_{\text{NBS}}$ (mm)
Tank #1		Temperature, 18.7°C 11-21-79		
1	Aft Vert.	1.7224	1.7223	-0.1
		20.1815	20.1819	+0.4
		20.6383	20.6389	+0.6
2	For. Vert.	1.2825	1.2823	-0.2
		20.5991	20.5982	-0.9
		21.0468	21.0463	-0.5
3	Port Vert.	0.5545	0.5548	+0.3
		16.7708	16.7720	+1.2

by the intersection of only two rays. This fact, coupled with the difficulty of positively identifying the targets on the photographs placed in these locations, suggested that the targets had been incorrectly identified on one plate and the other two intersections of the four rays (from the two plates to the two targets) might be the actual target positions. We used the appropriate camera and coordinate positions to derive the coordinates of the other two intersections for both tapes, and found in terms of both length and alignment, these intersections were the true target positions.

Of the 27 tapes and well over 100 targets used in the analysis of these five tanks, the only length disagreements between the NBS and photogrammetric length determinations of any consequence occurred on one tape and two other targets. Since an erroneous measurement, especially when only a few occur, is of much less significance than a correct measurement, the evidence that the photogrammetric method accurately determines the target coordinates is overwhelming.

4.2b Method of Analyzing Tape Data

The photogrammetrically determined i th length from the j th tape on a particular tank is assumed to be related to the corresponding NBS length l_{ij} in the following way:

$$l'_{ij} = a \cdot l_{ij} + \epsilon_{ij} \quad (2)$$

where a is a constant which ideally would be 1, l'_{ij} , and l_{ij} have been substituted for the symbols $(d_p)_{ij}$ and $(d_{NBS})_{ij}$, respectively, and ϵ_{ij} is a random error associated with the photogrammetric technique. However, because any error in the position of target 1 is part of the ϵ_{ij} for all the l'_{ij} , it may appear as a significant offset and hence affect the estimate for a . To avoid this, equation 2 was modified to the following relationship and fitted to the l'_{ij} :

$$l'_{ij} - l_{ij} = c + s \cdot (l_{ij} - \bar{l}_j) + \epsilon_{ij} \quad (3)$$

where \bar{l}_j is the average of the l_{ij} for the j th tape. For this relationship s ($=a-1$) would ideally be 0, as would the value for c ($=s\bar{l}_j$). In this form the estimate for s is unaffected by the error in the position of target 1.

The information derived from the l'_{ij} data are: an estimated value for s , an estimate of how this s value would affect the volume and an estimated value for the standard deviation (std. dev.) of the l'_{ij} .

4.2c Results of Analysis

Table IV gives this derived information for the vertically suspended targeted tapes by tank. Ninety-five percent confidence intervals (C.I.) are given for the s values and volume biases. The column headed d.f. (degrees of freedom) give the relative information available for estimating the std. dev.; the larger the d.f., the better the estimate. Only tank 3 shows a value of s that is judged to be different from zero. The 95% C.I. for the volume bias resulting from this s value is taken to be $-0.017\% \pm 0.012\%$. Figure 6 is a plot of $\bar{l}_{1j} - l_{1j}$ versus $l_{1j} - \bar{l}_j$ for all the tapes of tank 3. The point symbols are numbers giving the tape from which \bar{l}_{1j} was derived. This plot clearly indicates a value for s different from zero. The set of points for each of the three vertically suspended and four horizontally supported tapes (tape #6 targets were obscured) used for tank 3 each show a slightly different value of s .

Table V gives the results for each of the horizontally supported tapes. Each of these tapes are analyzed separately because they usually have more than four targets and have more problems to consider. Of the horizontal tapes of tank 3, only tape #5 shows a value for s significantly different from zero, but taken as an ensemble (see table VI), the case is clear.

As mentioned in the previous section, tape #5 on tank 4 gives data that are suspect and will not be considered in this analysis. The tape #5 data show a large value for s , but tape #3 hung on the same side shows no scale error (value of s not different from zero). However, tape #4 also shows a scale error, but of different sign from that of tape #5. Unfortunately, the vertical tape #1 hung on the same side as tape #4 and could not be used to shed any additional information on a non-zero value for s . Tape #4 is on the forward end of the tank and there are no tapes on the port side. Since the tapes on the other two sides show no scale error, it is assumed that half the tank has a scale error and other half does not. A 95% C.I. for the volume bias due to the scale error is taken to be $0.010\% \pm 0.007\%$.

As also discussed in the previous section, one of the \bar{l}_{1j} values on tape #7 of tank 5 is judged to be in error and not included in the analysis. The results for the remaining three \bar{l}_{1j} contain a large estimated std. dev. considered to be atypical. The tape was on the side adjacent to another tank. This higher uncertainty is expected since the camera positions are definitely

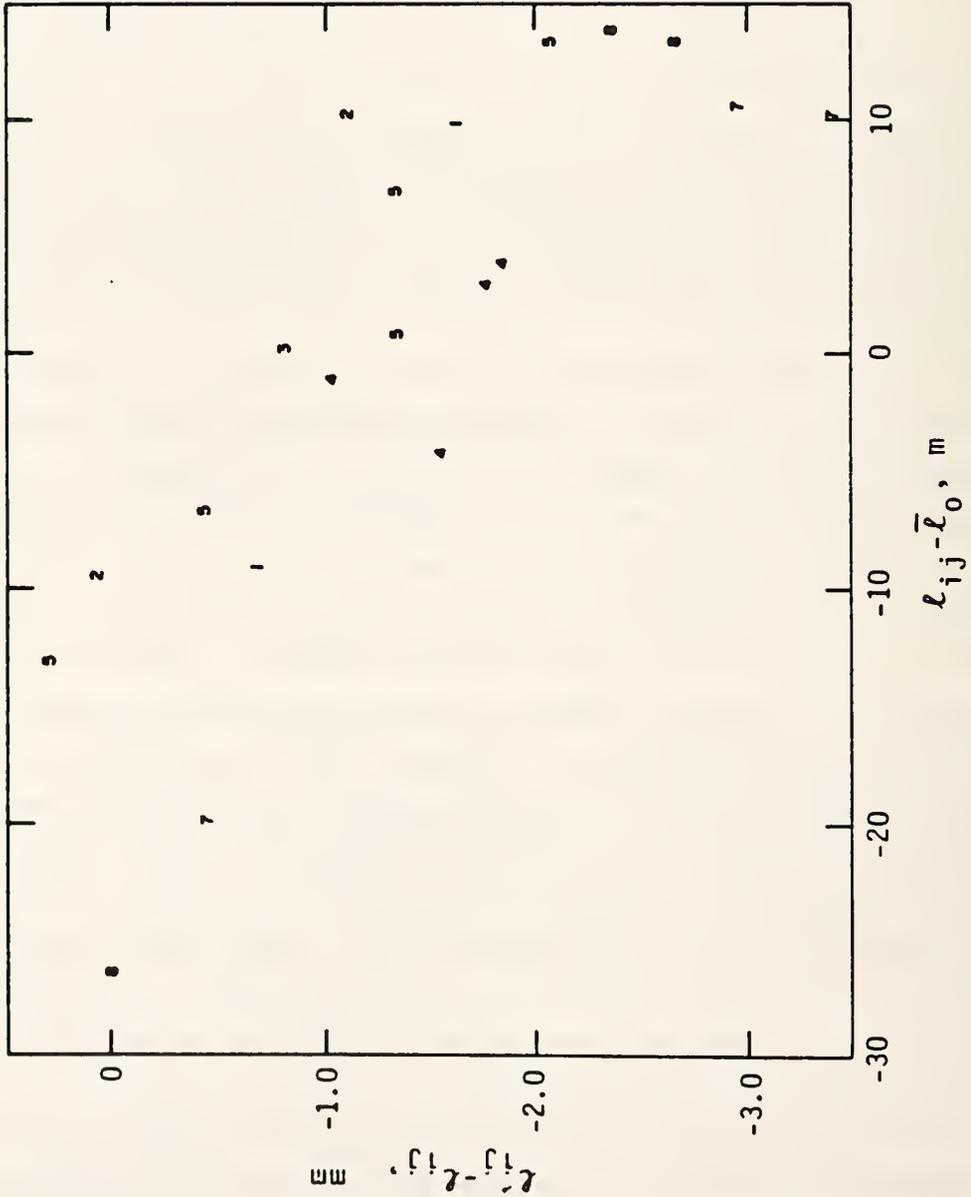


Figure 6. Deviation $\lambda'_{ij} - \lambda_{ij}$ of the photogrammetrically determined test tape length from the NBS determined length versus NBS length less the NBS average length, $\lambda_{ij} - \bar{\lambda}$, for all tapes used on Tank 3 of the Cove Point. The symbols refer to tape numbers given in Table III.

Table IV. Results From the Analyses of the Photogrammetrically Measured Target Spacings of the Vertically Hung Tapes on the Cove Point Tanks

<u>Tank</u>	<u>s value with 95% C.I.</u>	<u>Std. dev. for length measurements</u>	<u>d.f.</u>	<u>Volume Bias with 95% C.I.</u>
1	1.4 \pm 5.0 (10^{-5})	0.63 mm	8	0.004 \pm 0.015%
2	3.8 \pm 4.1 (10^{-5})	0.65 mm	7	0.011 \pm 0.012%
3	-5.8 \pm 4.1 (10^{-5})	0.34 mm	3	-0.017 \pm 0.012%
4	-1.2 \pm 2.9 (10^{-5})	0.33 mm	3	-0.004 \pm 0.009%
5	-0.7 \pm 5.0 (10^{-5})	0.53 mm	5	-0.002 \pm 0.015%
Combined		0.55 mm	28	

Table V. Results From Analyses of the Photogrammetrically Measured Target Spacings for Each of the Horizontally Supported Tapes of the Cove Point Tanks.

<u>Tank</u>	<u>Tape</u>	<u>s value with 95% C.I.</u>	<u>Std. dev. for length measurements</u>	<u>d.f.</u>	<u>Volume Bias with 95% C.I.</u>
2	1	$-3.9 \pm 5.6 (10^{-5})$	0.40 mm	3	$0.011 \pm 0.017\%$
3	4	$-5.7 \pm 24. (10^{-5})$	0.50 mm	3	$-0.017 \pm 0.072\%$
3	5	$-8.4 \pm 3.5 (10^{-5})$	0.32 mm	3	$-0.025 \pm 0.010\%$
3	7	$-9.0 \pm 16. (10^{-5})$	0.43 mm	1	$-0.027 \pm 0.047\%$
3	8	$-6.2 \pm 8.7 (10^{-5})$	0.31 mm	1	$-0.017 \pm 0.026\%$
4	4	$7.0 \pm 5.1 (10^{-5})$	0.22 mm	2	$0.021 \pm 0.015\%$
4	5	$-16.7 \pm 3.0 (10^{-5})$	0.35 mm	4	$-0.050 \pm 0.009\%$
5	4	$-1.2 \pm 3.9 (10^{-5})$	0.25 mm	4	$-0.004 \pm 0.012\%$
5	5	$3.0 \pm 3.9 (10^{-5})$	0.42 mm	4	$0.009 \pm 0.012\%$
5	6	$5.7 \pm 3.1 (10^{-5})$	0.08 mm	1	$0.017 \pm 0.009\%$
5	7	---	2.81 mm	3	---
5	8	$0.56 \pm 6.7 (10^{-5})$	0.95 mm	3	$0.002 \pm 0.02\%$

Table VI. Results From Analyses of the Photogrammetrically Measured Target Spacings for the Vertical and Horizontal Tapes of Each of the Cove Point Tanks.

<u>Tank</u>	<u>Tape</u>	<u>s value with 95% C.I.</u>	<u>Std. dev. for length measurements</u>	<u>d.f.</u>	<u>Volume Bias with 95% C.I.</u>
1	A11	$1.4 \pm 5.0 (10^{-5})$	0.63 mm	8	$0.004 \pm 0.015\%$
2	A11	$1.5 \pm 3.0 (10^{-5})$	0.58 mm	11	$0.004 \pm 0.009\%$
3	A11	$-7.2 \pm 1.8 (10^{-5})$	0.59 mm	18	$-0.022 \pm 0.005\%$
4	1,2,3	$-1.2 \pm 2.9 (10^{-5})$	0.33 mm	3	$-0.004 \pm 0.009\%$
4	4	$7.0 \pm 5.1 (10^{-5})$	0.22 mm	2	$-0.021 \pm 0.015\%$
5	1,2,3 4,5,6 8	$1.7 \pm 2.4 (10^{-5})$	0.73 mm	20	$0.005 \pm 0.007\%$
Combined			0.65 mm	57	

not optimum because of the narrow gap between the tanks in the storage area. The camera positions are close to the extended plane of the tank wall which is required to obtain a view of the full tank wall and dictates that the photogrammetrist must use ball targets. This camera positioning reduces the resolution of the target positions in the horizontal component parallel to the tank wall, but not the other two components. The increased uncertainty in target positions in this direction contributes negligibly to the tank volume uncertainty. The data for tape #7 are excluded from further analysis of tank 5.

Table VI is a summary combining the results for the vertical and horizontal tapes for each tank. Tank 4 is a special case and has been given two lines in the table. The combined std. dev. is based on all the tanks except 4, and will be the value used to represent the random error of the photogrammetric technique in this set of tanks.

The photogrammetric consultant uses six 15 1/4 meter lengths to determine the scale factor for each tank survey. If we assume that the standard deviation for the measurement of such lengths to be 1 mm, which is conservative based on our information from the photogrammetric consultant, the standard deviation for the scale factor would be 2.7×10^{-5} . For 99% of the time, we should then expect values of s in the interval $\pm 6.9 \times 10^{-5}$. The values observed for s for tank 3 falls outside this interval.

NBS estimates a standard deviation for the tape lengths of 0.3 mm. This includes all errors of laboratory length measurement, catenary correction, temperature correction, and errors in positioning the targets with respect to the tape markings. The photogrammetric consultant gives standard deviations for these lengths from 0.4 mm to 0.8 mm. The combined overall standard deviation for the length measurements from all tanks has a value of 0.65 mm (57 degrees of freedom) which is in good agreement with these values.

4.3 El Paso Columbia Tape Results

4.3a. Tape Descriptions and Locations

Each calibration tape used on the Columbia tanks had two or more targets attached. The positions of these targets, as determined by the survey, are contained in the coordinate data supplied to NBS by the photogrammetrist. The n targets on a tape represent only $n-1$ independent distances. One target on a tape was chosen as target 1 and the distances to the other targets were determined from this target. If targets 1 and i on a tape had photogrammetric coordinates (x_1, y_1, z_1) and (x_i, y_i, z_i) , then the distances between them as determined from the coordinate data, assuming an orthogonal coordinate system, is given by equation (1).

The temperature of the air near some of the calibration tapes was measured during the course of the photography and the target separations in table VII are determined at the temperature of the photogrammetric survey. The values d_{NBS} are the target spacings determined by NBS. The target separations determined by the photogrammetric survey, d_p , appear in the next to the last column of table VII.

The invar calibration tapes are labeled #1 through #6 in table VII. On tank 3, the vertical tapes #1, #2, and #3 were placed near the starboard corner of the forward end of the tank, near the port corner of the aft end of the tank and on the port side near the aft end of the tank respectively. Tape #4 with six targets was placed on edge horizontally alongs the port side of the tank and supported at 3 m intervals on laser aligned brackets. Tape #5 was similarly mounted along the starboard side again with seven targets. Tape #6 was mounted diagonally under the tank with ball targets on each end. The tape was laid flat on laser aligned wire hangers placed at 3 m intervals and extended from the after port corner to the forward center. Tape #3 fell from the tank and was destroyed before the photography.

TABLE VII. Comparison of NBS Determined Target Spacings and Photogrammetrically Measured Target Spacings on the Tanks of the El Paso Columbia.

Tape # and Location	NBS Length (m) d_{NBS}	Photogrammetric Length (m) d_P	$d_P - d_{NBS}$ (mm)
Tank #3			
Temperature, 16.2°C 3-7-79			
1 For. Vert.	Target slipped 19.3188	1.7293 19.3208	2.0
2 Aft Vert.	1.3097 21.0939	1.3097 21.0957	0.0 1.8
4 Port Horiz.	2.7010 13.0541 16.0187 20.2495 20.9134	2.7018 13.0544 16.0200 20.2496 20.9133	0.8 0.3 1.3 0.1 -0.1
5 Stbd. Horiz.	5.9329 7.0678 12.0095 20.4700 25.7629 29.2678	5.9331 7.0670 12.0091 20.4686 25.7606 29.2651	0.2 -0.8 -0.4 -1.4 -2.3 -2.7
6 Diag. Horiz.	38.2304	38.2252	-5.2
Tank #4			
Temperature 20.8°C 3-26-79			
1 Aft Vert.	1.7282 20.1726 20.6686	1.7287 20.1741 20.6693	0.5 1.5 0.7
2 For. Vert.	1.2993 2.0679 20.0884 21.0865	1.2996 2.0680 20.0879 21.0861	0.3 0.1 -0.5 -0.4
5 Port. Horiz. (between tanks)	7.6633 12.6909 13.7533 19.8007 0.7533 3.1924 6.0586 9.4419 12.2814	7.6571 12.6890 13.7541 19.7968 0.7542 3.1937 6.0620 9.4429 12.2810	-6.2 -1.9 0.8 -3.9 0.9 1.3 3.4 1.0 -0.4

TABLE VII--continued

Tank #5		Temperature, 18.5°C 3-28-79		
1	For. Vert.	0.9297	0.9297	0.0
		1.7593	1.7595	0.2
		20.1349	20.1361	1.5
2	Aft Vert.	2.0328	2.0325	-0.3
		20.1108	20.1126	1.6
		21.0181	21.0200	1.9
4	For. Horiz.	2.6784	2.6791	0.7
		13.0876	13.0874	-0.2
		16.0188	16.0199	1.1
		20.1990	20.1993	0.3
Tank #1		Temperature, 24.7°C 5-23-79		
1	Aft Vert.	1.7386	1.7383	-0.3
		20.1699	20.1692	-0.7
		20.6586	20.6575	-1.1
2	For. Vert.	1.2819	1.2821	0.2
		2.0652	2.0653	0.1
		20.1041	20.1037	-0.4
4	Aft Horiz.	21.0747	21.0741	-0.6
		2.6252	2.6256	0.4
		13.0695	13.0693	-0.2
		15.8852	15.8861	0.9
		20.1759	20.1764	0.5
		20.8753	20.8759	0.6
Tank #2		Temperature 26.2°C 5-24-79		
1	For. Vert.	1.6832	1.6834	0.2
		20.1539	20.1527	-1.2
		20.6307	20.6292	-1.5
2	Aft Vert.	1.2717	1.2718	0.1
		2.0356	2.0360	0.4
		20.5514	20.5524	1.0
		21.0639	21.0648	0.9
5	Stbd. Horiz.	6.0299	6.0298	-0.1
		7.1261	7.1265	0.4
		12.0906	12.0900	-0.6
		19.7938	19.7942	0.4
		20.4345	20.4347	0.2
		23.0050	23.0047	-0.3
		23.1019	23.1021	0.2
		25.8528	25.8529	0.1
		29.3218	29.3211	-0.7
		32.0650	32.0648	-0.2

On tank 4, the vertical tapes #1 and #2 were placed, respectively, on the forward end of the tank near the starboard corner with four targets and on the after end of the tank near the starboard corner with five targets. Tape #5 was placed horizontally along the port side of the tank.

Tape #1 was placed on forward end of tank 5; while tape #2 was placed on the aft end near the starboard corner. The tapes held five and four targets, respectively. Tape #4 with five targets was placed horizontally across the forward end.

On tank 1, tape #1 with four targets was placed near the starboard corner on the aft end and tape #2 with five targets was placed near the starboard corner on the forward end. Tape #4 was installed horizontally across the aft end of the tank with six targets attached.

On tank 2 tape #1 with four targets was placed on the forward end near the starboard corner and tape #2 with five targets was placed near the starboard corner on the aft end. Tape #5 with eleven targets was installed horizontally along the starboard side.

The differences of the NBS and the photogrammetry determination of reference target spacings is, again for this shipset, generally less than 2 mm. The diagonal tape on tank 3, tape #6, shows a difference exceeding 5 mm and tape #5 on tank 4 shows differences larger than 2 mm. In the case of the latter tape, this higher uncertainty is expected since it was located again in the narrow gap between the tanks in the storage area. The extra uncertainty in target positions in this direction contributes negligibly to the tank volume uncertainty. Only one ball target was placed on each end of tape #6; so insufficient information exists to determine whether the difference between the measured lengths is random or systematic. More information is available on the calibration of tank 3 in Appendix D. This tank has been dimensioned by a modification of the laser plane method developed by NBS for membrane tank calibration.

4.3b Method of Analyzing Tape Data

The method used on the Columbia tanks is the same as used on the Cove Point tanks, section 4.2b.

4.3c Results of Analysis

A 95% confidence interval is given in Table VIII for the s value of each tape. The corresponding estimated standard deviations for length measurements, shown in the third column, are based on the best linear fit for that tape. The column headed "degrees of freedom" give the relative information available for estimating the standard deviation; the larger the degrees of freedom, the better the estimate. The data for vertical tapes #1 and #2 on tank 3 were combined to give an estimate for s . There are only three length measurements between them, and the plot of these measurements suggest that s is approximately the same for both; the alternative would have been to discard these data.

A test of these estimated standard deviations shows them to be consistent with the assumption that the standard deviation for length measurements is the same for all tapes. There was one exception to this. As explained earlier, tape #5 on tank 4 is expected to have a larger standard deviation because of the oblique angles at which it was photographed. The data from this tape was not used in determining the overall, combined estimated standard deviation of 0.37 mm (34 degrees of freedom) for length measurements. This estimate is in good agreement with that of the photogrammetrist, who states the standard deviations for length measurements to be from 0.4 mm to 0.8 mm.

The 95% confidence intervals in table VIII for the various s values show evidence contrary to the assumption that each tank has a single value for s . Figures 7-11 are plots of the $l'_{ij} - l_{ij}$ versus l_{ij} for tanks 1-5, respectively. These plots illustrate the variability in the values of s for the various tapes on each tank. We assume for this set of tanks that the values for s are randomly variable from place to place on a tank. There are three estimated values for s for each tank. Each is given equal weight in estimating the average value of s for each tank and its standard deviation.

The average value of s computed for each tank and is given in table IX with a 95% confidence interval (C.I.). This 95% C.I. is based on pooling the five estimates of the standard deviations of s derived from the values of s obtained for each tank. These five values, also given in the table, were judged not statistically different. The last column of table IX gives the volume bias attributed to each of the averaged s values. None of the biases are judged to be significant, but the variability in the estimates for s introduce an uncertainty in the tank volumes of $\pm 0.025\%$.

Table VIII. Results from Analyses of the Photogrammetrically Measured Target Spacing for the Invar Tapes on the Columbia Tanks.

Tank	Tape	s value with 95% C.I.*	Std. dev. for length measurements	degrees of freedom
1	1	$-4.5 \pm 2.7 (10^{-5})$	0.24 mm	1
1	2	$-2.4 \pm 2.7 (10^{-5})$	0.17	2
1	4	$2.7 \pm 2.2 (10^{-5})$	0.42	2
2	1	$-6.6 \pm 2.6 (10^{-5})$	0.26	1
2	2	$4.6 \pm 2.5 (10^{-5})$	0.19	2
2	5	$-0.4 \pm 1.1 (10^{-5})$	0.38	8
3	1&2	$9.9 \pm 4.8 (10^{-5})$	0.27	1
3	4	$-3.8 \pm 5.1 (10^{-5})$	0.57	3
3	5	$-10.8 \pm 3.5 (10^{-5})$	0.40	5
4	1	$5.4 \pm 2.6 (10^{-5})$	0.50	1
4	2	$-3.4 \pm 4.0 (10^{-5})$	0.11	2
4	5	$-6.6 \pm 2.3 (10^{-5})$	2.7	7
5	1	$6.6 \pm 2.7 (10^{-5})$	0.12	3
5	2	$11.6 \pm 5.2 (10^{-5})$	0.004	1
5	4	$2.7 \pm 2.7 (10^{-5})$	0.63	2

*Confidence intervals based on overall observed standard deviations of 0.37 mm with 34 degrees of freedom.

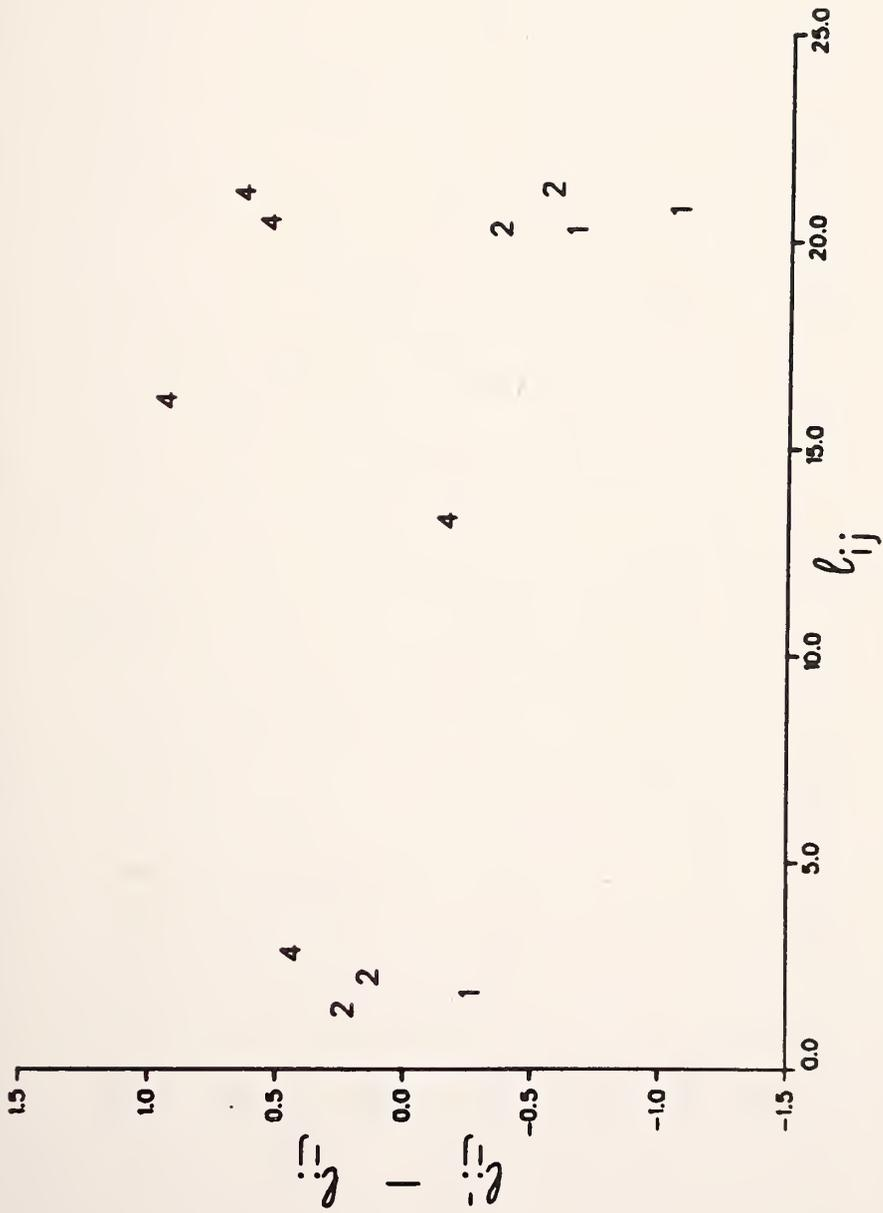


Figure 7. Deviations of photogrammetrically determined test tape lengths from NBS determined lengths versus length for Tank 1 of the Columbia.



Figure 8. Deviations of photogrammetrically determined test tape lengths from NBS determined test tape lengths from NBS determined length versus length for Tank 2 of the Columbia.

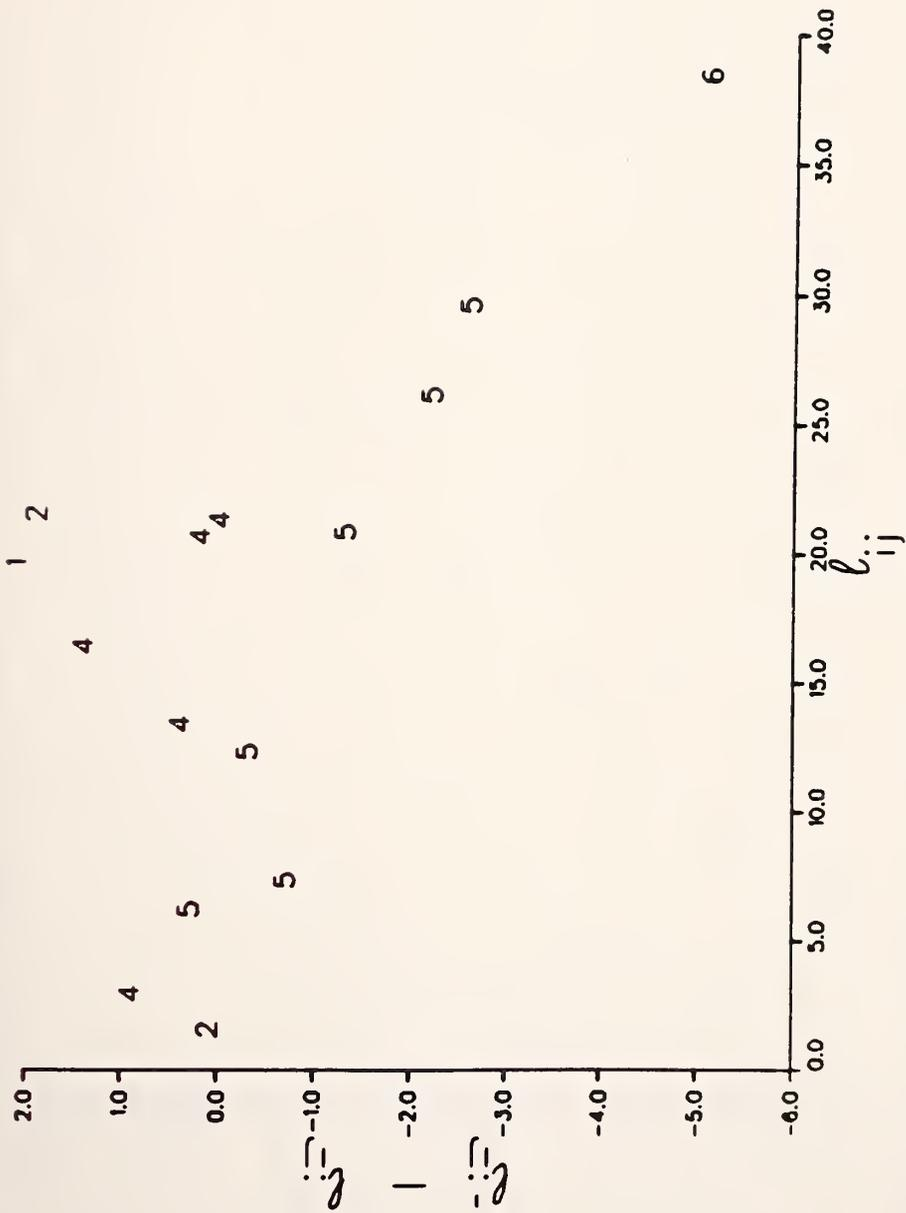


Figure 9. Deviations of photogrammetrically determined test tape lengths from NBS determined lengths versus length for Tank 3 of the Columbia.

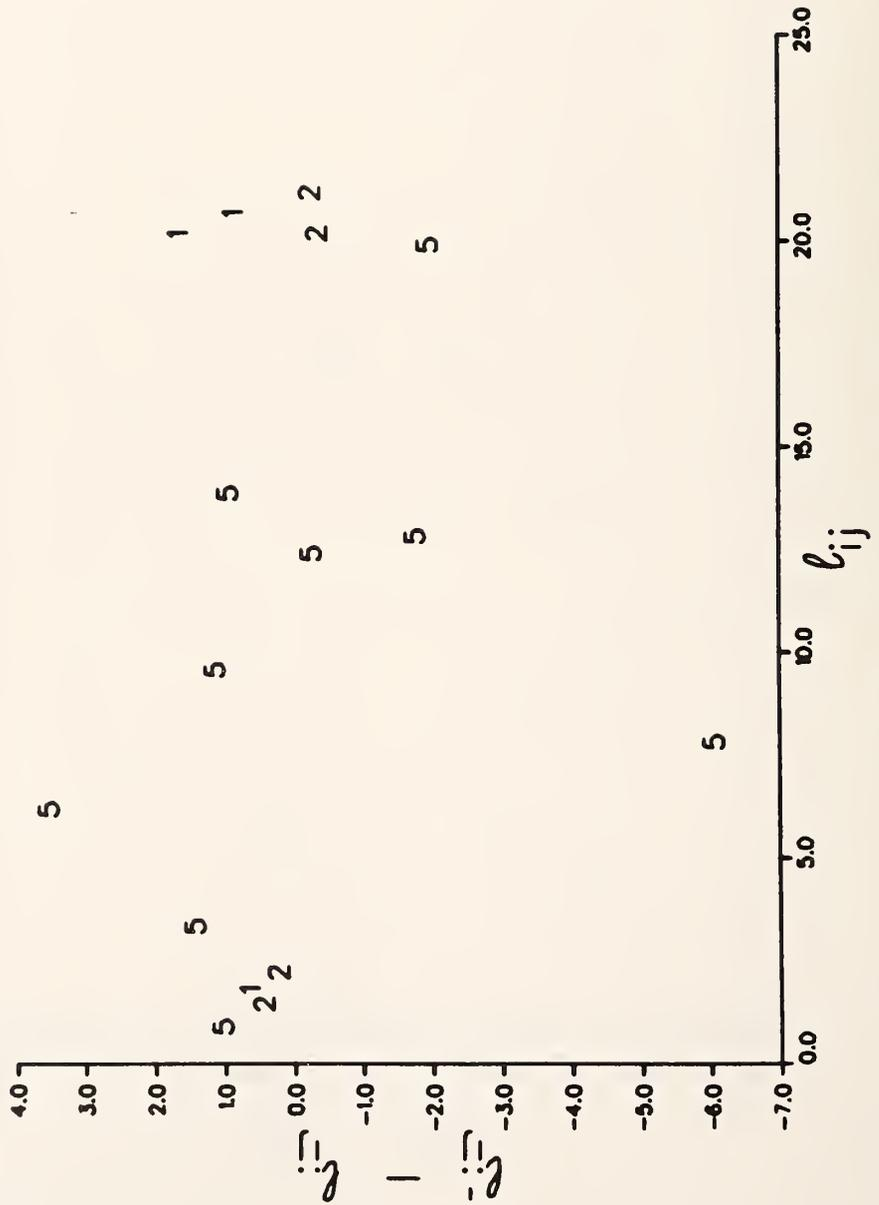


Figure 10. Deviations of photogrammetrically determined test tape lengths from NBS determined lengths versus length for Tank 4 of the Columbia.



Figure 11. Deviations of photogrammetrically determined test tape lengths from NBS determined lengths versus length for Tank 5 of the Columbia.

Table IX. Scale Error Estimates for Each of the Five Tanks of the El Paso Columbia

Tank	s value with 95% C.I.*	Std. dev. for s value of a tape	Number of tapes	Volume Bias with 95% C.I.
1	$-1.4 \pm 8.4 (10^{-5})$	$3.7 (10^{-5})$	3	$-0.004 \pm 0.025 (\%)$
2	$-0.8 \pm 8.4 (10^{-5})$	$5.6 (10^{-5})$	3	$-0.002 \pm 0.025 (\%)$
3	$-1.6 \pm 8.4 (10^{-5})$	$10.5 (10^{-5})$	3	$-0.005 \pm 0.025 (\%)$
4	$-1.5 \pm 8.4 (10^{-5})$	$6.2 (10^{-5})$	3	$-0.004 \pm 0.025 (\%)$
5	$7.0 \pm 8.4 (10^{-5})$	$4.5 (10^{-5})$	3	$0.021 \pm 0.025 (\%)$

*Confidence intervals are based on the combined standard deviations of the s values for each tank, i.e., $6.6 (10^{-5})$ with 10 degrees of freedom.

NBS estimates a standard deviation for the tape lengths of 0.3 mm. This includes all errors of laboratory length measurement, catenary correction, temperature correction, and errors in positioning the targets with respect to the tape markings.

5. Tape Data Summary and Comments

In these analyses of the length measurement data, the basic model has been

$$l_{ij} = A + B l'_{ij}$$

where l_{ij} and l'_{ij} are the corresponding length values as determined by the photogrammetrist and NBS for the i^{th} length on the j^{th} tape for a particular tank, and where A ideally has the value 0 and B the value 1. The constant A reflects any error in the reference target coordinates. For the analyses of the tape data for the ship sets 1 and 2, it had been assumed that B can change magnitude from tank to tank, but is a constant for all tapes on a particular tank. The analysis of the data showed no reason to alter this assumption. However, the data for ship set 3 (El Paso Columbia) suggested B might vary from tape to tape, and the data were handled accordingly.

As discussed in section 4.3, a separate value of B was estimated for each tape used on ship set 3 and the appropriate values averaged for each tank to obtain the estimated scale correction for the tank, see table IX. For the other two ship sets, where B was estimated on the assumption that it was not random from tape to tape but only from tank to tank, the uncertainty of the scale factor is smaller than estimated using the model for ship set 3. Larger uncertainties are obtained for the scale factor because the amount of information available to estimate uncertainties is now proportional to the number of tapes rather than the number of lengths, as was the case for ship sets 1 and 2. If we handle the Savannah (ship set 1) tape data as we did the Columbia (ship set 3), we get the estimates in table X for the average $s (= B-1)$ for each tank, rather than those shown in table II.

The major change in table X over table II is that the uncertainties (width of the 95% confidence intervals) are now twice as large because we now have only one-fourth the information with which to estimate uncertainty. We see no reason, therefore, to substitute a new analysis for the tape data from the Savannah.

Table X. Values of s When Allowed to Vary for Each Tape on the Tanks of the Savannah.

<u>Tank</u>	<u>s Value with 95% C.I.*</u>	<u>Number of Tapes</u>	<u>Volume Bias with 95% C.I.</u>
1	$-14.5 \pm 6.4 (10^{-5})$	3	$-0.04\% \pm 0.02\%$
2	$-22.6 \pm 6.4 (10^{-5})$	3	$-0.06\% \pm 0.02\%$
3	$2.4 \pm 7.9 (10^{-5})$	2	$0.01\% \pm 0.02\%$
4	$-9.8 \pm 7.9 (10^{-5})$	2	$-0.03\% \pm 0.02\%$
5	$-9.8 \pm 7.9 (10^{-5})$	2	$-0.03\% \pm 0.02\%$

* confidence intervals based on overall standard deviation of $4.8 (10^{-5})$ with 7 degrees of freedom.

Table XI. Values of s When Allowed to Vary for Each Tape on the Tanks of the Cove Point.

<u>Tank</u>	<u>s Value with 95% C.I.</u>	<u>Number of Tapes</u>	<u>Volume Bias with 95% C.I.</u>
1	$2.0 \pm 5.5 (10^{-5})$	3	$0.006 \pm 0.016\%$
2	$2.1 \pm 4.8 (10^{-5})$	4	$0.006 \pm 0.014\%$
3	$-6.7 \pm 1.7 (10^{-5})$	6	$-0.021 \pm 0.005\%$
4	$-7.6 \pm 16.1 (10^{-5})$	5	$-0.024 \pm 0.050\%$
5	$1.3 \pm 3.4 (10^{-5})$	8	$0.004 \pm 0.010\%$

Table XI gives the results of analyzing the Cove Point (ship set 2) tape data as we did that of the Columbia replacing table VI. The confidence intervals for s for tanks 1, 2, 5 are based on an estimated standard deviation of 4.4×10^{-5} (12 d.f.) that combines the individual estimates from the three tanks. For tank 3 the standard deviation is too small to be considered like those of the above three tanks, and was not combined with them. For tank 4 the estimated standard deviation is too large. Also, in the analysis of the tank 4 data in section 4.2, the tape 5 data was not used and one length from tape 1 was not used. However, in this analysis, all the data were used. The new results are little different from the results in section 4.2 except for those of tank 4. The new method of analysis allows us to treat all the tape data in the same way as in the analysis of tank 4 and not exclude data as in the previous analysis. The uncertainty in the determination of scale factor for tank 4 is about three times larger for the new analysis, but the uncertainties of the scale factor for the other four tanks remain as they are in section 4.2

The random uncertainty in length measurements as determined by the photogrammetric survey has been estimated for each of the three ship sets as follows:

<u>Ship</u>	<u>Standard deviation of length measurement</u>	<u>Degrees of freedom</u>
Savannah	0.58 mm	27
Cove Point	0.65 mm	57
Columbia	0.37 mm	34

The difference in standard deviations between the first two ship sets and the last may result from the method used to analyze the data. For the first two ship sets, the length measurements for a tank were analyzed without regard to what tape they came from, and so no allowance was made for different tapes having different scale factors; this method increases the apparent random scatter in the length measurements.

The imprecision of the length measurements and, indirectly, of the target locations should have little effect on the uncertainties of the tank calibrations. When determining the height of each of the levels of targets, the actual deviations of targets from the average may be several centimeters, and the deviation of the tank wall between targets may also be several centimeters.

In trying to predict the uncertainty due to scale error on future photogrammetric surveys of large tanks, we have pooled our three estimates of the standard deviation for s : 6.6×10^{-5} with 10 degrees of freedom for the Columbia from section 4.3, 4.8×10^{-5} (7 d.f.) for the Savannah, and 4.4×10^{-5} (12 d.f.) for the Cove Point, the last two from this section. The pooled value is 5.3×10^{-5} with 29 degrees of freedom. A two-sided 99% confidence interval for the true standard deviation of s is 3.9×10^{-5} to 7.8×10^{-5} . If, as we have assumed in similar exercises in the previous sections, the standard deviation of the length measurements is 1 mm, then the standard deviation for s obtained by the photogrammetrist using his vertical tapes should be 6.6×10^{-5} , which is certainly within this confidence interval. However, from the tape data it appears that his standard deviation for length measurements is actually smaller than 1 mm. Using the tapes the way the photogrammetrist uses them, a value of 0.6 mm may be more correct. This would give a standard deviation for s of 3.9×10^{-5} , the lower end of the interval.

Taking the upper end of the 99% confidence interval as our prediction for the standard deviation s , and assuming the use of six calibration tapes in the manner we have employed there, the uncertainty in volume calibration due to scale uncertainty would be $\pm 0.025\%$ (99% confidence interval)--it is 0.035% if only three tapes were used, as was done by the photogrammetrist.

6. References

[1] Hidnert, D. and Kirby, R. K., 1953. A New Method for Determining Thermal Expansion of Invar Geodetic Surveying Tapes. J.Res., NBS 50, 179.

UNITED STATES DEPARTMENT OF COMMERCE
NATIONAL BUREAU OF STANDARDS
WASHINGTON, D.C. 20234

R E P O R T O F C A L I B R A T I O N

M1465

page 1 of 4

For: Eight Invar Length Measuring Tapes

Submitted by: National Bureau of Standards
Center for Chemical Engineering
Thermophysical Properties Division
Boulder, Colorado 80303

The tapes were calibrated using a helium-neon laser interferometer as the length standard while under tension and uniformly supported on a horizontal flat surface. The distances between the terminal points of the indicated intervals at 20 degrees Celsius (68 degrees Fahrenheit) under 5 kilograms tension are given on the following pages. The terminal points of the indicated intervals are the centers of the graduations at the edge of the tape ribbon nearest the observer when the zero graduation is to his left.

All measurements were made in a controlled environment near 20 degrees Celsius and an assumed coefficient of thermal expansion of 0.0000004 per degree was used to correct the lengths to 20 degrees.

The linear density and AE values were determined and are given on the following pages. The AE value is the product of the average cross-sectional area of the tape ribbon and its Young's Modulus of Elasticity.

The uncertainty of the reported lengths is 0.000005 meter per meter and is taken to be the sum of the random and systematic components of error. The random component is taken to be three times the observed standard deviation. The systematic component consists solely of the uncertainty of the laser interferometer and is estimated to be 0.000002 meter per meter.

Measurements were made by

Clarence Leon Carroll, Jr.

For the Director,

Robert J. Hocken
Robert J. Hocken, Chief
Automated Production Technology Div.
Center for Manufacturing Engineering

Date: April 13, 1981

20-Meter Invar Tape

NBS No. 14811

Interval (graduations)	Feb 78 Length (millimeters)	Feb 79 Length (millimeters)	Jul 80 Length (millimeters)
A to B		865.96	
A to E	1712.85	1712.86	
A to F		8936.27	
A to G		14007.47	
A to C	20185.53	20185.54	
A to D	20631.02	20631.01	

The linear density is 0.026918 kilogram/meter and the AE value is 49499 kilograms for tape 14811.

21-Meter Invar Tape

NBS No. 14812

Interval (graduations)	Feb 78 Length (millimeters)	Feb 79 Length (millimeters)	Jul 80 Length (millimeters)
A to B	1262.48	1262.50	
A to E		2042.85	
A TO F		20113.47	
A to C	20585.07	20584.93	
A to D	21053.10	21052.91	21052.67

The linear density is 0.026961 kilogram/meter and the AE value is 49097 kilograms for tape 14812.

16-Meter Invar Tape

NBS No. 14813

Interval (graduations)	Feb 78 Length (millimeters)	Feb 79 Length (millimeters)	Jul 80 Length (millimeters)
A to B	553.36	553.43	
A to E		1079.34	
A to F		15709.98	
A to G		16174.44	
A to C	16576.98	16577.01	
A to D	16624.93	16624.99	16622.08

The linear density is 0.026923 kilogram/meter and the AE value is 49656 kilograms for tape 14813.

20-Meter Invar Tape

NBS No. 14814

Interval (graduations)	Feb 78 Length (millimeters)	Feb 79 Length (millimeters)	Jul 80 Length (millimeters)
A to B	2641.90	2641.94	2642.03
A to E		13048.44	13048.50
A to G		15890.82	15890.94
A to F		15979.84	15979.92
A to C	20188.90	20188.93	20189.05
A to D	20854.30	20854.34	20854.50

The linear density is 0.027063 kilogram/meter and the AE value is 48771 kilograms for tape 14814.

32-Meter Invar Tape

NBS No. 14815

Interval (graduations)	Feb 78 Length (millimeters)	Mar 79 Length (millimeters)	Jul 80 Length (millimeters)
A to S		128.15	
A to E		5969.11	
A to B		7063.30	
A to F		12052.66	
A to G		19729.28	
A to H		20469.28	
A to I		22941.33	
A to J	23035.63	23034.82	
A to K		25786.50	
A to L		29179.92	
A to M		29262.54	
A to S		31782.03	
A to C		31909.72	
A to D	31999.32	31998.36	31998.34

The linear density is 0.027043 kilogram/meter and the AE value is 47702 kilograms for tape 15815.

39-Meter Invar Tape

NBS No. 14916

Interval (graduations)	Feb 78 Length (millimeters)	Feb 79 Length (millimeters)	Jul 80 Length (millimeters)
A to B		328.33	
A to E		29209.82	
A to F		29521.08	
A to C		38917.69	
A to D		39110.93	39110.98

The linear density is 0.026762 kilogram/meter and the AE value is 48513 kilograms for tape 14916.

30-Meter Invar Tape

NBS No. 14917

Interval (graduations)	Feb 78 Length (millimeters)	Mar 79 Length (millimeters)	Jul 80 Length (millimeters)
A to B		198.93	
A to E		6278.48	
A to F		12223.08	
A to G		16729.43	
A to H		21433.55	
A to I		24383.88	
A to C		30074.29	
A to D		30367.46	

The linear density is 0.027020 kilogram/meter and the AE value is 48666 kilograms for tape 14917.

40-Meter Invar Tape

NBS No. 14918

Interval (graduations)	Feb 78 Length (millimeters)	Mar 79 Length (millimeters)	Jul 80 Length (millimeters)
A to B		168.75	
A to E		29514.73	
A to F		29790.67	
A to C		39583.23	
A to D		39811.76	39811.73

The linear density is 0.027100 kilogram/meter and the AE value is 48386 kilograms for tape 14918.

Appendix B

**Uncertainty in the Tank Volume Determination
Introduced by the Computational Method**

By

J. F. LaBrecque

Contents for Appendix B

	Page
Volume Calculation from Coordinate Data.	B-1
Comparisons of Volume Determination.	B-3
Target Distribution on Tank.	B-19
References	B-21

Uncertainty in the Tank Volume Determination
Introduced by the Computational Method

J. F. LaBrecque

The photogrammetric surveys of the freestanding prismatic tanks for the Savannah, Cove Point, and Columbia provide representations of each tank in the form of the X, Y, Z coordinates of the photogrammetric targets attached to the external tank walls. From these coordinate points, a mathematical model of the tank must be contrived from which the tank volume as a function of height can be calculated. In this report, the methods used by both the photogrammetrist and by NBS are outlined and the results of the two methods compared at selected elevations for all fifteen tanks of these three ships.

Volume Calculation from Coordinate Data

The photogrammetric consultant calculates the volume of a tank from a height times area relationship. Using the target coordinate data, he approximates the horizontal cross sectional area of the tank at various heights; the volume between two such adjacent areas is then their average times the distance between them. A linear interpolation is used to obtain the tank volume at a height falling between two adjacent cross sections. These volumes include the walls and internal support structure of the tank since the targets are located on the outer walls. To obtain the actual cargo volume, the volume of the structural materials or "deadwood" must be subtracted.

To check this calculation technique, we have separately calculated the external volume using the target coordinate data supplied by the photogrammetric consultant. The uncertainty in deadwood corrections are examined in a later section of this report.

Targets on a tank are arranged along each side in horizontal rows with vertical separations of about 1.5 m. Sixteen such rows span the approximate 23 m height of each tank. The bottom row of targets is just above the rounded

bottom edge and the top most row is just below the rounded top edge. The row of targets approximately the same height on all sides defines the boundary of a horizontal cross section of the tank. In our calculations, the height of each cross section is taken as the average height of all targets defining the cross section. The error introduced by this approximation should be small since deviations from the average level are small. Of course, on the chines, virtual adjustment in the z (vertical) direction must be accompanied by a virtual adjustment in the y direction (starboard to port).

We calculated the area of a cross section by summing the areas of triangles with vertices $(0,0,z)$, (x_i, y_i, z) , (x_{i+1}, y_{i+1}, z) , where z is the average height of targets for that cross section, i represents a perimeter point (target), $i+1$ is the next adjacent point on the perimeter and $(0,0,z)$ is a point on the vertical axis through the center of the tank. As there are no targets defining the cross sectional areas at the corners of the tank wall, virtual corner points for each cross section were determined by fitting least squares lines to the rows of targets defining a cross section and then solving for the intersections of these lines. The virtual corners were then included in the points defining the cross section. As a test of this point-to-point method, the area defined by the lines joining the virtual corners was also calculated. As a rule, these two values for the area differed only by small amounts. The point-to-point integration value should generally be closer to the true value.

As with the photogrammetrist's method, the volume between two cross sections is assumed to be the product of the average of the two areas and the vertical distance between them. This assumes that any volume effects of the variations in the tank walls between the two levels cancel. However, at the top of the chines there is sharp change with no level of targets to help define the cross sectional area at this height. To get a value for both the area and height at the top of the chines, planes were fit by the method of least squares to the coordinate data, six planes for each tank. Using those planes, a vertical height z was determined for the chine intersection with the vertical sides at each of the four corners of a tank. The average of these four values was taken as the height of the area at the top of the chine. For the El Paso Savannah and El Paso Cove Point the area

corresponding to this height was also determined using the six planes. This, however, is an overall average, and the determined areas closest to the top of the chines should be more predictive of what could be expected at the top of the chines. For the third ship, the El Paso Columbia, a linear extrapolation to the value of height as described above, from the two determined areas directly below was averaged with the linear extrapolation from the two determined areas directly above. For these ships the two methods for chine area determination produce values that are a little different. Fitting the planes to the tank walls allows us to check the conformance of the tank walls to planes, as well as provide another test of the volume calculation. This second volume calculation again uses the cross sectional areas and separations as discussed in the preceding paragraph but the areas are now defined by the planes fitted to the walls. The difference in the volumes obtained using the two methods was less than 0.04% of total volume for each of the five tanks of the Savannah, 0.03% for those of the Cove Point and 0.015% for those of the Columbia.

Comparisons of Volume Determinations

Our volume tables are compared with those of the photogrammetrist in tables 1 through 5 for the tanks of the Savannah, in tables 6 through 10 for the tanks of the Cove Point, and in tables 11 through 15 for those of the Columbia. These tables give the outside volume of the tanks at -160°C only [6]. No deadwood corrections have been made to these volumes. The volume between the bottom of a tank and the first level of targets has been subtracted out, as that part of the volume involves corrections for the bottom survey which we have not made. The temperature adjustments are presumed the same for both methods; so any differences in results cannot be attributed to this factor. The differences between the methods are generally 0.01% or less except for some values of volume toward the bottom of the tanks. The correction used by the photogrammetrist for the rounded tank corners amounts to 1.8 m^3 per tank. This correction is in the form of a 0.08 m^2 subtraction for each cross section. This correction is already accounted for in the volume comparisons for the tanks of the Cove Point and Columbia, but not for the Savannah. Subtracting 1.8 m^3 from each of the NBS total volumes gives the following differences between the two methods for tanks 1-5 of the Savannah, respectively; -0.072 m^3 , $.010 \text{ m}^3$, 0.431 m^3 ,

TABLE 1
 COMPARISON OF VOLUME CALCULATION
 FOR
 TANK 1 - SAVANNAH

HEIGHT	V1(PC)	V2(NBS)	%DIF
.398	0.000	-.000	0.0000
1.238	466.900	466.854	.0098
2.750	1373.200	1373.574	-.0272
4.288	2383.200	2383.283	-.0035
4.981	2867.000	2866.813	.0065
5.828	3469.600	3469.713	-.0033
7.353	4554.600	4555.215	-.0135
8.871	5635.200	5635.904	-.0125
10.388	6715.200	6715.710	-.0076
11.908	7796.700	7797.274	-.0074
13.427	8876.900	8877.756	-.0096
14.947	9957.800	9958.665	-.0087
16.463	11034.900	11036.335	-.0130
17.982	12114.300	12115.802	-.0124
19.502	13194.500	13195.844	-.0102
21.022	14274.300	14275.865	-.0110
22.460	15295.800	15297.672	-.0122

TABLE 2
 COMPARISON OF VOLUME CALCULATION
 FOR
 TANK 2 - SAVANNAH

HEIGHT	V1(PC)	V2(NBS)	%DIF
.390	0.000	-0.000	0.0000
1.257	965.600	965.667	-0.0070
2.756	2725.800	2726.219	-0.0154
4.303	4663.600	4663.480	.0026
4.991	5563.100	5563.757	-0.0118
5.826	6669.400	6669.439	-0.0006
7.346	8681.500	8682.406	-0.0104
8.865	10694.600	10694.683	-0.0008
10.385	12708.400	12708.413	-0.0001
11.904	14718.900	14720.245	-0.0091
13.422	16729.300	16730.257	-0.0057
14.941	18740.900	18741.258	-0.0019
16.458	20748.000	20749.038	-0.0050
17.975	22754.900	22756.143	-0.0055
19.494	24764.600	24765.378	-0.0031
21.014	26774.500	26776.009	-0.0056
22.454	28679.600	28681.390	-0.0062

TABLE 3
 COMPARISON OF VOLUME CALCULATION
 FOR
 TANK 3 - SAVANNAH

HEIGHT	V1(PC)	V2(NBS)	%DIF
.404	0.000	-.000	0.0000
1.236	957.700	957.803	-.0108
2.754	2796.600	2797.321	-.0258
4.280	4764.300	4765.671	-.0288
4.973	5697.600	5698.311	-.0125
5.815	6846.300	6846.944	-.0094
7.333	8917.200	8918.084	-.0099
8.852	10990.700	10990.929	-.0021
10.370	13061.100	13062.371	-.0097
11.890	15135.100	15136.171	-.0071
13.408	17205.600	17207.012	-.0082
14.927	19278.300	19279.185	-.0046
16.445	21348.800	21349.617	-.0038
17.964	23419.500	23420.802	-.0056
19.483	25490.400	25491.559	-.0045
21.002	27560.200	27561.962	-.0064
22.520	29630.000	29631.368	-.0046

TABLE 4
 COMPARISON OF VOLUME CALCULATION
 FOR
 TANK 4 - SAVANNAH

HEIGHT	V1(PC)	V2(NBS)	%DIF
.395	0.000	.000	0.0000
1.251	984.800	984.767	.0034
2.782	2839.700	2839.705	-.0002
4.294	4789.100	4789.106	-.0001
4.988	5723.700	5722.973	.0127
5.832	6874.600	6874.653	-.0008
7.351	8946.800	8947.096	-.0033
8.870	11018.900	11019.349	-.0041
10.385	13085.100	13085.789	-.0053
11.903	15155.700	15155.746	-.0003
13.421	17225.300	17225.288	.0001
14.940	19295.100	19296.009	-.0047
16.456	21361.700	21362.161	-.0022
17.975	23431.100	23431.795	-.0030
19.494	25499.800	25501.160	-.0053
21.008	27563.300	27563.711	-.0015
22.531	29637.900	29639.044	-.0039

TABLE 5
COMPARISON OF VOLUME CALCULATION
FOR

TANK 5 - SAVANNAH

HEIGHT	V1 (PC)	V2 (NBS)	%DIF
.398	0.000	.000	0.0000
1.256	703.400	703.683	-.0402
2.794	2033.200	2033.673	-.0233
4.314	3434.600	3434.653	-.0015
4.992	4087.400	4086.876	.0128
5.816	4891.200	4891.025	.0036
7.335	6373.200	6373.503	-.0047
8.853	7854.600	7855.047	-.0057
10.370	9335.900	9335.438	.0049
11.889	10817.600	10817.268	.0031
13.408	12298.600	12298.512	.0007
14.927	13779.400	13779.380	.0001
16.445	15258.900	15258.973	-.0005
17.963	16738.000	16738.211	-.0013
19.483	18218.800	18219.108	-.0017
20.999	19696.100	19695.965	.0007
22.447	21106.000	21106.482	-.0023

TABLE 6
 COMPARISON OF VOLUME CALCULATION
 FOR
 TANK 1 - COVE POINT

HEIGHT	V1(PC)	V2(NBS)	%DIF
.401	0.000	-.000	0.0000
1.302	501.500	501.463	.0075
2.745	1368.500	1368.512	-.0009
4.277	2375.900	2375.901	-.0000
4.979	2867.000	2866.427	.0200
5.828	3472.300	3471.526	.0223
7.351	4557.900	4557.109	.0173
8.862	5635.400	5634.591	.0144
10.380	6716.500	6715.746	.0112
11.902	7800.000	7799.256	.0095
13.420	8880.500	8879.659	.0095
14.935	9958.300	9957.464	.0084
16.453	11038.700	11037.850	.0077
17.975	12120.800	12119.943	.0071
19.485	13195.200	13194.406	.0060
21.011	14280.700	14279.903	.0056
22.449	15305.500	15304.741	.0050

TABLE 7
 COMPARISON OF VOLUME CALCULATION
 FOR
 TANK 2 - COVE POINT

HEIGHT	V1(PC)	V2(NBS)	%DIF
.399	0.000	.000	0.0000
1.187	875.500	875.496	.0004
2.663	2602.000	2602.015	-.0006
4.249	4581.000	4581.022	-.0005
4.964	5516.100	5516.122	-.0004
5.763	6574.400	6574.434	-.0005
7.281	8586.800	8586.752	.0006
8.802	10602.700	10602.745	-.0004
10.310	12601.300	12601.265	.0003
11.838	14626.100	14626.110	-.0001
13.356	16635.500	16635.522	-.0001
14.877	18650.000	18650.048	-.0003
16.393	20656.400	20656.430	-.0001
17.909	22662.400	22662.411	-.0000
19.426	24668.900	24668.866	.0001
20.946	26679.900	26679.921	-.0001
22.451	28671.300	28671.320	-.0001

TABLE 8
 COMPARISON OF VOLUME CALCULATION
 FOR
 TANK 3 - COVE POINT

HEIGHT	V1 (PC)	V2 (NBS)	%DIF
.427	0.000	.000	0.0000
1.307	1013.900	1013.859	.0041
2.731	2739.400	2739.459	-.0021
4.262	4712.000	4712.059	-.0013
4.977	5674.100	5673.948	.0027
5.832	6840.100	6839.697	.0059
7.351	8910.800	8910.453	.0039
8.865	10974.400	10974.030	.0034
10.387	13050.000	13049.650	.0027
11.905	15121.000	15120.623	.0025
13.422	17189.200	17188.871	.0019
14.941	19261.100	19260.722	.0020
16.457	21327.400	21327.060	.0016
17.975	23396.700	23396.385	.0013
19.494	25466.000	25465.647	.0014
21.011	27534.600	27534.298	.0011
22.450	29498.000	29497.742	.0009

TABLE 9
 COMPARISON OF VOLUME CALCULATION
 FOR
 TANK 4 - COVE POINT

HEIGHT	V1 (PC)	V2 (NBS)	%DIF
.431	0.000	.000	0.0000
1.240	932.600	932.648	-.0051
2.753	2764.900	2764.927	-.0010
4.286	4742.900	4742.920	-.0004
4.981	5679.000	5678.433	.0100
5.832	6838.900	6838.620	.0041
7.351	8911.000	8910.653	.0039
8.866	10977.800	10977.511	.0026
10.386	13050.700	13050.377	.0025
11.902	15118.900	15118.589	.0021
13.422	17191.200	17190.914	.0017
14.939	19260.500	19260.303	.0010
16.460	21334.100	21333.851	.0012
17.975	23399.600	23399.402	.0008
19.492	25466.000	25465.776	.0009
21.013	27541.000	27540.844	.0006
22.445	29494.900	29494.686	.0007

TABLE 10
 COMPARISON OF VOLUME CALCULATION
 FOR
 TANK 5 - COVE POINT

HEIGHT	V1(PC)	V2(NBS)	%DIF
.410	0.000	-.000	0.0000
1.263	698.300	698.304	-.0005
2.740	1973.300	1973.320	-.0010
4.302	3411.100	3411.190	-.0026
4.986	4069.400	4070.047	-.0159
5.841	4903.900	4903.865	.0007
7.365	6390.000	6389.939	.0009
8.882	7868.800	7868.645	.0020
10.403	9351.300	9351.114	.0020
11.917	10827.700	10827.475	.0021
13.438	12309.700	12309.465	.0019
14.954	13787.400	13787.060	.0025
16.474	15268.400	15268.058	.0022
17.990	16744.700	16744.331	.0022
19.509	18224.100	18223.674	.0023
21.029	19705.300	19704.806	.0025
22.467	21107.600	21107.114	.0023

TABLE 11
 COMPARISON OF VOLUME CALCULATION
 FOR
 TANK 1 - COLUMBIA

HEIGHT	V1(PC)	V2(NBS)	%DIF
.401	0.000	.000	0.0000
1.233	462.200	462.222	-.0048
2.698	1339.800	1339.718	.0062
4.259	2363.400	2363.193	.0088
4.973	2862.400	2862.307	.0032
5.808	3457.300	3456.946	.0102
7.323	4536.000	4535.694	.0067
8.822	5603.100	5602.771	.0059
10.366	6702.000	6701.669	.0049
11.884	7782.200	7781.869	.0043
13.401	8860.700	8860.328	.0042
14.915	9937.300	9936.895	.0041
16.437	11019.800	11019.370	.0039
17.952	12096.200	12095.813	.0032
19.466	13171.500	13171.096	.0031
20.984	14250.300	14249.811	.0034
22.473	15308.800	15308.388	.0027

TABLE 12
 COMPARISON OF VOLUME CALCULATION
 FOR
 TANK 2 - COLUMBIA

HEIGHT	V1(PC)	V2(NBS)	%DIF
.392	0.000	-.000	0.0000
1.228	929.900	929.925	-.0027
2.672	2620.900	2620.882	.0007
4.260	4602.900	4602.911	-.0002
4.975	5537.700	5537.904	-.0037
5.822	6659.800	6659.913	-.0017
7.336	8665.700	8665.855	-.0018
8.841	10660.300	10660.368	-.0006
10.374	12690.800	12690.951	-.0012
11.891	14701.600	14701.677	-.0005
13.410	16712.300	16712.427	-.0008
14.929	18723.900	18723.994	-.0005
16.444	20730.100	20730.222	-.0006
17.964	22742.200	22742.309	-.0005
19.482	24750.400	24750.574	-.0007
20.999	26759.000	26759.233	-.0009
22.480	28720.500	28720.732	-.0008

TABLE 13
 COMPARISON OF VOLUME CALCULATION
 FOR
 TANK 3 - COLUMBIA

HEIGHT	V1(PC)	V2(NBS)	%DIF
.398	0.000	-.000	0.0000
1.218	943.400	943.412	-.0013
2.567	2570.900	2570.896	.0001
4.274	4764.600	4764.667	-.0014
4.973	5704.800	5705.393	-.0104
5.788	6817.600	6817.579	.0003
7.306	8889.800	8889.850	-.0006
8.823	10959.600	10959.664	-.0006
10.342	13033.200	13033.301	-.0008
11.864	15109.400	15109.437	-.0002
13.382	17180.700	17180.818	-.0007
14.900	19251.600	19251.711	-.0006
16.416	21317.500	21317.677	-.0008
17.935	23389.100	23389.324	-.0010
19.454	25459.500	25459.704	-.0008
20.972	27527.500	27527.769	-.0010
22.446	29537.300	29537.522	-.0008

TABLE 14
 COMPARISON OF VOLUME CALCULATION
 FOR
 TANK 4 - COLUMBIA

HEIGHT	V1 (PC)	V2 (NBS)	%DIF
.432	0.000	-.000	0.0000
1.231	920.500	920.507	-.0008
2.672	2663.200	2663.255	-.0020
4.309	4771.900	4771.869	.0007
4.986	5683.000	5683.636	-.0112
5.832	6837.600	6837.567	.0005
7.349	8907.800	8907.741	.0007
8.859	10968.700	10968.672	.0003
10.384	13050.700	13050.646	.0004
11.901	15121.300	15121.238	.0004
13.420	17194.000	17193.956	.0003
14.937	19264.200	19264.166	.0002
16.454	21333.200	21333.202	-.0000
17.973	23404.700	23404.714	-.0001
19.491	25474.000	25473.991	.0000
21.010	27546.100	27546.122	-.0001
22.492	29568.400	29568.437	-.0001

TABLE 15
 COMPARISON OF VOLUME CALCULATION
 FOR
 TANK 5 - COLUMBIA

HEIGHT	V1(PC)	V2(NBS)	%DIF
.410	0.000	-.000	0.0000
1.247	685.300	685.311	-.0017
2.741	1974.500	1974.491	.0005
4.310	3420.300	3420.184	.0034
4.987	4071.600	4072.117	-.0127
5.837	4901.600	4901.493	.0022
7.347	6375.600	6375.437	.0026
8.857	7850.100	7849.925	.0022
10.387	9343.000	9342.852	.0016
11.907	10825.600	10825.374	.0021
13.422	12303.900	12303.744	.0013
14.940	13783.700	13783.494	.0015
16.467	15272.500	15272.305	.0013
17.978	16745.800	16745.562	.0014
19.493	18222.900	18222.679	.0012
21.013	19704.600	19704.312	.0015
22.492	21147.600	21147.368	.0011

0.656 m³ and 1.318 m³. The increase in the differences with tank number is considered coincidental. The major differences occur in the volumes adjacent to the chine top because of the difference in the methods used to determine the height and area at the top of the chines. The remaining differences are attributed to round off error.

The largest source of error arising from the volume calculation results from having to estimate the height and area at the chines where there are no targets. We judge that the height should be good to + 5 cm and the area to within + 1 m². These together produce an uncertainty in total volume of + 01%. Other sources of error in these calculations are judged to be negligible.

Target Distribution on Tank

The targets placed on the tanks for photographic reference are uniformly distributed on the tank surfaces. Again, in the vertical direction, the rows or targets are spaced about 1.5 meters apart with the first two rows only about half that distance apart, for a total of sixteen rows; and in the horizontal direction, the spacing between columns of targets is about 3 meters with the two columns at the right edge, left edge and in the middle being 1.5 meters apart. As discussed above, rows or targets at the same nominal height form the boundary of a horizontal cross section, and the height of the cross section is taken to be the average height of these targets. In computing tank volume tables, the photogrammetrist assumes that the targets on the boundary of a horizontal cross section are close enough together to give a good definition of the shape of the cross section, and that the computation of the cross sectional area is unaffected by the any smaller intermediate variations in the tank wall, since the area contributions of these variations tend to cancel. In the same way, he assumes that the effect on the volume of the variations in the tank walls between cross sections also cancel. To test the adequacy of the 3 meter spacing between columns of targets, additional targets were placed on tanks 3, 4 and 5 of the Savannah such that the spacing between columns of targets on these tanks was generally 1.5 m. On the larger tanks (3 or 4), the more dense spacing results in twenty-five columns of targets per side, rather than the fifteen per side of the less dense spacing. Tables 16, 17, and 18 show

the average heights and the areas for the sixteen levels (rows) for tanks 3, 4, and 5, respectively, for both the more and the less dense target spacings.

The area calculation method was as described above. As can be seen, in only one instance is the area difference for the two target densities as large as 0.01%. The volume error at the highest level of targets is: for tank 3, 0.66 m³ larger for the dense survey; for tank 4, 0.41 m³ larger for the dense survey; and for tank 5, 0.27 m³ smaller for the dense survey. These differences are very small. The largest difference, tank 3, is 0.002% of total volume.

The number and placement of targets on the tanks seem adequate from two standpoints. The closer spaced targets used on tanks 3, 4 and 5 yield a difference in total volume over the wider spaced targets of less than 1.0 m³ and the volume calculations that assumed the tank sides to be planes differed from those of the cross sectional method by at most 9 m³ -- this was for tank 3 -- for the other tanks it was 3 m³ or less. So for these tanks, increasing the number of targets would likely yield little results in terms of increased accuracy.

While it is not known exactly how the tank wall deviates from a flat surface between targets 3 m apart, a study of the 1.5 m horizontal spacings for tanks 3, 4 and 5 of the Savannah gave the standard deviations at the midpoint between 3m spacings of 5.7 mm, 4.7 mm and 5.3 mm, respectively. For tanks 1 and 2, the standard deviations for midpoints for 6 to 8 m spacings were 7.1 mm and 6.4 mm, respectively; we expect that these would be larger because of the larger spacings. A study of the vertical spacings for all five tanks gave standard deviations at the midpoint of 3 m spacings in the range of 2.5 mm to 3.2 mm. This would suggest that the deviations between 3 m spacings for tanks 1 and 2 are much like those for tanks 3, 4 and 5. Using a simplified model similar to that used for volume calculations, we estimate that the use of the 3 m spacings over the 1.5 m spacings contributes an uncertainty of + 1.0 m³ for the larger tank volumes. We must point out, however, that the systematic differences shown in tables 16, 17, and 18 indicate that the 3 m spacings do miss tank features that are the same for all or many levels of the tank; i.e., a vertical wrinkle would effect more than one level. Another way of looking at this is to consider as random the

percentage differences between the volume determinations for the 1.5 m spacings and the 3.0 m spacings for tanks 3, 4 and 5. These are, respectively, 0.00223%, 0.00183% and -0.00128%. The standard deviation based on these three values is 0.0018%. The prediction for tanks 1 and 2 of the Savannah and tanks of the other two ships is that the percentage differences would be in the interval $\pm 0.014\%$ [1]. This interval is rather large, but the prediction is based on only three numbers. Since tanks 3, 4 and 5 had the more dense spacings, the uncertainty from target placement for these tanks is taken to be negligible.

References

- [1] Natrella, M. B., 1963. Experimental Statistics. National Bureau of Standards Handbook 91.

Appendix C

Uncertainties Due to Temperature Effects

By

J. D. Siegwarth and J. F. LaBrecque

Uncertainties Due to Temperature Effects

J. D. Siegwarth and J. F. LaBrecque

1. INTRODUCTION

Since the measurements required to provide the volume of an LNG transport tank as a function of height are done at ambient temperature, a significant correction is required to adjust the tank volume to the operating temperature of 110 K. If the tank is not isothermal during the calibration measurements, not only is the temperature from which the correction is made uncertain, but the actual shape of the tank may likewise be altered from the shape at operating temperature. The portion of the tank in contact with the liquid cargo can be expected to be nearly isothermal except in the event that the contents stratify.

2. VARIOUS TEMPERATURE RELATED UNCERTAINTIES

Below is a discussion of the various ways temperature contributed to the volume uncertainty of the prismatic free standing tanks. An estimate of the maximum error is included in each case.

2.1 Uncertainty of the thermal expansion coefficient of the aluminum.

The uncertainty in the thermal expansion coefficient for 5083 aluminum is estimated to be $\pm 3\%$ [1]. The tanks are surveyed in the temperature range of 5 to 25°C and the volume is adjusted to -160°C. For this adjustment, the $\pm 3\%$ uncertainty in the expansion coefficient translates into a volume uncertainty of $\pm 0.03\%$.

2.2 Uncertainty contributed by the interior wall temperatures.

A small systematic error in tank volume arises due to the temperature distribution in the tank structure at the time of the photogrammetric survey. Measurements of the temperature of the outer walls of the tanks suggest they could be relatively isothermal though the degree of uniformity certainly depends on the wind, cloud cover and rate of change of ambient temperature. The inner quadrant

walls of the tank, however, can be as much as 8°C warmer than the outer walls because the temperature of the large volume of air within the tank lags the outside temperature. This difference will vary with the difference between day and night time temperatures and the rate of change of the external temperature. The higher temperature of the internal walls should cause a bulge in the side walls of the tank. If the quadrant walls are 8°C warmer, the outer walls should bulge 3.4 mm on the largest tanks assuming no constraining forces reduce this strain. The temperature distribution on the quadrant walls of tank 4 of shipset #3 were measured at the time of the survey to estimate this effect on volume.

The internal temperatures gradually increased from values within 1°C of the outside wall temperature at the bottom of the tank to 8°C warmer at the top. Measurements of the top and bottom outside temperatures on a number of points on the curved edge of the tank on tank 5 of the third shipset showed that, on that night, top and bottom temperatures were the same to about $\pm 1^\circ\text{C}$.

To estimate the effect of the internal quadrant wall temperature on volume, assume that the bulge in a wall is an isosceles triangle with an amplitude of zero at the bottom and 3.4 mm at the top. The volume, ΔV , added for all four sides is then

$$\begin{aligned}\Delta V &= \frac{.0034}{2} \times 22.9 \times \frac{36.6}{2} \times 4 \\ &= 2.85 \text{ m}^3,\end{aligned}$$

where 22.9 m and 36.6 m are the height and width of the tank respectively.

Hence, the actual volume of the tank is about 0.01% less than the volume given by the calibration. The tank height is similarly increased during the survey resulting in an additional decrease in volume of a similar amount but this does not affect the liquid content as determined from tank tables.

The magnitude of this systematic error should be the worst case estimate since the top of the tank must constrain the sides at the quadrant walls so they cannot move out. Also, the internal wall temperatures do decrease toward the outside wall.

2.3 Uncertainty contribution from tank wall temperature measurements.

An error of 1 C in the measurement of tank wall temperature generates an 0.007% error in tank volume assuming a temperature coefficient of 23×10^{-6} K.

During the time period of the photography, we noted a tank wall temperature change of 3°C maximum. Generally, the temperature change was much smaller over the course of the photography. Temperatures of the top plates were found to be as much as 1°C warmer. We estimate the temperature uncertainty of the tank to be $\pm 2^\circ\text{C}$ maximum so the tank temperature uncertainty at the time of the photogrammetric survey results in a volume uncertainty of $\pm 0.014\%$.

2.4 Error from calibration tape temperature differences.

The temperature of the NBS calibration tapes differed as much as -5°C from the tank wall temperature. The photogrammetric calibration tapes like the NBS tapes were suspended in the air away from the tank walls thus, may have differed from the tank wall temperature by -5°C also. The iron-36% nickel tapes used by NBS were corrected to the air temperature, though the correction is negligible, while the photogrammetrists' tapes were corrected to tank temperature. Assuming the photogrammetrists' tapes were steel, we assume stainless steel, with a coefficient of 16×10^{-6} per $^\circ\text{C}$ the tank volume would be over estimated by 0.024% if the tapes were indeed 5°C cooler.

3. DISCUSSION

Though it is possible to reduce the magnitude of the volume uncertainties caused by temperature uncertainties, it is not easy to do so in most cases. The volume uncertainty resulting from the coefficient of expansion of aluminum (section 2.1) could be reduced by carefully measuring the thermal contraction of samples of the aluminum plates comprising the tank walls and structure. Reducing the volume uncertainties due to tank temperature distribution and uncertainty (section 2.2 and 2.3) is difficult under the conditions of the measurement. The most stable conditions could probably be obtained on a cloudy windless night and around the time the tank reached the minimum temperature. A vigorous circulation

of air through the interior to bring the inside temperatures down to the exterior temperature is desirable.

The elimination of the three contributions discussed above, generally, will increase tank calibration costs. The uncertainty in volume resulting from tape temperature uncertainty can be eliminated at little additional cost by using a low thermal expansion alloy like iron-36% nickel for the calibration tapes rather than stainless steel.

4. REFERENCES

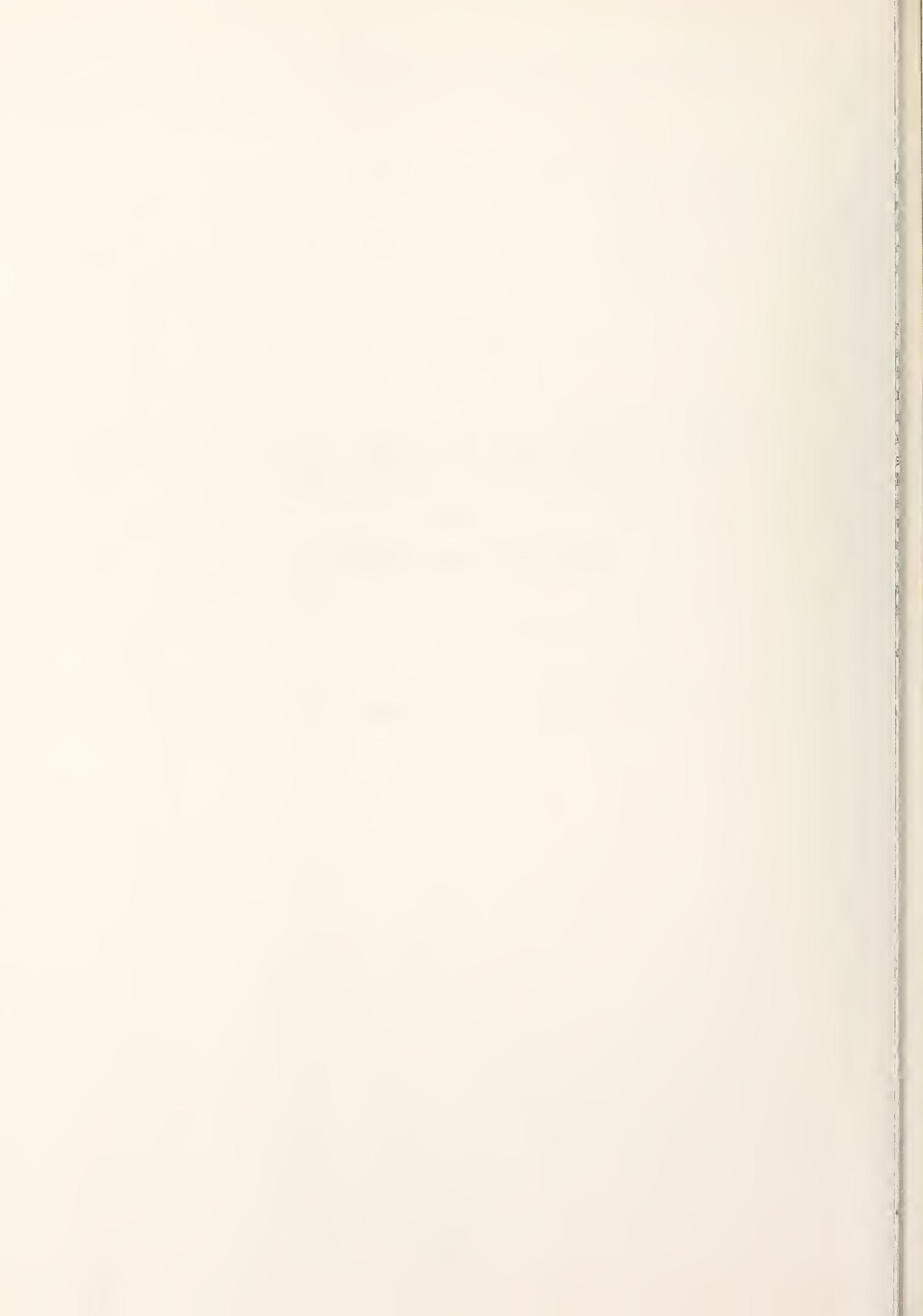
[1] Mann, D. B., Editor, 1977. LNG Materials and Fluids. Thermophysical Properties Division, National Bureau of Standards, Boulder, Colorado.

Appendix D

A Laser-Based Calibration of Tank #3
on the
LNG Tanker El Paso Columbia

By

W. C. Haight, F. Scire, R. G. Hartsock, and R. J. Hocken



A Laser-Based Calibration of Tank #3
on the LNG Tanker El Paso Columbia

This Appendix presents the results of a dimensional calibration of Tank #3 on the LNG tanker Columbia conducted by NBS personnel while the tank was in storage at the construction yard in Mobile, Alabama. This calibration is completely independent, both metrologically and computationally, of any other surveys conducted on this same tank.

The NBS measurement method is similar to the technique described in references [1] and [2] for membrane-type LNG tanks, with the exception being that all measurements were made from the tank exterior rather than the interior. All reference gage points were established by laser planes just outside the tank surfaces, and marked on aluminum plates attached to the exterior tank surface with high-strength epoxy. The dimensions of the laser plane solid were measured with an invar tape, and angles between planes were measured with a first-order theodolite. Offsets from the laser planes to the tank walls were measured on a 3 x 3 m grid, that is, on every other photogrammetric target whenever possible. An ultrasonic thickness gage was used to record the wall thickness at every offset point. The survey was conducted at night to minimize the effects of non-uniform temperature distributions on the tank surfaces caused by solar heating.

The following information is provided for this tank:

- a. A calibration report providing the measurement conditions and error estimate;
- b. Two summary main gaging tables showing the tank volume as a function of gage height at selected intervals;
 - ° Table 1 presents the tank interior volume as a function of gage height, exclusive of internal structural deadwood,
 - ° Table 2 presents the tank exterior volume as a function of gage height, exclusive of internal structural deadwood.
- c. A comparison of the NBS exterior main gaging table at selected intervals to the gaging table provided by the calibration contractor.

U.S. DEPARTMENT OF COMMERCE
NATIONAL BUREAU OF STANDARDS
WASHINGTON, D.C. 20234

REPORT OF CALIBRATION

For: Tank #3 on the LNG Tanker
El Paso Columbia

Requested by: El Paso Marine Company
2919 Allen Parkway
P.O. Box 1592
Houston, TX 77001

The following tables have been calculated from dimensional measurements on tank number 3 of the liquified natural gas tanker El Paso Columbia while the tank was in storage at the Kaiser Aluminum Company construction yard in Mobile, Alabama. These tables represent the volume of a liquid enclosed in the tank as a function of the height of the liquid surface, measured along a straight line, fixed with respect to the tank. This line is defined as being located at the longitudinal center line of the tank's capacitance gage. Both the measurement method and the computational algorithms are outlined in the paper "Multiple Redundancy in the Measurement of Large Structures", Annals of the International Institution of Production Engineering Research (CIRP), Volume 27/1, 1978.

All measurements relating to this survey were made from the tank exterior except those needed to locate the capacitance gage. The tank wall thickness at each survey point was measured with an ultrasonic thickness gage and these values are used to report the volume relative to the tank interior surfaces as a function of gage height in Table 1. Table 2 presents the corresponding relationship relative to the tank exterior surfaces. No correction has been made in either case for the volume occupied by internal structures (deadwood).

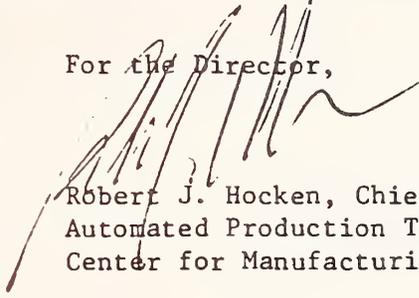
The tank was measured empty while at an average temperature of 13.5°Celsius. The tabulated volumes and the error estimates apply to the tank under these conditions.

The measurement method used includes geometrically redundant cross checks which allow assessment of the random error in the measurement process. For this tank, the total volume, excluding the vapor dome, was

- ° Interior volume = 30821.5 m³
- ° Exterior volume = 30929.5 m³

The uncertainty of these values is 3.1 m^3 (0.01% of total volume) at the three standard deviation limit of random error. Including an analysis of probable systematics by adding the absolute magnitude of the error sources, we estimate that the total uncertainty, at the 99% confidence level, is $\pm 0.05\%$ of the total volume. No estimates of the errors in the individual table entries are included, since without an estimate of the height error introduced by the liquid level gage such estimates of necessity would be incomplete.

For the Director,



Robert J. Hocken, Chief
Automated Production Technology Division
Center for Manufacturing Engineering

Date: March 5-8, 1979

TABLE 1

EL PASO COLUMBIA

CARGO TANK NO. 3, HULL 2266

MAIN VOLUME VS. HEIGHT TABLE, INTERIOR VOLUME

TANK TEMPERATURE: 13.5°C

GAGE HEIGHT (meters)	VOLUME (cubic meters)
.000	8.3
.050	64.1
.100	120.1
.200	232.4
.300	345.3
.400	458.7
.500	572.6
1.000	1149.7
2.000	2342.4
3.000	3586.4
4.000	4881.8
5.000	6228.4
6.000	7599.2
7.000	8970.0
8.000	10340.8
9.000	11711.6
10.000	13082.3
11.000	14453.0
12.000	15823.7
13.000	17194.4
14.000	18565.1
15.000	19935.7
16.000	21306.4
17.000	22677.0
18.000	24047.6
19.000	25418.1
20.000	26788.7
21.000	28159.2
22.000	29529.7
22.500	30215.0
23.000	30821.5

TOTAL INTERIOR VOLUME OF TANK = 30821.5 cubic meters

TABLE 2

EL PASO COLUMBIA

CARGO TANK NO. 3, HULL 2266

MAIN VOLUME VS. HEIGHT TABLE, EXTERIOR VOLUME

TANK TEMPERATURE: 13.5°C

GAGE HEIGHT (meters)	VOLUME (cubic meters)
.000	32.5
.050	88.5
.100	144.6
.200	257.3
.300	370.5
.400	484.2
.500	598.4
1.000	1177.2
2.000	2373.4
3.000	3620.8
4.000	4919.7
5.000	6269.9
6.000	7643.8
7.000	9017.6
8.000	10391.4
9.000	11765.1
10.000	13138.7
11.000	14512.3
12.000	15885.8
13.000	17259.2
14.000	18632.5
15.000	20005.7
16.000	21378.9
17.000	22752.0
18.000	24125.0
19.000	25497.9
20.000	26870.8
21.000	28243.6
22.000	29616.3
22.500	30302.6
23.000	30929.5

TOTAL EXTERIOR VOLUME OF TANK = 30929.5 cubic meters

Comparison of the NBS and
Photogrammetric Exterior Calibrations
of Tank 3 of the Columbia

Table 3 shows the photogrammetrically-determined external tank volume as a function of height compared to the NBS volume measured by the laser plane survey. The tables have been adjusted so the volume is zero at the zero of the level gage, which is the point on the internal floor of the tank immediately under the gage. This eliminates the tank bottom profile. Since the photogrammetric coordinate origin was at the inside surface of the lowest point of the tank, an additional 6.37 m^3 has been added to the photogrammetric volume in the vertical wall region. This correction drops linearly to zero from $Z=5$ to $Z=0$ m, which is the chine region. A value of 29.08 m^3 is added to all the photogrammetric volume table entries since that much volume was removed to correct for undulations of the bottom. With these adjustments, the bottom is now a horizontal gravitational plane through the zero of the gage and at the time the tank yard bottom survey was done.

The volume table derived from the laser survey is referenced to a horizontal plane containing the same zero point by subtracting 32.5 m^3 from each of the volume readings in table 2 of the calibration report at the end of this Appendix. This plane is, however, the best fit plane to the bottom survey rather than a gravitational plane. Neither plane offers advantages for the volume calculation since the orientation of the tank in the ship relative to the surveys is the one needed. For small relative tilts of these planes with respect to each other, a few centimeters makes no detectable error in the tank volume when the bottom is subtracted out, but could if the bottom is left in. Thus the two survey methods are best compared with the bottom effects removed.

The photogrammetric volume versus height tables are derived from planes fit to each level of targets as described in Appendix B and the volume versus external height data supplied by the photogrammetrist is given at each target level in table 3 for 16.2°C . The laser plane volume versus height table is given at meter intervals and since the horizontal cross sectional areas at each level are defined by planes fit to each surface of the tank, the laser measurements are

Table 3
Volume Versus Height Table
Columbia, Tank #3

Height (m)	Volume Laser Planes (m ³)	Volume Photogrammetry (m ³)
0.0	0.0	0.0
0.398	449.5	448.7
1.218	1401.3	1399.8
2.567	3042.2	3041.5
4.274	5252.7	5251.8
4.973		
5.788	7320.9	7320.0
7.306	9406.6	9406.8
8.823	11490.8	11491.1
10.342	13577.5	13579.2
11.864	15668.3	15670.0
13.382	17753.4	17755.8
14.900	19838.3	19841.3
16.415	21918.9	21921.7
17.935	24006.2	24007.8
19.454	26091.9	26092.7
20.971	28174.8	28175.2
22.445	30198.4	30199.1

easier to extrapolate to the photogrammetrists levels than vice-versa. The laser-determined volume from Z=0 to 4.8 m given in table 3 is:

$$V(Z) = 1119Z + 25.7Z^2 + 0.15Z \text{ (m}^3\text{)}$$

and from Z=5.2 to 22.5 m as

$$V(Z) = -163.26 + 1374.314Z - 0.0368Z^2 + 0.17Z - .09 \text{ (m}^3\text{)}$$

The last term of the first equation and the last two terms of the second convert the volumes at 13.5°C to the volumes at 16.2°C so the photogrammetric and laser surveys can be compared with the tank at the same temperature. A gap between Z values of about 4.8 to 5.2 m exists where neither expression is correct because the wall actually rounds into the chine with a radius of about 15 cm rather than meeting it at a sharp angle.

The two calibrations shown in table 3 agree in volume to within 2 m³ over the height of the tank except for the 13 to 17 m range where the disagreement is less than 3 m³.

If the tank bottom shape is included, then 8.3 m³ must be added to the laser volumes given in table 3. The photogrammetrists volume with the bottom included is 30,198.2 m³ at 22.445 m height. This is 8.5 m³ or about 0.03% less than the NBS value. This is well within the estimated uncertainty of both calibrations. This difference probably arises from differences in the zero location, approximately 1 m³/mm and the different choices of reference plane which when coupled with the offset of the level gage, horizontally adds 1.2 m³ of difference per centimeter of tilt. The best fit plane was used as the level plane for the NBS calibration and the gravitational plane was used for the photogrammetric calibration. The offset from the coordinate origin of the best fit plane supplied the bottom correction for former calibration while numerical integration supplied the correction for the latter. The orientation of the tanks to the level ship is the information needed to finally determine the volume to be included in the tank bottom.

The close agreement between the volume tables calculated by the two independent

surveys indicates that the uncertainty estimates given for the two surveys, +0.05% of total volume for the laser method and 0.1% for the photogrammetric method, are conservative.

REFERENCES

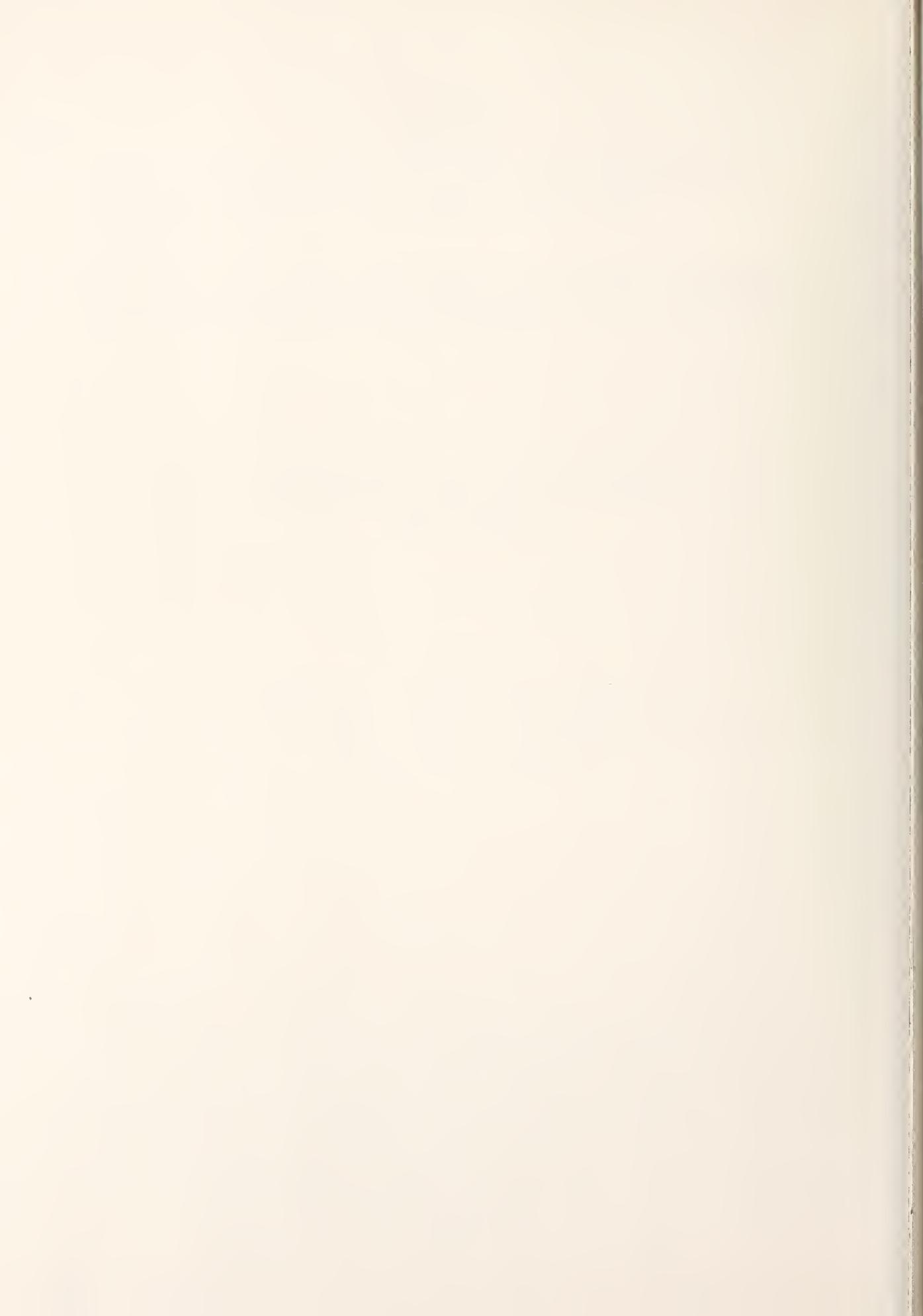
- [1] Hocken, R.J. and Haight, W.C., 1978; "Multiple Redundancy in the Measurement of Large Structures", Annals of the International Institution of Production Engineering Research (CIRP), Volume 27, p. 1.
- [2] Haight, W.C., R.J. Hocken, B.R. Borchardt, C.L. Carroll, R.G. Hartsock, C.P. Reeve, F.E. Scire, and R.C. Veale, 1981; "Estimated Accuracy of Calibration of Some Membrane-Type LNG Transport Tanks", NBSIR 80-2141.

Appendix E

Deformation Measurements on Freestanding
LNG Cargo Tanks

By

W. C. Haight, B. Borchardt, R. G. Hartsock,
R. C. Veale, and R. J. Hocken



NBSIR 81-2332

**DEFORMATION MEASUREMENTS ON
FREESTANDING LNG CARGO TANKS**

W. C. Haight, B. Borchardt, R. G. Hartsock,
R. C. Veale and R. J. Hocken

U.S. DEPARTMENT OF COMMERCE
National Bureau of Standards
National Engineering Laboratory
Center for Manufacturing Engineering
Automated Production Technology Division
Washington, DC 20234

October 1981

U.S. DEPARTMENT OF COMMERCE
National Bureau of Standards

Table of Contents

Page

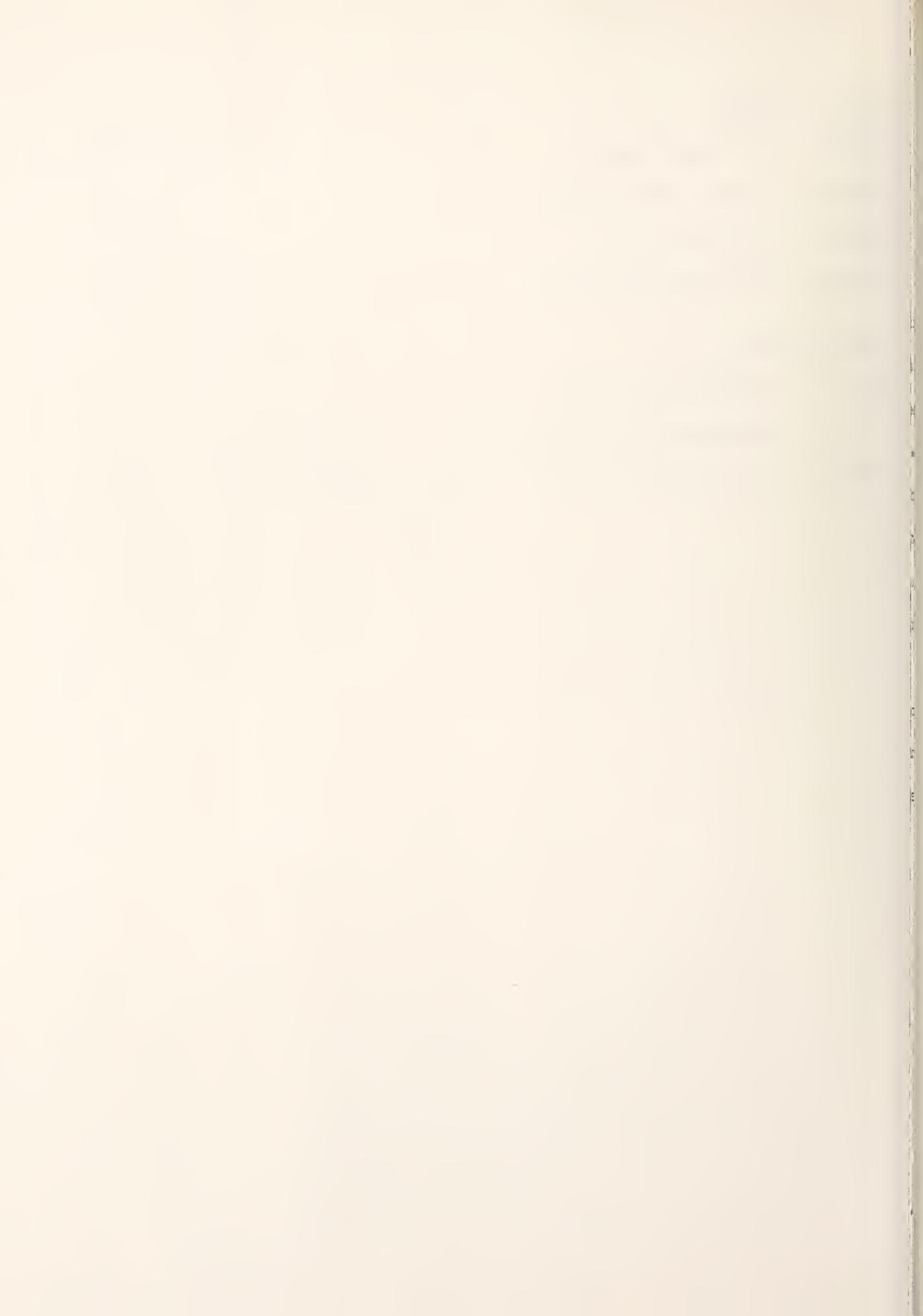
Abstract	1
I. Introduction	2
II. The Measurement Method	5
II.1 Top Survey	5
II.2 Bottom Survey	9
III. Data Analysis	12
III.1 General Comments	12
III.2 Tank Top Data	12
III.3 Tank Bottom Data	13
III.4 Calculation of Distortion	13
IV. Error Analysis	14
V. Results and Conclusions	17
VI. Tables of Survey Data	20
VII. References	39

List of Figures

	<u>Page</u>
Figure 1 - LNG Tank Schematic	4
Figure 2 - Laser Level Schematic	6
Figure 3 - LNG Tank Top Plan	7
Figure 4 - LNG Tank Bottom Plan	10

List of Tables

Table 1 - Random Error Sources	14
Table 2 - Temperature Profile Summaries	16
Table 3 - RMS Distortion Results	19



Deformation Measurements on Freestanding
LNG Cargo Tanks

W. C. Haight, B. Borchardt, R. G. Hartsock
R. C. Veale, and R. J. Hocken

ABSTRACT

Large Liquid Natural Gas (LNG) cargo tanks in a variety of configurations are presently under construction worldwide. Metrologists are being called upon to measure their capacity, their deformation under load, and their mechanical deformation due to handling after calibration. In this paper, we present the results of a series of measurements made on aluminum tanks to determine the extent of permanent distortion caused by loading them into a ship with a large crane. These measurements are intended to be used to determine the validity of land-based photogrammetric calibrations conducted prior to installation of the tanks in the ships.

It is shown that the permanent tank deformation is insignificant to the level of accuracy of the measurement method used, and that the volumetric change can be no more than 0.02% of the total tank volume when the technique described herein is employed.

I. Introduction

Measurement of LNG cargo volume determines one of three essential quantities upon which the dollar value of LNG shipments is based, the other two being LNG composition and density. The volume of a shipboard cargo is typically determined from a measurement of the liquid-gas interface level relative to the tank bottom in each tank. This measurement, in conjunction with a prior determination of the tank size and shape can be used to compute a liquid volume at the time of gaging.

Metrologists are being challenged by the LNG industry to develop a variety of measurement techniques for parameters affecting total cargo volume. The most fundamental of these, tank size and shape, has been studied for certain container types and reported by Hocken and Haight [1] and by Jelffs [2]. The rising price of LNG is motivating a further extension of such measurement accuracy to parts in 10^5 over distances of 30 meters and beyond.

A second study area is the effect of cryogenic temperatures on container size and shape. Since methane liquifies at -162°C , this effect can be substantial. The present literature is limited to physical property data for various container materials and fluids at cryogenic temperatures [3] but no field measurements of tank dimensional changes at cryogenic temperature are known to have been made.

A third area is the hydrostatic deformation of tanks under the load of their cargo. Even though the density of liquid methane is approximately 0.5 g/cm^3 , the average volume of $25,000 \text{ m}^3$ per tank can lead to potentially significant distortions that may introduce errors in gaging tables based on empty tank calibrations. This effect has been investigated by Haight et. al. for large freestanding prismatic tanks and reported in reference [4].

The area of study for this paper is distortion of freestanding prismatic tanks due to a lifting procedure used to place them in a ship after construction. The ship under study contained 5 cargo tanks, with a typical tank shown schematically in Figure 1. They are constructed from aluminum plate up to 25 mm thick. All tank structural support is provided by a complex structure of internal beams, and when installed in the ship the tank is uniformly supported on wood blocks at its base and is clamped to the ship's deck at the top to prevent movement. Insulation is provided by a polyurethane foam, sprayed directly onto the inner hull of the ship, and covered with layers of fiberglass.

When tank construction is completed on land, the ship's deck plates are removed and the tanks are lifted into the ship's hull with a large crane. All lifting is along the longitudinal centering of the tank using multiple hydraulically equalized cables, with lifting hooks attached to brackets on the tank top.

Primary tank calibrations are done photogrammetrically while the tanks are in a storage yard prior to loading into the ship. It is the desire of the sponsor to know if the photogrammetric calibrations remain valid after the tanks have been loaded into the ship and are resting on a base other than the one on which they were calibrated. To meet this end, two sets of measurements have been made by NBS. One set is made when the tanks are in the storage yard in the same position in which they were photographed. The second set is a repeat of the first set but is made after tank loading into the ship is complete. A comparison of the two data sets yields an estimate of the permanent distortion due to the loading process.

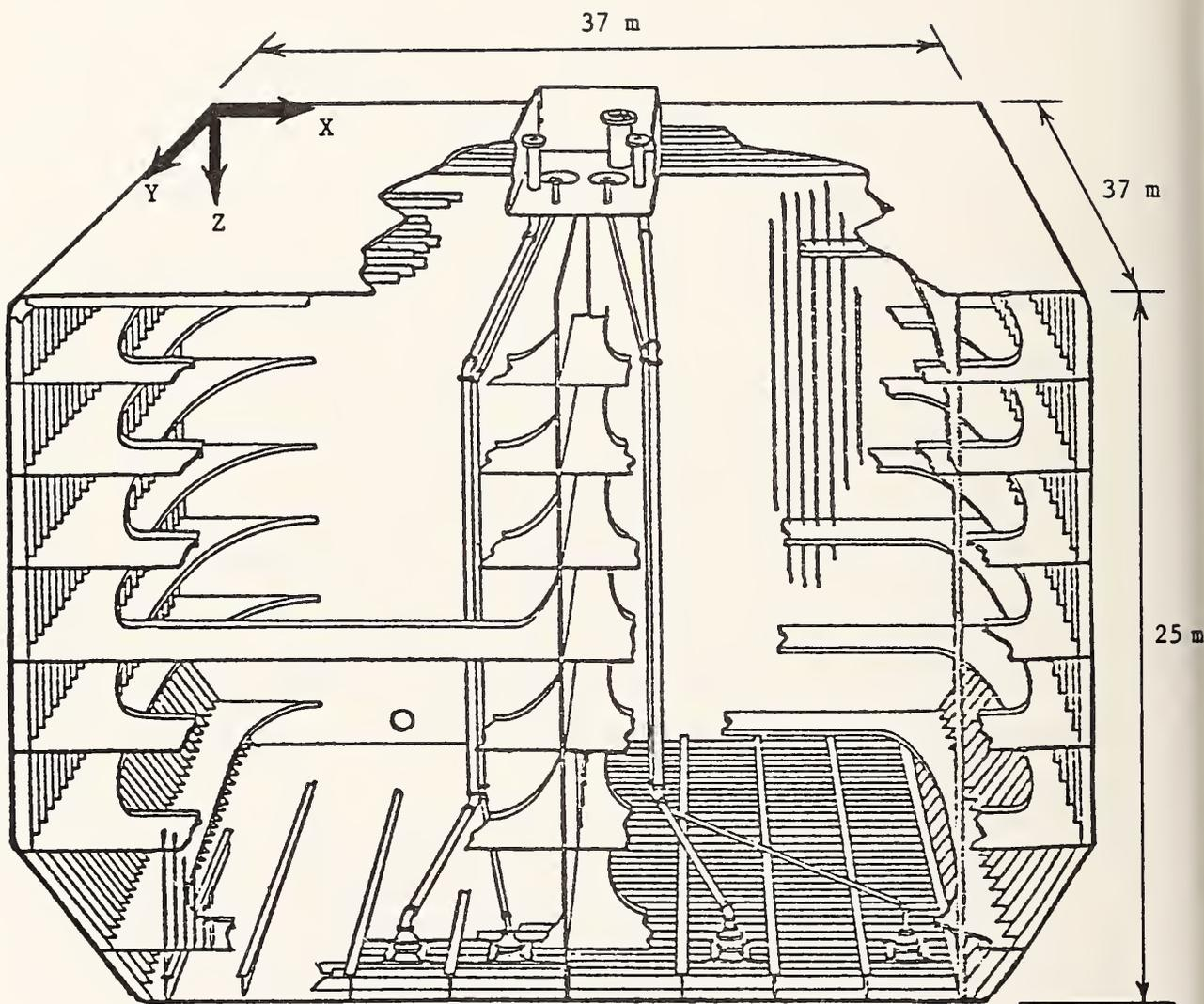


Figure 1 - A typical LNG tank of the freestanding prismatic type. The tank is internally divided into quadrants and is uniformly supported on the bottom while in the ship. The coordinate system used to report the measurement data is shown here. (View from Aft)

II. The Measurement Method

In order to characterize permanent distortion due to lifting the free-standing LNG cargo tanks, the following technique is used. Two "flatness" surveys are conducted on each tank, one on the tank exterior top and one on the tank interior bottom. Each survey is conducted both before and after the tank is loaded into the ship's hull.

The flatness surveys utilize a rotating laser, schematized in Figure 2, to define a plane flat to ± 10 sec of arc and approximately parallel to the tank surface. This laser has a self leveling feature that permits the plane to be established perpendicular to the earth's gravitational field. For the surveys reported herein, the laser is always allowed to self-level after initial setup, and is then locked to insure that the reference plane remains fixed throughout the survey. Offsets from this swept plane are measured to the actual tank surface using a beam seeking laser rod. These commercially available rods have been refitted with higher accuracy scales, kinematic base plates, and a circular bubble level to insure the rod is perpendicular to the survey plane. The laser rod contains an active detector that searches for the laser beam, averages a large number of readings, and then locks so a reading can be taken. The offset measurements are made at a large number of points on a uniform two-dimensional grid to fully characterize the contours of the surface being surveyed.

II.1 Top Survey

The top survey details will be presented first. A grid approximately 3 m x 3 m (actually 10 ft x 10 ft) is marked off on the tank top by placing small aluminum markers around the tank perimeter at the grid interval.

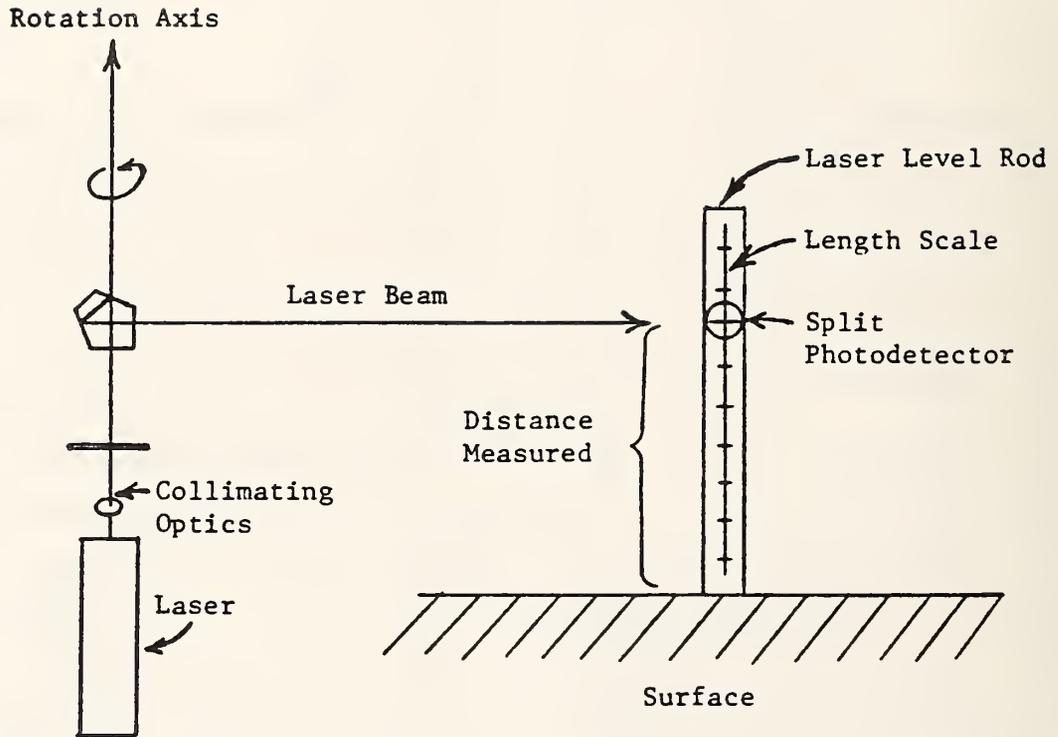


Figure 2 - Schematic of laser level with beam seeking laser rod. The rotating pentaprism causes the beam to be swept in a plane. Manufacturer's specifications are ± 10 seconds of arc flatness. Resolution of rod is 0.1 mm.

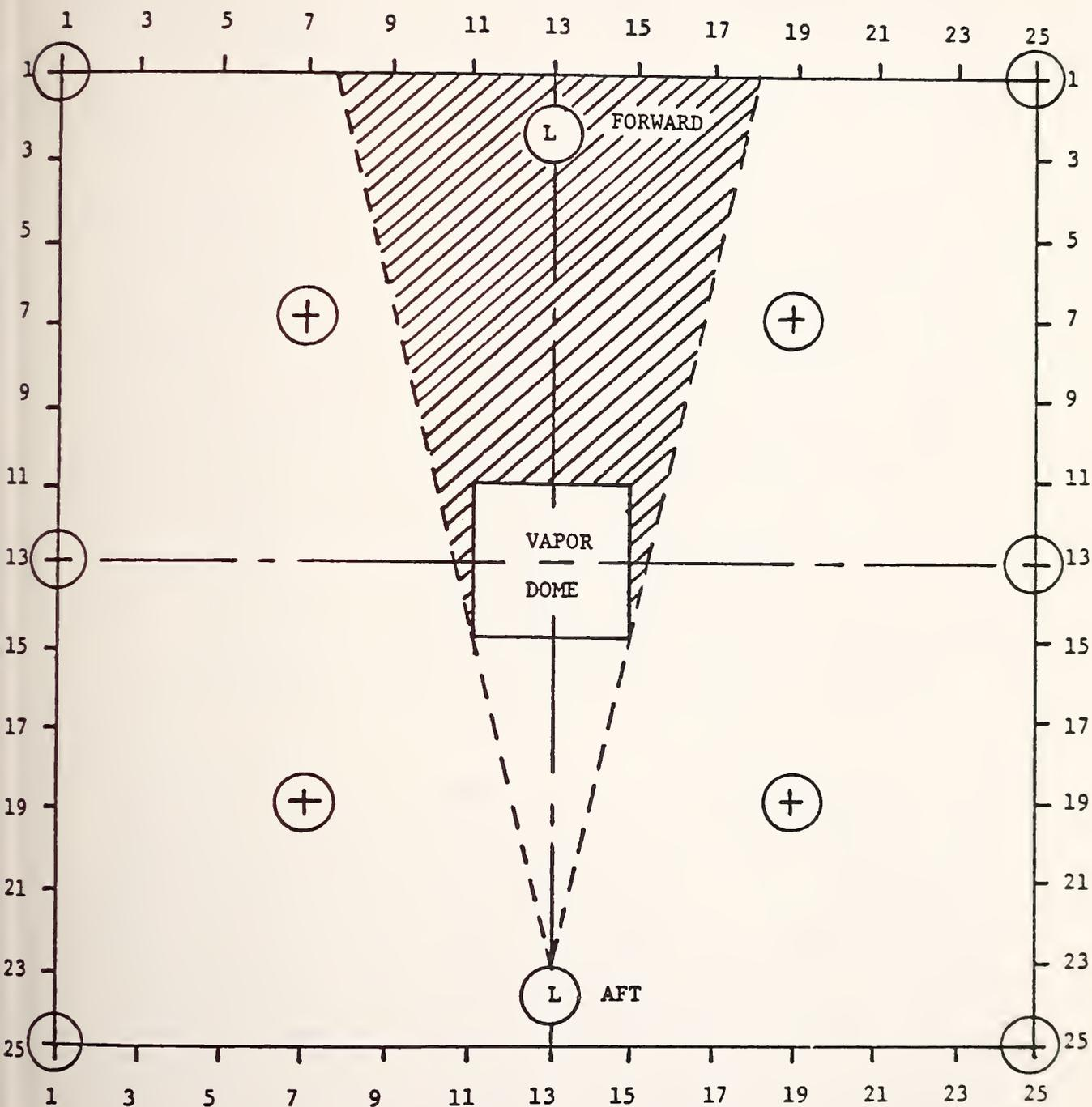


Figure 3 - Top plan of a typical LNG tank showing grid point definitions. \odot L represents laser set-up points and \oplus represents tie-in points. The shaded area is not visible from the aft laser set-up, but is instead measured from the forward laser set-up. One grid unit equals approx. 1.5m (5 feet).

This is shown in detail in Figure 3. Markers are placed at every other one of the photogrammetric targets along the tank edge so the top survey can be referenced to an independent exterior photogrammetric survey. The grid is measured from tank centerlines, since not all tanks are rectangular in plan.

A uniform grid spacing is chosen since the tank is constructed from large aluminum plates braced internally by a cross section of beams. The plate size and support spacing lead to periodic variations in the top profile due to welding the various members together. The uniform 3 m grid spacing avoids the periodicity of these supports, with grid point positions sometimes lying on high ridges over a beam, dips between beams, or at various intermediate points. (Transverse beams are spaced at 0.65 m, longitudinal beams are spaced at 3.66 m and top plates are half the length of the tank long by approximately 3.60 m wide.)

No point on the surface exists from which all other points are visible because of the rectangular vapor dome in the center of the tank. To survey the grid points in the laser shadow, we chose to make two laser set-ups, one on the aft lifting bracket and one on the forward lifting bracket. In addition, 10 points on the tank top were carefully marked (see Figure 3) so that they could be included in both the aft and forward surveys. The aft survey is conducted first, and includes all visible grid points and the 10 tie-in points. The laser is then moved to the forward set-up point and all remaining grid points are surveyed and the 10 tie-in points are included. These tie-in points are used in the analysis to reference the entire tank top to a single plane.

Characterizing the thermal profile of the tank top during the survey presents a problem. When the tanks are in the storage yard, top

surveys are conducted at night when the tanks are in a near isothermal state. When the tanks are loaded into the ship, top surveys must be conducted immediately after loading since insulation on the tank top is installed within a few hours after loading is complete. This survey is often conducted in direct sunlight with surface temperatures as high as 48 °C. A temperature profile on a 5 x 5 point grid over the entire tank top was recorded first while the tank was in the storage yard, and was then repeated at the start of the in-ship survey and again when the laser was moved from the aft to the forward set-up point during the in-ship survey. Since the tank walls were not accessible after the tanks were loaded into the ship, no temperature readings were taken there, even though gradients in the side walls could distort the top non-uniformly. The results of these thermal profiles and the thermal distortion error introduced into the flatness surveys will be discussed in Section IV.

II.2 Bottom Survey

The bottom survey is conducted in a manner similar to the top, but is complicated by the fact that the tank is divided into quadrants with a longitudinal liquid tight bulkhead and a transverse swash bulkhead. It is further complicated by the fact that floor beams up to 1.4 m high are present. A schematic of the tank bottom is shown in Figure 4. The method used is as follows: Four separate flatness surveys are conducted, one in each tank quadrant, using a nominal 2 m x 2 m grid spacing. These surveys may be done on four different days if necessary. The laser is mounted on the top flange of a floor beam and the intersection of the laser plane with the wall beam flanges is marked at the four

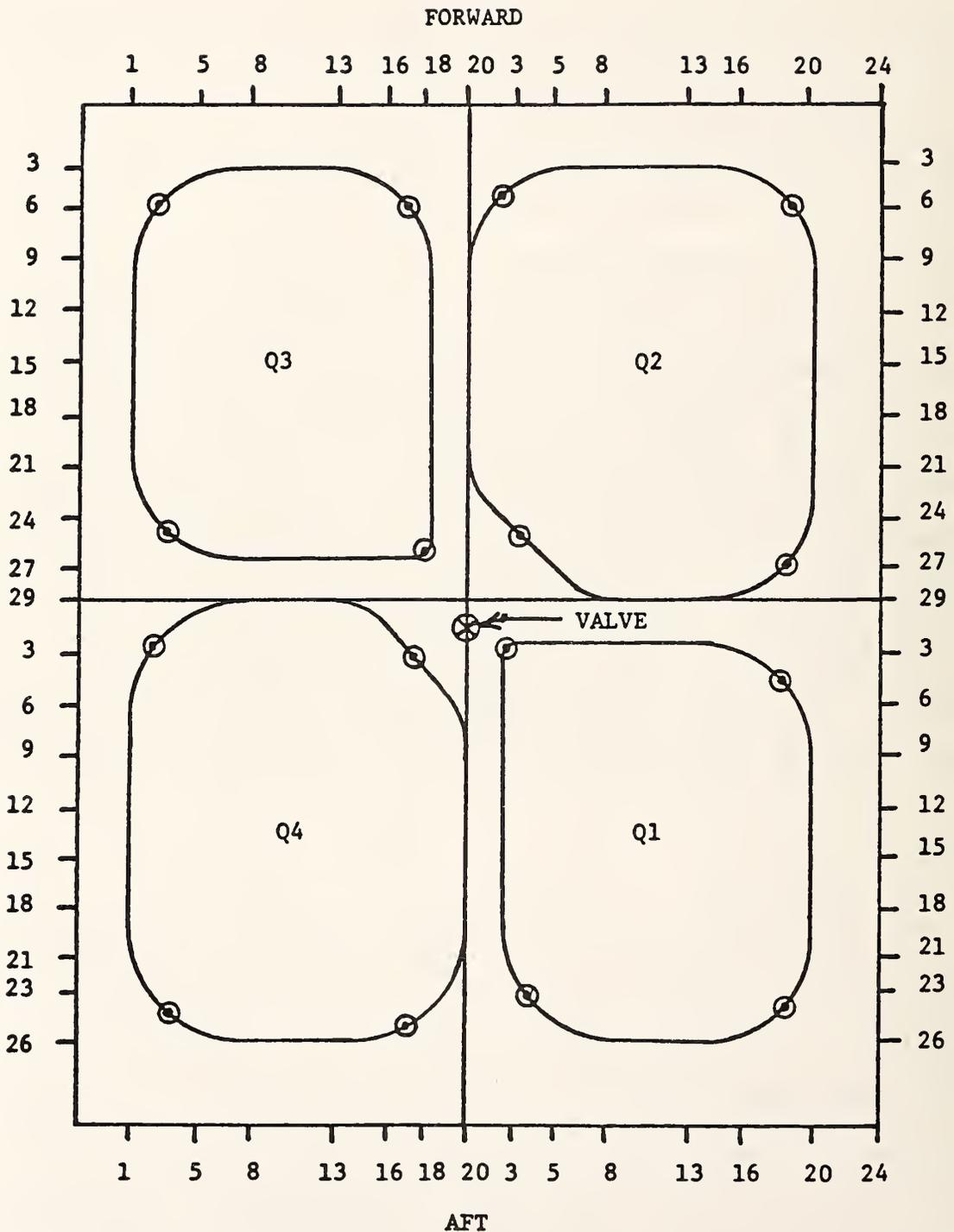


Figure 4 - Bottom plan of a typical LNG tank showing grid point definitions. Points marked \odot are water tube tie-in points. Grid numbers are based on small floor and wall beam locations. One grid unit equals approx. 0.6 m (2 feet).

extremes of each quadrant. The laser level is locked after initially allowing the unit to self-level. Offsets from the laser plane to the tank floor are measured with the beam seeking level rod in the usual manner. Extreme care is taken to insure the rod is perpendicular to the laser plane since the offset measurements are approximately 1.9 m in length and the chance of a significant cosine error is substantial. A circular bubble level on the rod is used for this purpose.

Once the four quadrant surveys are complete, water tubes are used as a differential level to define a level plane throughout the tank. Then, short offset measurements from laser plane locations in each quadrant can be used to reference the four quadrant surveys to a single surface. The water tube technique involves establishing a reference point in one quadrant by keeping one end of the tube fixed at that point. The other end of the tube is then moved to 15 additional points in the appropriate quadrants. The approximate location of these points is shown in Figure 4. At each point, a mark is made at the same height as the reference mark, based on the water level. It is important for this procedure to be completed as quickly as possible on all 15 points. Access to various quadrants is through a valve in the liquid tight bulkhead and through manways in the swash bulkhead. The water tubes used for this survey are made from tygon and have aluminum scales attached to each end for clamping to the tank beams.

Finally, a number of angular measurements were made on the tank interiors in the event that the top and bottom survey data showed significant distortions. These are not reported, since they add no new information to the tank distortion profiles.

III. Data Analysis

III.1 General Comments

Field data for any tank surface consists of a set of deviation measurements from a plane, typically a gravitational plane defined by a rotating laser or by a set of water tube readings. Since the tank surface is likely to be tilted with respect to the gravitational plane, it is more convenient to reference the surface deviations to the hypothetical plane which best fits the surface in the least squares sense. It is reasonable to compute such a plane because at least four data points will always be available. In fact, there will usually be many more available so that no single data point has undue influence on the location of the fitted plane.

III.2 Tank Top Data

The basic raw data from one complete top survey consists of two sets of X, Y, and Z coordinates. The X and Y values are approximate and are expressed as index numbers. The Z values, measured with the beam seeking laser rod, have a resolution of 0.1 mm.

Before any further analysis can be made, the forward survey data must be tied-in to the aft survey data. This is accomplished by fitting separate least squares planes to each set of data using only the ten points common to both sets. All of the Z values from the forward survey are rotated until the least squares planes are coincidental. This completes the tie-in procedure. The differences between the pairs of Z values at the ten tie-in points provides a measure of the closure of the process. The root-mean-square (rms) value of these differences was typically about 2 mm.

The final adjustment is made by fitting a least squares plane to the combined Z values and then computing the deviations of the Z values from that plane. These deviations, which describe the profile of the tank surface, are reported in Section VI. The rms value of the deviations from the plane are also reported in Table 3 as a measure of the "flatness" of the surface.

III.3 Tank Bottom Data

The problem is only slightly more complicated with the bottom survey data. There are five gravitational planes; one for each quadrant, generated by the rotating laser, and the fifth, for the entire tank, generated by the water tube measurements. The water tube plane is taken to be absolute and uniform throughout the tank.

In each quadrant there are four tie-in points where the offset from the laser plane to the water tube plane has been measured. A least squares plane is fit to these four offset values, and corrections are obtained for converting Z values. The set of deviations of the Z values from this plane then describes the profile of the bottom surface of the tank.

III.4 Calculation of Changes

On both the bottom and top planes, the individual data points are carefully selected to be at the same positions for both the before and after surveys. Thus, the problem of the change in the shape reduces to one of subtraction at each data point. It is only necessary to decide which set of deviations is most likely to be representative of the tank itself. The best fit least squares plane through the whole surface was chosen as the best reference to use. A point-by-point subtraction is made, the rms value for the differences is found, and the differences are reported in Section VI.

IV. Error Analysis

Errors associated with the flatness surveys used to quantify mechanical deformation due to loading LNG tanks into a ship are of several types. We will discuss 3 types in this paper; random, systematic, and model errors.

The random errors currently identified in tank flatness surveys are shown in Table 1.

Table 1 - Random Errors in Free-Standing Tank Measurements

<u>Physical Source</u>	<u>Error Value</u>	<u>Error Source</u>
Laser plane	<u>+1.5mm</u>	Manufacturer Spec (1)
Laser rods		
Reading Error	<u>+0.3 mm</u>	Estimated (2)
Cosine error	<u>+0.6 mm</u>	Computed (3)
Grid point definition	<u>+4.0 mm</u>	Estimated (4)
Total Random Error	<u>+4.3 mm</u>	Sum of errors in quadrature

Notes for Table 1

(1) Specifications on the laser plane include wobble, lack of flatness, and deviation from level when self-leveling feature is used. The manufacturer specifies that the sum of these errors will not exceed +10 arc sec. For the maximum length of a tank, $L \approx 30$ m, this error is +1.5 mm.

(2) Scales on the laser rods are blank lines in mm increments on a light background. The random error estimate for this type of scale is based on years of laboratory experience.

(3) For an absolute displacement measurement, a rod cosine error is systematic. For relative measurements, this becomes random. For a discussion of the calculation method used to predict this error, see Reference 1.

(4) For comparison of the "before" and "after" survey data, the same grid point must be repeated. Due to local surface curvature around some points, an error can result from inability to remeasure exactly the same point. This estimate is based on remeasurement at a number of points.

It must be noted that the laser rod calibration cannot contribute an error in this survey since only relative displacement from flatness of two planes is being computed.

The major systematic error in this type of survey is the thermal distortion due to uneven heating of the tank surfaces from the sun. The worst case observed was on the top of Tank 5 after it was loaded into the ship. Gradients of up to 18 °C were recorded on the top, which over a 30 m length in aluminum amount to a dimensional change of 11 mm. Gradients in the tank walls are equally important in establishing this error, however it was not possible to measure these. Table 2 presents a summary of the thermal profiles recorded on each surface surveyed, with bottom profiles

being based on a 16 point grid and top profiles being based on 25 or more points. A clear picture of the thermal distortion effect is not presently available.

Table 2

El Paso Savannah
Temperature Profile Summaries - Readings in °C

TOP PLANES			BOTTOM PLANES		
Tank 4			Tank 4		
	Avg.	Range		Avg.	Range
Before lifting	26.1	21.3-29.7	Before lifting	18.7	18.1-19.3
After lifting	31.3	27.0-37.0	After lifting	22.8	21.9-23.5
Tank 5			Tank 5		
Before lifting	6.8	6.2- 7.4	Before lifting	13.3	13.2-13.4
After lifting	39.8	30.0-48.0	After lifting	25.9	25.6-26.4

Finally, model errors will be considered. The previous discussion dealt with expected errors in measurement, but one must also examine how well the model of flat planes represents the true tank surface. In performing this distortion survey, we measured two tanks of the El Paso Savannah, both before and after loading into the ship, and top and bottom surfaces of each tank. This yielded 8 flatness surfaces, and the rms deviations from the "best fit" plane for each case is shown in Table 3. These deviations vary from 7.9 mm to 23.0 mm for surfaces up to 37 m square. We therefore conclude that the tank surfaces are modeled sufficiently well by a plane.

V. Results and Conclusions

The results of lifting distortion measurements on Tanks 4 and 5 of the El Paso Savannah are presented in Table 3. Two planes per tank for two tanks were measured, both before and after lifting, yielding 8 data sets. The rms deviations of each of these 8 data sets from a "best fit" plane are reported, and most importantly the rms values of the before and after differences taken on a point-by-point basis for each surface are given. From this table, it is seen that these rms differences range from 3.4 mm to 5.1 mm, with the exception of the bottom of Tank 5. The difference value for Tank 5 is invalid because of a failure of the water tube survey to successfully tie the four quadrant surveys together before tank lifting. A true measure of tank bottom flatness is given by the "flatness from underneath" value, but because different survey points were used inside and outside the tank these two data sets cannot be differenced. The failure of the water tube apparatus was probably due to an undetected constriction of the tubing while level points were being marked on the tank.

The estimated random error of this survey technique, exclusive of thermal effects, is ± 4.3 mm at the one-standard deviation limit of uncertainty, and ± 13.0 mm at the three-standard deviation limit. Systematic distortion would therefore be indicated by any rms difference value exceeding 13.0 mm. Since no surface, except the one on which the measurement method failed, exceeds this value, we conclude the effect of lifting distortion on land-based tank calibrations is negligible.

An estimate of the volume error caused by a systematic deformation of the tank bottom can be made as follows. Consider the largest tank, Tank 4, with bottom dimensions of approximately 30 m x 37 m. Assume that the edges of the bottom surface are constrained and only the center deflects. Further assume that the deflection profile is parabolic so that the deformed bottom is a paraboloid with a rectangular base. If the center of the paraboloid is 13.0 mm from the plane formed by the base, the enclosed volume is 6.4 m³. Alternatively, if it is assumed that the interior bulkhead constrains the bottom in quadrants, that is four surfaces 15 m x 18.5 m each are deflected, then the total enclosed volume remains 6.4 m³. For a tank with a total volume of approximately 30,800 m³, this represents an uncertainty of only 0.02% of total volume.

Table 3

El Paso Savannah
Deviations (RMS) from "best fit" Plane

TOP PLANES

BOTTOM PLANES

Tank 4		Tank 4	
Before lifting	23.0 mm	Before lifting	9.8 mm
After lifting	22.2 mm	After lifting	8.2 mm
RMS value of differences	3.4 mm	RMS value of differences	5.1 mm
Tank 5		Tank 5	
Before lifting	18.0 mm	Before lifting	13.7 mm*
After lifting	18.5 mm	After lifting	7.9 mm
RMS value of differences	4.6 mm	RMS value of differences	13.8 mm
		* Flatness from underneath	7.7 mm

VI. Tables of Survey Data

For completeness, tables of the actual deviations of each data point from the "best fit" plane applicable to that surface are included here. Also included are the difference tables for each point of each surface in the before and after surveys. All deviations are reported in millimeters. The composition of each table is as follows:

<u>Table</u>	<u>Contents</u>
A1	Tank 4, Top before lifting
A2	Tank 4, Top after lifting
A3	Tank 4, Top differences
A4	Tank 4, Bottom before lifting
A5	Tank 4, Bottom after lifting
A6	Tank 4, Bottom differences
A7	Tank 5, Top before lifting
A8	Tank 5, Top after lifting
A9	Tank 5, Top differences
A10	Tank 5, Bottom before lifting
A11	Tank 5, Bottom after lifting
A12	Tank 5, Bottom differences

Any point on the top surfaces with a entry of "*****" is one that could not be measured either because the laser was mounted too close to the point or the vapor dome was installed where the point would have been.

The coordinate system orientation used for reporting data in these tables is shown in Figure 1. The X-Y origin is at the forward port corner of each surface, as shown in Figures 3 and 4 for top and bottom surfaces respectively. The Z-axis is positive downward, and the Z=0 point is defined by the best fit plane.

TABLE A1

El Paso Savannah, Tank 4 Top Shape Data Before Lifting

X \ Y	1	3	5	7	9	11	13	15	17	19	21	23	25
1	2.8	-4.1	-13.1	-14.8	-30.6	-6.1	-10.5	-21.4	-36.3	-32.2	-33.0	-31.7	-41.9
3	-4.9	-28.9	-27.1	-10.0	2.5	23.6	*	27.1	6.7	-12.9	-14.8	-24.5	-10.6
5	0.6	-30.7	-23.1	0.9	22.5	41.8	-1.0	39.1	21.7	11.6	-16.9	-22.1	11.5
7	-5.8	-28.8	-9.1	4.5	28.5	48.4	5.4	49.1	22.6	6.8	-17.3	-16.2	15.1
9	-0.7	-19.7	-31.1	7.3	31.0	...	5.1	47.2	29.6	6.4	-6.7	-9.6	8.3
11	-9.5	-16.4	-26.7	-4.0	3.4	17.5	2.6	15.0	10.7	-7.7	-14.4	-8.3	2.1
13	-11.0	-14.3	-10.7	-10.9	-4.0	-1.6	*	0.5	-9.9	-9.7	-2.6	-10.5	-6.4
15	-13.6	-21.0	1.2	6.2	4.0	24.3	23.8	16.1	6.5	-2.2	-2.7	-1.9	-6.3
17	-30.6	-17.5	-8.6	17.1	36.6	52.5	13.3	45.1	33.2	9.4	-9.8	2.6	3.5
19	-21.7	-10.5	-10.0	17.7	43.1	69.4	10.0	47.9	36.3	17.7	-9.9	-7.4	3.8
21	-28.1	-18.9	1.1	20.5	42.2	64.2	7.9	32.4	30.0	20.0	-20.1	-10.6	-13.9
23	-39.0	-15.1	-3.4	12.3	30.0	40.4	*	4.5	8.9	-7.2	-20.4	-21.7	-28.4
25	-46.4	-26.3	-26.3	-28.3	-22.3	-1.7	2.2	-24.7	-33.8	-29.2	-32.2	-20.4	-37.4

TABLE A2
El Paso Savannah, Tank 4 Top Shape Data After Lifting

X \ Y	1	3	5	7	9	11	13	15	17	19	21	23	25
1	4.5	-3.4	-8.1	-13.1	-26.7	-7.0	-10.2	-22.7	-37.0	-34.7	-31.9	-28.4	-38.5
3	-0.6	-25.6	-27.4	-14.7	-1.5	27.8	*	25.1	10.0	-9.5	-16.1	-22.4	-8.0
5	3.7	-27.1	-24.3	-7.9	15.6	42.6	-2.9	36.9	34.7	11.8	-17.6	-18.8	11.8
7	-1.2	-25.3	-23.8	1.1	31.0	46.9	2.5	53.8	26.5	6.0	-15.6	-14.5	17.8
9	1.2	-18.1	-33.8	2.6	31.1	31.9	0.9	43.7	27.4	7.3	-6.7	-11.3	9.3
11	-10.5	-15.2	-19.9	-10.6	6.1	14.3	-0.8	12.8	7.8	-7.4	-17.7	-7.2	2.6
13	-11.4	-13.2	-11.5	-14.1	-6.9	-1.7	*	-0.5	-8.2	-8.0	-4.1	-7.6	-5.0
15	-13.2	-17.8	1.9	3.9	11.5	18.9	19.5	13.3	5.9	-2.1	-6.4	-1.4	-6.2
17	-29.5	-12.8	-8.3	14.5	36.3	49.8	11.1	41.6	32.6	10.0	-10.2	1.9	4.6
19	-19.1	-9.6	-11.6	15.9	42.2	67.8	6.3	35.6	35.8	16.2	-11.1	-11.0	4.7
21	-26.3	-15.6	4.8	18.7	50.3	61.9	4.1	32.7	28.7	19.5	-19.1	-19.2	-13.5
23	-36.9	-12.6	-1.7	9.9	27.1	44.8	*	14.2	9.7	-6.1	-18.3	-19.0	-25.9
25	-42.2	-25.1	-26.9	-26.3	-22.6	-4.6	1.0	-25.5	-34.0	-28.5	-27.8	-18.5	-34.2

TABLE A3

El Paso Savannah, Tank 4 Top Changes Due To Lifting

X \ Y	1	3	5	7	9	11	13	15	17	19	21	23	25
1	1.7	0.6	4.9	1.6	3.8	-0.9	0.3	-1.3	-0.6	-2.6	1.0	3.2	3.4
3	4.3	3.3	-0.2	-4.6	-3.9	4.3	*	-2.1	3.3	3.5	-1.2	2.2	2.7
5	3.1	3.6	-1.2	-8.8	-6.9	0.8	-1.9	-2.2	13.0	0.2	-0.7	3.3	0.3
7	4.6	3.5	-14.7	-3.4	2.5	-1.5	-2.9	4.7	3.9	-0.8	1.7	1.7	2.7
9	1.9	1.6	-2.7	-4.7	-0.8	-2.8	-4.2	-3.5	-2.2	0.9	0.0	-1.7	1.0
11	-1.0	1.2	6.8	-6.6	2.7	-3.2	-3.4	-2.2	-2.9	0.3	-3.3	1.1	0.5
13	-0.4	1.1	-0.8	-3.2	-2.9	-0.1	*	-1.0	1.7	1.7	-1.4	3.0	1.4
15	0.4	3.2	0.7	-2.3	7.5	-5.4	-4.3	-2.8	-0.6	0.1	-3.7	0.5	0.1
17	1.1	4.7	0.3	-2.6	-0.3	-2.7	-2.2	-3.5	-0.6	0.6	-0.4	-0.7	1.1
19	2.6	0.9	-1.6	-1.8	-0.9	-1.6	-3.7	-12.3	-0.5	-1.5	-1.2	-3.7	0.8
21	1.8	3.3	3.7	-1.8	8.1	-2.3	-3.8	0.3	-1.3	-0.5	1.0	-8.6	0.4
23	2.1	2.5	1.7	-2.4	-2.9	4.4	*	9.7	0.8	1.1	2.1	2.7	2.5
25	4.2	1.2	-0.6	2.0	-0.3	-2.9	-1.2	-0.8	-0.2	0.7	4.4	1.9	3.2

TABLE A4 (Quadrants 1 & 2)

El Paso Savannah, Tank 4 Bottom Shape Data Before Lifting

X \ Y	27	29	31	34	39	42	44	45	46
4	*	*	*	*	*	*	*	*	*
5	*	*	*	-5.7	*	*	*	*	*
6	*	-11.9	*	*	1.3	3.9	5.2	*	*
8	*	-14.3	*	-4.7	*	*	*	*	*
9	-29.1	*	-14.3	-4.5	*	4.2	*	*	4.9
10	*	*	*	*	0.7	*	*	*	*
12	-22.2	*	-13.8	-3.3	1.9	6.0	*	*	1.8
14	*	*	*	0.9	*	*	*	*	*
15	-23.1	*	-9.6	*	3.6	4.3	*	*	0.6
17	*	*	*	3.0	*	*	*	*	*
18	-23.8	*	-7.2	2.3	5.5	6.5	*	*	3.7
20	*	*	*	*	*	*	*	*	*
21	-23.2	*	-5.7	*	8.1	8.8	*	*	4.1
23	-26.4	*	*	5.1	*	*	*	*	*
24	*	*	-4.9	*	10.4	9.4	0.9	*	*
26	*	*	*	8.8	*	*	*	*	*
27	*	*	4.1	*	10.2	8.9	0.8	*	*
29	*	*	*	9.4	14.3	12.6	*	*	*
30	*	*	*	*	*	*	*	*	*
32	*	*	-2.9	5.7	10.9	7.3	*	*	*
35	*	-11.9	-4.9	3.9	11.1	9.1	*	0.4	*
38	*	-17.9	-8.0	-0.1	10.9	4.3	*	*	2.2
41	*	-15.7	-7.2	-0.2	8.8	3.8	*	*	-3.0
44	*	-18.9	-9.1	1.2	8.7	6.4	*	*	1.0
46	*	*	*	*	*	6.3	*	*	*
47	*	-23.9	-6.5	3.5	10.6	*	*	*	1.6
49	*	*	*	*	*	*	*	*	*
50	*	*	-4.4	3.0	12.5	9.1	*	*	1.3
52	*	*	-0.7	9.2	16.0	12.8	*	3.9	*
54	*	*	*	8.6	*	17.4	*	*	*
55	*	*	*	*	17.3	*	*	*	*

TABLE A4 (Quadrants 3 & 4)
 El Paso Savannah, Tank 4 Bottom Shape Data Before Lifting

X \ Y	1	3	5	8	13	16	18	20
4	*	*	*	2.1	0.7	*	*	*
5	*	*	*	*	*	*	*	*
6	*	-4.5	-0.2	2.5	-0.4	-8.4	*	*
8	*	*	*	*	*	*	*	*
9	-13.4	*	-1.3	3.2	-0.6	-7.9	-12.5	*
10	*	*	*	*	*	*	*	*
12	-13.5	*	-7.0	0.8	-4.2	-9.5	-17.6	*
14	*	*	*	*	*	*	*	*
15	-14.3	*	-6.6	-3.7	-4.6	-12.3	-17.8	*
17	*	*	*	*	*	*	*	*
18	-14.5	*	-6.4	1.1	-4.4	-9.7	-16.9	*
20	*	*	*	*	*	*	*	*
21	-14.0	*	-6.4	0.0	-0.4	-9.4	-17.3	*
23	*	*	*	*	*	*	*	*
24	-13.7	*	-2.0	5.3	0.2	-6.2	-14.6	*
26	*	*	*	*	*	*	*	*
27	*	*	-1.2	8.4	-0.8	-7.3	*	*
29	*	*	*	*	*	*	*	*
30	*	*	*	4.8	3.5	*	*	*
32	*	-2.8	1.3	2.8	-4.4	-9.7	*	*
35	*	*	-2.7	1.8	-3.9	-8.2	-24.7	*
38	-8.2	*	1.1	7.0	-4.0	-10.0	*	-22.4
41	-6.3	*	4.2	7.1	0.6	-8.2	*	-18.7
44	-5.8	*	4.2	6.1	2.2	-7.6	*	-20.9
44	-1.9	*	7.7	6.8	2.8	-6.0	*	-20.0
46	*	*	*	*	*	*	*	*
47	-0.1	*	*	*	*	*	*	*
49	2.9	*	11.0	9.3	8.0	-1.9	*	-17.2
50	*	*	*	*	*	*	*	*
52	*	7.5	10.8	10.8	10.4	0.5	-8.4	*
54	*	*	13.8	17.5	17.5	1.7	*	*
55	*	*	*	12.7	*	*	*	*

TABLE A5 (Quadrants 1 & 2)
 El Paso Savannah, Tank 4 Bottom Shape Data After Lifting

X \ Y	27	29	31	34	39	42	44	45	46
4	*	*	*	*	*	*	*	*	*
5	*	*	*	2.8	*	*	*	*	*
6	*	*	0.0	2.2	5.8	5.7	7.6	*	*
8	*	*	-1.8	4.8	*	6.5	*	*	*
9	-11.7	*	-1.4	4.1	2.7	4.7	*	*	4.6
10	*	*	-1.4	6.5	1.4	*	*	*	-1.1
12	-10.6	*	-1.4	7.4	2.1	0.5	*	*	-4.4
14	*	*	2.6	6.7	2.0	2.7	*	*	-3.7
15	-13.3	*	2.2	7.8	3.9	1.7	*	*	-6.0
17	*	*	3.0	7.7	3.5	1.3	-3.9	*	*
18	-8.5	*	3.6	5.0	2.1	0.8	-8.3	*	*
20	*	*	*	6.4	2.8	1.5	*	*	*
21	-11.6	*	1.3	6.4	7.8	2.6	*	*	*
23	-13.8	*	-0.6	6.4	9.2	3.6	*	*	*
24	*	*	-2.7	3.5	7.8	3.5	*	*	*
26	*	*	-3.4	4.3	7.7	0.8	*	*	*
27	*	*	-4.2	1.9	6.5	3.0	*	*	*
29	*	*	-3.6	4.4	5.9	4.6	*	*	*
30	*	*	-1.0	5.6	10.6	*	*	*	-3.6
32	*	*	2.3	11.0	13.2	7.3	*	*	*
35	*	*	*	6.7	16.8	10.9	*	*	-2.5
38	*	*	*	*	*	13.9	*	-5.8	*
41	*	*	*	*	*	*	*	*	*
44	*	*	*	*	*	*	*	*	*
46	*	*	*	*	*	*	*	*	*
47	*	*	*	*	*	*	*	*	*
49	*	*	*	*	*	*	*	*	*
50	*	*	*	*	*	*	*	*	*
52	*	*	*	*	*	*	*	*	*
54	*	*	*	*	*	*	*	*	*
55	*	*	*	*	*	*	*	*	*

TABLE A5 (Quadrants 3 & 4)

El Paso Savannah, Tank 4 Bottom Shape Data After Lifting

X \ Y	1	3	5	8	13	16	18	20
4	*	*	*	2.3	1.0	*	*	*
5	*	*	*	*	*	*	*	*
6	*	1.7	4.9	8.3	4.5	-6.0	*	*
8	*	*	*	*	*	*	*	*
9	-7.8	*	5.1	5.2	3.8	-6.1	-11.1	*
10	*	*	*	*	*	*	*	*
12	-6.2	*	-0.2	1.9	-2.0	-7.5	-15.7	*
14	*	*	*	*	*	*	*	*
15	-8.3	*	-3.1	-0.9	-2.7	-9.4	-19.4	*
17	*	*	*	*	*	*	*	*
18	-10.2	*	-5.0	0.5	-2.6	-10.2	-17.3	*
20	*	*	*	*	*	*	*	*
21	-9.2	*	-3.2	1.0	-0.7	-9.4	-18.5	*
23	*	*	*	*	*	*	*	*
24	-14.5	*	-1.4	6.5	1.2	-5.8	-15.9	*
26	*	*	1.9	10.1	0.2	-5.8	*	*
27	*	*	*	*	*	*	*	*
29	*	*	*	*	*	*	*	*
30	*	*	6.7	2.4	4.6	*	*	*
32	*	-0.7	2.8	-0.4	-1.4	-9.1	*	*
35	-6.4	*	2.1	3.3	0.8	-10.7	-24.8	*
38	-5.3	*	3.3	8.2	-2.5	-13.5	*	-26.7
41	-0.7	*	5.5	8.2	1.8	-11.1	*	-24.0
44	-0.3	*	6.5	5.9	3.1	-10.2	*	-28.3
46	*	*	8.0	8.3	3.7	-9.0	*	-25.8
47	2.1	*	*	*	*	*	*	*
49	5.6	*	11.2	8.1	5.4	-6.1	*	-22.6
50	*	*	*	*	*	*	*	*
52	*	11.0	11.5	8.8	6.5	-2.0	-7.5	*
54	*	*	14.2	9.2	9.1	-2.7	*	*
55	*	*	*	*	*	*	*	*

TABLE A6 (Quadrants 1 & 2)

El Paso Savannah, Tank 4 Bottom Changes Due To Lifting

X \ Y	27	29	31	34	39	42	44	45	46
4	*	*	*	*	*	*	*	*	*
5	*	*	*	8.5	*	*	*	*	*
6	*	*	11.9	*	4.4	1.8	2.4	*	*
8	*	*	12.5	6.9	*	2.3	*	*	*
9	17.4	*	12.4	9.3	2.0	*	*	*	-0.3
10	*	*	*	*	-0.5	-1.4	*	*	-2.9
12	11.5	*	12.4	7.5	*	*	*	*	*
14	*	*	*	5.7	*	*	*	*	*
15	9.8	*	8.2	*	-1.5	-3.8	*	*	-5.0
17	*	*	*	4.3	*	*	*	*	*
18	15.3	*	9.8	*	-3.5	-3.8	*	*	-7.4
20	*	*	*	4.4	*	*	*	*	*
21	11.6	*	7.9	*	-4.2	-7.0	*	*	-10.1
23	12.7	*	*	2.7	*	*	*	*	*
24	*	*	7.9	*	-6.9	-8.1	-4.7	*	*
26	*	*	*	-1.0	*	*	*	*	*
27	*	*	-0.5	*	-8.1	-8.2	-9.1	*	*
29	*	*	*	-4.4	-11.5	-11.1	*	*	*
30	*	*	*	*	*	*	*	*	*
32	*	*	4.1	0.7	-3.1	-4.7	*	*	*
35	*	4.3	4.3	2.5	-1.9	-5.5	*	-5.2	*
38	*	7.9	5.3	3.6	-3.1	-0.7	*	*	-5.2
41	*	6.7	3.8	4.5	-1.0	-3.0	*	*	-4.8
44	*	6.9	4.9	0.8	-2.2	-3.4	*	*	-7.1
46	*	*	*	*	*	-1.7	*	*	*
47	*	15.5	3.0	1.0	-4.8	*	*	*	-5.2
49	*	*	*	*	*	*	*	*	*
50	*	*	3.5	2.5	-2.0	-1.8	*	*	-3.8
52	*	*	3.0	1.8	-2.8	-1.9	*	-9.6	*
54	*	*	*	-1.8	*	-3.6	*	*	*
55	*	*	*	*	-0.5	*	*	*	*

TABLE A6 (Quadrants 3 & 4)

El Paso Savannah, Tank 4 Bottom Changes Due To Lifting

X \ Y	1	3	5	8	13	16	18	20
4	*	*	*	0.2	0.2	*	*	*
5	*	*	*	5.8	4.9	*	*	*
6	*	6.1	5.1	*	4.9	2.4	*	*
8	*	*	*	6.4	4.4	1.8	*	*
9	5.6	*	*	2.0	4.4	1.8	1.4	*
10	*	*	*	1.1	2.2	2.0	1.9	*
12	7.3	*	*	*	1.9	2.9	-1.6	*
14	*	*	*	2.8	1.8	-0.5	-0.4	*
15	6.0	*	3.5	1.0	-0.2	0.1	-1.2	*
17	*	*	1.4	-0.6	1.8	0.4	-1.3	*
18	4.3	*	*	1.0	1.0	1.5	*	*
20	*	*	3.2	1.7	1.0	*	*	*
21	4.9	*	*	1.3	1.1	*	*	*
23	*	*	0.6	3.2	1.0	0.6	*	*
24	-0.8	*	*	1.7	1.1	*	*	*
26	*	*	3.1	1.8	3.0	0.6	*	*
27	*	*	1.9	-3.2	4.7	-2.5	0.0	-4.3
29	*	*	1.5	1.5	1.5	-3.5	*	-5.3
30	*	*	2.2	1.2	1.1	-2.9	*	-7.4
32	*	2.1	1.2	1.0	0.9	-2.6	*	-5.8
35	1.7	*	9.1	-0.2	0.9	-3.0	*	-5.4
38	1.0	*	0.2	1.5	0.9	-4.2	*	*
41	5.1	*	*	0.2	-2.6	*	*	*
44	1.6	*	0.2	-1.2	-2.6	-2.5	0.9	*
46	*	*	*	0.7	-3.9	-4.4	*	*
47	2.3	*	*	0.4	-8.4	*	*	*
49	2.7	*	0.2	-3.5	*	*	*	*
50	*	*	*	*	*	*	*	*
52	*	3.4	0.7	-2.1	-3.9	-2.5	0.9	*
54	*	*	0.4	*	-8.4	-4.4	*	*
55	*	*	*	*	*	*	*	*

TABLE A7
 El Paso Savannah, Tank 5 Top Shape Data Before Lifting

X \ Y	1	2	4	6	8	10	12	14	16	18	20	22	23
1	4.3	-16.4	-26.1	-23.1	-4.3	3.3	15.1	-3.9	-9.7	-5.8	-21.5	-9.5	14.8
3	16.7	-16.9	-37.7	-34.3	-19.2	-3.0	*	-1.4	-2.4	-20.3	-22.0	-3.9	44.3
5	46.3	-8.6	-33.1	-30.5	-14.7	8.1	25.8	10.0	1.5	-17.9	-17.5	3.1	26.3
7	50.0	-7.1	-31.7	-27.8	-10.0	11.5	25.5	8.0	-11.9	-7.9	-13.9	5.4	37.2
9	46.6	6.3	-17.3	-19.6	5.0	18.0	28.6	13.4	1.3	-6.4	2.5	9.8	22.6
11	20.6	5.5	10.3	1.9	3.4	0.9	*	7.4	-5.3	-0.3	-5.2	-4.8	18.6
13	48.1	14.3	0.9	-4.1	5.5	4.4	8.4	3.2	2.6	-2.9	-10.3	-4.2	13.3
15	46.9	8.3	-14.0	-12.0	-6.7	-0.5	7.0	-4.2	1.4	-3.1	-13.5	-7.6	13.3
17	36.7	0.6	-12.5	-21.3	-9.2	-2.2	*	-6.9	-1.1	-5.5	-18.5	-5.7	23.6
19	0.0	-23.3	-18.6	-23.9	-25.4	-18.2	11.8	-7.1	-11.6	-3.5	-12.4	1.2	11.8

TABLE A8
El Paso Savannah, Tank 5 Top Shape Data After Lifting

X \ Y	1	2	4	6	8	10	12	14	16	18	20	22	23
1	-6.1	-5.7	-21.0	-19.5	-12.9	-5.5	4.1	-14.8	-14.5	-6.1	-20.3	-8.1	20.0
3	17.4	-10.5	-28.2	-34.7	-17.2	-7.0	"	-10.6	-11.8	-13.5	-20.9	2.1	53.1
5	47.8	-6.9	-33.5	-35.7	-17.3	1.0	18.5	5.8	-6.6	-16.1	-16.9	5.3	30.1
7	51.4	0.0	-26.9	-31.5	-10.5	5.9	16.7	10.0	-1.4	-10.0	-14.4	10.3	37.5
9	44.6	10.8	-16.8	-15.9	4.8	15.8	21.9	16.4	6.5	-9.4	-0.6	8.9	25.2
11	23.3	7.9	7.0	5.6	4.0	4.5	"	8.9	4.9	-1.4	-3.0	-4.7	23.2
13	51.1	19.9	0.9	-4.3	0.7	2.4	7.2	3.1	7.3	-0.7	-12.0	-2.0	13.8
15	50.0	10.4	-15.9	-13.3	-5.6	-4.0	4.6	-4.1	1.5	-2.0	-9.8	-3.5	6.6
17	42.6	3.7	-17.5	-18.5	-11.7	-8.3	"	-6.0	-4.0	-5.1	-19.9	-2.8	22.6
19	4.7	-28.5	-20.2	-23.5	-28.6	-28.3	11.1	-10.0	-13.9	-7.6	-13.1	2.6	17.9

TABLE A9
El Paso Savannah, Tank 5 Top Changes Due To Lifting

X \ Y	1	2	4	6	8	10	12	14	16	18	20	22	23
1	-10.4	10.7	5.1	3.6	-8.6	-8.7	-11.0	-10.8	-4.8	-0.4	1.2	1.4	5.2
3	0.7	6.4	9.5	-0.4	2.1	-4.0	-9.2	-9.2	-9.4	6.8	1.0	6.0	8.8
5	1.5	1.7	-0.3	-5.2	-2.6	-7.1	-7.2	-4.2	-8.1	1.8	0.7	2.2	3.8
7	1.4	7.1	4.8	-3.7	-0.6	-5.6	-8.7	1.9	10.5	-2.1	-0.5	4.8	0.3
9	-1.9	4.5	0.5	3.8	-0.2	-2.3	-6.7	3.0	5.2	-3.1	-3.1	-0.8	2.6
11	2.7	2.5	-3.3	3.7	0.6	3.6	*	1.6	10.2	-1.1	2.2	0.1	4.7
13	3.0	5.6	-0.1	-0.2	-4.7	-2.0	-1.2	-0.1	4.7	2.3	-1.7	2.1	0.5
15	3.1	2.1	-1.8	-1.3	1.1	-3.5	-2.4	0.1	0.1	1.1	3.8	4.1	-6.8
17	5.8	3.1	-5.0	2.8	-2.6	-6.1	*	0.9	-2.9	0.4	-1.4	2.9	-1.0
19	4.7	-5.2	-1.7	0.5	-3.2	-10.1	-0.7	-2.9	-2.3	-4.1	-0.8	1.5	6.1

TABLE A10 (Quadrants 1 & 2)

El Paso Savannah, Tank 5 Bottom Shape Data Before Lifting

X \ Y	27	28	29	31	34	35	38	39	40	41	42	44	45	46
4	*	*	*	*	-12.5	*	*	-5.7	*	*	*	*	*	*
5	*	*	*	-18.3	*	*	*	*	*	*	*	*	*	*
6	*	*	-24.6	-17.0	-10.1	*	*	-4.0	*	*	-0.9	*	*	*
7	*	*	*	*	*	*	*	*	*	*	*	*	*	*
9	*	-24.8	*	-17.6	-7.4	*	*	-1.7	*	*	-0.3	*	-0.5	*
10	*	*	*	*	*	*	*	*	*	*	*	*	*	*
12	-29.7	*	*	-17.8	-7.7	*	*	2.7	*	*	4.3	*	1.5	*
13	*	*	*	*	*	*	*	*	*	*	*	*	*	*
15	-32.7	*	*	-19.0	-5.9	*	*	5.9	*	*	8.2	*	*	4.2
16	*	*	*	*	*	*	*	*	*	*	*	*	*	*
18	*	-30.4	*	-14.9	-1.9	*	*	8.1	*	*	8.8	*	4.2	*
19	*	*	*	-5.1	3.4	*	*	13.8	*	*	14.1	*	*	*
21	*	*	*	*	*	*	*	*	*	*	*	*	*	*
22	*	*	*	*	*	*	*	*	*	*	*	*	*	*
25	*	*	*	*	8.4	*	8.6	*	*	*	*	*	*	*
28	*	*	-1.0	7.6	9.3	*	11.6	*	*	11.9	12.0	*	*	*
31	2.2	*	*	9.8	8.3	*	11.7	*	*	12.2	9.3	1.0	*	*
33	2.9	*	*	9.6	7.1	*	11.7	*	*	11.3	10.5	*	*	-0.2
34	*	*	*	*	*	*	*	*	*	12.0	11.5	*	*	1.8
36	*	*	*	*	*	*	*	*	*	*	*	*	1.4	*
37	*	*	10.6	10.9	8.7	*	11.1	*	*	12.8	9.7	*	*	*
38	*	*	*	*	*	*	*	*	*	*	*	*	*	*
39	*	*	*	10.2	*	*	*	*	*	*	*	*	*	*
40	*	*	*	*	*	15.7	10.1	*	17.6	*	*	*	*	*

TABLE A10 (Quadrants 3 & 4)
 El Paso Savannah, Tank 5 Bottom Shape Data Before Lifting

X \ Y	1	2	3	5	8	10	12	13	16	18
4	*	*	*	*	-19.4	*	*	-20.1	*	*
5	*	*	*	-21.0	*	*	*	*	*	*
6	*	*	*	*	*	*	*	*	*	*
7	*	*	-31.7	-21.1	-18.1	*	*	-23.0	-18.6	*
9	*	*	*	-20.1	-16.6	*	*	-19.9	-17.4	-22.3
10	-27.8	*	*	*	*	*	*	*	*	*
12	*	*	*	*	*	*	*	*	*	*
13	-32.3	*	*	-17.2	-7.1	*	*	-12.9	-16.0	-20.6
15	*	*	*	*	*	*	*	*	*	*
16	-27.1	*	*	-12.9	-3.5	*	*	-12.2	-23.9	-23.4
18	*	*	*	*	*	*	*	*	*	*
19	*	-29.6	*	-9.4	0.5	*	*	-9.2	-11.8	-22.1
21	*	*	*	-6.2	*	*	*	*	*	*
22	*	*	*	*	2.1	*	*	-3.0	-11.6	*
25	*	*	*	-15.2	-3.5	*	*	0.0	*	*
28	*	*	-14.5	-11.8	1.3	*	*	5.5	-0.8	*
31	-18.0	*	*	-6.1	*	3.7	*	2.4	0.1	*
33	*	*	*	*	*	*	*	*	*	*
34	-14.1	*	*	-3.3	2.6	*	*	5.9	2.6	-11.3
36	*	*	*	*	*	*	*	*	*	*
37	*	-7.3	*	6.3	-0.5	*	*	3.8	*	*
38	*	*	*	*	*	*	*	*	1.7	*
39	*	*	*	12.5	*	*	*	*	*	*
40	*	*	*	*	2.4	*	6.9	*	*	*

TABLE All (Quadrants 1 & 2)

El Paso Savannah, Tank 5 Bottom Shape Data After Lifting

X \ Y	27	28	29	31	34	35	38	39	40	41	42	44	45	46
4	*	*	*	*	1.9	*	*	-9.7	*	*	*	*	*	*
5	*	*	*	-3.8	*	*	*	*	*	*	*	*	*	*
6	*	*	2.8	3.2	1.4	*	*	-10.5	*	*	-12.0	*	*	*
7	*	*	*	*	*	*	*	*	*	*	*	*	*	*
9	*	5.4	*	2.4	3.8	*	*	-6.5	*	*	-11.6	*	-19.4	*
10	*	*	*	*	*	*	*	-2.0	*	*	-8.5	*	-18.6	*
12	2.1	*	*	2.1	2.5	*	*	*	*	*	*	*	*	*
13	*	*	*	*	*	*	*	-0.5	*	*	-7.0	*	*	-21.7
15	-4.5	*	*	-0.3	4.5	*	*	*	*	*	*	*	*	*
16	*	*	*	2.2	6.8	*	*	0.7	*	*	-4.5	*	-15.6	*
18	*	-3.3	*	*	*	*	*	7.5	*	*	-3.6	*	*	*
19	*	*	*	9.4	10.4	*	*	*	*	*	*	*	*	*
21	*	*	*	*	*	*	*	*	*	*	*	*	*	*
22	*	*	*	*	*	*	*	*	*	*	*	*	*	*
25	*	*	*	*	7.7	*	3.4	*	*	5.2	8.4	*	*	*
28	*	*	-2.4	9.8	7.2	*	11.8	*	*	4.2	3.8	*	*	*
31	6.2	*	*	9.3	7.4	*	10.2	*	*	3.3	2.2	-14.9	*	-10.1
33	5.8	*	*	8.7	6.8	*	12.1	*	*	4.7	2.2	*	*	-9.2
34	*	*	*	*	*	*	*	*	*	*	*	*	*	*
36	*	*	*	*	*	*	*	*	*	*	*	*	-11.5	*
37	*	*	9.7	7.7	1.6	*	8.2	*	*	4.6	2.2	*	*	*
38	*	*	*	*	*	*	*	*	*	*	*	*	*	*
39	*	*	*	6.9	*	*	*	*	*	*	*	*	*	*
40	*	*	*	*	*	8.5	6.3	*	6.2	*	*	*	*	*

TABLE All (Quadrants 3 & 4)

El Paso Savannah, Tank 5 Bottom Shape Data After Lifting

X \ Y	1	2	3	5	8	10	12	13	16	18
4	*	*	*	*	5.9	*	*	1.0	*	*
5	*	*	*	5.1	*	*	*	*	*	*
6	*	*	*	*	*	*	*	*	*	*
7	*	*	-6.5	1.7	4.5	*	*	0.6	1.0	*
9	*	*	*	*	*	*	*	*	*	*
10	-5.7	*	*	0.1	5.8	*	*	-0.1	1.3	-3.5
12	*	*	*	*	*	*	*	*	*	*
13	-11.3	*	*	3.6	10.5	*	*	4.1	1.1	-6.8
15	*	*	*	*	*	*	*	*	*	*
16	-11.6	*	*	3.8	10.9	*	*	4.2	-0.5	-7.4
18	*	*	*	*	*	*	*	*	*	*
19	*	-17.9	*	0.9	11.2	*	*	4.8	-3.0	-11.5
21	*	*	*	4.0	*	*	*	*	*	*
22	*	*	*	*	12.9	*	*	5.9	-2.6	*
25	*	*	*	-27.2	2.4	*	*	7.7	*	*
28	*	*	-5.3	-1.2	3.1	*	*	7.3	1.3	*
31	-16.6	*	*	-6.7	*	4.1	*	2.5	-0.5	*
33	*	*	*	*	*	*	*	*	*	*
34	-11.8	*	*	-7.9	-4.5	*	*	1.2	-1.3	-11.4
36	*	*	*	*	*	*	*	*	*	*
37	*	-11.6	*	-8.9	-6.6	*	*	-3.3	*	*
38	*	*	*	*	*	*	*	*	-9.3	*
39	*	*	*	-8.9	*	*	*	*	*	*
40	*	*	*	*	-9.3	*	-4.0	*	*	*

TABLE A12 (Quadrants 1 & 2)
 El Paso Savannah, Tank 5 Bottom Changes Due To Lifting

X \ Y	27	28	29	31	34	35	38	39	40	41	42	44	45	46
4	*	*	*	*	14.4	*	*	-4.0	*	*	*	*	*	*
5	*	*	*	14.5	*	*	*	*	*	*	*	*	*	*
6	*	27.4	*	20.2	11.5	*	*	-6.5	*	*	-11.1	*	*	*
7	*	*	*	*	*	*	*	*	*	*	*	*	*	*
9	*	30.2	*	20.0	11.2	*	*	-4.8	*	*	-11.3	*	-18.9	*
10	*	*	*	19.9	10.2	*	*	-4.7	*	*	-12.8	*	-20.1	*
12	31.7	*	*	*	*	*	*	*	*	*	*	*	*	*
13	*	*	*	18.7	10.4	*	*	-6.4	*	*	-15.2	*	*	-25.9
15	28.2	*	*	17.1	8.8	*	*	-7.4	*	*	-13.3	*	-19.8	*
16	*	27.1	*	14.6	7.1	*	*	-6.3	*	*	-17.7	*	*	*
18	*	*	*	*	*	*	*	*	*	*	*	*	*	*
19	*	*	*	*	*	*	*	*	*	*	*	*	*	*
21	*	*	*	*	*	*	*	*	*	*	*	*	*	*
22	*	*	*	*	*	*	*	*	*	*	*	*	*	*
25	*	*	*	*	-0.8	*	-5.3	*	*	-6.7	-3.6	*	*	*
28	*	*	-1.4	2.2	-2.0	*	0.3	*	*	-8.0	-5.5	-15.9	*	*
31	4.0	*	*	-0.6	-0.9	*	-1.5	*	*	-8.0	-8.3	*	*	-10.0
33	2.9	*	*	-0.9	-0.2	*	0.4	*	*	-7.3	-9.3	*	*	-11.0
34	*	*	*	*	*	*	*	*	*	*	*	*	*	*
36	*	*	*	*	*	*	*	*	*	*	*	*	-12.9	*
37	*	*	-0.9	-3.2	-7.0	*	-2.9	*	*	-8.2	-7.5	*	*	*
38	*	*	*	*	*	*	*	*	*	*	*	*	*	*
39	*	*	*	-3.2	*	*	*	*	*	*	*	*	*	*
40	*	*	*	*	*	-7.2	-3.8	*	-11.4	*	*	*	*	*

TABLE A12 (Quadrants 3 & 4)
 El Paso Savannah, Tank 5 Bottom Changes Due To Lifting

X \ Y	1	2	3	5	8	10	12	13	16	18
4	*	*	*	*	25.2	*	*	24.1	*	*
5	*	*	*	26.1	*	*	*	*	*	*
6	*	*	*	*	*	*	*	*	*	*
7	*	*	25.3	22.8	22.5	*	*	23.6	19.6	*
9	*	*	*	20.2	22.5	*	*	19.8	18.7	18.8
10	22.1	*	*	*	*	*	*	*	*	*
12	*	*	*	*	*	*	*	*	*	*
13	21.0	*	*	20.9	17.6	*	*	17.0	17.1	13.8
15	*	*	*	*	*	*	*	*	*	*
16	15.5	*	*	16.7	14.5	*	*	16.3	23.4	16.0
18	*	*	*	*	*	*	*	*	*	*
19	*	11.7	*	10.3	10.8	*	*	14.0	8.8	10.6
21	*	*	*	10.2	*	*	*	*	*	*
22	*	*	*	*	10.8	*	*	8.9	9.0	*
25	*	*	*	-12.0	5.8	*	*	7.6	*	*
28	*	*	9.1	10.6	1.7	*	*	1.8	2.0	*
31	1.3	*	*	-0.6	*	0.4	*	0.1	-0.6	*
33	*	*	*	*	*	*	*	*	*	*
34	2.2	*	*	-4.6	-7.1	*	*	-4.7	-3.8	-0.1
36	*	*	*	*	*	*	*	*	*	*
37	*	-4.3	*	-15.2	-6.1	*	*	-7.1	*	*
38	*	*	*	*	*	*	*	*	-10.9	*
39	*	*	*	-21.4	*	*	*	*	*	*
40	*	*	*	*	-11.7	*	-10.9	*	*	*

VII. References

1. Hocken, R. J. and Haight, W. C., "Multiple Redundancy in the Measurement of Large Structures," *Annals of the CIRP* (1978).
2. Jelffs, P. A., "Calibration of Containers and Gages," *J. Inst. Pet.*, Vol. 58, No. 561, p 117-25 (May 1972).
3. Mann, D. B., Editor, "LNG Materials and Fluids. A User's Manual of Property Data in Graphic Format - 1st Edition," NBS Cryogenic Data Center (1977).
4. Haight, W. C., Scire, F., Hartsock, R. G., and Hocken, R. J., "Hydrostatic Deformation of Freestanding LNG Cargo Tanks," NBSIR (in preparation).



Appendix F

**Hydrostatic Deformation
of
Freestanding LNG Cargo Tanks**

By

W. C. Haight, F. Scire, R. G. Hartsock, and R. J. Hocken



Tables of Tank Surface Flatness Data

The following tables present the results of the hydrostatic distortion survey conducting on Tank 3 of the El Paso Columbia. The following plane numbering scheme is used:

<u>Plane #</u>	<u>Location</u>
1	Tank Bottom
2	Starboard Chine
3	Starboard Wall
4	Tank Top
5	Port Wall
6	Port Chine
7	Aft Wall
8	Forward Wall

The coordinate system orientation for each surface is as follows:

<u>Plane #</u>	<u>Plane Location</u>	<u>X-Y Origin Location</u>	<u>X-Axis</u>	<u>Y-Axis</u>
2	Starboard Chine	Bottom Aft	Bottom to Top	Aft to Fwd
3	Starboard Wall	Bottom Aft	Bottom to Top	Aft to Fwd
5	Port Wall	Bottom Aft	Bottom to Top	Aft to Fwd
6	Port Chine	Bottom Aft	Bottom to Top	Aft to Fwd
7	Aft Wall	Bottom Port	Bottom to Top	Port to Stbd
8	Fwd Wall	Bottom Port	Bottom to Top	Port to Stbd

For all planes, a smaller Z value indicates an outward displacement of the surface as referenced to the tank interior. The X-Y coordinate spacing is approximately 1524 mm (5 feet) per unit of X or Y. The bottom row of targets on the forward and aft walls starts approximately 914 mm (3 feet) from the weld seam joining the wall to the curved section at the tank bottom.

For this survey, planes 2, 3, 5, 6, 7 and 8 were measured twice; first while the tank was under hydrostatic test and later when the tank was empty in the storage yard. Plane 1 was not measured because the presence of concrete supports beneath the tank in the hydrotest area completely obscured the tank bottom. Plane 4 was not measured because the tank was not completely filled with water and top deformation does not contribute to the tank capacity error in normal tank usage, that is, the tank is not filled with cargo to 100% capacity.

Table 1 presents a summary of the rms deviations from flatness for each tank surface measured, and also reports the rms deviations from flatness for the surfaces comparing the tank containing water vs. not containing water.

From an examination of Table 1, it is concluded that no systematic distortion of the tank occurred during the hydrotest. The reasoning used is as follows. The estimated random error of the survey technique is ± 2.2 mm (refer to Table 1 of "Deformation Measurements on Freestanding LNG Cargo Tanks"). This means the three-standard deviation limit of uncertainty of the survey is ± 6.6 mm. Systematic distortion would be indicated by any rms difference value exceeding this value. Since only one surface exceeded that value, namely plane 6, and since that surface had unique characteristics discussed below, we conclude that systematic distortion due to hydrotesting does not exist.

Tables 2 through 31 present flatness data for each plane measured. Two unique cases exist.

- a) Plane 3, the starboard wall, is reported from Y=1 to Y=20, not to Y=25 as in the case of the other surfaces. This was caused by the laser plane being too close to the wall from Y=21 to Y=25 for the detector rod to function. This surface was not re-measured with a new laser setup because of the hazardous working conditions and time pressure from the tank construction crew for NBS to clear the tank.
- b) Plane 6, the port chine, shows an rms difference deviation 9.0 mm. A closer examination of Table 21 shows that the largest deviations occur at the forward and aft extremes of the surface. For the survey conducted on the hydrostand (reported in Table 19), these end points could not be surveyed because of the tank lifting brackets. The

construction yard staff would not allow these brackets to be removed for the NBS survey, so the points were dropped. Therefore, a detailed comparison of before and after survey data in these regions is invalid.

Table 1

El Paso Columbia - Summary of Flatness Measurements

<u>Plane</u>	<u>Flatness without water, mm</u>	<u>Flatness with water, mm</u>	<u>Flatness differences, mm</u>
2	9.9	11.5	4.8
3	7.7	8.6	3.8
5	6.2	7.9	3.5
6	10.3	11.9	9.0
7	11.1	10.2	5.0
8	12.9	14.5	4.8

NOTE: All table entries represent the rms deviations from flatness in millimeters.

Table 2

El Paso Columbia

Plane 2

Flatness data without water - Z is normal to the plane.

<u>X</u>	<u>Y</u>	<u>Z (mm)</u>
5.	1.	165.40
3.	1.	152.60
1.	1.	135.20
5.	2.	155.70
5.	3.	160.00
3.	3.	152.10
1.	3.	147.30
5.	5.	162.70
3.	5.	156.60
1.	5.	142.30
5.	7.	175.00
3.	7.	151.40
1.	7.	139.30
5.	9.	170.50
3.	9.	160.80
1.	9.	148.30
5.	11.	181.00
3.	11.	165.30
1.	11.	153.20
5.	13.	184.30
3.	13.	163.30
5.	14.	145.30
3.	14.	149.00
1.	14.	151.10
5.	16.	151.10
3.	16.	148.40
1.	16.	149.30
5.	18.	161.00
3.	18.	155.90
1.	18.	157.30
5.	20.	163.50
3.	20.	162.30
1.	20.	161.20
5.	22.	168.60
3.	22.	168.90
1.	22.	166.20
5.	24.	171.00
3.	24.	172.00
1.	24.	167.00
5.	25.	191.20
3.	25.	196.90
1.	25.	180.70

RMS deviation from flatness 9.9 mm

Table 3

El Paso Columbia

Plane 2

Flatness map without water.

Y/X	1	2	3	4	5
1	-11.	-5.	1.	4.	8.
2	-6.	-3.	-0.	2.	-2.
3	-1.	-1.	-1.	-0.	1.
4	-4.	-2.	0.	1.	2.
5	-7.	-3.	2.	2.	2.
6	-10.	-6.	-2.	3.	8.
7	-12.	-9.	-5.	4.	13.
8	-8.	-5.	-1.	4.	10.
9	-4.	-1.	3.	5.	7.
10	-3.	1.	4.	8.	11.
11	-1.	2.	6.	11.	16.
12	-7.	-2.	4.	10.	17.
13	-14.	-6.	2.	10.	18.
14	-6.	-9.	-13.	-18.	-22.
15	-7.	-11.	-14.	-17.	-20.
16	-9.	-12.	-15.	-17.	-18.
17	-6.	-9.	-12.	-13.	-14.
18	-2.	-6.	-9.	-9.	-10.
19	-1.	-4.	-7.	-8.	-9.
20	-0.	-2.	-4.	-6.	-9.
21	2.	-0.	-2.	-4.	-7.
22	3.	2.	1.	-2.	-5.
23	3.	2.	1.	-2.	-5.
24	3.	2.	2.	-1.	-4.
25	15.	21.	26.	21.	15.

Table 4

El Paso Columbia

Plane 2

Flatness data with water - Z is normal to the plane.

<u>X</u>	<u>Y</u>	<u>Z (mm)</u>
3.	1.	234.00
3.	3.	222.90
5.	5.	246.00
3.	5.	214.40
1.	5.	194.00
5.	7.	244.00
3.	7.	204.80
1.	7.	185.00
5.	9.	235.20
3.	9.	208.00
1.	9.	187.20
5.	11.	241.00
3.	11.	206.70
1.	11.	184.80
5.	13.	222.30
3.	13.	200.40
5.	14.	192.50
3.	14.	181.80
1.	14.	174.50
5.	16.	190.20
3.	16.	172.70
1.	16.	171.00
5.	18.	186.40
3.	18.	170.00
1.	18.	171.50
5.	20.	188.80
3.	20.	170.80
1.	20.	169.60
3.	22.	173.00
3.	24.	174.20
3.	25.	198.00

RMS Deviation from flatness 11.5 mm

Table 5

El Paso Columbia

Plane 2

Flatness map with water.

Y/X	1	2	3	4	5
1	-2.	0.	3.	3.	2.
2	-4.	-2.	1.	2.	4.
3	-6.	-4.	-2.	2.	6.
4	-7.	-5.	-3.	2.	8.
5	-9.	-7.	-5.	2.	10.
6	-11.	-9.	-7.	2.	12.
7	-12.	-11.	-9.	2.	13.
8	-9.	-7.	-5.	3.	12.
9	-5.	-3.	-0.	5.	10.
10	-3.	-1.	2.	9.	16.
11	-1.	1.	4.	13.	22.
12	-2.	1.	4.	9.	15.
13	-2.	1.	3.	6.	9.
14	-3.	-8.	-13.	-16.	-18.
15	-2.	-8.	-14.	-16.	-17.
16	-1.	-9.	-16.	-16.	-15.
17	2.	-6.	-15.	-14.	-14.
18	5.	-4.	-13.	-13.	-13.
19	7.	-2.	-10.	-10.	-9.
20	9.	1.	-7.	-6.	-5.
21	11.	4.	-4.	-2.	-1.
22	12.	6.	1.	1.	3.
23	14.	9.	3.	5.	7.
24	16.	11.	8.	8.	11.
25	18.	14.	35.	12.	15.

Table 6

El Paso Columbia

Plane 2

Difference between "with water" and "without water" - Z heights in mm.

Y/X	1	2	3	4	5
1	9.	5.	2.	-2.	-6.
2	2.	2.	1.	0.	7.
3	-5.	-2.	-1.	3.	5.
4	-3.	-3.	-3.	1.	6.
5	-2.	-4.	-7.	0.	7.
6	-1.	-3.	-5.	-1.	4.
7	-1.	-2.	-4.	-2.	0.
8	-0.	-2.	-4.	-1.	2.
9	-0.	-2.	-3.	0.	3.
10	-0.	-1.	-2.	1.	4.
11	-0.	-1.	-2.	2.	6.
12	6.	3.	-0.	-1.	-2.
13	11.	6.	1.	-4.	-9.
14	2.	1.	0.	2.	4.
15	5.	2.	-0.	1.	3.
16	8.	3.	-1.	1.	3.
17	8.	3.	-2.	-1.	-1.
18	7.	2.	-4.	-4.	-4.
19	8.	2.	-3.	-2.	-0.
20	9.	3.	-2.	0.	3.
21	9.	4.	-2.	2.	6.
22	9.	4.	0.	3.	8.
23	11.	6.	2.	6.	11.
24	14.	9.	6.	9.	15.
25	2.	-7.	8.	-9.	-0.

RMS deviation from flatness 4.8 mm

Table 7

El Paso Columbia

Plane 3

Flatness data without water - Z is normal to the plane.

<u>X</u>	<u>Y</u>	<u>Z (mm)</u>	<u>X</u>	<u>Y</u>	<u>Z (mm)</u>
12.	1.	120.90	2.	11.	153.70
10.	1.	138.30	1.	11.	156.90
8.	1.	140.00	10.	13.	156.10
6.	1.	148.00	8.	13.	154.50
4.	1.	147.10	6.	13.	157.90
2.	1.	149.70	4.	13.	158.00
1.	1.	144.90	2.	13.	154.30
10.	2.	119.00	1.	13.	154.90
8.	2.	129.30	10.	14.	159.70
6.	2.	146.80	8.	14.	160.50
4.	2.	143.90	6.	14.	166.50
2.	2.	141.00	4.	14.	164.90
1.	2.	138.50	2.	14.	159.10
10.	3.	120.70	1.	14.	160.30
8.	3.	133.80	12.	16.	131.30
6.	3.	144.50	10.	16.	149.20
4.	3.	141.40	8.	16.	151.90
2.	3.	141.30	6.	16.	155.30
1.	3.	140.20	4.	16.	156.20
10.	5.	122.30	2.	16.	156.60
8.	5.	131.20	1.	16.	156.10
6.	5.	139.30	12.	18.	121.00
4.	5.	140.40	10.	18.	145.90
2.	5.	142.30	8.	18.	152.30
1.	5.	141.50	6.	18.	156.30
10.	7.	124.30	4.	18.	162.20
8.	7.	129.50	2.	18.	161.80
6.	7.	139.80	1.	18.	162.00
4.	7.	142.70	12.	20.	125.00
2.	7.	143.30	10.	20.	146.00
1.	7.	141.80	8.	20.	153.90
12.	9.	121.30	6.	20.	160.00
10.	9.	124.30	4.	20.	161.80
8.	9.	134.70	2.	20.	163.10
6.	9.	141.30	1.	20.	164.70
4.	9.	144.90			
2.	9.	146.90			
1.	9.	151.30			
12.	11.	119.30			
10.	11.	135.90			
8.	11.	143.70			
6.	11.	146.20			
4.	11.	151.20			

RMS deviation from flatness 7.7 mm

Table 8

El Paso Columbia

Plane 3

Flatness map without water.

Y/X	1	2	3	4	5	6	7	8	9	10	11	12
1	-2.	5.	6.	7.	10.	13.	11.	9.	11.	12.	6.	-1.
2	-10.	-5.	-1.	3.	7.	10.	4.	-3.	-5.	-8.	-11.	-14.
3	-9.	-6.	-3.	-1.	3.	7.	4.	1.	-3.	-8.	-12.	-16.
4	-9.	-6.	-4.	-2.	0.	3.	1.	-1.	-5.	-8.	-11.	-14.
5	-10.	-7.	-5.	-4.	-2.	-0.	-2.	-4.	-6.	-8.	-10.	-12.
6	-11.	-7.	-6.	-4.	-2.	-1.	-3.	-6.	-7.	-8.	-9.	-10.
7	-12.	-8.	-6.	-4.	-3.	-2.	-5.	-8.	-8.	-8.	-8.	-9.
8	-8.	-7.	-5.	-4.	-3.	-2.	-4.	-6.	-8.	-9.	-9.	-9.
9	-4.	-6.	-5.	-4.	-3.	-3.	-4.	-5.	-7.	-10.	-9.	-9.
10	-2.	-4.	-3.	-2.	-1.	-1.	-1.	-1.	-3.	-5.	-8.	-11.
11	-1.	-2.	-1.	1.	0.	0.	1.	2.	1.	-1.	-7.	-13.
12	-3.	-2.	0.	3.	4.	5.	6.	7.	8.	8.	7.	5.
13	-5.	-3.	1.	5.	8.	10.	10.	11.	14.	17.	20.	24.
14	-0.	1.	6.	11.	14.	17.	17.	16.	18.	20.	22.	24.
15	-4.	-2.	2.	6.	8.	11.	11.	11.	12.	14.	11.	9.
16	-7.	-4.	-2.	0.	2.	4.	5.	5.	6.	7.	1.	-6.
17	-5.	-2.	0.	2.	3.	4.	4.	4.	5.	5.	-4.	-12.
18	-3.	-1.	2.	4.	4.	3.	3.	4.	3.	2.	-8.	-18.
19	-3.	-1.	1.	3.	3.	4.	4.	3.	2.	1.	-8.	-17.
20	-2.	-2.	0.	2.	3.	5.	4.	3.	2.	-0.	-8.	-16.

Table 9

El Paso Columbia

Plane 3

Flatness data with water - Z is normal to the plane.

<u>X</u>	<u>Y</u>	<u>Z (mm)</u>	<u>X</u>	<u>Y</u>	<u>Z (mm)</u>
12.	1.	159.30	2.	11.	135.90
10.	1.	171.40	1.	11.	137.30
8.	1.	171.70	10.	13.	144.70
6.	1.	175.90	8.	13.	140.20
4.	1.	172.00	6.	13.	142.00
2.	1.	171.30	4.	13.	136.00
12.	2.	134.10	2.	13.	128.30
10.	2.	149.50	1.	13.	129.00
8.	2.	159.90	12.	14.	123.30
6.	2.	171.20	10.	14.	144.00
4.	2.	165.20	8.	14.	141.10
2.	2.	160.10	6.	14.	144.80
12.	3.	135.20	4.	14.	138.10
10.	3.	148.90	2.	14.	128.50
8.	3.	158.40	1.	14.	127.20
6.	3.	165.70	12.	16.	112.00
4.	3.	159.10	10.	16.	125.30
2.	3.	157.40	8.	16.	125.10
12.	5.	135.30	6.	16.	125.30
10.	5.	141.10	4.	16.	123.10
8.	5.	148.30	2.	16.	118.00
6.	5.	153.90	1.	16.	112.20
4.	5.	150.10	10.	18.	113.30
2.	5.	149.10	8.	18.	118.10
1.	5.	148.90	6.	18.	118.50
12.	7.	122.00	4.	18.	118.30
10.	7.	137.00	2.	18.	112.10
8.	7.	138.00	6.	20.	114.20
6.	7.	144.70			
4.	7.	141.40			
2.	7.	132.90			
1.	7.	138.50			
12.	9.	128.30			
10.	9.	128.30			
8.	9.	132.90			
6.	9.	138.00			
4.	9.	137.90			
2.	9.	141.10			
1.	9.	138.50			
12.	11.	118.00			
10.	11.	133.80			
8.	11.	136.10			
6.	11.	136.00			
4.	11.	135.10			

RMS Deviation from flatness 8.6 mm

Table 10

El Paso Columbia

Plane 3

Flatness map with water.

Y/X	1	2	3	4	5	6	7	8	9	10	11	12
1	4.	6.	7.	8.	11.	14.	13.	12.	12.	13.	8.	3.
2	-6.	-3.	0.	4.	8.	12.	7.	2.	-2.	-6.	-13.	-20.
3	-5.	-3.	-1.	1.	5.	9.	6.	4.	-0.	-4.	-10.	-16.
4	-6.	-5.	-3.	-1.	2.	6.	4.	1.	-2.	-5.	-9.	-13.
5	-7.	-6.	-5.	-3.	-0.	3.	1.	-1.	-4.	-6.	-8.	-10.
6	-10.	-11.	-8.	-5.	-2.	1.	-1.	-4.	-5.	-6.	-10.	-14.
7	-12.	-17.	-12.	-6.	-4.	-1.	-4.	-6.	-6.	-5.	-12.	-18.
8	-9.	-10.	-8.	-6.	-4.	-2.	-4.	-6.	-6.	-7.	-10.	-12.
9	-7.	-3.	-4.	-5.	-4.	-3.	-4.	-6.	-7.	-9.	-8.	-7.
10	-5.	-3.	-3.	-3.	-2.	-1.	-1.	-2.	-2.	-3.	-6.	-9.
11	-3.	-3.	-3.	-2.	-1.	1.	2.	3.	3.	2.	-5.	-12.
12	-4.	-4.	-2.	1.	4.	6.	7.	7.	9.	10.	9.	7.
13	-6.	-5.	-1.	4.	8.	12.	12.	12.	15.	19.	22.	25.
14	-5.	-3.	3.	9.	13.	18.	17.	16.	18.	21.	11.	2.
15	-10.	-5.	-0.	4.	7.	10.	10.	10.	12.	14.	6.	-1.
16	-14.	-8.	-4.	-1.	1.	3.	4.	5.	6.	7.	1.	-4.
17	-13.	-8.	-4.	-0.	1.	3.	3.	4.	4.	4.	0.	-3.
18	-12.	-8.	-4.	-0.	1.	2.	3.	3.	2.	1.	-1.	-2.
19	-11.	-8.	-4.	0.	1.	1.	2.	3.	0.	-3.	-2.	-1.
20	-10.	-9.	-4.	0.	0.	3.	1.	2.	-2.	-6.	-3.	-1.

Table 11

El Paso Columbia

Plane 3

Difference between "with water" and "without water" - Z heights in mm.

Y/X	1	2	3	4	5	6	7	8	9	10	11	12
1	6.	1.	1.	1.	1.	1.	2.	2.	2.	1.	2.	4.
2	3.	2.	2.	1.	1.	2.	3.	5.	4.	2.	-2.	-6.
3	4.	3.	2.	1.	2.	2.	2.	3.	3.	4.	2.	0.
4	3.	2.	1.	1.	2.	3.	3.	3.	3.	3.	2.	1.
5	3.	1.	1.	1.	2.	3.	3.	3.	2.	2.	2.	2.
6	1.	-4.	-3.	-1.	0.	2.	2.	2.	2.	2.	-1.	-4.
7	-1.	-9.	-6.	-3.	-1.	1.	1.	2.	2.	3.	-3.	-10.
8	-2.	-3.	-2.	-2.	-1.	0.	0.	0.	1.	2.	-1.	-4.
9	-3.	3.	1.	-1.	-0.	0.	-1.	-1.	0.	2.	2.	2.
10	-2.	1.	-1.	-2.	-1.	0.	-0.	-0.	1.	2.	2.	2.
11	-2.	-2.	-2.	-3.	-1.	1.	0.	0.	2.	3.	2.	1.
12	-1.	-2.	-2.	-2.	-0.	1.	1.	1.	1.	2.	2.	1.
13	-1.	-2.	-2.	-1.	1.	2.	2.	1.	1.	1.	1.	1.
14	-4.	-3.	-3.	-2.	-1.	0.	0.	-0.	0.	1.	-11.	-22.
15	-6.	-3.	-2.	-2.	-1.	-0.	-0.	-0.	0.	0.	-5.	-10.
16	-8.	-4.	-2.	-1.	-1.	-1.	-0.	-0.	-0.	-0.	1.	2.
17	-8.	-6.	-4.	-3.	-2.	-1.	-1.	-0.	-0.	-1.	4.	9.
18	-9.	-7.	-6.	-4.	-3.	-1.	-1.	-0.	-1.	-1.	7.	16.
19	-8.	-7.	-5.	-3.	-3.	-3.	-2.	-1.	-2.	-4.	6.	16.
20	-8.	-7.	-4.	-1.	-3.	-2.	-3.	-1.	-4.	-6.	5.	16.

RMS deviation from flatness 3.8 mm

Table 12

El Paso Columbia

Plane 5

Flatness data without water - Z is normal to the plane.

<u>X</u>	<u>Y</u>	<u>Z (mm)</u>	<u>X</u>	<u>Y</u>	<u>Z (mm)</u>	<u>X</u>	<u>Y</u>	<u>Z (mm)</u>
12.	1.	145.70	6.	11.	119.90	8.	23.	127.00
12.	1.	144.30	4.	11.	119.50	6.	23.	134.70
8.	1.	140.30	2.	11.	121.30	4.	23.	135.00
6.	1.	132.60	1.	11.	122.80	2.	23.	132.30
4.	1.	127.20	12.	12.	124.90	1.	23.	135.70
2.	1.	137.20	10.	12.	130.80	10.	24.	118.70
1.	1.	139.90	8.	12.	123.30	8.	24.	124.50
12.	2.	139.60	6.	12.	123.20	6.	24.	135.60
10.	2.	140.00	4.	12.	121.20	4.	24.	135.30
8.	2.	138.20	2.	12.	125.30	2.	24.	131.30
6.	2.	135.30	1.	12.	123.90	1.	24.	133.30
4.	2.	132.30	10.	13.	134.30	12.	25.	118.40
2.	2.	137.10	8.	13.	132.20	10.	25.	122.00
1.	2.	134.10	6.	13.	130.90	8.	25.	122.60
12.	3.	137.20	4.	13.	129.50	6.	25.	129.90
10.	3.	140.30	2.	13.	125.80	4.	25.	130.20
8.	3.	135.60	1.	13.	125.30	2.	25.	130.90
6.	3.	129.80	12.	15.	127.70	1.	25.	133.30
4.	3.	128.40	10.	15.	124.40			
2.	3.	131.90	8.	15.	130.80			
1.	3.	133.10	6.	15.	133.60			
12.	5.	124.60	4.	15.	125.90			
10.	5.	133.30	2.	15.	121.90			
8.	5.	127.20	1.	15.	121.80			
6.	5.	120.90	12.	17.	124.90			
4.	5.	119.60	10.	17.	120.90			
2.	5.	127.20	8.	17.	124.90			
1.	5.	131.70	6.	17.	132.30			
10.	7.	129.10	4.	17.	126.80			
8.	7.	122.90	2.	17.	124.70			
6.	7.	119.30	1.	17.	123.00			
4.	7.	119.30	10.	19.	118.00			
2.	7.	124.90	8.	19.	122.90			
1.	7.	130.30	6.	19.	127.90			
12.	9.	124.90	4.	19.	124.90			
10.	9.	129.40	2.	19.	125.30			
8.	9.	121.90	1.	19.	126.20			
6.	9.	119.10	10.	21.	117.60			
4.	9.	118.40	8.	21.	127.50			
2.	9.	122.90	6.	21.	132.00			
1.	9.	129.90	4.	21.	129.20			
12.	11.	126.30	2.	21.	128.70			
1.	11.	127.20	1.	21.	132.70			
8.	11.	120.30	10.	23.	114.90			

RMS deviation from flatness 6.2 mm

Table 13

El Paso Columbia

Plane 5

Flatness map without water.

Y/X	1	2	3	4	5	6	7	8	9	10	11	12
1	7.	5.	-0.	-5.	-2.	1.	5.	9.	10.	11.	12.	13.
2	2.	5.	2.	0.	2.	4.	5.	7.	8.	9.	9.	9.
3	1.	-0.	-2.	-3.	-2.	-2.	1.	5.	7.	10.	8.	7.
4	0.	-2.	-5.	-7.	-7.	-6.	-3.	1.	4.	6.	4.	1.
5	0.	-4.	-8.	-12.	-11.	-10.	-7.	-3.	0.	3.	-1.	-5.
6	-0.	-5.	-8.	-11.	-11.	-10.	-8.	-5.	-2.	1.	1.	1.
7	-1.	-6.	-9.	-11.	-11.	-11.	-9.	-7.	-4.	-0.	3.	6.
8	-1.	-7.	-9.	-11.	-11.	-11.	-9.	-7.	-4.	0.	1.	1.
9	-1.	-7.	-9.	-12.	-11.	-10.	-9.	-7.	-3.	1.	-2.	-4.
10	-4.	-8.	-9.	-11.	-10.	-10.	-9.	-8.	-5.	-2.	-2.	-3.
11	-7.	-8.	-9.	-10.	-9.	-9.	-9.	-8.	-7.	-5.	-3.	-2.
12	-6.	-4.	-6.	-8.	-7.	-5.	-5.	-5.	-1.	3.	0.	-3.
13	-4.	-3.	-1.	1.	2.	3.	3.	4.	5.	7.	8.	9.
14	-5.	-5.	-3.	-1.	2.	4.	4.	4.	3.	2.	4.	5.
15	-7.	-7.	-4.	-2.	2.	6.	5.	3.	0.	-3.	-1.	1.
16	-6.	-5.	-3.	-1.	2.	5.	3.	1.	-2.	-4.	-2.	-0.
17	-5.	-3.	-2.	-1.	2.	5.	2.	-2.	-4.	-6.	-3.	-1.
18	-3.	-3.	-2.	-1.	1.	3.	0.	-3.	-5.	-7.	-7.	-7.
19	-1.	-2.	-2.	-2.	-0.	1.	-1.	-3.	-6.	-8.	-10.	-12.
20	2.	0.	0.	0.	2.	4.	1.	-1.	-4.	-8.	-11.	-15.
21	6.	2.	2.	3.	4.	6.	4.	2.	-3.	-8.	-12.	-17.
22	8.	4.	5.	6.	7.	8.	5.	2.	-3.	-9.	-14.	-19.
23	9.	6.	8.	9.	9.	9.	6.	2.	-4.	-10.	-16.	-22.
24	7.	6.	8.	10.	10.	11.	5.	-0.	-3.	-6.	-8.	-11.
25	13.	5.	5.	5.	5.	5.	2.	-2.	-2.	-2.	-4.	-5.

Table 14

El Paso Columbia

Plane 5

Flatness data with water - Z is normal to the plane.

<u>X</u>	<u>Y</u>	<u>Z (mm)</u>	<u>X</u>	<u>Y</u>	<u>Z (mm)</u>	<u>X</u>	<u>Y</u>	<u>Z (mm)</u>
12.	1.	143.70	8.	11.	137.90	2.	21.	160.00
10.	1.	146.10	6.	11.	135.20	1.	21.	161.00
8.	1.	133.50	4.	11.	129.30	12.	23.	145.20
6.	1.	125.00	2.	11.	132.00	10.	23.	156.80
4.	1.	123.00	1.	11.	130.80	8.	23.	169.20
2.	1.	131.10	12.	12.	147.00	6.	23.	175.00
1.	1.	133.30	10.	12.	150.90	4.	23.	172.10
12.	2.	139.80	8.	12.	144.10	2.	23.	169.00
10.	2.	144.00	6.	12.	141.30	1.	23.	171.10
8.	2.	136.00	4.	12.	136.80	12.	24.	145.90
6.	2.	133.30	2.	12.	138.10	10.	24.	161.10
4.	2.	129.30	1.	12.	134.00	8.	24.	168.00
2.	2.	134.30	10.	13.	155.10	6.	24.	179.30
1.	2.	129.50	8.	13.	152.30	4.	24.	176.70
12.	3.	135.30	6.	13.	150.30	2.	24.	174.10
10.	3.	142.00	4.	13.	148.10	1.	24.	172.50
8.	3.	132.10	2.	13.	142.30	12.	25.	169.70
6.	3.	129.70	1.	13.	140.10	10.	25.	173.00
4.	3.	125.10	12.	15.	157.40	8.	25.	166.00
2.	3.	130.90	10.	15.	153.20	6.	25.	168.00
1.	3.	127.30	8.	15.	156.50	4.	25.	169.20
12.	5.	131.10	6.	15.	159.50	2.	25.	164.00
10.	5.	139.00	4.	15.	149.50	1.	25.	178.00
8.	5.	129.00	2.	15.	143.00			
6.	5.	123.20	1.	15.	139.70			
4.	5.	119.20	12.	17.	158.80			
2.	5.	127.10	10.	17.	152.40			
1.	5.	129.30	8.	17.	157.30			
12.	7.	119.90	6.	17.	159.50			
10.	7.	141.30	4.	17.	153.60			
8.	7.	134.00	2.	17.	151.50			
6.	7.	126.80	1.	17.	147.30			
4.	7.	125.00	12.	19.	141.00			
2.	7.	129.30	10.	19.	151.50			
1.	7.	131.40	8.	19.	156.80			
12.	9.	141.10	6.	19.	165.60			
10.	9.	141.90	4.	19.	156.30			
8.	9.	135.20	2.	19.	155.00			
6.	9.	129.70	1.	19.	155.60			
4.	9.	126.80	12.	21.	149.00			
2.	9.	127.00	10.	21.	154.20			
1.	9.	132.30	8.	21.	161.20			
12.	11.	142.80	6.	21.	166.80			
10.	11.	146.70	4.	21.	163.10			

RMS Deviation from flatness 7.9 mm

Table 15

El Paso Columbia

Plane 5

Flatness map with water.

Y/X	1	2	3	4	5	6	7	8	9	10	11	12
1	6.	4.	-0.	-5.	-4.	-3.	1.	6.	12.	18.	17.	15.
2	1.	5.	3.	0.	2.	4.	5.	6.	10.	14.	12.	10.
3	-3.	0.	-3.	-6.	-3.	-1.	-0.	1.	6.	11.	7.	4.
4	-4.	-3.	-7.	-10.	-8.	-6.	-4.	-2.	3.	8.	4.	0.
5	-4.	-7.	-11.	-15.	-13.	-11.	-8.	-5.	-0.	4.	0.	-4.
6	-5.	-7.	-10.	-13.	-12.	-11.	-8.	-4.	-0.	4.	-3.	-11.
7	-5.	-8.	-10.	-12.	-11.	-11.	-7.	-4.	0.	4.	-7.	-18.
8	-7.	-10.	-12.	-13.	-12.	-11.	-8.	-5.	-1.	2.	-3.	-9.
9	-8.	-13.	-13.	-13.	-12.	-11.	-8.	-6.	-2.	1.	0.	0.
10	-10.	-12.	-13.	-14.	-12.	-10.	-8.	-6.	-2.	2.	0.	-1.
11	-12.	-11.	-13.	-14.	-11.	-9.	-7.	-6.	-2.	3.	0.	-2.
12	-11.	-7.	-8.	-8.	-6.	-4.	-3.	-1.	2.	5.	3.	1.
13	-6.	-4.	-1.	1.	2.	3.	4.	5.	6.	8.	9.	10.
14	-8.	-5.	-2.	1.	3.	6.	6.	6.	5.	5.	7.	9.
15	-10.	-7.	-3.	-0.	5.	9.	8.	6.	4.	3.	5.	7.
16	-8.	-4.	-2.	0.	4.	8.	6.	5.	3.	1.	3.	6.
17	-5.	-1.	-0.	1.	3.	6.	5.	4.	1.	-1.	2.	5.
18	-3.	-1.	-0.	0.	4.	8.	5.	2.	-1.	-3.	-4.	-6.
19	-0.	-1.	-0.	0.	5.	9.	5.	0.	-3.	-5.	-11.	-16.
20	1.	0.	1.	2.	5.	8.	4.	1.	-2.	-6.	-10.	-14.
21	2.	1.	2.	4.	5.	7.	4.	1.	-2.	-6.	-9.	-11.
22	5.	4.	5.	7.	8.	10.	7.	4.	-1.	-6.	-10.	-15.
23	9.	7.	8.	10.	11.	12.	9.	6.	-0.	-6.	-12.	-18.
24	9.	10.	11.	13.	14.	15.	9.	3.	-0.	-4.	-11.	-19.
25	13.	-2.	1.	3.	3.	2.	1.	-0.	3.	7.	5.	3.

Table 16

El Paso Columbia

Plane 5

Difference between "with water" and "without water" - Z heights in mm.

Y/X	1	2	3	4	5	6	7	8	9	10	11	12
1	-1.	-1.	0.	1.	-1.	-3.	-3.	-3.	2.	7.	4.	2.
2	-1.	1.	0.	-0.	0.	0.	0.	-0.	2.	5.	3.	1.
3	-4.	1.	-1.	-2.	-1.	0.	-2.	-4.	-1.	1.	-1.	-3.
4	-4.	-1.	-2.	-3.	-2.	-0.	-2.	-3.	-1.	1.	0.	-1.
5	-4.	-2.	-3.	-3.	-2.	-1.	-2.	-2.	-0.	1.	1.	1.
6	-4.	-2.	-2.	-2.	-1.	-0.	0.	1.	2.	3.	-4.	-11.
7	-5.	-2.	-1.	-1.	-0.	0.	2.	3.	4.	4.	-10.	-24.
8	-6.	-4.	-3.	-1.	-1.	0.	1.	3.	2.	2.	-4.	-10.
9	-7.	-6.	-4.	-2.	-1.	-0.	1.	2.	1.	0.	2.	4.
10	-6.	-4.	-4.	-3.	-2.	0.	1.	2.	3.	4.	3.	2.
11	-5.	-3.	-4.	-4.	-2.	1.	1.	2.	5.	3.	4.	0.
12	-5.	-3.	-2.	-0.	1.	1.	3.	4.	3.	2.	3.	4.
13	-2.	-1.	-0.	1.	1.	1.	1.	1.	1.	1.	1.	1.
14	-3.	-0.	0.	1.	2.	2.	2.	2.	3.	3.	3.	3.
15	-3.	0.	1.	2.	3.	4.	3.	3.	4.	5.	6.	6.
16	-2.	1.	1.	2.	2.	2.	3.	4.	5.	5.	5.	6.
17	-0.	2.	2.	1.	1.	1.	3.	6.	5.	4.	5.	6.
18	0.	1.	2.	2.	3.	4.	5.	5.	4.	3.	2.	1.
19	1.	1.	2.	2.	5.	8.	6.	3.	3.	2.	-1.	-4.
20	-2.	-0.	1.	1.	3.	4.	3.	1.	2.	2.	2.	1.
21	-4.	-1.	-0.	1.	1.	1.	0.	-1.	1.	2.	4.	6.
22	-2.	-0.	0.	1.	1.	2.	2.	2.	2.	3.	4.	5.
23	-1.	0.	0.	0.	2.	3.	4.	4.	4.	3.	3.	3.
24	1.	5.	4.	3.	3.	4.	4.	4.	3.	2.	-3.	-8.
25	-0.	-7.	-4.	-2.	-2.	-3.	-1.	2.	5.	9.	8.	8.

RMS deviation from flatness 3.5 mm

Table 17

El Paso Columbia

Plane 6

Flatness data without water - Z is normal to the plane.

<u>X</u>	<u>Y</u>	<u>Z (mm)</u>
5.	1.	142.10
3.	1.	165.80
5.	2.	132.00
3.	2.	138.10
5.	3.	131.10
3.	3.	139.80
5.	5.	130.10
3.	5.	138.30
1.	5.	136.20
5.	7.	134.30
3.	7.	132.90
1.	7.	147.90
5.	9.	137.30
3.	9.	131.30
1.	9.	137.90
5.	11.	137.30
3.	11.	136.20
1.	11.	142.30
5.	12.	133.50
3.	12.	130.30
1.	12.	141.00
5.	13.	145.80
3.	13.	142.10
5.	15.	149.10
3.	15.	148.60
1.	15.	147.10
5.	17.	154.10
3.	17.	149.60
1.	17.	145.20
5.	19.	161.30
3.	19.	150.30
1.	19.	144.70
5.	21.	168.90
3.	21.	152.00
1.	21.	133.10
5.	23.	175.10
3.	23.	156.20
1.	23.	137.80
5.	25.	181.30
3.	25.	175.70
1.	25.	164.90

RMS deviation from flatness 10.3 mm

Table 18

El Paso Columbia

Plane 6

Flatness map without water.

Y/X	1	2	3	4	5
1	56.	43.	31.	18.	6.
2	9.	6.	2.	-2.	-5.
3	13.	8.	3.	-2.	-7.
4	6.	3.	1.	-4.	-9.
5	-1.	-1.	-1.	-5.	-10.
6	3.	-0.	-4.	-7.	-9.
7	8.	0.	-8.	-8.	-8.
8	2.	-4.	-10.	-8.	-7.
9	-4.	-8.	-11.	-9.	-7.
10	-2.	-6.	-10.	-9.	-8.
11	-1.	-5.	-8.	-9.	-9.
12	-3.	-9.	-15.	-14.	-13.
13	-7.	-6.	-4.	-3.	-2.
14	-4.	-3.	-2.	-2.	-1.
15	-0.	0.	0.	-0.	-1.
16	-2.	-1.	-0.	0.	1.
17	-4.	-2.	-1.	1.	2.
18	-5.	-3.	-1.	2.	5.
19	-6.	-4.	-2.	3.	8.
20	-13.	-8.	-2.	4.	11.
21	-20.	-11.	-2.	6.	13.
22	-19.	-10.	-1.	7.	16.
23	-17.	-9.	0.	9.	18.
24	-5.	2.	9.	14.	20.
25	8.	13.	18.	20.	22.

Table 19

El Paso Columbia

Plane 6

Flatness data with water - Z is normal to the plane.

<u>X</u>	<u>Y</u>	<u>Z (mm)</u>
3.	1.	261.80
1.	1.	234.60
3.	2.	231.00
3.	3.	226.70
5.	5.	239.50
3.	5.	216.00
1.	5.	198.20
5.	7.	229.40
3.	7.	200.00
1.	7.	203.30
5.	9.	228.00
3.	9.	193.90
1.	9.	187.10
5.	11.	223.10
3.	11.	196.00
1.	11.	186.00
5.	12.	217.00
3.	12.	194.10
5.	13.	227.40
3.	13.	198.00
1.	13.	172.60
5.	15.	222.50
3.	15.	196.70
1.	15.	178.30
5.	17.	222.40
3.	17.	190.30
1.	17.	173.70
5.	19.	221.10
3.	19.	182.60
1.	19.	159.60
5.	21.	226.50
3.	21.	181.40
1.	21.	147.10
3.	23.	183.10
3.	25.	203.10
1.	25.	168.80

RMS Deviation from flatness 11.9 mm

Table 20

El Paso Columbia

Plane 6

Flatness map with water.

Y/X	1	2	3	4	5
1	22.	26.	30.	33.	37.
2	15.	18.	1.	24.	27.
3	9.	10.	-1.	14.	17.
4	2.	2.	2.	5.	7.
5	-5.	-6.	-7.	-5.	-3.
6	0.	-6.	-12.	-9.	-6.
7	5.	-7.	-18.	-13.	-8.
8	-1.	-10.	-19.	-13.	-7.
9	-7.	-13.	-19.	-12.	-5.
10	-5.	-10.	-16.	-10.	-5.
11	-3.	-8.	-12.	-9.	-5.
12	-15.	-14.	-12.	-10.	-9.
13	-12.	-9.	-6.	-1.	4.
14	-6.	-5.	-4.	0.	4.
15	-1.	-2.	-2.	1.	4.
16	-1.	-2.	-3.	2.	6.
17	-1.	-2.	-4.	2.	9.
18	-6.	-5.	-5.	2.	10.
19	-10.	-9.	-7.	3.	12.
20	-14.	-10.	-5.	6.	17.
21	-18.	-11.	-3.	9.	22.
22	-10.	-3.	4.	16.	27.
23	-2.	5.	3.	22.	32.
24	5.	13.	20.	29.	37.
25	13.	21.	28.	35.	43.

Table 21

El Paso Columbia

Plane 6

Difference between "with water" and "without water" - Z heights in mm.

Y/X	1	2	3	4	5
1	-34.	-17.	-1.	15.	31.
2	6.	12.	-1.	25.	32.
3	-4.	2.	-4.	16.	24.
4	-4.	-1.	1.	8.	16.
5	-3.	-5.	-6.	0.	7.
6	-3.	-6.	-8.	-2.	3.
7	-3.	-7.	-10.	-5.	-0.
8	-3.	-6.	-9.	-4.	1.
9	-3.	-5.	-8.	-3.	2.
10	-2.	-4.	-6.	-2.	3.
11	-2.	-3.	-4.	-0.	4.
12	-12.	-4.	3.	4.	5.
13	-5.	-3.	-1.	2.	6.
14	-3.	-2.	-2.	2.	5.
15	-1.	-2.	-2.	1.	5.
16	1.	-1.	-3.	1.	5.
17	3.	0.	-3.	1.	6.
18	-0.	-2.	-4.	1.	5.
19	-4.	-4.	-5.	-0.	4.
20	-1.	-2.	-3.	2.	6.
21	2.	0.	-1.	4.	9.
22	8.	7.	6.	9.	12.
23	15.	14.	3.	13.	15.
24	10.	11.	11.	14.	18.
25	5.	8.	10.	15.	21.

RMS deviation from flatness 9.0 mm

Table 22

El Paso Columbia

Plane 7

Flatness data without water - Z is normal to the plane.

<u>X</u>	<u>Y</u>	<u>Z (mm)</u>	<u>X</u>	<u>Y</u>	<u>Z (mm)</u>	<u>X</u>	<u>Y</u>	<u>Z (mm)</u>
15.	25.	217.10	15.	15.	215.30	7.	6.	235.80
13.	25.	247.30	13.	15.	245.30	5.	6.	245.30
11.	25.	241.50	11.	15.	245.10	3.	6.	255.00
9.	25.	239.20	9.	15.	238.90	1.	6.	260.00
7.	25.	236.00	7.	15.	244.10	15.	4.	195.20
5.	25.	231.10	5.	15.	249.10	13.	4.	212.30
15.	24.	213.50	3.	15.	260.00	11.	4.	220.00
13.	24.	247.20	1.	15.	274.30	9.	4.	227.00
11.	24.	252.70	13.	13.	234.10	7.	4.	231.80
9.	24.	244.30	11.	13.	238.70	5.	4.	242.30
7.	24.	242.70	9.	13.	242.00	3.	4.	248.90
5.	24.	232.50	7.	13.	245.30	15.	2.	183.80
15.	23.	206.30	5.	13.	255.50	13.	2.	210.00
13.	23.	244.30	3.	13.	266.20	11.	2.	221.70
11.	23.	247.30	1.	13.	270.80	9.	2.	232.50
9.	23.	241.10	15.	12.	213.30	7.	2.	239.10
7.	23.	239.00	13.	12.	229.00	5.	2.	244.80
5.	23.	233.00	11.	12.	235.30	15.	1.	173.80
3.	23.	235.60	9.	12.	236.30	13.	1.	195.10
15.	21.	204.80	7.	12.	243.50	11.	1.	206.80
13.	21.	242.00	5.	12.	251.30	9.	1.	213.30
11.	21.	247.40	3.	12.	269.30	7.	1.	222.50
9.	21.	245.90	1.	12.	278.30	5.	1.	231.30
7.	21.	242.80	15.	10.	210.90			
5.	21.	238.00	13.	10.	222.40			
3.	21.	244.50	11.	10.	227.80			
1.	21.	259.00	9.	10.	232.50			
15.	19.	199.00	7.	10.	240.20			
13.	19.	240.50	5.	10.	250.10			
11.	19.	248.20	3.	10.	264.80			
9.	19.	244.60	1.	10.	268.80			
7.	19.	242.30	15.	8.	201.00			
5.	19.	244.90	13.	8.	211.40			
3.	19.	252.10	11.	8.	229.10			
1.	19.	267.10	9.	8.	231.00			
15.	17.	207.30	7.	8.	238.70			
13.	17.	240.50	5.	8.	248.70			
11.	17.	243.30	3.	8.	261.90			
9.	17.	243.00	1.	8.	264.20			
7.	17.	248.10	15.	6.	210.00			
5.	17.	249.30	13.	6.	212.30			
3.	17.	237.30	11.	6.	225.40			
1.	17.	270.20	9.	6.	231.00			

RMS deviation from flatness 11.1 mm

Table 23

El Paso Columbia

Plane 7

Flatness map without water.

Y/X	1	2	3	4	5	6	7	8	9	10	11	12	13	14	15
1	-8.	-9.	-10.	-10.	-11.	-12.	-12.	-13.	-14.	-14.	-13.	-15.	-18.	-24.	-31.
2	-2.	-1.	0.	1.	2.	3.	4.	4.	4.	3.	1.	-1.	-3.	-13.	-22.
3	-3.	-2.	-1.	-1.	0.	-0.	-1.	0.	1.	0.	-0.	-2.	-3.	-10.	-17.
4	-3.	-3.	-3.	-2.	-2.	-3.	-5.	-4.	-2.	-2.	-2.	-2.	-2.	-7.	-12.
5	-2.	-1.	-0.	-1.	-1.	-2.	-4.	-2.	-1.	-0.	0.	-1.	-3.	-4.	-5.
6	-0.	1.	2.	1.	-0.	-1.	-2.	-1.	0.	1.	2.	-1.	-4.	-1.	2.
7	1.	3.	5.	3.	1.	-0.	-1.	-1.	-0.	2.	3.	-1.	-5.	-4.	-4.
8	3.	5.	8.	5.	2.	1.	-1.	-1.	-1.	2.	5.	-1.	-6.	-7.	-9.
9	4.	6.	9.	5.	3.	1.	-1.	-1.	-1.	1.	3.	1.	-1.	-3.	-4.
10	6.	8.	9.	6.	3.	1.	-0.	-1.	-1.	1.	2.	3.	4.	2.	0.
11	10.	10.	11.	6.	2.	1.	1.	1.	1.	3.	5.	6.	7.	4.	0.
12	14.	13.	13.	7.	3.	2.	2.	2.	2.	5.	8.	9.	9.	5.	1.
13	6.	7.	9.	7.	6.	4.	3.	5.	7.	9.	11.	12.	14.	15.	17.
14	7.	6.	5.	3.	2.	2.	1.	3.	5.	9.	14.	16.	19.	14.	9.
15	8.	5.	1.	-0.	-2.	-1.	0.	1.	2.	9.	16.	20.	24.	12.	1.
16	6.	-3.	-11.	-7.	-3.	-1.	2.	3.	4.	9.	15.	18.	21.	9.	-4.
17	3.	-10.	-23.	-13.	-3.	-0.	3.	4.	5.	9.	13.	15.	18.	5.	-3.
18	1.	-8.	-16.	-11.	-6.	-3.	-1.	2.	5.	10.	15.	16.	17.	2.	-13.
19	-2.	-5.	-9.	-9.	-9.	-7.	-4.	1.	6.	11.	17.	16.	16.	-1.	-18.
20	-6.	-10.	-14.	-13.	-13.	-9.	-5.	1.	6.	11.	16.	16.	16.	0.	-16.
21	-11.	-14.	-18.	-18.	-17.	-11.	-5.	0.	6.	10.	15.	16.	17.	2.	-13.
22	-22.	-23.	-23.	-22.	-20.	-14.	-7.	-2.	3.	8.	14.	15.	17.	2.	-13.
23	-33.	-31.	-28.	-26.	-23.	-17.	-10.	-5.	-0.	6.	13.	15.	18.	2.	-13.
24	-60.	-51.	-42.	-33.	-25.	-16.	-7.	-2.	2.	10.	18.	19.	20.	7.	-7.
25	-51.	-45.	-39.	-33.	-27.	-20.	-14.	-9.	-4.	1.	6.	13.	19.	3.	-4.

Table 24

El Paso Columbia

Plane 7

Flatness data with water - Z is normal to the plane.

<u>X</u>	<u>Y</u>	<u>Z (mm)</u>	<u>X</u>	<u>Y</u>	<u>Z (mm)</u>	<u>X</u>	<u>Y</u>	<u>Z (mm)</u>
13.	25.	298.50	3.	15.	260.60	3.	6.	254.50
11.	25.	282.20	1.	15.	262.00	1.	6.	247.50
9.	25.	267.50	13.	13.	287.00	13.	4.	267.50
7.	25.	255.80	11.	13.	279.90	11.	4.	265.50
5.	25.	239.00	9.	13.	272.80	9.	4.	262.80
13.	24.	300.70	7.	13.	266.00	7.	4.	256.00
11.	24.	293.30	5.	13.	264.80	5.	4.	252.90
9.	24.	274.60	3.	13.	265.20	3.	4.	251.60
7.	24.	260.50	1.	13.	262.10	13.	2.	266.40
5.	24.	240.00	13.	12.	284.10	11.	2.	266.30
3.	24.	227.90	11.	12.	277.40	9.	2.	267.50
11.	23.	288.70	9.	12.	269.00	7.	2.	261.00
9.	23.	272.20	7.	12.	262.00	5.	2.	256.10
7.	23.	257.50	5.	12.	260.00	3.	2.	247.80
5.	23.	239.90	3.	12.	267.50	13.	1.	253.00
3.	23.	235.30	1.	12.	262.80	11.	1.	252.80
1.	23.	243.80	13.	10.	279.00	9.	1.	251.20
13.	21.	295.20	11.	10.	272.30	7.	1.	247.00
11.	21.	288.10	9.	10.	265.20	5.	1.	244.40
9.	21.	275.50	7.	10.	260.90			
7.	21.	259.50	5.	10.	258.00			
5.	21.	243.50	3.	10.	264.00			
3.	21.	241.50	1.	10.	257.10			
1.	21.	245.00	13.	8.	274.10			
13.	19.	294.00	11.	8.	273.80			
11.	19.	290.30	9.	8.	265.10			
9.	19.	274.70	7.	8.	259.50			
7.	19.	262.10	5.	8.	255.90			
5.	19.	249.20	3.	8.	261.00			
3.	19.	249.90	1.	8.	255.50			
1.	19.	255.90	13.	6.	272.10			
13.	17.	296.90	11.	6.	273.60			
11.	17.	296.90	9.	6.	266.70			
9.	17.	273.00	7.	6.	256.60			
7.	17.	264.70	5.	6.	255.60			
5.	17.	253.90						
3.	17.	256.00						
1.	17.	256.70						
13.	15.	299.80						
11.	15.	286.10						
9.	15.	270.40						
7.	15.	263.10						
5.	15.	257.80						

RMS Deviation from flatness 10.2 mm

Table 25

El Paso Columbia

Plane 7

Flatness map with water.

Y/X	1	2	3	4	5	6	7	8	9	10	11	12	13
1	-5.	-6.	-8.	-9.	-11.	-12.	-14.	-14.	-15.	-17.	-19.	-21.	-24.
2	-5.	-3.	-2.	-1.	1.	0.	0.	1.	1.	-2.	-6.	-8.	-11.
3	0.	-0.	-0.	-1.	-1.	-2.	-3.	-2.	-2.	-4.	-6.	-8.	-11.
4	5.	3.	1.	-1.	-3.	-4.	-5.	-5.	-4.	-6.	-7.	-9.	-10.
5	4.	3.	2.	0.	-2.	-4.	-5.	-4.	-3.	-3.	-3.	-6.	-8.
6	2.	3.	3.	1.	-1.	-3.	-5.	-3.	-1.	-0.	1.	-3.	-6.
7	6.	6.	6.	3.	-1.	-3.	-4.	-3.	-2.	-1.	0.	-3.	-6.
8	9.	9.	9.	4.	-1.	-2.	-3.	-3.	-3.	-1.	0.	-2.	-5.
9	10.	10.	11.	5.	-0.	-2.	-3.	-3.	-3.	-2.	-1.	-2.	-3.
10	10.	11.	12.	6.	0.	-1.	-2.	-3.	-4.	-3.	-2.	-1.	-1.
11	13.	13.	13.	7.	1.	-1.	-2.	-2.	-2.	-1.	0.	1.	1.
12	15.	15.	15.	8.	2.	0.	-2.	-1.	-0.	1.	3.	3.	4.
13	14.	13.	12.	9.	6.	4.	2.	3.	3.	4.	5.	6.	6.
14	14.	12.	9.	6.	2.	1.	0.	1.	2.	5.	8.	10.	12.
15	14.	10.	7.	3.	-1.	-2.	-2.	-1.	0.	5.	10.	14.	19.
16	11.	8.	4.	0.	-4.	-2.	-1.	0.	1.	8.	15.	16.	17.
17	8.	5.	2.	-2.	-6.	-3.	-1.	1.	2.	11.	21.	18.	15.
18	7.	3.	-2.	-5.	-9.	-5.	-2.	0.	3.	10.	17.	15.	13.
19	6.	1.	-5.	-8.	-11.	-8.	-4.	-0.	3.	8.	13.	12.	12.
20	1.	-4.	-10.	-12.	-14.	-10.	-5.	-1.	3.	8.	12.	12.	12.
21	-5.	-10.	-14.	-16.	-18.	-12.	-7.	-2.	3.	7.	11.	11.	12.
22	-6.	-12.	-17.	-19.	-20.	-14.	-8.	-3.	2.	6.	11.	14.	17.
23	-7.	-14.	-21.	-21.	-22.	-16.	-10.	-5.	-0.	5.	11.	16.	22.
24	-35.	-32.	-29.	-25.	-22.	-14.	-7.	-3.	2.	8.	15.	16.	17.
25	-46.	-40.	-35.	-29.	-23.	-18.	-12.	-9.	-6.	-1.	3.	9.	14.

Table 26

El Paso Columbia

Plane 7

Difference between "with water" and "without water" - Z heights in mm.

Y/X	1	2	3	4	5	6	7	8	9	10	11	12	13
1	3.	3.	2.	1.	0.	-0.	-1.	-1.	-1.	-3.	-6.	-6.	-7.
2	-3.	-3.	-2.	-2.	-1.	-2.	-3.	-3.	-3.	-5.	-7.	-7.	-8.
3	3.	2.	1.	-0.	-1.	-2.	-2.	-2.	-3.	-4.	-6.	-7.	-8.
4	9.	6.	4.	1.	-1.	-1.	-0.	-1.	-2.	-3.	-5.	-7.	-8.
5	6.	4.	3.	1.	-1.	-1.	-2.	-2.	-2.	-2.	-3.	-4.	-6.
6	2.	2.	1.	0.	-1.	-2.	-3.	-2.	-1.	-1.	-2.	-2.	-3.
7	4.	3.	1.	-0.	-2.	-2.	-3.	-2.	-2.	-2.	-3.	-2.	-1.
8	7.	4.	2.	-1.	-3.	-3.	-3.	-2.	-2.	-3.	-4.	-2.	1.
9	6.	4.	2.	-0.	-3.	-2.	-2.	-2.	-2.	-3.	-4.	-3.	-2.
10	4.	3.	2.	0.	-2.	-2.	-2.	-2.	-3.	-3.	-4.	-4.	-5.
11	3.	3.	2.	1.	-1.	-2.	-3.	-3.	-2.	-4.	-5.	-5.	-5.
12	1.	2.	2.	1.	-0.	-2.	-3.	-3.	-2.	-4.	-6.	-6.	-6.
13	8.	6.	3.	2.	1.	-0.	-1.	-2.	-4.	-5.	-6.	-7.	-7.
14	7.	6.	4.	3.	1.	-0.	-1.	-2.	-3.	-4.	-6.	-6.	-6.
15	6.	6.	6.	3.	1.	-1.	-2.	-2.	-2.	-4.	-6.	-5.	-5.
16	5.	10.	15.	7.	-1.	-2.	-3.	-3.	-3.	-1.	1.	-1.	-4.
17	5.	15.	24.	11.	-3.	-3.	-4.	-3.	-3.	2.	8.	3.	-3.
18	7.	10.	14.	6.	-2.	-2.	-2.	-2.	-3.	-0.	2.	-1.	-4.
19	8.	6.	4.	1.	-2.	-1.	0.	-1.	-2.	-3.	-3.	-4.	-5.
20	7.	6.	4.	1.	-1.	-1.	-1.	-2.	-2.	-3.	-4.	-4.	-5.
21	6.	5.	4.	2.	-0.	-1.	-2.	-2.	-2.	-3.	-4.	-4.	-4.
22	16.	11.	6.	3.	1.	-0.	-1.	-1.	-1.	-2.	-3.	-2.	-0.
23	26.	17.	7.	5.	2.	1.	0.	0.	0.	-1.	-3.	1.	4.
24	25.	19.	14.	8.	3.	1.	0.	-0.	-0.	-2.	-3.	-3.	-3.
25	5.	5.	4.	4.	3.	3.	2.	0.	-2.	-2.	-3.	-4.	-5.

RMS deviation from flatness 5.0 mm

Table 27

El Paso Columbia

Plane 8

Flatness data without water - Z is normal to the plane.

<u>X</u>	<u>Y</u>	<u>Z (mm)</u>	<u>X</u>	<u>Y</u>	<u>Z (mm)</u>	<u>X</u>	<u>Y</u>	<u>Z (mm)</u>
15.	1.	298.90	11.	11.	283.30	13.	22.	274.30
13.	1.	311.30	9.	11.	275.50	11.	22.	256.80
11.	1.	313.20	7.	11.	278.40	9.	22.	242.60
9.	1.	313.50	5.	11.	277.70	7.	22.	234.30
7.	1.	307.70	3.	11.	282.50	5.	22.	241.30
5.	1.	295.80	1.	11.	290.90	3.	22.	267.30
15.	2.	290.40	13.	13.	285.20	15.	24.	275.20
13.	2.	305.90	11.	13.	285.60	13.	24.	274.30
11.	2.	309.80	9.	13.	274.70	11.	24.	253.30
9.	2.	309.30	7.	13.	273.50	9.	24.	243.60
7.	2.	309.80	5.	13.	275.10	7.	24.	239.30
5.	2.	289.30	3.	13.	282.20	5.	24.	247.00
15.	3.	287.40	1.	13.	281.90	15.	25.	259.30
13.	3.	304.00	13.	14.	303.10	13.	25.	257.20
11.	3.	300.50	11.	14.	277.30	11.	25.	250.90
9.	3.	298.70	9.	14.	264.90	9.	25.	245.30
7.	3.	299.10	7.	14.	257.80	7.	25.	244.40
5.	3.	283.50	5.	14.	259.30	5.	25.	251.50
3.	3.	278.30	3.	14.	279.50			
15.	5.	271.30	1.	14.	296.00			
13.	5.	292.30	15.	16.	307.20			
11.	5.	294.50	13.	16.	293.10			
9.	5.	291.50	11.	16.	267.90			
7.	5.	289.80	9.	16.	255.30			
5.	5.	280.30	7.	16.	249.10			
3.	5.	281.10	5.	16.	252.40			
1.	5.	288.80	3.	16.	276.00			
15.	7.	271.70	1.	16.	291.30			
13.	7.	288.90	15.	18.	289.00			
11.	7.	294.30	13.	18.	281.50			
9.	7.	285.10	11.	18.	270.10			
7.	7.	284.00	9.	18.	248.10			
5.	7.	279.80	7.	18.	241.20			
3.	7.	283.90	5.	18.	250.00			
1.	7.	290.00	3.	18.	274.00			
15.	9.	270.00	1.	18.	297.10			
13.	9.	286.40	15.	20.	286.70			
11.	9.	285.70	13.	20.	279.70			
9.	9.	278.50	11.	20.	264.10			
7.	9.	281.50	9.	20.	246.50			
5.	9.	278.00	7.	20.	238.50			
3.	9.	285.40	5.	20.	248.80			
1.	9.	290.30	3.	20.	270.00			
15.	11.	277.50	1.	20.	293.20			
13.	11.	287.30	15.	22.	280.40			

RMS deviation from flatness 12.9 mm

El Paso Columbia

Plane 8

Flatness map without water.

Y/X	1	2	3	4	5	6	7	8	9	10	11	12	13	14	15
1	-28.	-23.	-17.	-11.	-5.	0.	6.	9.	11.	11.	11.	9.	8.	2.	-5.
2	-50.	-40.	-30.	-20.	-10.	0.	10.	10.	9.	9.	9.	7.	5.	-3.	-11.
3	-23.	-21.	-18.	-16.	-14.	-6.	1.	1.	1.	1.	2.	4.	5.	-3.	-12.
4	-13.	-14.	-15.	-14.	-13.	-7.	-1.	-1.	-1.	0.	1.	1.	1.	-3.	-18.
5	-3.	-7.	-12.	-12.	-13.	-8.	-4.	-3.	-2.	-1.	0.	-1.	-3.	-13.	-24.
6	-1.	-4.	-8.	-10.	-11.	-8.	-5.	-4.	-4.	-1.	2.	-0.	-2.	-12.	-22.
7	2.	-1.	-5.	-7.	-9.	-7.	-5.	-5.	-5.	-0.	4.	1.	-2.	-11.	-20.
8	4.	1.	-2.	-5.	-8.	-6.	-5.	-5.	-6.	-2.	2.	0.	-1.	-10.	-18.
9	6.	4.	1.	-3.	-7.	-5.	-4.	-6.	-7.	-4.	-1.	-0.	-0.	-9.	-17.
10	9.	5.	2.	-2.	-5.	-4.	-3.	-5.	-7.	-3.	0.	1.	2.	-5.	-11.
11	11.	7.	2.	-0.	-3.	-3.	-3.	-5.	-6.	-3.	1.	3.	5.	-0.	-6.
12	9.	6.	4.	1.	-2.	-3.	-3.	-4.	-5.	0.	4.	5.	6.	3.	0.
13	6.	6.	6.	2.	-2.	-3.	-4.	-3.	-3.	2.	3.	7.	7.	6.	6.
14	22.	14.	5.	-5.	-15.	-16.	-17.	-14.	-11.	-5.	1.	14.	27.	99.	52.
15	22.	14.	6.	-6.	-17.	-18.	-20.	-16.	-13.	-7.	-1.	11.	24.	93.	43.
16	22.	14.	6.	-6.	-18.	-20.	-22.	-19.	-16.	-10.	-4.	8.	21.	29.	34.
17	27.	17.	7.	-5.	-17.	-21.	-24.	-21.	-18.	-9.	-1.	8.	17.	22.	27.
18	32.	20.	8.	-4.	-16.	-21.	-26.	-22.	-19.	-8.	2.	8.	13.	17.	30.
19	32.	20.	8.	-3.	-15.	-20.	-25.	-21.	-18.	-8.	1.	8.	14.	18.	21.
20	32.	20.	8.	-3.	-14.	-19.	-24.	-21.	-17.	-8.	0.	8.	16.	19.	22.
21	34.	21.	9.	-3.	-15.	-20.	-24.	-20.	-17.	-9.	-1.	7.	15.	18.	21.
22	36.	23.	10.	-4.	-17.	-21.	-24.	-20.	-17.	-10.	-3.	6.	14.	17.	20.
23	23.	14.	5.	-3.	-12.	-16.	-20.	-17.	-14.	-8.	-3.	7.	16.	13.	19.
24	9.	5.	1.	-3.	-7.	-11.	-15.	-13.	-11.	-7.	-2.	8.	18.	19.	19.
25	15.	11.	7.	3.	-1.	-4.	-8.	-8.	-8.	-5.	-3.	0.	3.	4.	5.

Table 29

El Paso Columbia

Plane 8

Flatness data with water - Z is normal to the plane.

<u>X</u>	<u>Y</u>	<u>Z (mm)</u>	<u>X</u>	<u>Y</u>	<u>Z (mm)</u>	<u>X</u>	<u>Y</u>	<u>Z (mm)</u>
13.	1.	302.00	13.	13.	272.30	5.	22.	215.80
9.	1.	295.20	11.	13.	266.10	3.	22.	237.00
7.	1.	284.60	9.	13.	256.80	1.	22.	249.30
5.	1.	269.90	7.	13.	249.30	15.	24.	268.00
15.	2.	286.50	5.	13.	247.20	13.	24.	260.90
13.	2.	297.30	3.	13.	252.10	11.	24.	238.20
11.	2.	297.20	1.	13.	251.60	9.	24.	224.00
9.	2.	293.50	15.	14.	292.20	7.	24.	214.90
7.	2.	287.90	13.	14.	290.00	5.	24.	217.10
5.	2.	263.80	11.	14.	262.00	3.	24.	235.70
15.	3.	281.20	9.	14.	244.20	15.	25.	254.30
13.	3.	290.30	7.	14.	234.20	13.	25.	249.50
11.	3.	284.70	5.	14.	230.80	11.	25.	235.20
9.	3.	282.30	3.	14.	248.30	9.	25.	226.30
7.	3.	268.30	1.	14.	261.00	7.	25.	220.10
5.	3.	248.70	15.	16.	299.10	5.	25.	224.00
15.	5.	264.30	13.	16.	282.10			
13.	5.	283.50	11.	16.	253.20			
11.	5.	282.10	9.	16.	233.90			
9.	5.	273.40	7.	16.	222.50			
5.	5.	251.70	5.	16.	222.20			
3.	5.	251.10	3.	16.	244.90			
15.	7.	264.10	1.	16.	258.50			
13.	7.	279.70	15.	18.	279.80			
11.	7.	279.90	13.	18.	271.30			
9.	7.	255.30	11.	18.	254.20			
7.	7.	260.10	9.	18.	227.00			
3.	7.	253.00	7.	18.	213.00			
15.	9.	264.00	5.	18.	216.30			
13.	9.	276.90	3.	18.	242.20			
11.	9.	272.20	1.	18.	263.70			
9.	9.	258.90	15.	20.	279.60			
7.	9.	254.80	13.	20.	267.20			
5.	9.	254.50	11.	20.	248.80			
3.	9.	251.70	9.	20.	226.00			
15.	11.	271.30	7.	20.	210.60			
13.	11.	278.70	5.	20.	215.10			
11.	11.	269.70	3.	20.	237.20			
9.	11.	257.00	1.	20.	262.10			
7.	11.	253.50	15.	22.	271.00			
5.	11.	246.90	13.	22.	264.90			
3.	11.	251.00	11.	22.	242.70			
1.	11.	258.20	9.	22.	223.70			
15.	13.	285.10	7.	22.	209.30			

RMS Deviation from flatness 14.5 mm

Table 30

El Paso Columbia

Plane 8

Flatness map with water.

Y/X	1	2	3	4	5	6	7	8	9	10	11	12	13	14	15
1	-27.	-22.	-17.	-12.	-6.	-1.	4.	7.	11.	10.	10.	10.	9.	3.	-4.
2	-50.	-40.	-30.	-20.	-10.	-0.	10.	10.	11.	11.	11.	9.	7.	-1.	-8.
3	-54.	-45.	-39.	-31.	-23.	-16.	-8.	-3.	2.	1.	0.	1.	2.	-5.	-12.
4	-32.	-29.	-26.	-23.	-20.	-14.	-9.	-4.	-0.	0.	1.	1.	0.	-9.	-18.
5	-9.	-11.	-13.	-14.	-16.	-13.	-9.	-6.	-3.	-0.	2.	1.	-1.	-13.	-24.
6	-7.	-8.	-9.	-11.	-12.	-10.	-8.	-9.	-10.	-3.	3.	1.	-1.	-11.	-22.
7	-6.	-6.	-6.	-7.	-7.	-7.	-8.	-12.	-17.	-6.	4.	2.	-0.	-10.	-20.
8	-4.	-4.	-5.	-5.	-6.	-7.	-8.	-10.	-13.	-5.	2.	1.	0.	-9.	-18.
9	-2.	-3.	-3.	-4.	-5.	-7.	-9.	-9.	-9.	-4.	0.	1.	1.	-8.	-16.
10	5.	1.	-2.	-4.	-7.	-7.	-7.	-7.	-8.	-3.	1.	3.	4.	-9.	-10.
11	11.	6.	0.	-4.	-8.	-7.	-6.	-6.	-6.	-2.	2.	5.	7.	1.	-5.
12	10.	6.	3.	-2.	-6.	-6.	-6.	-5.	-4.	-1.	2.	4.	6.	5.	4.
13	9.	7.	5.	1.	-4.	-5.	-6.	-4.	-2.	0.	3.	4.	5.	9.	13.
14	21.	12.	4.	-7.	-18.	-18.	-19.	-16.	-13.	-6.	1.	13.	25.	24.	33.
15	21.	13.	4.	-8.	-20.	-21.	-22.	-19.	-16.	-9.	-2.	11.	23.	26.	33.
16	22.	13.	5.	-9.	-22.	-24.	-26.	-23.	-19.	-11.	-4.	9.	21.	27.	34.
17	27.	16.	5.	-9.	-23.	-26.	-29.	-25.	-20.	-11.	-1.	3.	13.	22.	36.
18	32.	19.	6.	-9.	-24.	-28.	-31.	-27.	-22.	-10.	1.	8.	14.	17.	19.
19	33.	19.	6.	-8.	-23.	-27.	-31.	-25.	-20.	-10.	1.	8.	14.	18.	21.
20	34.	20.	5.	-8.	-21.	-25.	-30.	-24.	-18.	-9.	0.	7.	15.	19.	23.
21	30.	19.	7.	-6.	-19.	-23.	-28.	-23.	-17.	-9.	-1.	7.	15.	18.	21.
22	26.	17.	9.	-3.	-16.	-21.	-27.	-22.	-16.	-9.	-2.	7.	16.	17.	18.
23	30.	21.	11.	-1.	-13.	-18.	-22.	-18.	-14.	-9.	-3.	7.	17.	18.	19.
24	35.	24.	12.	1.	-11.	-14.	-17.	-14.	-12.	-7.	-3.	7.	17.	18.	20.
25	15.	11.	7.	2.	-2.	-6.	-10.	-9.	-8.	-5.	-3.	9.	7.	9.	8.

Table 31

El Paso Columbia

Plane 8

Difference between "with water" and "without water" - Z heights in mm.

	1	2	3	4	5	6	7	8	9	10	11	12	13	14	15
1	1.	0.	0.	-0.	-1.	-1.	-2.	-1.	-1.	-1.	-1.	0.	1.	1.	1.
2	-0.	-0.	-0.	-0.	-0.	-0.	-0.	1.	2.	2.	1.	2.	2.	2.	3.
3	-31.	-26.	-20.	-15.	-10.	-9.	-9.	-4.	1.	-0.	-2.	-3.	-3.	-1.	0.
4	-18.	-15.	-11.	-9.	-6.	-7.	-7.	-3.	1.	0.	0.	-0.	-1.	-0.	0.
5	-6.	-3.	-1.	-2.	-3.	-4.	-2.	-3.	-0.	1.	2.	2.	2.	1.	-0.
6	-7.	-4.	-1.	-1.	-1.	-2.	-4.	-5.	-6.	-3.	1.	1.	2.	1.	-0.
7	-8.	-5.	-2.	0.	2.	0.	-2.	-7.	-12.	-6.	0.	1.	1.	0.	-1.
8	-8.	-6.	-3.	-1.	2.	-1.	-4.	-5.	-7.	-3.	0.	1.	1.	1.	0.
9	-8.	-6.	-4.	-1.	2.	-1.	-5.	-3.	-1.	-0.	1.	1.	1.	1.	1.
10	-4.	-4.	-3.	-2.	-3.	-3.	-4.	-2.	-1.	0.	1.	1.	2.	1.	1.
11	0.	-1.	-2.	-4.	-5.	-4.	-3.	-2.	-0.	0.	1.	2.	2.	2.	1.
12	2.	0.	-1.	-2.	-4.	-3.	-3.	-1.	0.	-1.	-2.	-1.	0.	2.	4.
13	3.	1.	-1.	-1.	-3.	-2.	-3.	-1.	1.	-2.	-5.	-3.	-2.	3.	3.
14	-2.	-2.	-3.	-2.	-3.	-2.	-1.	-2.	-2.	-1.	-1.	-1.	-2.	-16.	-23.
15	-1.	-1.	-2.	-3.	-4.	-3.	-3.	-3.	-3.	-1.	-0.	-1.	-1.	-3.	-15.
16	1.	-0.	-1.	-3.	-4.	-4.	-4.	-4.	-3.	-1.	-0.	0.	0.	-0.	-1.
17	0.	-1.	-2.	-4.	-5.	-5.	-5.	-4.	-3.	-1.	-0.	0.	1.	-0.	-3.
18	0.	-1.	-3.	-5.	-6.	-7.	-6.	-4.	-2.	-2.	-1.	-0.	1.	-0.	-0.
19	1.	-1.	-3.	-5.	-6.	-7.	-6.	-4.	-2.	-1.	-1.	-0.	0.	-0.	-0.
20	3.	-0.	-3.	-5.	-7.	-6.	-5.	-4.	-2.	-1.	-0.	-1.	-1.	-0.	1.
21	-4.	-3.	-3.	-2.	-3.	-4.	-4.	-2.	-1.	-0.	1.	1.	1.	0.	-0.
22	-10.	-5.	-0.	0.	1.	-1.	-2.	-1.	0.	1.	1.	2.	2.	0.	-2.
23	8.	7.	5.	2.	1.	-2.	-2.	-1.	-0.	0.	1.	0.	0.	0.	-0.
24	26.	18.	11.	4.	-3.	-3.	-2.	-1.	-1.	0.	0.	-1.	-2.	-0.	1.
25	0.	-0.	-0.	-1.	-1.	-1.	-1.	-1.	0.	0.	-0.	2.	4.	4.	3.

Appendix G

Deadwood Survey Data

El Paso Columbia, Hull 2266, Tank 3

By

W. C. Haight, R. G. Hartsock, and R. J. Hocken

Deadwood Survey Data

El Paso Columbia, Hull 2266, Tank 3

The first 26 tables presented in this appendix contain the results of a detailed dimensional survey of all deadwood members on Tank 3 of the El Paso Columbia, including the thickness of the eight exterior tank walls. In the context of this appendix, deadwood is defined to be any solid tank member whose volume reduces the internal liquid capacity of the tank. The deadwood members measured in this survey include all tank exterior walls, interior bulkheads, interior beams and interior stiffness.

Each table presents the actual measured data for a given deadwood component in millimeters, and the nominal component size in inches and millimeters as taken from Conch Methane Services, Ltd. drawing number 6043-125-3/OG-5, Alt. no. 12. These measured and nominal dimensions can be used in each case to determine the actual oversize or undersize of deadwood from the specified values. Each data point is referenced by an index number which, in conjunction with the diagrams provided, locates the measurement point physically on the tank. Exterior wall thickness measurements were made near every photogrammetric survey target, and the average values for a given plate are reported.

All thickness readings reported in these tables were taken with an ultrasonic thickness gage utilizing the pulse-echo technique. The instrument operates as follows. For each measurement, a small amount of liquid couplant is applied to the surface of the tank member to be measured, and a probe is held firmly on the tank at that point. The couplant eliminates any air gap between the probe and the material to be measured, insuring a good acoustic bond. A pulse of ultrasound is then emitted by the instrument through the probe. An echo occurs at the back wall of the member at the solid/air interface and the instrument times the interval for this pulse round trip. The thickness of the test piece is proportional to this time interval and the proportionality constant is a function of the velocity of sound in the test piece.

The instrument/probe assembly was field calibrated to determine the material sound velocity. For this purpose, a reference block was manufactured by NBS from a sample of Aluminum Alloy 5083-0 Temper obtained from the tank construction site in Mobile, Alabama. This block had steps of 25.40 mm, 19.05 mm, 12.70 mm and 6.35 mm and the instrument calibration was re-checked every hour during the

survey. The resolution of the instrument is 0.01 mm and the total uncertainty of all thickness measurements is estimated to be ± 0.05 mm.

All remaining dimensional measurements reported herein were made with a steel surveying tape, graduated in 1 mm increments and calibrated at NBS.

This survey was conducted while the tank was in storage at a construction yard in Mobile, Alabama and while the tank had an average exterior temperature of 13.5°C. All data reported herein is for the tank at these conditions.

The final two tables in this Appendix, Tables 27 and 28 report the results of the computation of the volume occupied by the surveyed deadwood. The computations were performed by representing deadwood elements by simple geometric figures. Except in the case of the balconies, these computations were straight forward and can easily be reproduced by quick examination of the drawings of the structural members shown in Tables 4 through 10.

For the balconies the following model was used. The web thickness was assumed to be constant at the average value. The web length was assumed to have one value along two walls and another along the other two. The rounded corners were approximated by triangles. The flange was assumed to have a constant length and thickness except in the four corners of the tank, (borders of the triangle sections) where different flange lengths and thicknesses were allowed. Implementation of this model required (11) eleven parameters. The model was altered slightly by the subtraction of some sections for balconies of the type in tank quadrants two (2) and four (4). Since only the balconies in quadrants one (1) and four (4) were measured. Quadrant three was assumed equal to one (1) and two (2) equal to four (4) when reporting the results. The results are reported by levels (balconies) with the deadwood volume of balcony one (1) being reported in level one, etc.

In Table 28 the percentage deviation of the deadwood from nominal is given. The exterior walls are not included since their deviations from nominal thickness are reported in Tables 1 through 3 by plate.

Table 1

Exterior Plate Thickness
Aft and Stbd Walls

<u>Plate Number</u>	<u>Nominal</u>		<u>Measured</u>
	<u>inch</u>	<u>mm</u>	<u>mm</u>
1.1	0.84	21.3	22.4
1.2	0.81	20.6	21.7
1.3	0.81	20.6	21.6
1.4	0.75	19.1	19.3
1.5	0.63	16.0	15.6
1.6	0.56	14.2	14.7
2.1	0.84	21.3	none
2.2	0.81	20.6	none
2.3	0.81	20.6	none
2.4	0.75	19.1	none
2.5	0.63	16.0	none
2.6	0.56	14.2	none
3.1	0.84	21.3	21.5
3.2	0.84	21.3	21.7
3.3	0.81	20.6	20.8
3.4	0.75	19.1	18.9
3.5	0.69	17.5	18.3
3.6	0.63	16.0	16.3
3.7	0.50	12.7	13.1
4.1	0.84	21.3	21.2
4.2	0.84	21.3	21.3
4.3	0.81	20.6	20.6
4.4	0.75	19.1	19.3
4.5	0.69	17.5	17.7
4.6	0.63	16.0	16.1
4.7	0.50	12.7	14.1

Location Diagram:

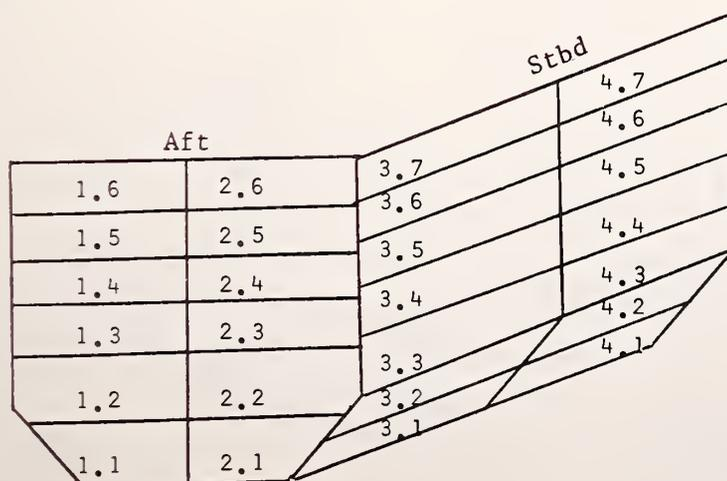


Table 2
Exterior Plate Thickness
Fwd and Port Walls

<u>Plate Number</u>	<u>Nominal</u>		<u>Measured</u>
	<u>inch</u>	<u>mm</u>	<u>mm</u>
5.1	0.84	21.3	21.6
5.2	0.81	20.6	21.3
5.3	0.81	20.6	22.0
5.4	0.75	19.1	19.3
5.5	0.63	16.0	16.9
5.6	0.56	14.2	13.8
6.1	0.84	21.3	22.3
6.2	0.81	20.6	22.3
6.3	0.81	20.6	21.2
6.4	0.75	19.1	18.4
6.5	0.63	16.0	16.1
6.6	0.56	14.2	14.9
7.1	0.84	21.3	21.2
7.2	0.84	21.3	21.3
7.3	0.81	20.6	20.5
7.4	0.75	19.1	19.9
7.5	0.69	17.5	18.9
7.6	0.63	16.0	16.0
7.7	0.50	12.7	13.4
8.1	0.84	21.3	21.5
8.2	0.84	21.3	21.7
8.3	0.81	20.6	20.6
8.4	0.75	19.1	18.9
8.5	0.69	17.5	17.3
8.6	0.63	16.0	17.0
8.7	0.50	12.7	13.7

Location Diagram:

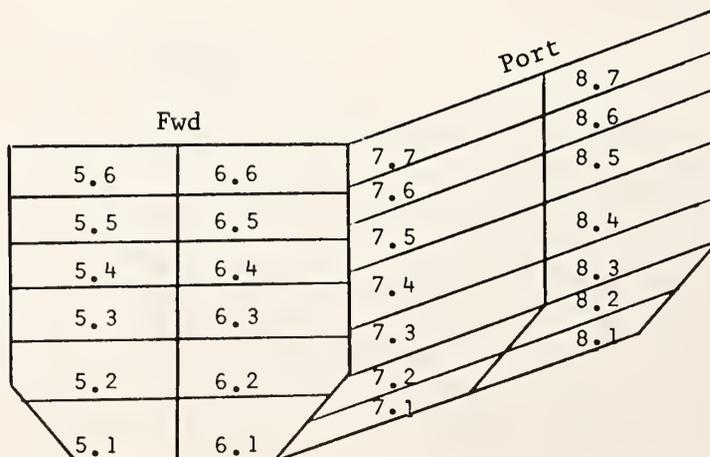


Table 3

Exterior Plate Thickness
Top and Bottom Surfaces

<u>Plate Number</u>	<u>Location</u>	<u>Nominal</u>		<u>Measured</u>
		<u>inch</u>	<u>mm</u>	<u>mm</u>
9.1	1	0.50	12.7	13.7
9.1	3	0.50	12.7	13.7
9.2	5	0.50	12.7	13.3
9.3	7	0.56	14.2	14.6
9.4	9	0.56	14.2	14.7
9.5	11	0.56	14.2	14.5
9.6	15	0.56	14.2	14.9
9.7	17	0.56	14.2	15.2
9.8	19	0.56	14.2	14.8
9.9	21	0.50	12.7	12.9
9.10	23	0.50	12.7	13.3
9.10	25	0.50	12.7	13.3
10.1	1	0.81	20.6	22.0
10.2	5	0.81	20.6	20.6
10.3	7	0.81	20.6	none
10.4	9	0.81	20.6	21.7
10.5	13	0.81	20.6	21.4
10.6	15	0.81	20.6	none
10.7	17	0.81	20.6	21.9
10.8	19	0.81	20.6	21.8

Location Diagram:

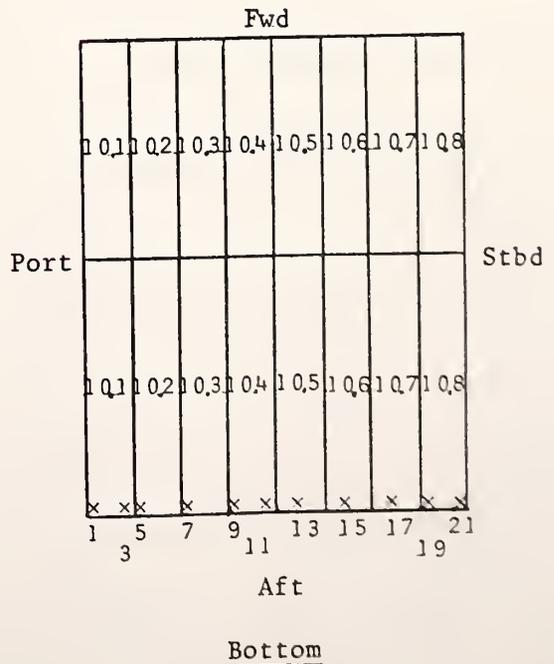
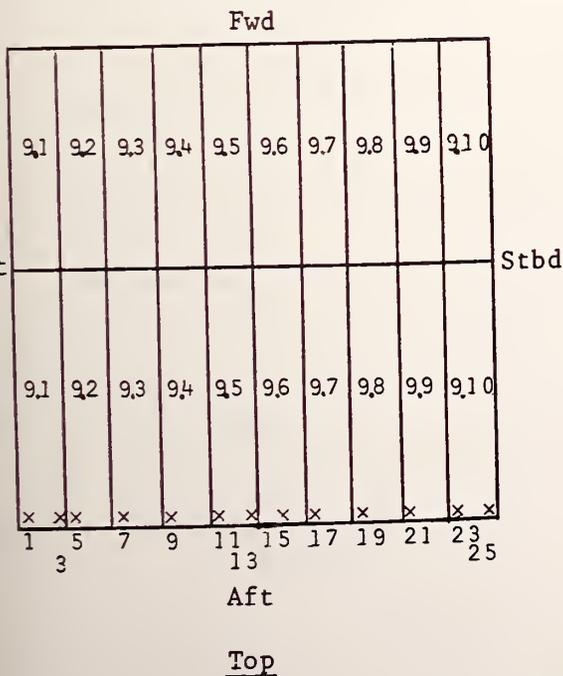


Table 4

Interior Bulkhead Thickness
Swash Bulkhead, Quadrants 1 and 4

<u>Location</u>	<u>Nominal</u>		<u>Quadrant 1</u>	<u>Quadrant 4</u>
	<u>inch</u>	<u>mm</u>	<u>measured</u> <u>mm</u>	<u>measured</u> <u>mm</u>
7.9	0.50	12.7	x	13.0
7.7	0.50	12.7	none	x
7.1	0.50	12.7	13.4	x
6.9	0.50	12.7	x	13.7
6.7	0.50	12.7	13.6	x
6.1	0.50	12.7	12.3	x
5.9	0.50	12.7	x	13.2
5.7	0.50	12.7	13.2	x
5.1	0.50	12.7	13.4	x
4.9	0.50	12.7	x	12.5
4.7	0.50	12.7	13.6	x
4.1	0.50	12.7	16.1	x
3.9	0.50	12.7	x	13.5
3.7	0.50	12.7	13.8	x
3.1	0.50	12.7	13.3	x
2.9	0.50	12.7	x	12.7
2.7	0.50	12.7	13.3	x
2.1	0.50	12.7	13.4	x
1.9	0.56	14.2	x	15.5
1.7	0.50	12.7	13.2	x
1.1	0.50	12.7	13.9	x
0.9	0.56	14.2	x	15.5
0.7	0.56	14.2	14.6	x
0.1	0.56	14.2	14.6	x

Location Diagrams (Location = i.j; where i = level, j = location):

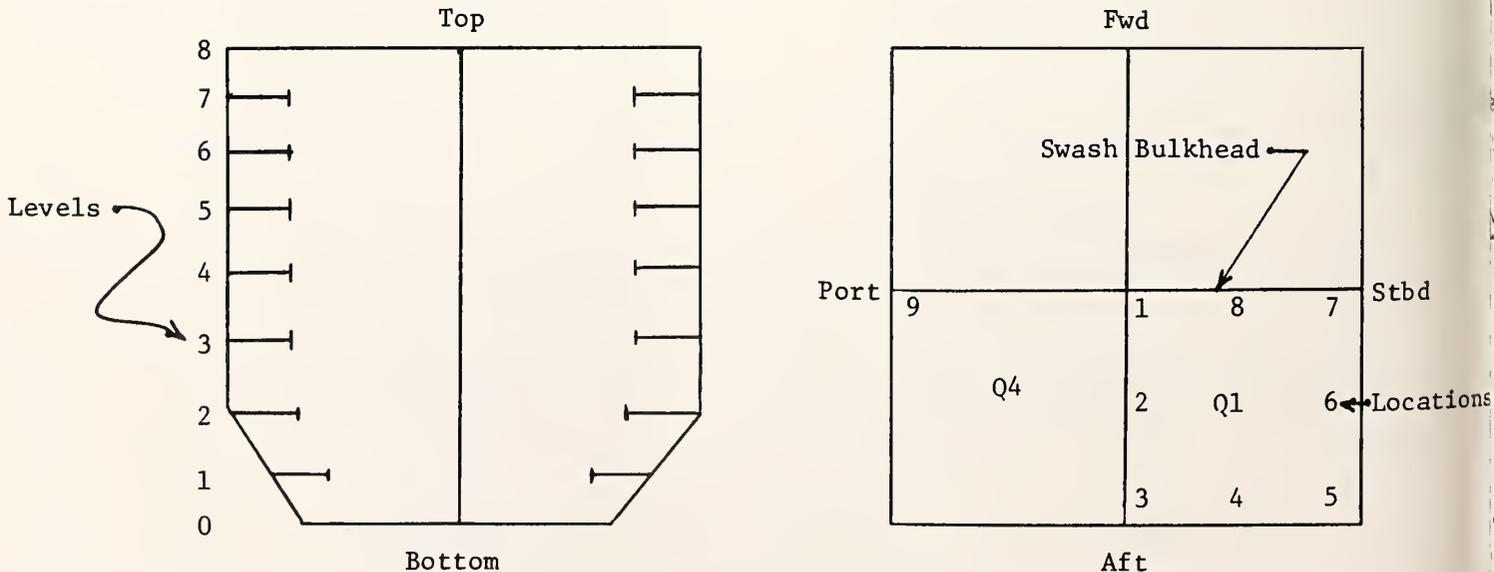


Table 5

Interior Bulkhead Thickness
Liquid Tight Bulkhead, Quadrants 1 and 4

<u>Location</u>	<u>Nominal</u>		<u>Measured</u>
	<u>inch</u>	<u>mm</u>	<u>mm</u>
7.3	0.50	12.7	13.0
7.1	0.50	12.7	13.0
6.3	0.50	12.7	12.7
6.1	0.50	12.7	13.5
5.3	0.50	12.7	13.0
5.1	0.50	12.7	12.8
4.3	0.50	12.7	13.4
4.1	0.50	12.7	13.3
3.3	0.50	12.7	13.2
3.1	0.50	12.7	13.0
2.3	0.50	12.7	13.9
2.1	0.50	12.7	14.0
1.3	0.50	12.7	13.9
1.1	0.50	12.7	13.9
0.3	0.56	14.2	15.0
0.1	0.56	14.2	15.1

Location Diagrams (Location = i.j; where i = level, j = location)

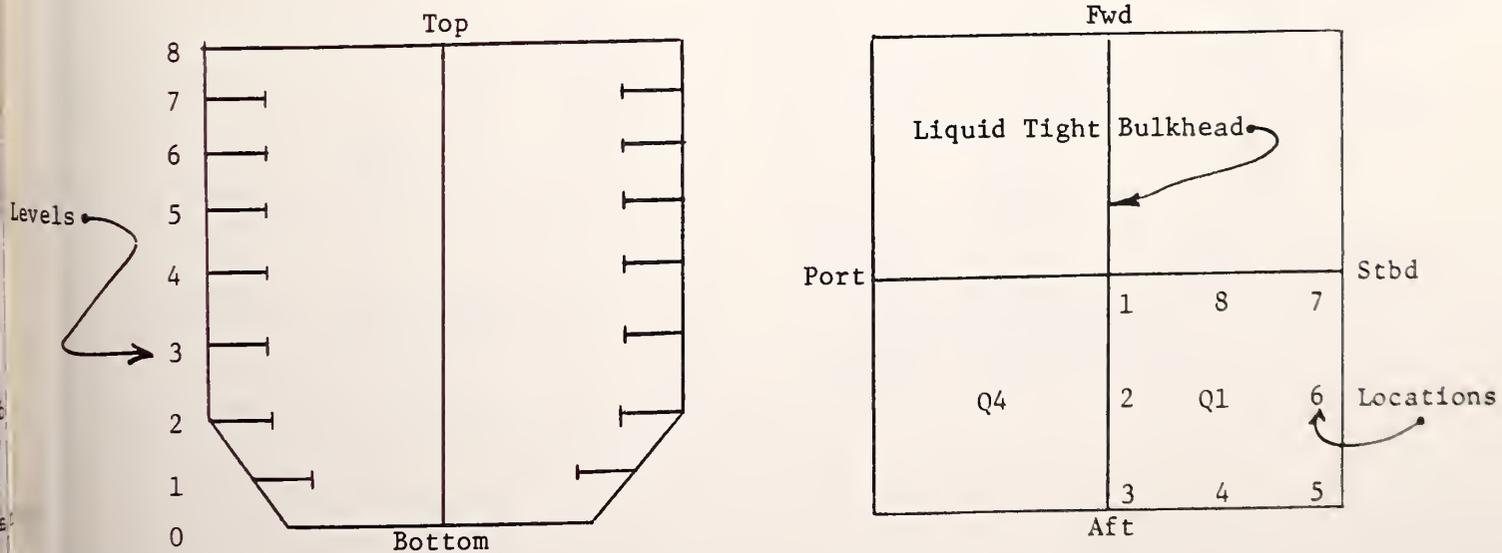


Table 6

Balcony Beam Locations, Vertical Positions
Quadrants 1 and 4

<u>Location</u>	<u>Nominal Vertical Separation</u>		<u>Measured Vertical Separation</u>	
	<u>ft, inch</u>	<u>mm</u>	<u>Quadrant 1</u> <u>mm</u>	<u>Quadrant 4</u> <u>mm</u>
8-7	11' 4"	3454.4	none	none
7-6	11' 4"	3454.4	3415.0	3407.0
6-5	10' 6"	3200.4	3186.7	3242.0
5-4	9' 11"	3022.6	3033.5	2984.7
4-3	9' 0"	2743.2	2728.8	2739.4
3-2	8' 7"	2616.2	2642.4	2612.4
2-1	7' 10"	2387.6	2365.6	2398.0
1-0	6' 10"	2082.8	2106.0	2090.5

Location Diagrams: [Location = Level (i) - Level (j)]

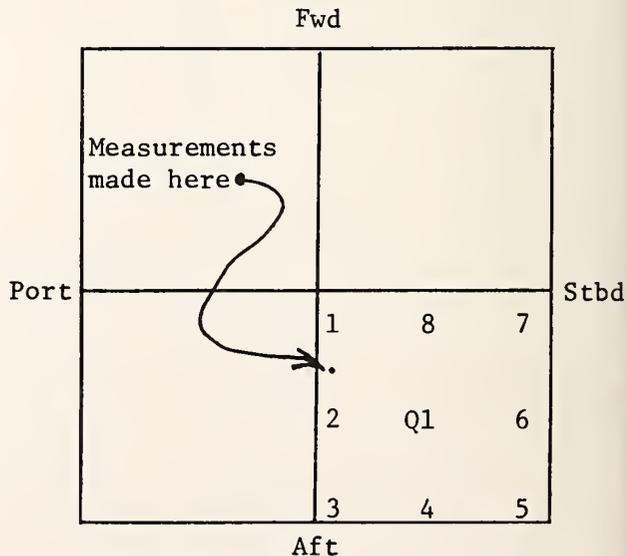
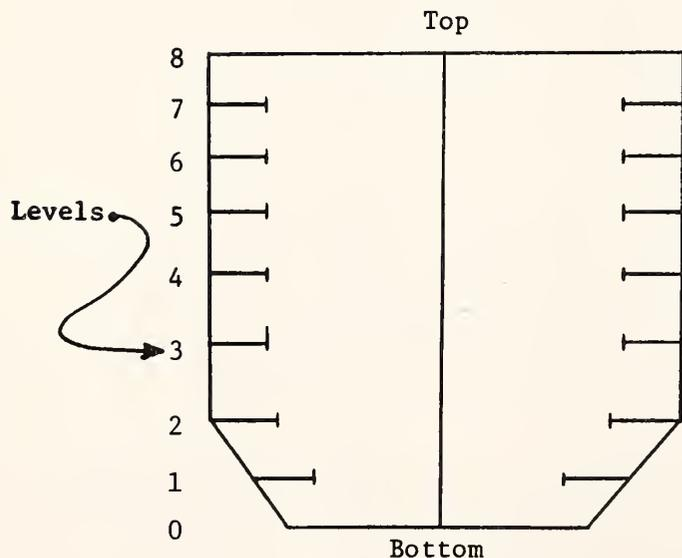
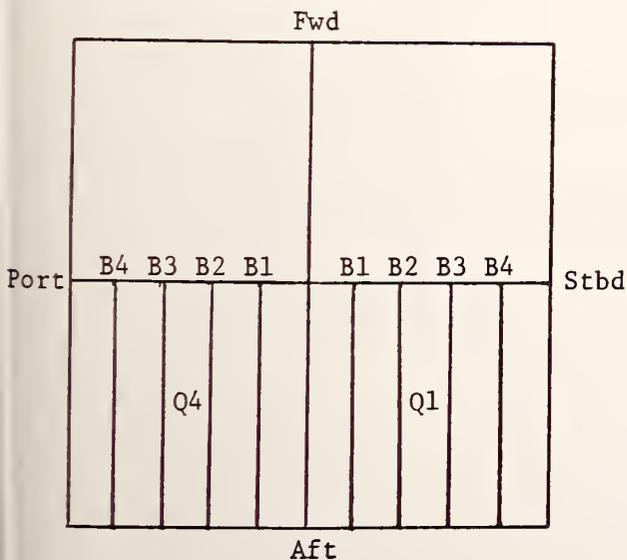


Table 7

Large Floor Beam Dimensions
Quadrants 1 and 4

<u>Dimension</u>	<u>Location</u>	<u>Nominal</u>		<u>Quadrant 1</u>	<u>Quadrant 4</u>
		<u>inch</u>	<u>mm</u>	<u>measured</u>	<u>measured</u>
				<u>mm</u>	<u>mm</u>
A	Beam 1	54	1371.6	1368	1373
	Beam 2	54	1371.6	1367	1370
	Beam 3	54	1371.6	1382	1377
	Beam 4	54	1371.6	1364	1370
B	Beam 1	16	406.4	412	413
	Beam 2	16	406.4	412	413
	Beam 3	16	406.4	411	410
	Beam 4	16	406.4	409	414
C	Beam 1	0.63	16.0	17.0	16.8
	Beam 2	0.63	16.0	17.1	16.5
	Beam 3	0.63	16.0	16.9	16.2
	Beam 4	0.63	16.0	16.4	16.2
D	Beam 1	1.38	35.1	35.4	35.3
	Beam 2	1.38	35.1	35.5	35.4
	Beam 3	1.38	35.1	36.2	35.9
	Beam 4	1.38	35.1	36.2	35.8

Location Diagram:



Dimension Diagram:

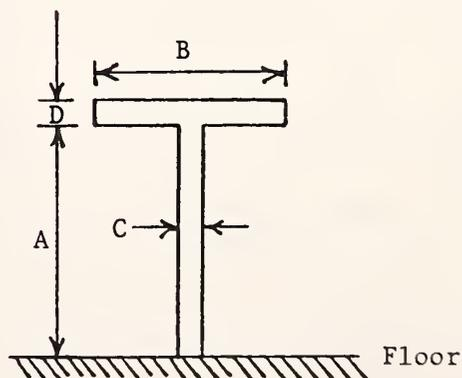


Table 8

Small Floor Beam Dimensions
Quadrants 1 and 4

<u>Dimension</u>	<u>Location</u>	<u>Nominal</u>		<u>Quadrant 1</u>	<u>Quadrant 4</u>
		<u>inch</u>	<u>mm</u>	<u>measured</u> <u>mm</u>	<u>measured</u> <u>mm</u>
A	Beam 1	16	406.4	406	409
	Beam 2	16	406.4	408	405
B	Beam 1	4.5	114.3	112	114
	Beam 2	4.5	114.3	114	114
C	Beam 1	0.56	14.2	14.5	14.6
	Beam 2	0.56	14.2	14.6	14.6
D	Beam 1	1.05	26.7	27.1	27.1
	Beam 2	1.05	26.7	27.0	27.0

Location Diagram:

Dimension Diagram:

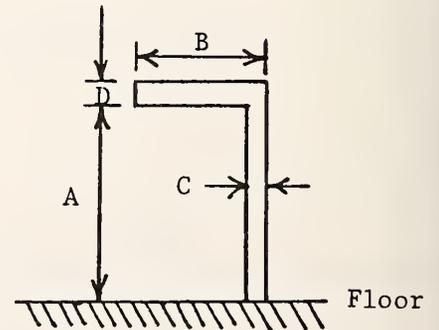
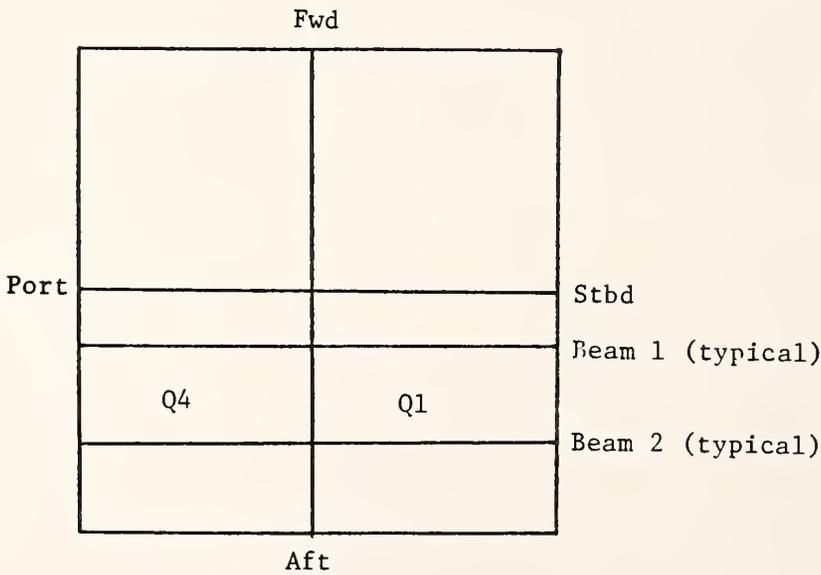


Table 9
(Sheet 1 of 2)

Vertical Stiffner Dimensions
Quadrant 1

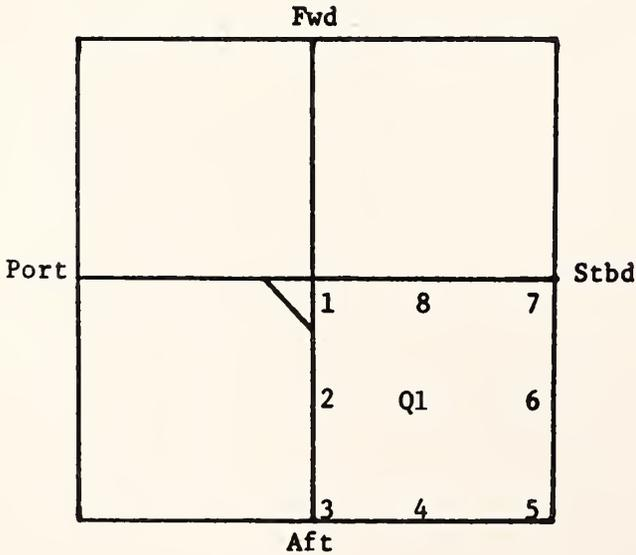
<u>Dimension</u>	<u>Location</u>	<u>Nominal</u>		<u>Level 7</u>	<u>Level 1</u>
		<u>inch</u>	<u>mm</u>	<u>Measured</u>	<u>Measured</u>
				<u>mm</u>	<u>mm</u>
A	1	9	228.6	228	228
	2	9	228.6	226	226
	3	13	330.2	330	327
	4	13	330.2	329	329
	5	13	330.2	328	331
	6	13	330.2	329	406
	7	9	228.6	225	227
	8	9	228.6	228	224
B	1	2.5	63.5	63.5	63.0
	2	2.5	63.5	63.2	64.0
	3	2.5	63.5	63.3	63.0
	4	2.5	63.5	63.2	63.0
	5	2.5	63.5	64.0	63.0
	6	2.5	63.5	63.1	64.0
	7	2.5	63.5	64.0	64.0
	8	2.5	63.5	65.0	64.0

Table 9
(Sheet 2 of 2)

Vertical Stiffner Dimensions
Quadrant 1

<u>Dimension</u>	<u>Location</u>	<u>Nominal</u>		<u>Level 7</u>	<u>Level 1</u>
		<u>inch</u>	<u>mm</u>	<u>mm</u>	<u>mm</u>
C	1	0.406	10.3	10.8	10.7
	2	0.406	10.3	10.7	10.7
	3	0.4375	11.1	11.9	10.7
	4	0.4375	11.1	11.6	11.2
	5	0.4375	11.1	11.5	11.0
	6	0.4375	11.1	11.3	11.5
	7	0.406	10.3	10.9	10.7
	8	0.406	10.3	10.9	10.7
D	1	0.875	22.2	22.4	22.4
	2	0.875	22.2	22.5	22.3
	3	0.875	22.2	22.4	22.4
	4	0.875	22.2	22.4	22.3
	5	0.875	22.2	22.8	22.4
	6	0.875	22.2	22.5	23.1
	7	0.406	10.3	11.5	11.0
	8	0.406	10.3	11.5	11.1

Location Diagram:



Dimension Diagram:

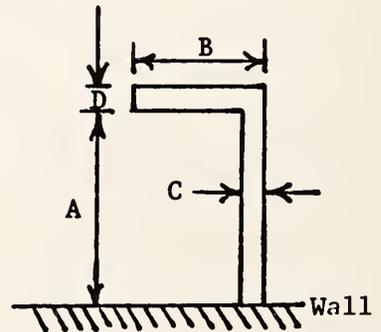
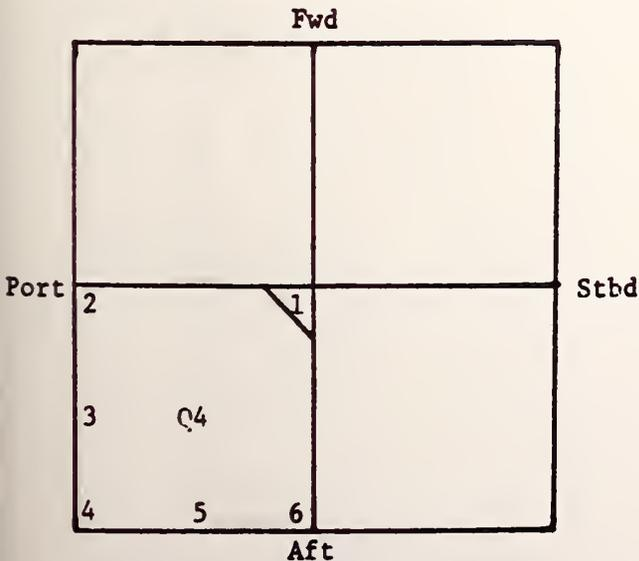


Table 10
Vertical Stiffner Dimensions
Quadrant 4

<u>Dimension</u>	<u>Location</u>	<u>Nominal</u>		<u>Level 7</u>	<u>Level 2</u>
		<u>inch</u>	<u>mm</u>	<u>Measured</u>	<u>Measured</u>
				<u>mm</u>	<u>mm</u>
A	2	13	330.2	327	328
	3	13	330.2	328	330
	4	13	330.2	329	328
	5	13	330.2	330	329
	6	13	330.2	329	331
	B	2	2.5	63.5	62.0
3		2.5	63.5	63.0	63.0
4		2.5	63.5	63.0	64.0
5		2.5	63.5	63.0	63.0
6		2.5	63.5	63.0	63.0
C		2	0.4375	11.1	11.3
	3	0.4375	11.1	11.7	11.6
	4	0.4375	11.1	11.7	11.5
	5	0.4375	11.1	11.4	11.2
	6	0.4375	11.1	11.6	11.3
	D	2	0.875	22.2	22.3
3		0.875	22.2	22.2	22.5
4		0.875	22.2	22.6	22.5
5		0.875	22.2	22.5	22.4
6		0.875	22.2	23.2	22.5

Location Diagram:



Dimension Diagram:

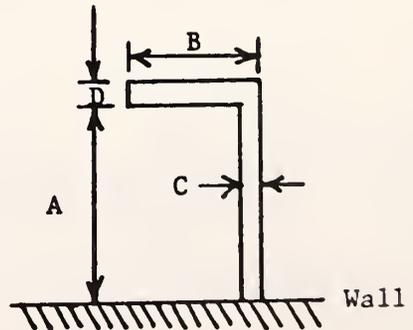


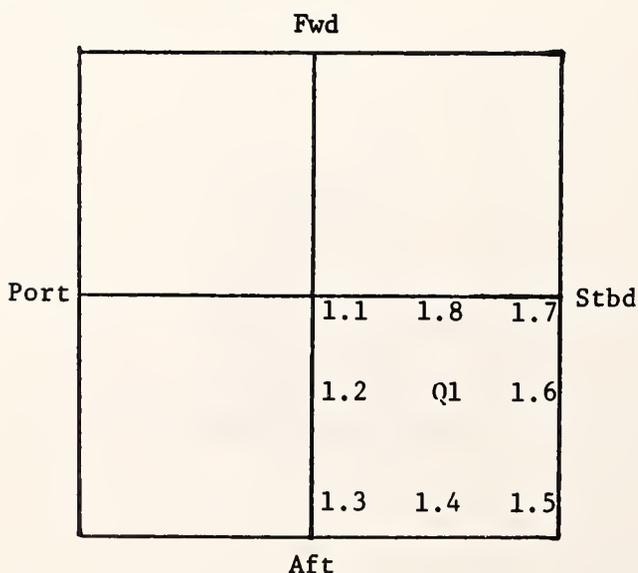
Table 11

Balcony Beam Dimensions
Quadrant 1, Level 1

<u>Location</u>	<u>Flange Length, FL</u>			<u>Flange Thickness, FT</u>		
	<u>Nominal</u>		<u>Measured</u>	<u>Nominal</u>		<u>Measured</u>
	<u>inch</u>	<u>mm</u>	<u>mm</u>	<u>inch</u>	<u>mm</u>	<u>mm</u>
1.1	18	457.2	461	1.19	30.2	31.4
1.2	18	457.2	463	1.00	25.4	25.4
1.3	18	457.2	476	1.00	25.4	25.8
1.4	18	457.2	463	1.00	25.4	25.8
1.5	21	533.4	538	1.50	38.1	38.9
1.6	18	457.2	463	1.00	25.4	25.9
1.7	18	457.2	461	1.19	30.2	31.6
1.8	18	457.2	466	1.00	25.4	26.3

<u>Location</u>	<u>Web Length, WL</u>			<u>Web Thickness, WT</u>		
	<u>Nominal</u>		<u>Measured</u>	<u>Nominal</u>		<u>Measured</u>
	<u>inch</u>	<u>mm</u>	<u>mm</u>	<u>inch</u>	<u>mm</u>	<u>mm</u>
1.1			2708	0.63	16.0	16.7
1.2	60	1524	1526	0.63	16.0	16.6
1.3			4517	0.63	16.0	16.9
1.4	78	1981	1981	0.63	16.0	16.7
1.5			5026	0.63	16.0	16.7
1.6	78	1981	1981	0.63	16.0	16.4
1.7			4459	0.63	16.0	16.6
1.8	60	1524	1523	0.63	16.0	16.9

Location Diagram:



Dimension Diagram:

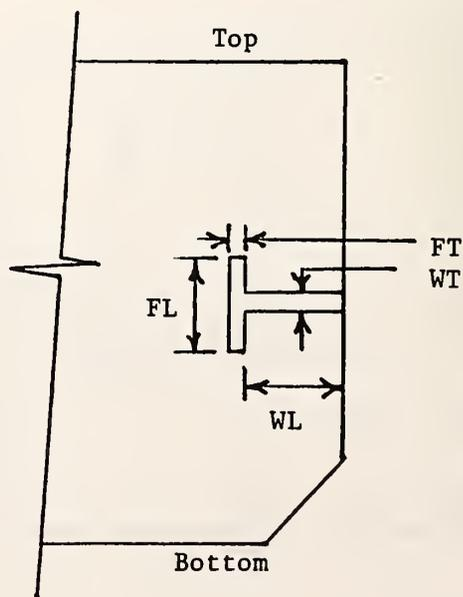


Table 12

Balcony Beam Dimensions
Quadrant 1, Level 2

<u>Location</u>	<u>Flange Length, FL</u>			<u>Flange Thickness, FT</u>		
	<u>Nominal</u>		<u>Measured</u>	<u>Nominal</u>		<u>Measured</u>
	<u>inch</u>	<u>mm</u>		<u>inch</u>	<u>mm</u>	
2.1	18	457.2	462	1.19	30.2	30.4
2.2	18	457.2	462	1.00	25.4	25.5
2.3	18	457.2	463	1.00	25.4	25.9
2.4	18	457.2	465	1.00	25.4	25.9
2.5	27	685.8	687	1.50	38.1	38.0
2.6	18	457.2	462	1.00	25.4	26.7
2.7	18	457.2	459	1.19	30.2	30.4
2.8	18	457.2	463	1.00	25.4	26.7

<u>Location</u>	<u>Web Length, WL</u>			<u>Web Thickness, WT</u>		
	<u>Nominal</u>		<u>Measured</u>	<u>Nominal</u>		<u>Measured</u>
	<u>inch</u>	<u>mm</u>		<u>inch</u>	<u>mm</u>	
2.1			2711	0.63	16.0	15.4
2.2	60	1524	1522	0.63	16.0	15.4
2.3			4495	0.63	16.0	16.0
2.4	78	1981	1981	0.63	16.0	16.0
2.5			5231	0.63	16.0	16.5
2.6	78	1981	1998	0.63	16.0	16.6
2.7			4789	0.63	16.0	16.5
2.8	60	1524	1528	0.63	16.0	16.4

Location Diagram:

Dimension Diagram:

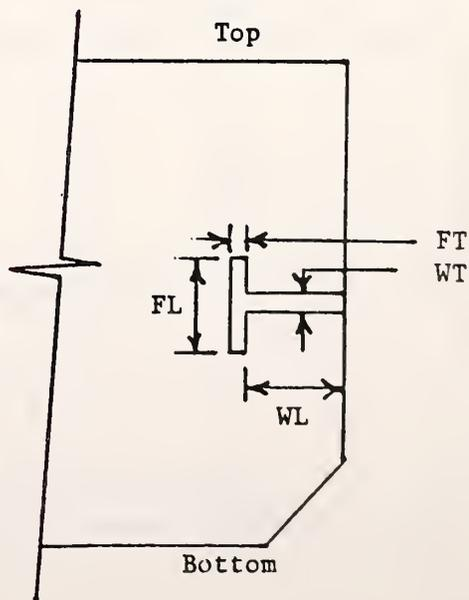
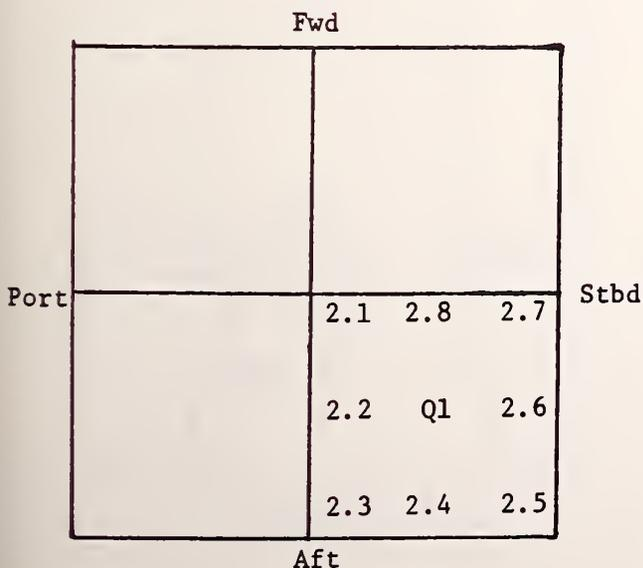


Table 13

Balcony Beam Dimensions
Quadrant 1, Level 3

<u>Location</u>	<u>Flange Length, FL</u>			<u>Flange Thickness, FT</u>		
	<u>Nominal</u>		<u>Measured</u>	<u>Nominal</u>		<u>Measured</u>
	<u>inch</u>	<u>mm</u>	<u>mm</u>	<u>inch</u>	<u>mm</u>	<u>mm</u>
3.1	18	457.2	465	1.19	30.2	30.7
3.2	18	457.2	465	1.00	25.4	26.7
3.3	18	457.2	466	1.00	25.4	26.0
3.4	18	457.2	466	1.00	25.4	26.0
3.5	27	685.8	692	1.50	38.1	38.9
3.6	18	457.2	462	1.00	25.4	26.1
3.7	18	457.2	458	1.19	30.2	30.9
3.8	18	457.2	465	1.00	25.4	25.9

<u>Location</u>	<u>Web Length, WL</u>			<u>Web Thickness, WT</u>		
	<u>Nominal</u>		<u>Measured</u>	<u>Nominal</u>		<u>Measured</u>
	<u>inch</u>	<u>mm</u>	<u>mm</u>	<u>inch</u>	<u>mm</u>	<u>mm</u>
3.1			2710	0.63	16.0	16.4
3.2	60	1524.0	1526	0.63	16.0	16.6
3.3			4478	0.63	16.0	16.2
3.4	78	1981.2	1983	0.63	16.0	16.2
3.5			4936	0.63	16.0	16.6
3.6	78	1981.2	1981	0.63	16.0	16.5
3.7			4485	0.63	16.0	16.2
3.8	60	1524.0	1524	0.63	16.0	16.2

Location Diagram:

Dimension Diagram:

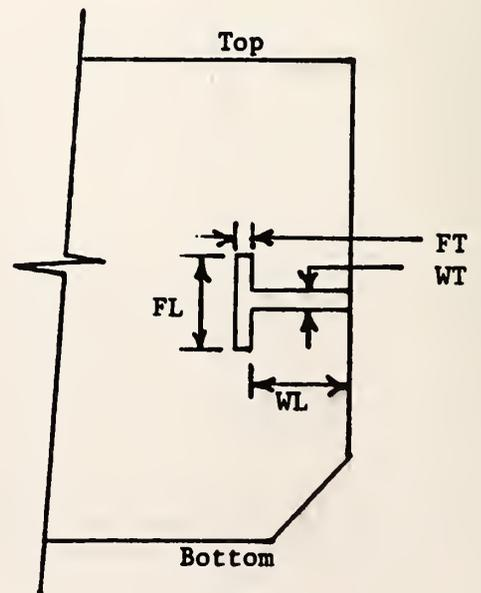
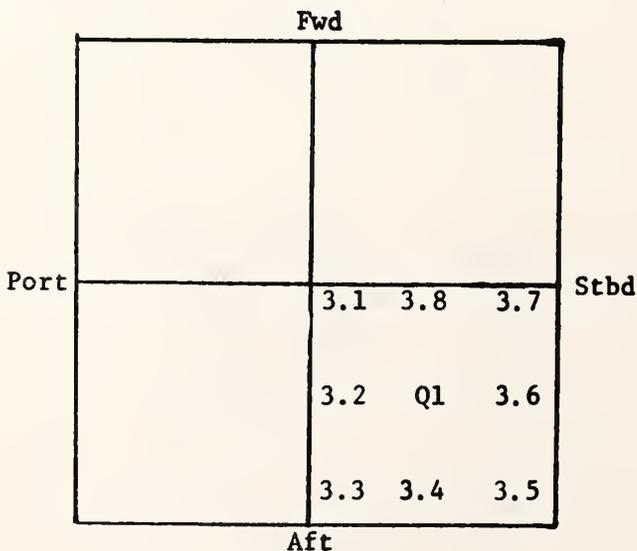


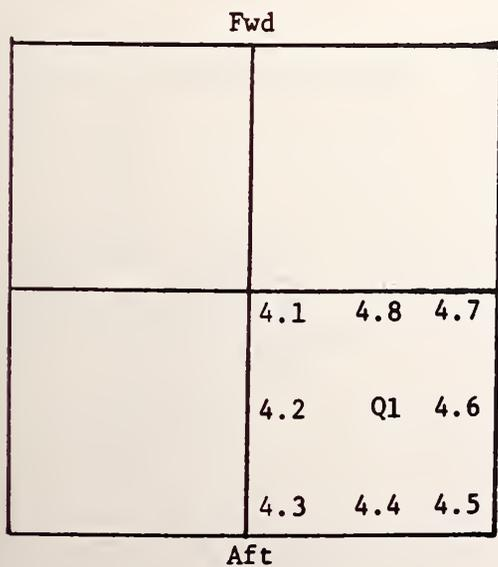
Table 14

Balcony Beam Dimensions
Quadrant 1, Level 4

<u>Location</u>	<u>Flange Length, FL</u>			<u>Flange Thickness, FT</u>		
	<u>Nominal</u>		<u>Measured</u>	<u>Nominal</u>		<u>Measured</u>
	<u>inch</u>	<u>mm</u>	<u>mm</u>	<u>inch</u>	<u>mm</u>	<u>mm</u>
4.1	18	457.2	468	1.19	30.2	30.5
4.2	18	457.2	463	1.00	25.4	25.6
4.3	18	457.2	463	1.00	25.4	26.1
4.4	18	457.2	466	0.75	19.1	19.1
4.5	24	609.6	615	1.50	38.1	38.3
4.6	18	457.2	464	0.75	19.1	19.0
4.7	18	457.2	462	1.19	30.2	30.7
4.8	18	457.2	465	1.00	25.4	26.1

<u>Location</u>	<u>Web Length, WL</u>			<u>Web Thickness, WT</u>		
	<u>Nominal</u>		<u>Measured</u>	<u>Nominal</u>		<u>Measured</u>
	<u>inch</u>	<u>mm</u>	<u>mm</u>	<u>inch</u>	<u>mm</u>	<u>mm</u>
4.1			2711	0.63	16.0	16.1
4.2	60	1524.0	1527	0.63	16.0	15.9
4.3			4486	0.63	16.0	16.4
4.4	78	1981.2	1983	0.63	16.0	16.5
4.5			4937	0.63	16.0	15.2
4.6	78	1981.2	1980	0.63	16.0	15.4
4.7			4505	0.63	16.0	16.2
4.8	60	1524.0	1581	0.63	16.0	16.2

Location Diagram:



Dimension Diagram:

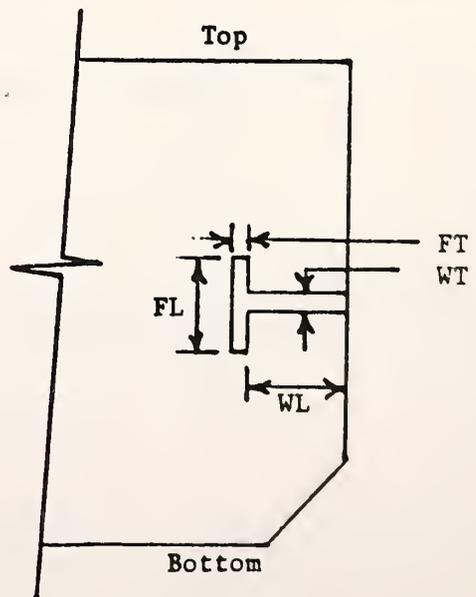


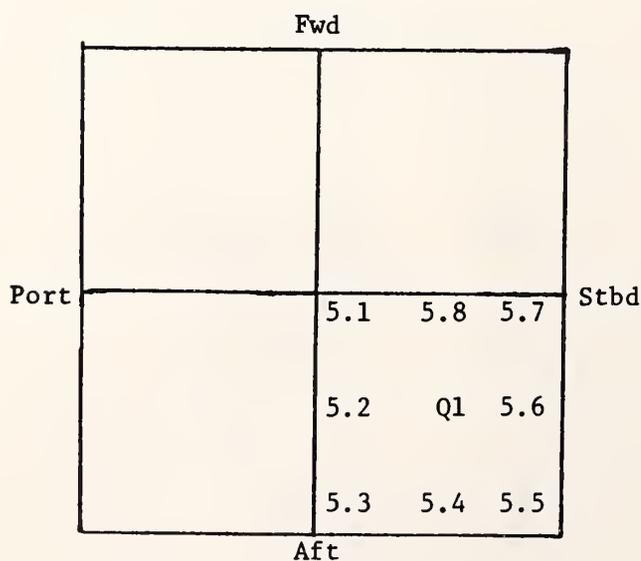
Table 15

Balcony Beam Dimensions
Quadrant 1, Level 5

<u>Location</u>	<u>Flange Length, FL</u>			<u>Flange Thickness, FT</u>		
	<u>Nominal</u>		<u>Measured</u>	<u>Nominal</u>		<u>Measured</u>
	<u>inch</u>	<u>mm</u>	<u>mm</u>	<u>inch</u>	<u>mm</u>	<u>mm</u>
5.1	18	457.2	461	1.19	30.2	30.4
5.2	18	457.2	465	1.00	25.4	25.3
5.3	18	457.2	460	1.00	25.4	26.1
5.4	18	457.2	460	0.75	19.1	19.3
5.5	24	609.6	615	1.50	38.1	38.5
5.6	18	457.2	464	0.75	19.1	19.0
5.7	18	457.2	465	1.19	30.2	30.8
5.8	18	457.2	478	1.00	25.4	25.9

<u>Location</u>	<u>Web Length, WL</u>			<u>Web Thickness, WT</u>		
	<u>Nominal</u>		<u>Measured</u>	<u>Nominal</u>		<u>Measured</u>
	<u>inch</u>	<u>mm</u>	<u>mm</u>	<u>inch</u>	<u>mm</u>	<u>mm</u>
5.1			2710	0.63	16.0	15.2
5.2	60	1524.0	1523	0.63	16.0	15.3
5.3			4490	0.63	16.0	15.6
5.4	78	1981.2	1981	0.63	16.0	16.4
5.5			4939	0.63	16.0	16.5
5.6	78	1981.2	1976	0.63	16.0	13.7
5.7			4486	0.63	16.0	16.5
5.8	60	1524.0	1522	0.63	16.0	16.4

Location Diagram:



Dimension Diagram:

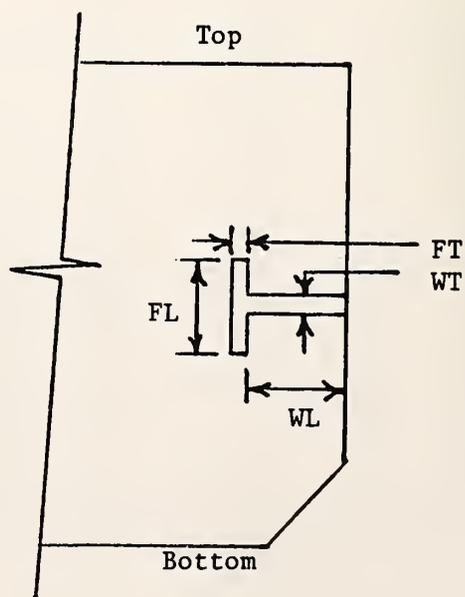


Table 16

Balcony Beam Dimensions
Quadrant 1, Level 6

<u>Location</u>	<u>Flange Length, FL</u>			<u>Flange Thickness, FT</u>		
	<u>Nominal</u>		<u>Measured</u>	<u>Nominal</u>		<u>Measured</u>
	<u>inch</u>	<u>mm</u>	<u>mm</u>	<u>inch</u>	<u>mm</u>	<u>mm</u>
6.1	16	406.4	411	1.00	25.4	25.2
6.2	16	406.4	411	0.75	19.1	19.7
6.3	16	406.4	411	1.00	25.4	26.3
6.4	16	406.4	409	0.75	19.1	19.6
6.5	20	508.0	511	1.50	38.1	40.0
6.6	16	406.4	410	0.75	19.1	19.7
6.7	16	406.4	410	1.00	25.4	26.0
6.8	16	406.4	409	0.75	19.1	19.6

<u>Location</u>	<u>Web Length, WL</u>			<u>Web Thickness, WT</u>		
	<u>Nominal</u>		<u>Measured</u>	<u>Nominal</u>		<u>Measured</u>
	<u>inch</u>	<u>mm</u>	<u>mm</u>	<u>inch</u>	<u>mm</u>	<u>mm</u>
6.1			2724	0.63	16.0	16.4
6.2	60	1524.0	1526	0.63	16.0	16.0
6.3			4503	0.63	16.0	16.8
6.4	78	1981.2	1982	0.63	16.0	16.6
6.5			4968	0.63	16.0	16.8
6.6	78	1981.2	1972	0.63	16.0	16.6
6.7			4496	0.63	16.0	16.6
6.8	60	1524.0	1522	0.63	16.0	16.6

Location Diagram:

Dimension Diagram:

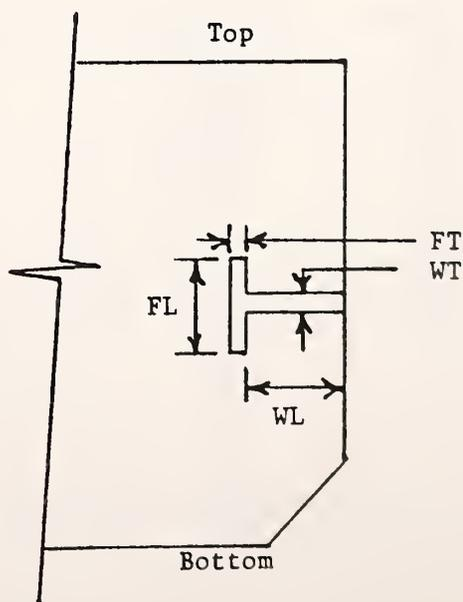
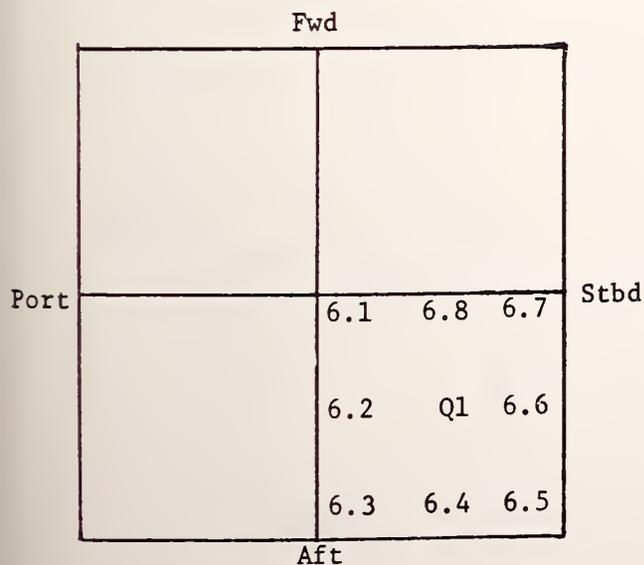


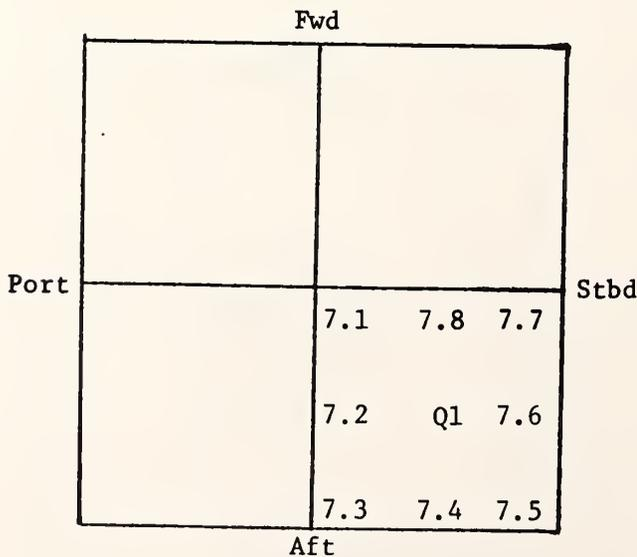
Table 17

Balcony Beam Dimensions
Quadrant 1, Level 7

<u>Location</u>	<u>Flange Length, FL</u>			<u>Flange Thickness, FT</u>		
	<u>Nominal</u>		<u>Measured</u>	<u>Nominal</u>		<u>Measured</u>
	<u>inch</u>	<u>mm</u>		<u>inch</u>	<u>mm</u>	
7.1	14	355.6	357	0.75	19.1	20.0
7.2	14	355.6	363	0.75	19.1	20.0
7.3	14	355.6	358	0.75	19.1	19.2
7.4	14	355.6	363	0.75	19.1	19.6
7.5	18	457.2	460	1.00	25.4	26.4
7.6	14	355.6	362	0.75	19.1	19.3
7.7	14	355.6	364	0.75	19.1	19.7
7.8	14	355.6	365	0.75	19.1	20.1

<u>Location</u>	<u>Web Length, WL</u>			<u>Web Thickness, WT</u>		
	<u>Nominal</u>		<u>Measured</u>	<u>Nominal</u>		<u>Measured</u>
	<u>inch</u>	<u>mm</u>		<u>inch</u>	<u>mm</u>	
7.1			2714	0.63	16.0	16.6
7.2	60	1524.0	1529	0.63	16.0	16.3
7.3			4521	0.63	16.0	16.1
7.4	78	1981.2	1978	0.63	16.0	16.1
7.5			4948	0.63	16.0	16.3
7.6	78	1981.2	1980	0.63	16.0	17.1
7.7			4487	0.63	16.0	25.5
7.8	60	1524.0	1520	0.63	16.0	25.5

Location Diagram:



Dimension Diagram:

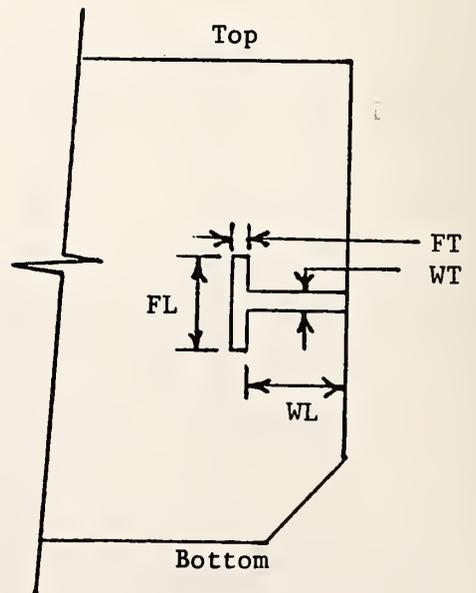


Table 18

Balcony Beam Dimensions
Quadrant 4, Level 1

<u>Location</u>	<u>Flange Length, FL</u>			<u>Flange Thickness, FT</u>		
	<u>Nominal</u>		<u>Measured</u>	<u>Nominal</u>		<u>Measured</u>
	<u>inch</u>	<u>mm</u>	<u>mm</u>	<u>inch</u>	<u>mm</u>	<u>mm</u>
1.2	18	457.2	456	1.19	30.2	30.1
1.3	18	457.2	464	1.00	25.4	26.2
1.4	21	533.4	539	1.50	38.1	39.1
1.5	18	457.2	460	1.00	25.4	25.5
1.6	18	457.2	459	1.00	25.4	25.9

<u>Location</u>	<u>Web Length, WL</u>			<u>Web Thickness, WT</u>		
	<u>Nominal</u>		<u>Measured</u>	<u>Nominal</u>		<u>Measured</u>
	<u>inch</u>	<u>mm</u>	<u>mm</u>	<u>inch</u>	<u>mm</u>	<u>mm</u>
1.2			3787	0.63	16.0	16.4
1.3	78	1981.2	1977	0.63	16.0	16.1
1.4			4904	0.63	16.0	16.3
1.5	78	1981.2	1980	0.63	16.0	16.2
1.6			3741	0.63	16.0	16.7

Location Diagram:

Dimension Diagram:

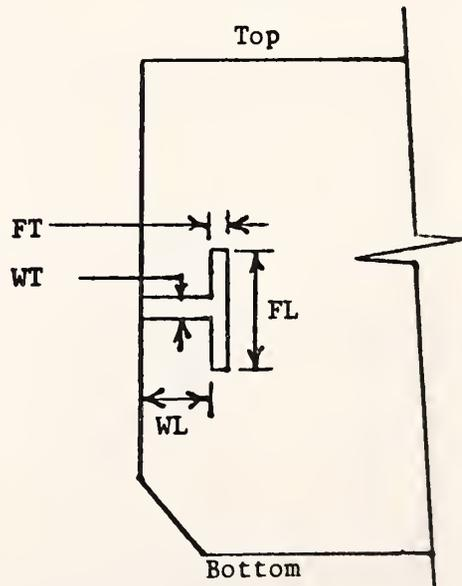
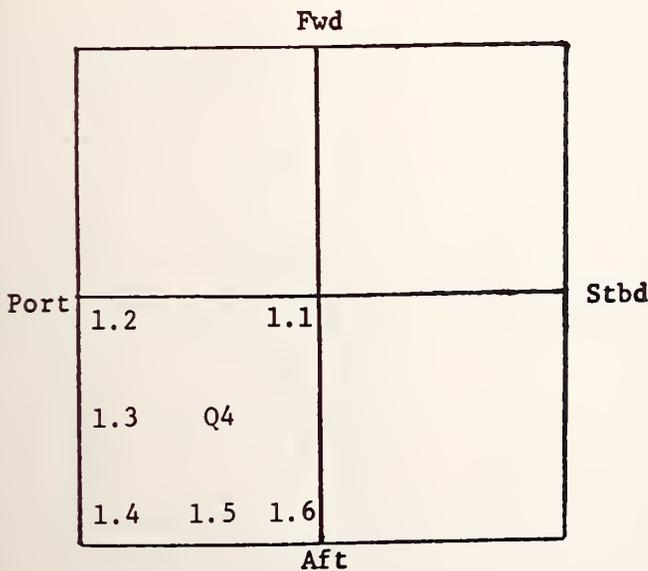


Table 19

Balcony Beam Dimensions
Quadrant 4, Level 2

<u>Location</u>	<u>Flange Length, FL</u>			<u>Flange Thickness, FT</u>		
	<u>Nominal</u>		<u>Measured</u>	<u>Nominal</u>		<u>Measured</u>
	<u>inch</u>	<u>mm</u>	<u>mm</u>	<u>inch</u>	<u>mm</u>	<u>mm</u>
2.2	18	457.2	459	1.19	30.2	30.9
2.3	18	457.2	464	1.00	25.4	26.2
2.4	27	685.8	688	1.50	38.1	39.5
2.5	18	457.2	464	1.00	25.4	25.4
2.6	18	457.2	463	1.00	25.4	26.0

<u>Location</u>	<u>Web Length, WL</u>			<u>Web Thickness, WT</u>		
	<u>Nominal</u>		<u>Measured</u>	<u>Nominal</u>		<u>Measured</u>
	<u>inch</u>	<u>mm</u>	<u>mm</u>	<u>inch</u>	<u>mm</u>	<u>mm</u>
2.2			3753	0.63	16.0	16.1
2.3	78	1981.2	1990	0.63	16.0	17.6
2.4			4948	0.63	16.0	16.5
2.5	78	1981.2	1980	0.63	16.0	16.8
2.6			3794	0.63	16.0	16.4

Location Diagram:

Dimension Diagram:

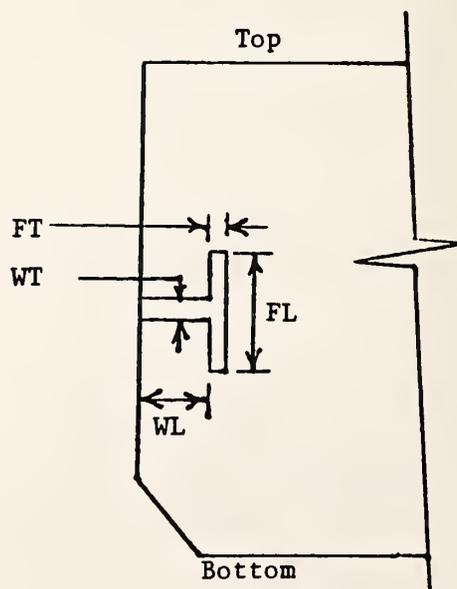
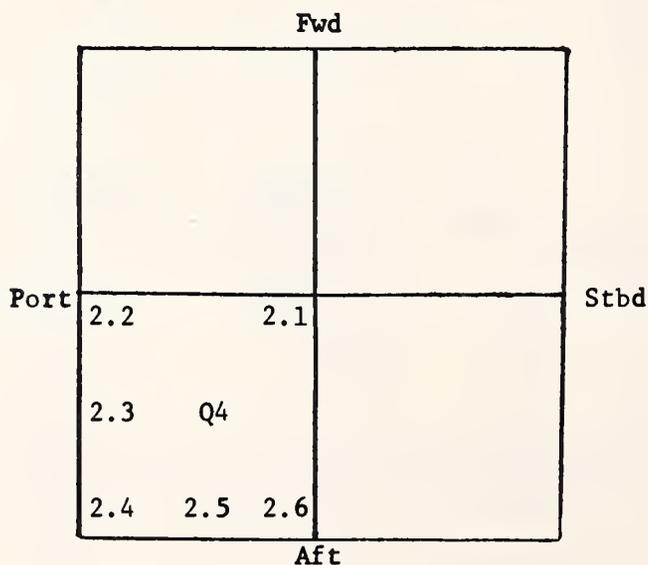


Table 20

Balcony Beam Dimensions
Quadrant 4, Level 3

Location	Flange Length, FL			Flange Thickness, FT		
	Nominal		Measured	Nominal		Measured
	inch	mm		inch	mm	
3.2	18	457.2	463	1.19	30.2	30.1
3.3	18	457.2	463	1.00	25.4	26.2
3.4	27	685.8	683	1.50	38.1	39.3
3.5	18	457.2	465	1.00	25.4	25.2
3.6	18	457.2	462	1.00	25.4	26.2

Location	Web Length, WL			Web Thickness, WT		
	Nominal		Measured	Nominal		Measured
	inch	mm		inch	mm	
3.2			3436	0.63	16.0	15.9
3.3	78	1981.2	1982	0.63	16.0	16.8
3.4			4935	0.63	16.0	16.7
3.5	78	1981.2	1982	0.63	16.0	16.5
3.6			3772	0.63	16.0	17.1

Location Diagram:

Dimension Diagram:

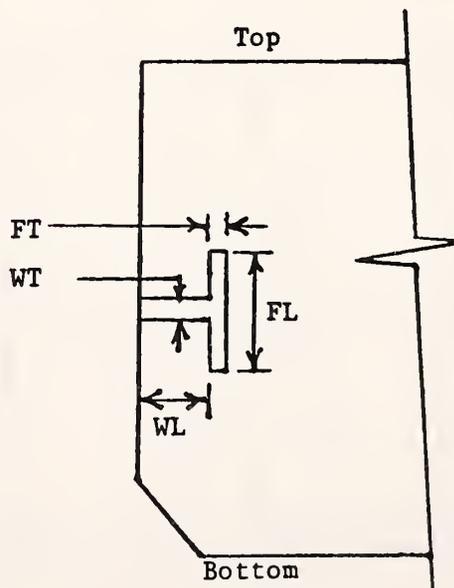
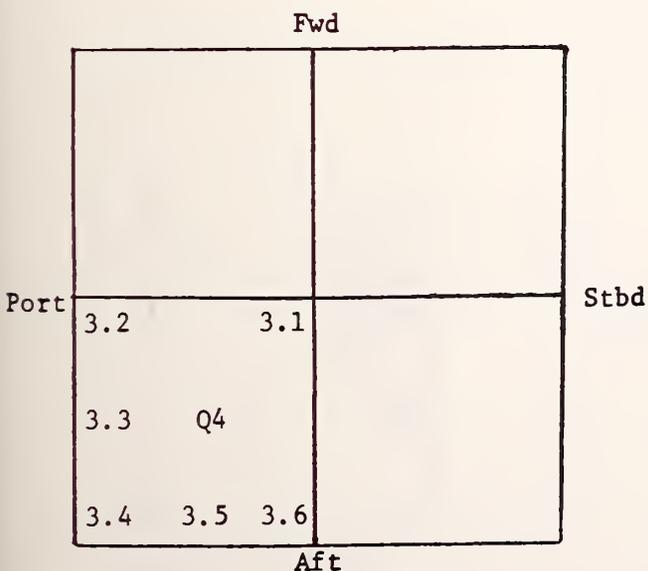


Table 21

Balcony Beam Dimensions
Quadrant 4, Level 4

<u>Location</u>	<u>Flange Length, FL</u>			<u>Flange Thickness, FT</u>		
	<u>Nominal</u>		<u>Measured</u>	<u>Nominal</u>		<u>Measured</u>
	<u>inch</u>	<u>mm</u>	<u>mm</u>	<u>inch</u>	<u>mm</u>	<u>mm</u>
4.2	18	457.2	466	1.19	30.2	30.1
4.3	18	457.2	461	0.75	19.1	19.6
4.4	24	609.6	614	1.50	38.1	38.6
4.5	18	457.2	460	0.75	19.1	19.5
4.6	18	457.2	461	1.00	25.4	26.0

<u>Location</u>	<u>Web Length, WL</u>			<u>Web Thickness, WT</u>		
	<u>Nominal</u>		<u>Measured</u>	<u>Nominal</u>		<u>Measured</u>
	<u>inch</u>	<u>mm</u>	<u>mm</u>	<u>inch</u>	<u>mm</u>	<u>mm</u>
4.2			3755	0.63	16.0	15.9
4.3	78	1981.2	1984	0.63	16.0	16.8
4.4			4931	0.63	16.0	16.1
4.5	78	1981.2	1982	0.63	16.0	16.0
4.6			3760	0.63	16.0	16.4

Location Diagram:

Dimension Diagram:

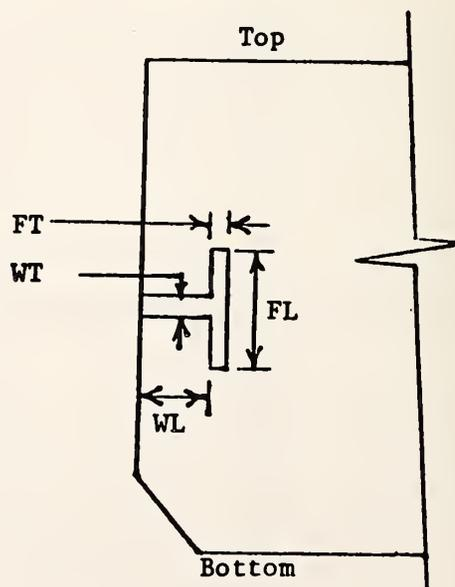
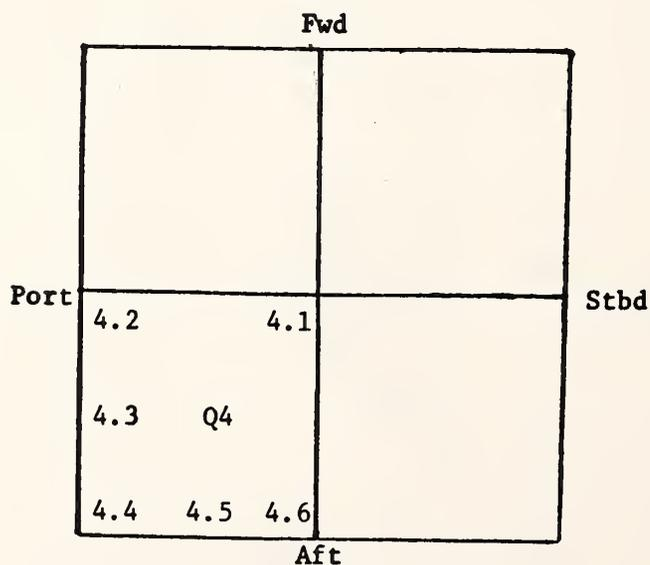


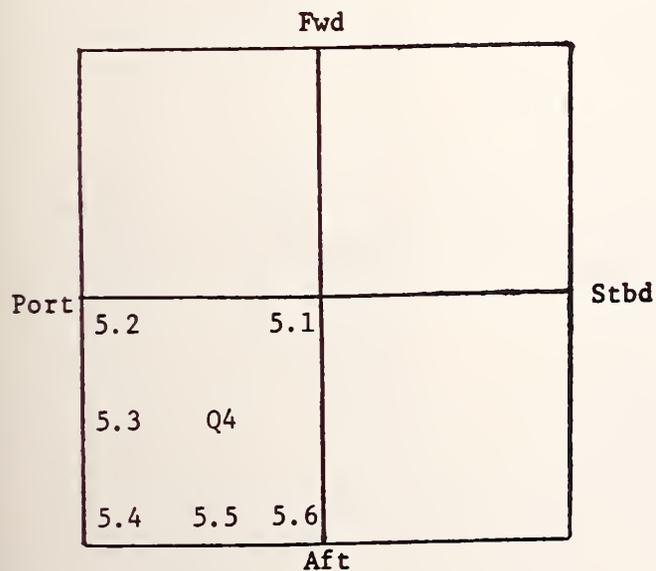
Table 22

Balcony Beam Dimensions
Quadrant 4, Level 5

<u>Location</u>	<u>Flange Length, FL</u>			<u>Flange Thickness, FT</u>		
	<u>Nominal</u>		<u>Measured</u>	<u>Nominal</u>		<u>Measured</u>
	<u>inch</u>	<u>mm</u>		<u>inch</u>	<u>mm</u>	
5.2	18	457.2	458	1.19	30.2	30.1
5.3	18	457.2	461	0.75	19.1	19.6
5.4	24	609.6	614	1.50	38.1	38.5
5.5	18	457.2	463	0.75	19.1	19.5
5.6	18	457.2	462	1.00	25.4	25.9

<u>Location</u>	<u>Web Length, WL</u>			<u>Web Thickness, WT</u>		
	<u>Nominal</u>		<u>Measured</u>	<u>Nominal</u>		<u>Measured</u>
	<u>inch</u>	<u>mm</u>		<u>inch</u>	<u>mm</u>	
5.2			3795	0.63	16.0	16.3
5.3	78	1981.2	1986	0.63	16.0	16.4
5.4			4953	0.63	16.0	16.7
5.5	78	1981.2	1989	0.63	16.0	16.7
5.6			3777	0.63	16.0	16.3

Location Diagram:



Dimension Diagram:

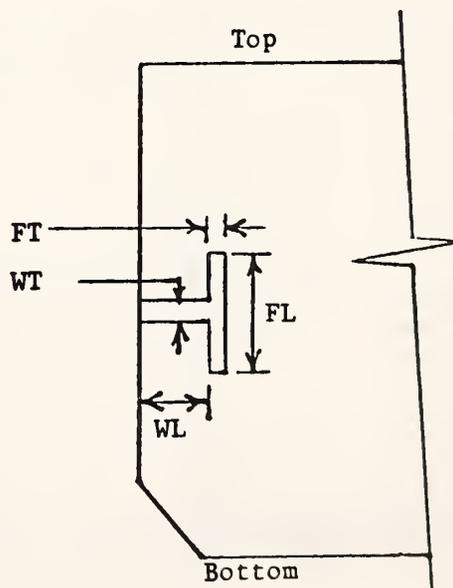


Table 23

Balcony Beam Dimensions
Quadrant 4, Level 6

<u>Location</u>	<u>Flange Length, FL</u>			<u>Flange Thickness, FT</u>		
	<u>Nominal</u>		<u>Measured</u>	<u>Nominal</u>		<u>Measured</u>
	<u>inch</u>	<u>mm</u>	<u>mm</u>	<u>inch</u>	<u>mm</u>	<u>mm</u>
6.2	16	406.4	412	1.00	25.4	26.5
6.3	16	406.4	414	0.75	19.1	19.5
6.4	20	508.0	508	1.50	38.1	38.8
6.5	16	406.4	411	0.75	19.1	19.3
6.6	16	406.4	412	1.00	25.4	26.5

<u>Location</u>	<u>Web Length, WL</u>			<u>Web Thickness, WT</u>		
	<u>Nominal</u>		<u>Measured</u>	<u>Nominal</u>		<u>Measured</u>
	<u>inch</u>	<u>mm</u>	<u>mm</u>	<u>inch</u>	<u>mm</u>	<u>mm</u>
6.2			3771	0.63	16.0	16.3
6.3	78	1981.2	1982	0.63	16.0	16.8
6.4			4945	0.63	16.0	16.4
6.5	78	1981.2	1982	0.63	16.0	16.6
6.6			3786	0.63	16.0	16.4

Location Diagram:

Dimension Diagram:

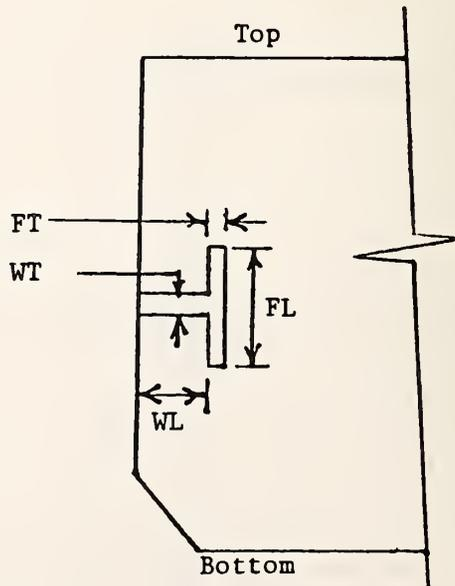
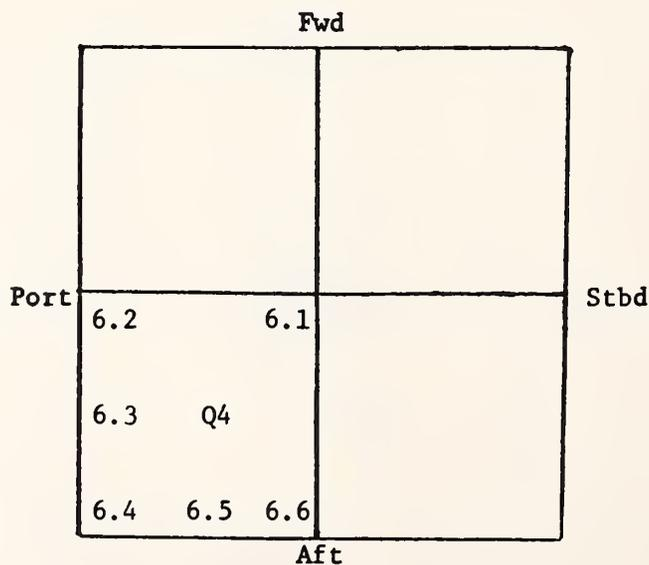


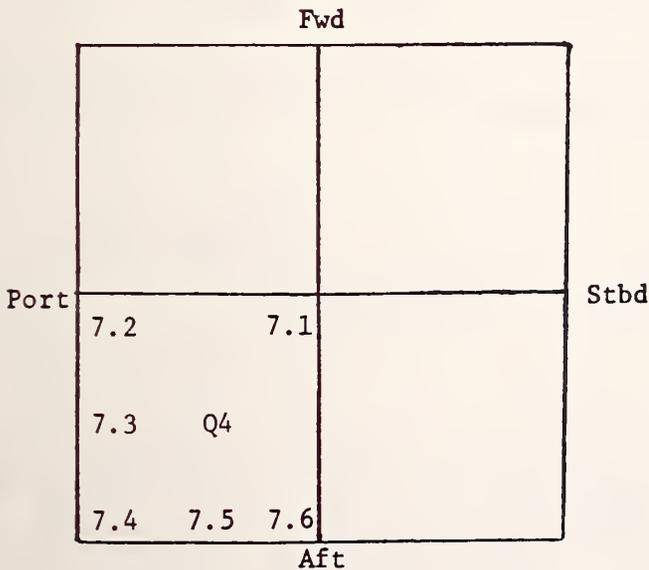
Table 24

Balcony Beam Dimensions
Quadrant 4, Level 7

Location	Flange Length, FL			Flange Thickness, FT		
	Nominal		Measured	Nominal		Measured
	inch	mm		inch	mm	
7.2	14	355.6	352	0.75	19.1	19.6
7.3	14	355.6	365	0.75	19.1	20.0
7.4	18	457.2	462	1.00	25.4	26.3
7.5	14	355.6	363	0.75	19.1	19.4
7.6	14	355.6	368	0.75	19.1	20.0

Location	Web Length, WL			Web Thickness, WT		
	Nominal		Measured	Nominal		Measured
	inch	mm		inch	mm	
7.2			3383	0.63	16.0	16.3
7.3	78	1981.2	1983	0.63	16.0	16.8
7.4			4950	0.63	16.0	16.4
7.5	78	1981.2	1988	0.63	16.0	16.6
7.6			3781	0.63	16.0	16.0

Location Diagram:



Dimension Diagram:

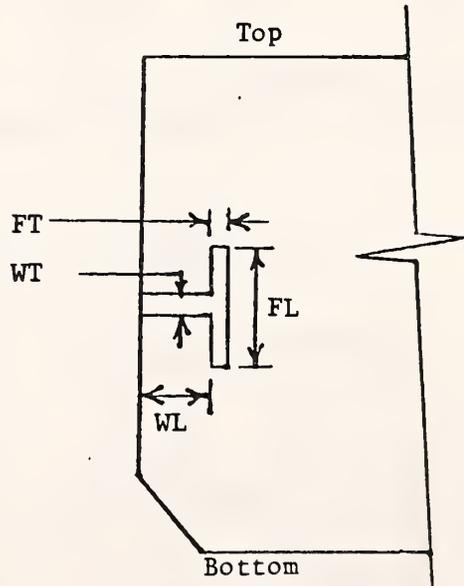


Table 25

Balcony Beam Dimensions
Quadrant 2, Level 1-7

<u>Location</u>	<u>Flange Length, FL</u>			<u>Flange Thickness, FT</u>		
	<u>Nominal</u>		<u>Measured</u>	<u>Nominal</u>		<u>Measured</u>
	<u>inch</u>	<u>mm</u>	<u>mm</u>	<u>inch</u>	<u>mm</u>	<u>mm</u>
1.5	18	457.2	460	1.00	25.4	25.7
2.5	18	457.2	464	1.00	25.4	25.2
3.5	18	457.2	463	1.00	25.4	25.2
4.5	18	457.2	458	0.75	19.1	18.1
5.5	18	457.2	461	0.75	19.1	19.6
6.5	16	406.4	412	0.75	19.1	19.7
7.5	14	355.6	361	0.75	19.1	19.6

<u>Location</u>	<u>Web Length, WL</u>			<u>Web Thickness, WT</u>		
	<u>Nominal</u>		<u>Measured</u>	<u>Nominal</u>		<u>Measured</u>
	<u>inch</u>	<u>mm</u>	<u>mm</u>	<u>inch</u>	<u>mm</u>	<u>mm</u>
1.5	78	1981.2	1982	0.63	16.0	16.5
2.5	78	1981.2	1975	0.63	16.0	16.6
3.5	78	1981.2	1981	0.63	16.0	16.5
4.5	78	1981.2	1980	0.63	16.0	16.5
5.5	78	1981.2	1983	0.63	16.0	16.9
6.5	78	1981.2	1978	0.63	16.0	16.1
7.5	78	1981.2	1975	0.63	16.0	16.2

Location Diagram:

Dimension Diagram:

(Location = i.j; where i = level, j = location)

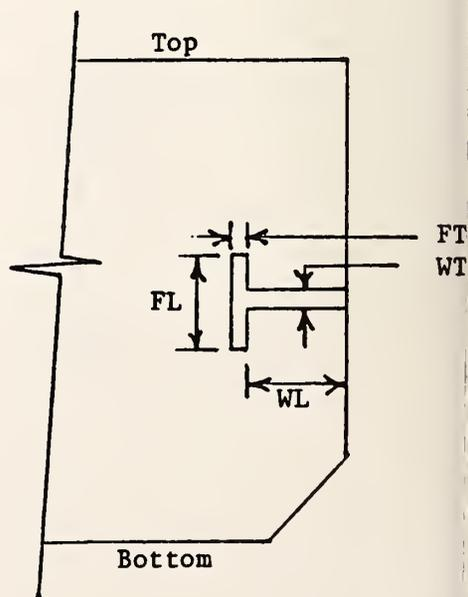
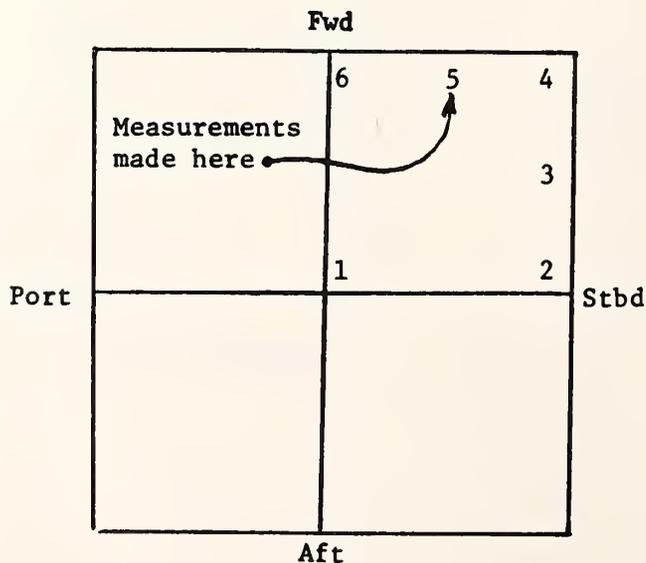


Table 26

Balcony Beam Dimensions
Quadrant 3, Level 1-6

<u>Location</u>	<u>Flange Length, FL</u>			<u>Flange Thickness, FT</u>		
	<u>Nominal</u>		<u>Measured</u>	<u>Nominal</u>		<u>Measured</u>
	<u>inch</u>	<u>mm</u>	<u>mm</u>	<u>inch</u>	<u>mm</u>	<u>mm</u>
1.8	18	457.2	467	1.00	25.4	26.3
2.8	18	457.2	464	1.00	25.4	26.3
3.8	18	457.2	462	1.00	25.4	26.6
4.8	18	457.2	463	1.00	25.4	26.0
5.8	18	457.2	463	1.00	25.4	26.7
6.8	16	406.4	409	0.75	19.1	19.4
7.8	Not accessible					

<u>Location</u>	<u>Web Length, WL</u>			<u>Web Thickness, WT</u>		
	<u>Nominal</u>		<u>Measured</u>	<u>Nominal</u>		<u>Measured</u>
	<u>inch</u>	<u>mm</u>	<u>mm</u>	<u>inch</u>	<u>mm</u>	<u>mm</u>
1.8	60	1524	1524	0.63	16.0	16.7
2.8	60	1524	1527	0.63	16.0	16.0
3.8	60	1524	1526	0.63	16.0	16.7
4.8	60	1524	1514	0.63	16.0	16.0
5.8	60	1524	1526	0.63	16.0	16.8
6.8	60	1524	1519	0.63	16.0	16.2
7.8	Not accessible					

Location Diagram:

(Location = i.j; where i = level, j = location)

Dimension Diagram:

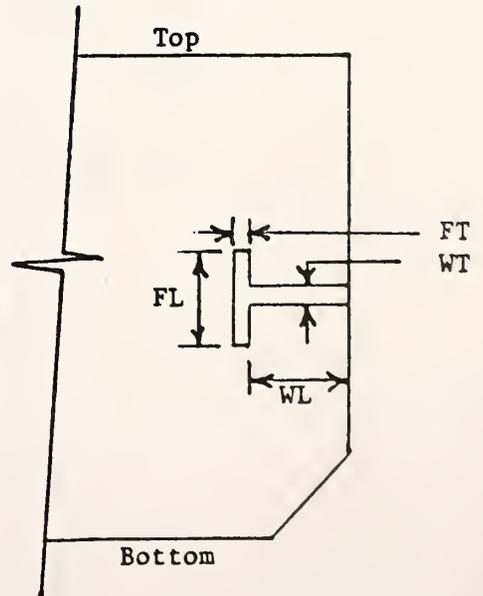
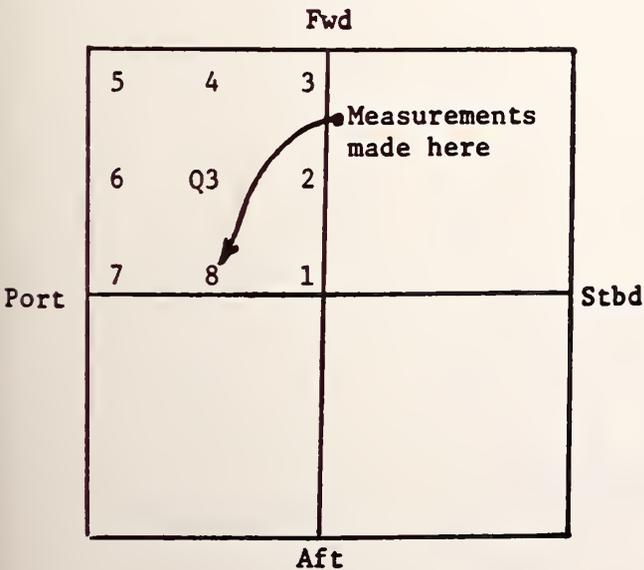


Table 27 Deadwood Volume - (All volumes in m³)

Level	Height 1	Height 2	Swash Bulkhead	Liquid Tight Bulkhead	Large Floor Beams	Small Floor Beams	Vertical Stiffeners	Balconies	Exterior Walls	Ceiling Beams	Total Volume by Level	Accumulated Deadwood Volume
0-1	0	2098.3	1.00	1.17	11.13	15.05	1.95	9.90	7.1	-	47.3	47.3
1-2	2098.3	4480.1	1.22	1.23	-	-	2.21	10.78	8.5	-	23.9	71.2
2-3	4480.1	7107.5	1.27	1.36	-	-	2.44	11.54	8.1	-	24.7	95.9
3-4	7107.5	9841.6	1.37	1.33	-	-	2.53	10.28	8	-	23.5	119.4
4-5	9841.6	12850.7	1.45	1.49	-	-	2.79	10.22	8.5	-	24.5	143.9
5-6	12850.7	16065.1	1.58	1.54	-	-	2.98	10.04	8.5	-	24.6	168.5
6-7	16065.1	19476.1	1.67	1.65	-	-	3.16	10.66	8.2	2.5	27.8	196.3
7-8	19476.1	22950.0	1.70	1.67	-	-	3.22	-	7.9	43.4	57.9	254.2

Volume of Tank Bottom = 24.2

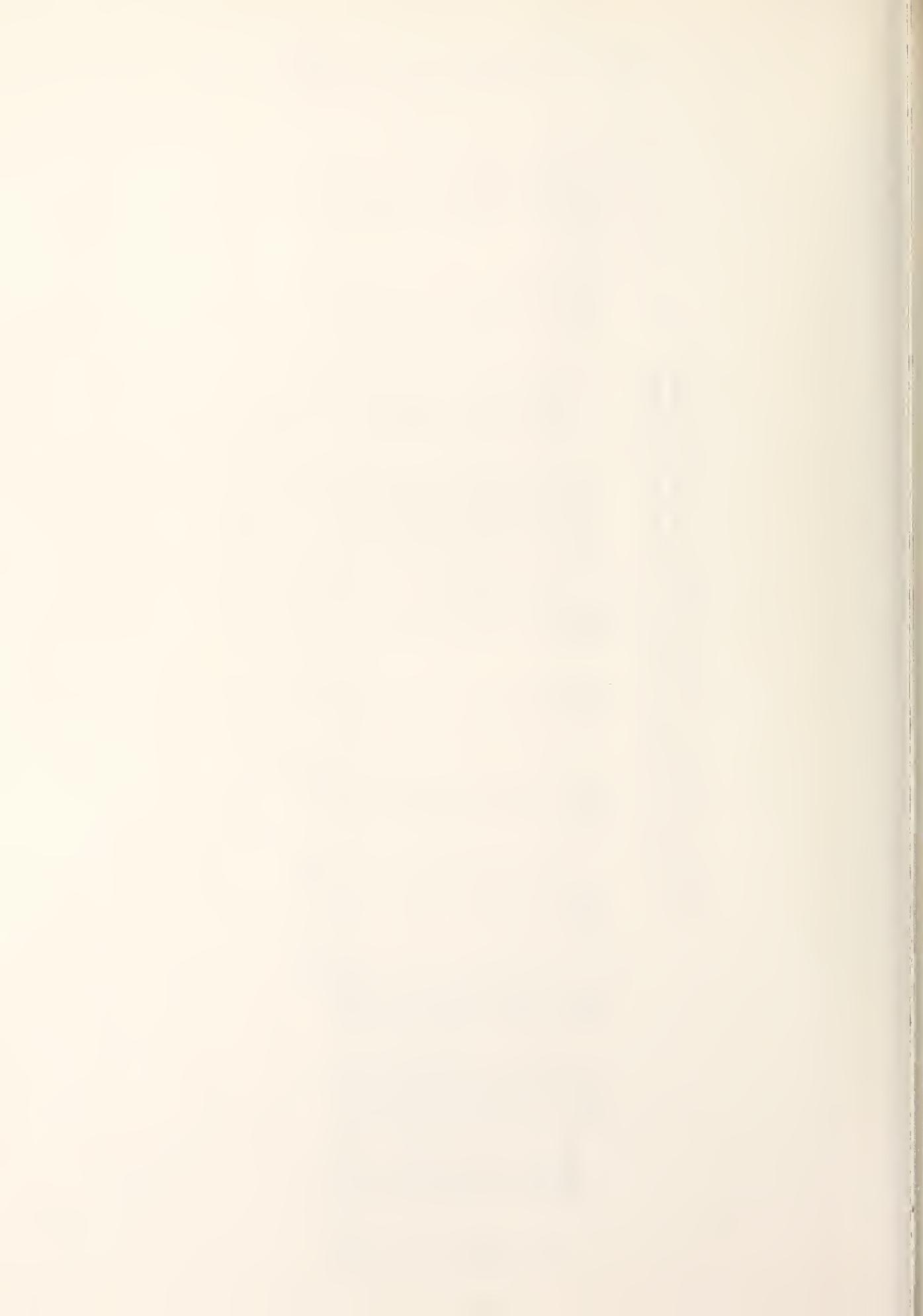
Volume of Tank Top = 19.2

Total Measured Deadwood = 297.6

Table 28 - Deviation of Interior Deadwood from Nominal -Percent[†]
 (Does not include bottom and top or exterior wall deviations)

Level	Height 1	Height 2	Swash Bulkhead	Liquid Tight Bulkhead	Large Floor Beams	Small Floor Beams	Vertical Stiffners	Balconies	Deviation by Level	Accumulated Deviation
0-1	0	2098.3	6.0	6.0	3.8	2.2	2.0	3.2	3.1	3.1
1-2	2098.3	4480.1	14.4	9.4	-	-	2.0	0.4	2.5	2.9
2-3	4480.1	7107.5	2.9	9.8	-	-	2.0	1.6	2.5	2.8
3-4	7107.5	9841.6	6.7	3.1	-	-	2.0	0	1.2	2.5
4-5	9841.6	12850.7	2.8	5.1	-	-	2.0	1.3	0	2.1
5-6	12850.7	16065.1	4.3	1.6	-	-	2.0	2.7	2.6	2.2
6-7	16065.1	19476.1	5.0	3.1	-	-	2.0	11.3	8.1	2.9
7-8	19476.1	22950.0	3.7	2.4	-	-	2.0	-	2.5	2.9

[†] Ceiling beams are not included because nominal size was assumed.



Appendix H

**Bottom Surveys of Freestanding
LNG Cargo Tanks**

By

**W. C. Haight, F. Scire, R. G. Hartsock,
C. Johnson, and R. J. Hocken**

Table of Contents

	<u>Page</u>
Abstract	H1
1. Introduction	H1
2. The Measurement Method	H2
3. Data Analysis	H9
4. Error Analysis	H10
5. Results and Conclusions	H11
6. Tables of Survey Data	H16
7. References	H58

List of Figures

Figure 1 - LNG Tank Schematic	H3
Figure 2 - Laser Level Schematic	H4
Figure 3 - LNG Tank Bottom Plan	H6

List of Tables

Table 1 - Random Error Sources	H10
Table 2 - El Paso Savannah, Bottom Flatness Summary	H12
Table 3 - El Paso Cove Point, Bottom Flatness Summary	H12
Table 4 - El Paso Savannah, Capacitance Gage Survey	H13
Table 5 - El Paso Cove Point, Capacitance Gage Survey	H15
Tables A1-A40 - Tables of Survey Data	H16

Bottom Surveys of Free-Standing
LNG Cargo Tanks

W. C. Haight, F. Scire, R. G. Hartsock,
C. Johnson, and R. J. Hocken

Abstract

Large Liquid Natural Gas (LNG) cargo tanks in a variety of configurations are presently under construction worldwide. Metrologists are being called upon to measure their (a) capacity, (b) deformation under load, and (c) mechanical deformation due to handling after calibration. The results of a series of measurements made on free standing aluminum tanks to determine the extent of the permanent distortion caused by loading them into a ship with a large crane were presented in a previous paper (1). In this paper, we present the results of the mapping surveys performed on the bottom (i.e. bottom survey) of ten (10) such tanks that were placed on the two ships, the El Paso Savannah and the El Paso Cove Point.

1. Introduction

Measurement of LNG cargo volume determines one of three essential quantities upon which the dollar value of LNG shipments is based, the other two being LNG composition and density. The volume of a shipboard cargo is typically determined from a measurement of the liquid-gas interface level relative to the tank bottom in each tank. This measurement, in conjunction with a prior determination of the tank size and shape, can be used to compute a liquid volume at the time of gaging. Techniques for calibration of tanks and computation of total volume have been reported elsewhere.

The area of concern for this paper is the flatness of the bottoms of freestanding prismatic tanks. Tank construction is conducted independently of ship construction. When the tanks are completed, the ship deck plates are removed and the tanks are lifted into the ship's hull by means of a large crane. Primary tank calibrations were done photogrammetrically, prior to loading into the ship, while the tanks were still in the storage yard. The tank bottoms were surveyed by the tank construction firm from beneath. It is the desire of the sponsor to know if these measurements remain valid after the tanks have been loaded into the ship and are resting on a base other than the one on which they were calibrated. To meet this end, the bottom profiles of every quadrant of each tank in the El Paso Savannah and the El Paso Cove Point were measured by NBS after the tanks were installed in the ships. A typical tank is shown in Figure 1.

2. The Measurement Method

"Flatness" mapping surveys were conducted for each tank on the tank interior bottom, after the tank was loaded into the ship's hull. The characterization of the bottom flatness involved the following technique:

A rotating laser, schematized in Figure 2, was used to define a plane flat to ± 10 sec of arc and approximately parallel to the tank surface. This laser has a self leveling feature that permits the plane to be established perpendicular to the earth's gravitational field. For the surveys reported herein, the laser was always allowed to self-level after initial setup, and was then locked to insure that the reference plane remained fixed throughout the survey. Offsets from this swept-plane were measured to the actual tank surface, which was marked with a nearly uniform grid of points, using a beam seeking laser rod. These commercially available rods had been refitted with higher accuracy scales, kinematic base plates, and a circular bubble level to

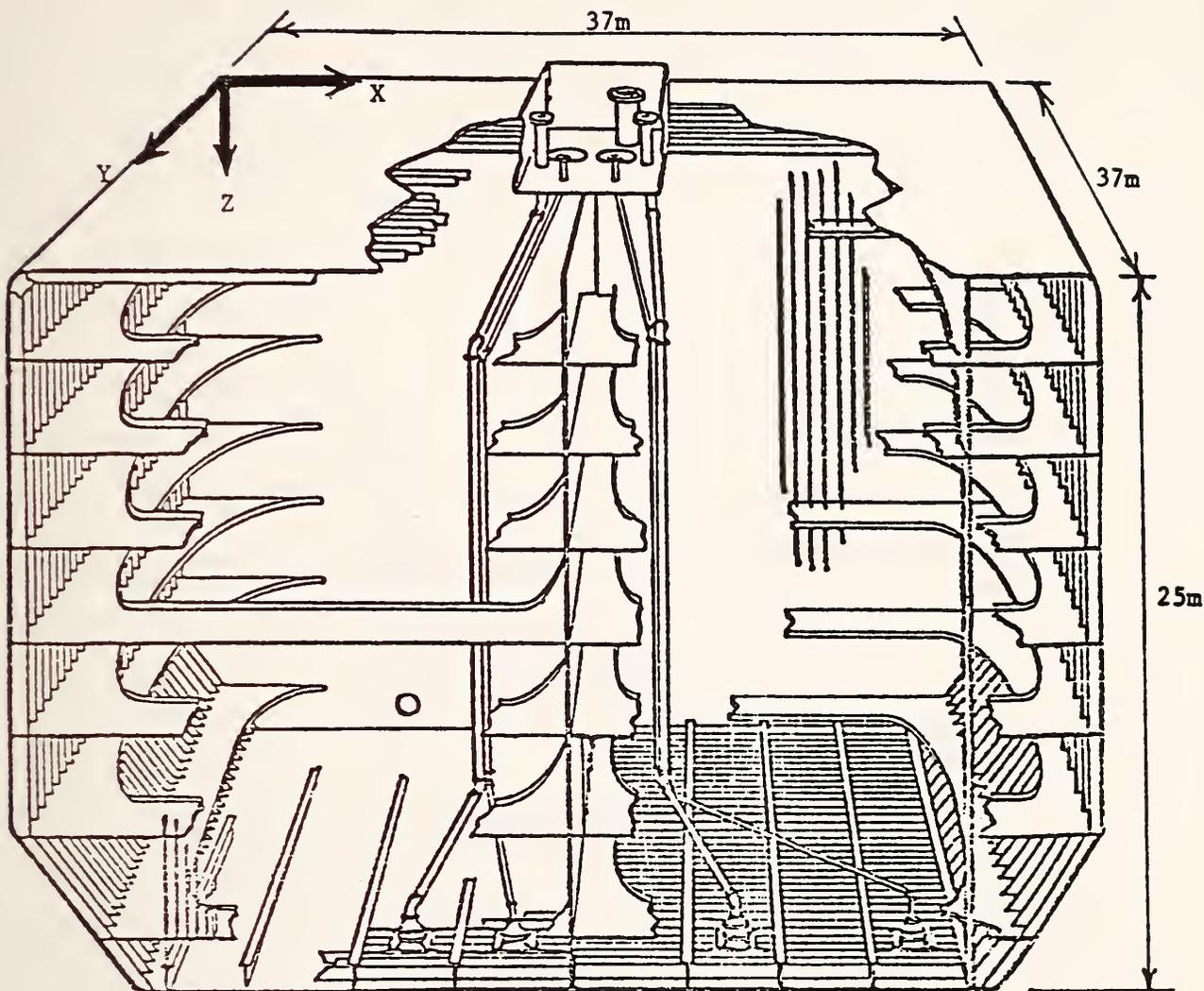


Figure 1 - A typical LNG tank of the freestanding prismatic type. The tank is internally divided into quadrants as shown and is uniformly supported on the bottom while in the ship. The coordinate system used to report the measurement data is shown here. (View from Aft)

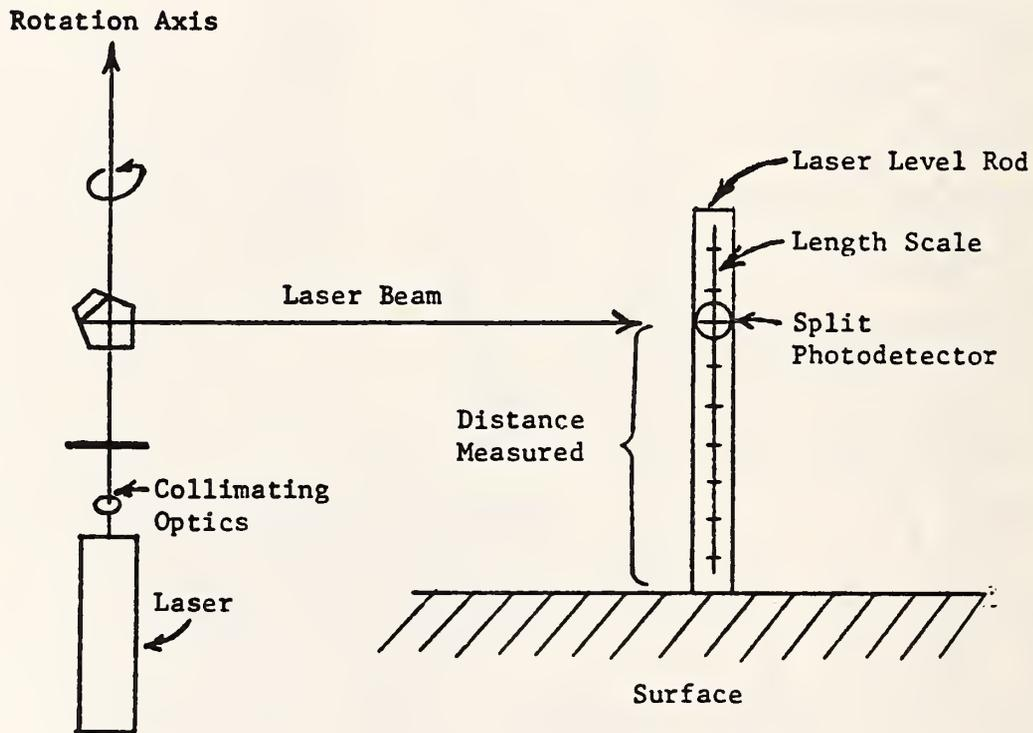


Figure 2 - Schematic of laser level with beam seeking "laser rod. The rotating pentaprism causes the beam to be swept in a plane. Manufacturer's specifications are ± 10 seconds of arc flatness. Resolution of rod is 0.1 mm.

insure that the rod was perpendicular to the survey plane. The laser rod contained an active detector that searched for the laser beam, averaged a large number of readings, and then locked so a reading could be taken. These offset measurements were made at a large number of points, to fully characterize the contours of the surface being surveyed.

The survey was complicated by the fact that the tank is divided into quadrants with a longitudinal liquid-tight bulkhead and a transverse swash bulkhead. A schematic of the tank bottom is shown in Figure 3. It was further complicated by the fact that floor beams up to 1372 mm high, are present. Consequently, four separate flatness surveys are conducted, one in each tank quadrant, using a nominal 2 m x 2 m grid spacing. The laser was mounted on the top flange of a floor beam and the intersection of the laser plane with the wall beam flanges was marked at the four water tube tie-in points shown in Figure 3 for each quadrant. Offsets from the laser plane to the tank floor were measured with the beam seeking level rod in the usual manner. Extreme care was taken to insure that the rod was perpendicular to the laser plane since the offset measurements are approximately 1.9 m in length and the chance of a significant cosine error is substantial. A circular bubble level on the rod was used for this purpose.

Upon completion of the four quadrant surveys, a hydrostatic differential level (water tube) was used to attempt to define a level plane throughout the tank. Short offset measurements from the laser plane intersection marks in each quadrant shown in Figure 3 were to be used to reference the four quadrant surveys to a single surface. The water tube technique involved using one mark in one quadrant as a reference and measuring the 15 additional points with the other end of the tube in the appropriate quadrants. Access to the various quadrants was through a valve in the liquid-tight bulkhead and through

FORWARD

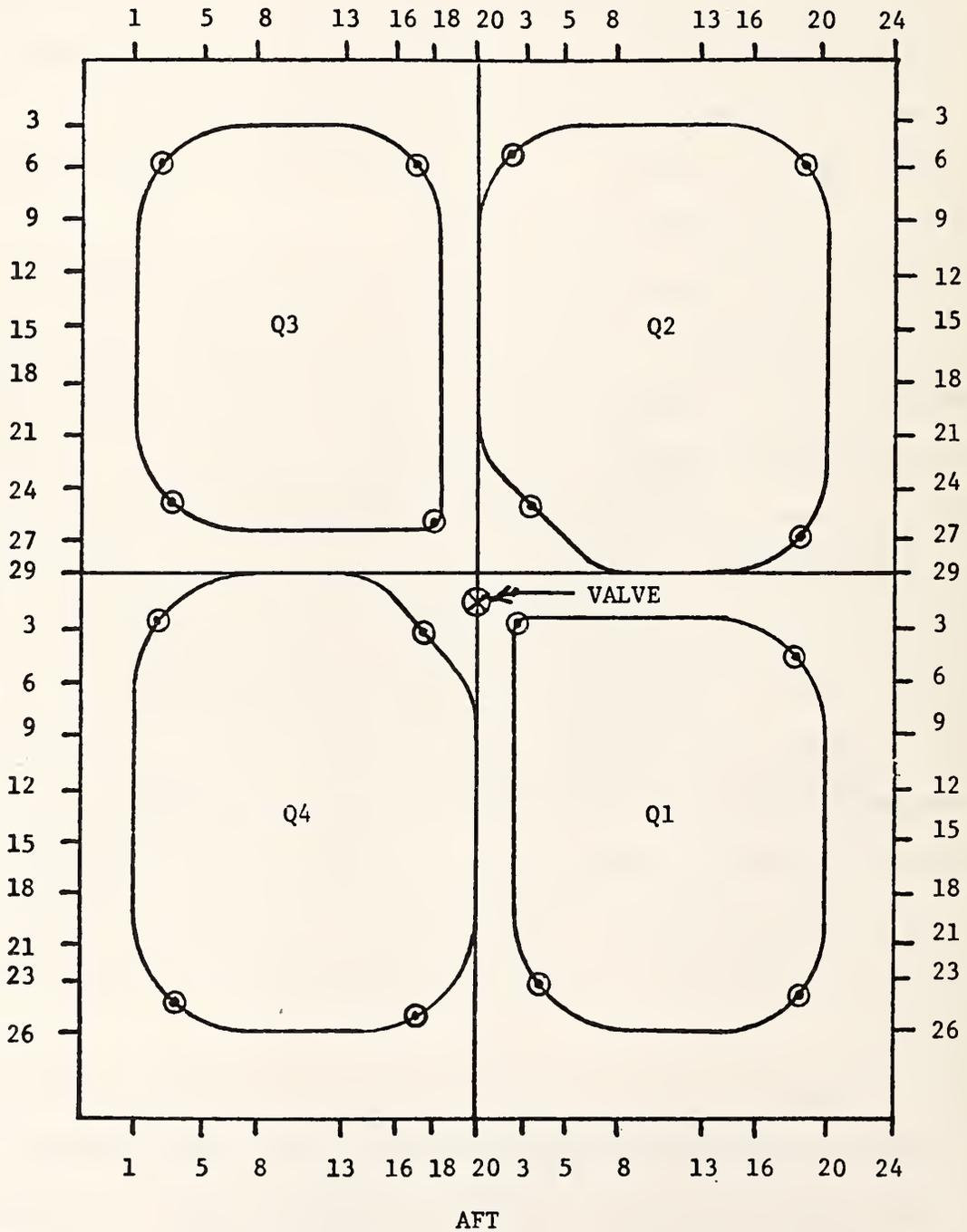


Figure 3 - Bottom plan of a typical LNG tank showing grid point definitions. Points marked ⊙ are water tube tie-in points. Grid numbers are based on small floor and wall beam locations.

manways in the swash bulkheads. The water tubes used for this survey were made from tygon and had aluminum scales attached to each end as a means of clamping to the tank beams. This technique, necessitated by the lack of optical access between the quadrants, was the principal source of error in the measurements.

Hydrostatic differential leveling is one of the oldest measurement techniques known for establishing elevation differences between two points. The water tube apparatus used by NBS for this technique was thoroughly tested in the laboratory under controlled conditions and found to have random errors on the order of ± 0.2 mm. The apparatus was also used in the field under controlled conditions and found to produce similar results. Unfortunately, it was not possible to make all measurements under carefully controlled conditions for reasons that will be discussed below. The most significant conditions that systematically affect water tube accuracy were found to be:

- a) Stability of the tank or ship
- b) Constrictions in the tygon tubing
- c) Thermal gradients in the apparatus

Each error source will be commented on.

a) Stability of the tank or ship - When the flatness surveys were made on the El Paso Savannah, the ship was berthed in the Mississippi River at Avondale Shipyard. Despite assurances to the contrary, the ship's ballast tanks were being loaded and unloaded while the NBS survey was underway. This leads to changes in ship trim on the order of 300 mm. Furthermore, a second El Paso ship was tied up along side the Savannah while our survey was being conducted. This completely disrupted the water tube survey by introducing a list in the ship of approximately 60 mm. Because of the difficult working conditions, a decision was made to not resurvey the entire ship, but to try and analyze the

data at NBS. This analysis was unsuccessful because of the random variation of the water survey tie-in points. In many cases, the four tie-in points in each quadrant did not form a plane to within 50 mm.

The El Paso Cove Point was surveyed in a floating dry dock, also in the Mississippi River. While the platform was more stable than the Savannah case, passing ship traffic still caused water tube elevation differences of 10-20 mm.

In our opinion, this hydrostatic leveling technique is only practical on land or in rivers with very light ship traffic, and then only when no changes in ship list/trim occur.

b) Constrictions in the tubing - This is a significant error source, often causing leveling errors of 20-30 mm or more. In tanks of the type reported on here, the tubing must be strung over many large I-beams on the tank floor. It must also be threaded through butterfly valve openings with sharp edges on the valve. Care must be taken to insure that the tubing does not constrict under its own weight when strung over a beam edge or through a valve. For these surveys, a tube approximately 30 meters long was used, and the operators were instructed to inspect the entire tube for constrictions before taking any data. Because there was no lighting in the tanks, this task was difficult at best, and some constrictions inevitably remained in the tubing.

c) Thermal gradients in the apparatus - A long tube of this type has an extreme sensitivity to changes in temperature of the water. Interior tank temperatures during these surveys was as high as 35°C and quite non-uniform. While this error source is difficult to quantify, it is felt to far exceed the +1.6 mm random survey error.

Because of these large errors, the quadrant surveys could not be tied together and referenced to a single water-level defined plane. Therefore, the data is reported by quadrants only.

During the course of the bottom surveys, the capacitance gage orientation with respect to the level plane was also established. This was done by using the laser level in the right angle mode, (with the reference plane parallel to gravity), in two orthogonal orientations with respect to the ship and measuring offsets from these planes to the capacitance gage at the bottom and near the top of each tank.

3. Data Analysis

The raw data from a complete bottom survey for each tank quadrant consisted of five sets of X, Y, Z coordinates. Data points on the X and Y directions are were approximate and expressed as index numbers, the data points in the Z direction, which were measured with the beam seeking laser rod, have a resolution of 0.1 mm. The intent was to determine the best-fit plane from the differences between these five data sets and then, by using those plane coefficients, bring the second set of Z's into coincidence with the first.

For practical purposes, we really have five planes -- one for each quadrant, generated by the rotating laser, and the fifth (which overlaps each of the other four) generated by the water tube measurements. In principle, all that is needed is to generate a value for the best fit "water tube" plane at each point in the other four planes, calculate the differences, and then transform the laser planes into the water tube plane, which is taken to be absolute and uniform. The final step planned was to fit a plane to the whole surface, storing deviations from that plane and the rms value of those deviations. However, since the water tube data did not form a plane within even one quadrant

(with four points the fit is slightly over-constrained) this data could not be used to determine the "whole-surface" planes. Instead the rms deviations from flatness are reported on a quadrant by quadrant basis.

4. Error Analysis

Several types of errors are associated with the individual flatness surveys. We will discuss three types in this paper: random, systematic, and model errors.

The random errors currently identified in tank flatness surveys are shown in Table 1.

Table 1 - Random Errors in Free-Standing Tank Measurements

<u>Physical Source</u>	<u>Error Value</u>	<u>Error Source</u>
Laser plane(1)	<u>+1.5</u> mm	Manufacturer Spec (1)
Laser rods(2)		
Reading Error	<u>+0.3</u> mm	Estimated (2)
Cosine Error(3)	<u>+0.6</u> mm	Computed (3)
Total Random Error	<u>+1.6</u> mm	Sum of errors in quadrature

(1) Specifications on the laser plane include wobble, lack of flatness, and deviation from level when a self-leveling feature is used. The manufacturer specifies that the sum of these errors will not exceed +10 arc sec. For the maximum length of a tank, $L \approx 30$ m, this error is +1.5 mm.

(2) Scales on the laser rods are blank lines in mm increments on a light background. The random error for this type of scale is based on years of laboratory experience.

(3) For an absolute displacement measurement, a rod cosine error is systematic. For relative measurements, this becomes random. For a discussion of the calculation method used to predict this error, see Reference 1.

It must be noted that the absolute laser rod calibration cannot contribute an error in this survey since only relative displacement from flatness of two planes are being computed.

5. Results and Conclusions

The results of the bottom surveys on the two ships, the El Paso Savannah and the El Paso Cove Point are summarized in Tables 2 and 3 by tank quadrant. These tables show the rms deviation of each of the surfaces from the best fit plane. The maximum deviation of 11.76 mm was observed in quadrant 2 of Tank 1 of the El Paso Savannah. The complete data sets are given in Section 6.

The results of the capacitance gage surveys are reported in Tables 4 and 5. These data are based on dimensional measurements made from within the tanks after the tanks were installed in the ships and all tank construction and fitting out was complete.

Table 2 - El Paso Savannah, Bottom Flatness Summary

<u>Tank</u>	<u>Quadrant</u>	<u>RMS Deviation from Flatness (mm)</u>
1	1	6.03
1	2	11.76
1	3	5.50
1	4	6.17
2	1	6.61
2	2	8.02
2	3	6.47
2	4	8.54
3	1	7.18
3	2	8.29
3	3	7.04
3	4	7.48
4	1	6.42
4	2	5.38
4	3	6.61
4	4	7.19
5	1	4.85
5	2	5.06
5	3	6.87
5	4	6.26

Table 3 - El Paso Cove Point, Bottom Flatness Summary

<u>Tank</u>	<u>Quadrant</u>	<u>RMS Deviation from Flatness (mm)</u>
1	1	4.42
1	2	4.77
1	3	4.26
1	4	5.33
2	1	2.90
2	2	2.43
2	3	4.21
2	4	4.05
3	1	6.27
3	2	7.45
3	3	9.15
3	4	10.43
4	1	6.10
4	2	9.31
4	3	6.98
4	4	7.28
5	1	7.72
5	2	7.22
5	3	4.01
5	4	4.50

Table 4 - El Paso Savannah, Capacitance Gage Survey

<u>Tank</u>	<u>Measurement Location Z, mm</u>	<u>X-liq. tight Bulkhead, mm</u>	<u>X-Port seam, mm</u>	<u>Y-Swash Bulkhead, mm</u>	<u>Y-Aft Wall, mm</u>
1	0 (Tank floor) 20500	631 628	9215 N/A	2873 2890	12399 N/A
2	0 (Tank floor) 20500	1783 1771	12673 N/A	2873 2895	15637 N/A
3	0 (Tank floor) 20500	2992 3000	11887 N/A	2228 2230	16278 N/A
4	0 (Tank floor) 20500	3004 2989	11886 N/A	2234 2248	16289 N/A
5	0 (Tank floor) 20500	2054 2057	12078 N/A	3487 3510	8515 8532

<u>Tank</u>	<u>Gage Height from Tank Floor, mm</u>
1	39.0
2	41.2
3	39.5
4	40.0
5	40.0

NOTES:

- a) All gages are located in the aft-port quadrant of the respective tank.
- b) N/A means either not applicable or not available because of lack of access to that point.
- c) X-Portseam refers to the weld seam between the floor and the port chine base plate.

Table 5 - El Paso Cove Point, Capacitance Gage Survey

<u>Tank</u>	<u>Measurement Location Z, mm</u>	<u>X-liq. tight Bulkhead, mm</u>	<u>X-Port seam, mm</u>	<u>Y-Aft Wall, mm</u>
1	0 (Tank floor)	562	9283	12373
2	0 (Tank floor)	1811	12635	15652
3	0 (Tank floor)	2995	11876	16274
4	0 (Tank floor)	2996	11878	16261
5	0 (Tank floor)	2060	12087	8511

<u>Tank</u>	<u>Gage Height from Tank Floor, mm</u>
1	40.3
2	38.3
3	39.1
4	40.5
5	41.0

Gage Orientation

<u>Tank</u>	<u>X-Offset, mm</u>		<u>Y-Offset, mm</u>	
	<u>Z=500 mm</u>	<u>Z=20500 mm</u>	<u>Z=500 mm</u>	<u>Z=20500 mm</u>
1	50.2	69.0	46.0	70.0
2	110.3	108.0	49.9	47.0
3	75.0	68.0	54.0	61.0
4	48.4	64.0	75.0	97.0
5	43.8	96.0	63.0	89.0

NOTES:

- a) For X-Offset measurements, the laser plane was on the port side of the gage (viewed from above).
- b) For Y-Offset measurements, the laser plane was aft of the gage (viewed from above).

6. Tables of Survey Data

For completeness, tables have been added to present the actual deviations of each data point from the "best fit" plane applicable to that surface. The composition of each table is as follows:

<u>Table</u>	<u>Contents</u>
A1	Savannah Tank 1, Quadrant 1
A2	Savannah Tank 1, Quadrant 2
A3	Savannah Tank 1, Quadrant 3
A4	Savannah Tank 1, Quadrant 4
A5	Savannah Tank 2, Quadrant 1
A6	Savannah Tank 2, Quadrant 2
A7	Savannah Tank 2, Quadrant 3
A8	Savannah Tank 2, Quadrant 4
A9	Savannah Tank 3, Quadrant 1
A10	Savannah Tank 3, Quadrant 2
A11	Savannah Tank 3, Quadrant 3
A12	Savannah Tank 3, Quadrant 4
A13	Savannah Tank 4, Quadrant 1
A14	Savannah Tank 4, Quadrant 2
A15	Savannah Tank 4, Quadrant 3
A16	Savannah Tank 4, Quadrant 4
A17	Savannah Tank 5, Quadrant 1
A18	Savannah Tank 5, Quadrant 2
A19	Savannah Tank 5, Quadrant 3
A20	Savannah Tank 5, Quadrant 4
A21	Cove Point Tank 1, Quadrant 1
A22	Cove Point Tank 1, Quadrant 2
A23	Cove Point Tank 1, Quadrant 3
A24	Cove Point Tank 1, Quadrant 4
A25	Cove Point Tank 2, Quadrant 1
A26	Cove Point Tank 2, Quadrant 2
A27	Cove Point Tank 2, Quadrant 3
A28	Cove Point Tank 2, Quadrant 4
A29	Cove Point Tank 3, Quadrant 1
A30	Cove Point Tank 3, Quadrant 2
A31	Cove Point Tank 3, Quadrant 3
A32	Cove Point Tank 3, Quadrant 4
A33	Cove Point Tank 4, Quadrant 1
A34	Cove Point Tank 4, Quadrant 2
A35	Cove Point Tank 4, Quadrant 3
A36	Cove Point Tank 4, Quadrant 4
A37	Cove Point Tank 5, Quadrant 1
A38	Cove Point Tank 5, Quadrant 2
A39	Cove Point Tank 5, Quadrant 3
A40	Cove Point Tank 5, Quadrant 4

Table A1

EL PASO SAVANNAH, TANK #1
BOTTOM SURVEY, TANK IN SHIP, QUADRANT#1

X	Y	DEV
5.	3.	10.12
5.	6.	-3.04
5.	9.	1.10
5.	12.	1.65
5.	15.	4.39
5.	18.	6.33
8.	3.	-11.71
8.	6.	-4.77
8.	9.	-10.23
8.	12.	-3.99
8.	15.	3.25
8.	18.	-.41
8.	21.	-1.87
13.	6.	9.61
13.	9.	2.75
13.	12.	4.59
13.	15.	4.23
13.	18.	-1.93
13.	21.	-8.89

RMS DEVIATION FROM A PLANE 6.03

Table A2

EL PASO SAVANNAH, TANK #1
BOTTOM SURVEY, TANK IN SHIP, QUADRANT#2

X	Y	DEV
3.	6.	-6.35
3.	9.	6.45
3.	12.	8.15
3.	15.	8.55
3.	18.	.75
6.	6.	-11.00
6.	9.	-7.70
6.	12.	13.20
6.	15.	6.41
6.	18.	-32.29
9.	6.	-10.24
9.	9.	6.76
9.	12.	16.36
9.	15.	3.86
9.	18.	-6.34

RMS DEVIATION FROM A PLANE 11.76

Table A3

EL PASO SAVANNAH, TANK #1
BOTTOM SURVEY, TANK IN SHIP, QUADRANT#3

X	Y	DEV
3.	6.	4.16
3.	9.	8.48
3.	12.	6.30
3.	15.	1.12
3.	18.	-8.37
6.	6.	-8.19
6.	9.	-1.07
6.	12.	-1.16
6.	15.	-2.74
6.	18.	-7.92
9.	6.	-4.24
9.	9.	-0.83
9.	12.	2.19
9.	15.	4.91
9.	18.	8.13

RMS DEVIATION FROM A PLANE 5.50

Table A4

EL PASO SAVANNAH, TANK #1
BOTTOM SURVEY, TANK IN SHIP, QUADRANT #4

X	Y	DEV
1.	6.	9.40
1.	9.	8.81
1.	12.	11.42
1.	15.	3.93
1.	18.	-4.46
1.	21.	-7.05
5.	3.	-9.22
5.	6.	-9.21
5.	9.	-8.30
5.	15.	-3.38
5.	18.	-4.47
5.	21.	-6.56
8.	3.	-4.03
8.	6.	-4.52
8.	9.	-1.81
8.	12.	5.30
8.	15.	5.41
8.	18.	6.42
8.	21.	-1.57
12.	6.	3.76
12.	9.	6.77
12.	12.	1.78
12.	15.	3.69
12.	18.	-4.50

RMS DEVIATION FROM A PLANE

6.17

Table A5

EL PASO SAVANNAH, TANK #2
 BOTTOM SURVEY, TANK IN SHIP, QUADRANT#1

X	Y	DEV
1.	9.	11.27
1.	12.	9.63
1.	15.	7.89
1.	18.	10.05
1.	21.	7.01
5.	6.	1.93
5.	9.	2.03
5.	12.	2.29
5.	15.	-1.05
5.	18.	.71
5.	21.	-.93
5.	24.	-3.67
8.	3.	-4.64
8.	6.	-3.98
8.	9.	-6.02
8.	12.	-6.06
8.	15.	-4.40
8.	18.	-3.24
8.	21.	-1.03
8.	24.	-5.42
13.	3.	1.44
13.	6.	-5.30
13.	9.	-6.74
13.	12.	-7.28
13.	15.	-6.92
13.	18.	-5.06
13.	21.	-5.60
13.	24.	-15.34
16.	6.	-4.65
16.	9.	-1.89
16.	12.	-.54
16.	15.	1.42
16.	18.	.53
16.	21.	-5.06
20.	6.	.71
20.	9.	6.17
20.	12.	8.73
20.	15.	16.09
20.	18.	9.45
20.	21.	11.30

RMS DEVIATION FROM A PLANE

6.61

Table A6

EL PASO SAVANNAH TANK #2
 BOTTOM SURVEY, TANK IN SHIP, QUADRANT#2

X	Y	DEV
1.	9.	14.73
1.	12.	15.15
1.	15.	10.77
1.	18.	10.69
1.	21.	12.71
1.	24.	10.92
5.	6.	-1.53
5.	9.	-1.91
5.	12.	1.81
5.	18.	2.95
5.	21.	1.57
5.	24.	-2.11
5.	27.	-5.49
8.	6.	-11.55
8.	9.	-7.04
8.	12.	-5.82
8.	15.	-4.30
8.	18.	-8.18
8.	21.	-6.26
8.	24.	-12.94
8.	27.	-11.72
8.	29.	-2.84
13.	6.	-11.20
13.	9.	-8.48
13.	12.	-4.86
13.	15.	-4.34
13.	18.	-6.92
13.	21.	-6.91
13.	24.	-7.29
13.	27.	-5.67
13.	29.	2.31
16.	6.	1.37
16.	9.	-5.01
16.	12.	-1.39
16.	15.	1.33
16.	18.	-.85
16.	21.	-2.83
16.	24.	1.39
16.	27.	-1.49
16.	29.	-2.61
20.	9.	8.35
20.	12.	8.37
20.	15.	14.89
20.	18.	14.51
20.	21.	10.63
20.	24.	11.45

RMS DEVIATION FROM A PLANE

8.02

Table A7

EL PASO SAVANNAH TANK #2
 BOTTOM SURVEY, TANK IN SHIP, QUADRANT#3

X	Y	DEV
1.	9.	2.94
1.	12.	8.39
1.	15.	8.25
1.	18.	12.00
1.	21.	13.35
1.	24.	8.61
5.	6.	-9.23
5.	9.	-11.88
5.	12.	-.62
5.	15.	.13
5.	18.	1.49
5.	21.	4.34
5.	24.	-1.51
5.	27.	-5.85
5.	29.	-2.75
9.	6.	-.92
9.	9.	-10.66
9.	12.	-5.21
9.	15.	-4.35
9.	18.	-4.50
9.	21.	-3.25
9.	24.	-6.19
9.	27.	-7.74
9.	29.	10.17
13.	4.	-3.06
13.	6.	-1.06
13.	9.	-3.70
13.	12.	.45
13.	15.	-.10
13.	18.	-3.54
13.	21.	-13.39
13.	24.	-6.13
13.	27.	-4.48
13.	29.	-3.88
16.	6.	3.06
16.	9.	.51
16.	12.	4.76
16.	15.	3.22
16.	18.	4.57
16.	21.	-.07
16.	24.	-3.12
16.	27.	-7.77
19.	9.	3.75
19.	12.	11.31
19.	15.	9.76
19.	18.	9.22
19.	21.	5.87
19.	24.	2.32

RMS DEVIATION FROM 5 PLANE

6.47

Table A8

EL PASO SAVANNAH, TANK #2
 BOTTOM SURVEY, TANK IN SHIP, QUADRANT#4

X	Y	DEV
3.	6.	6.52
3.	9.	12.48
3.	12.	13.04
3.	15.	18.20
3.	18.	13.37
3.	21.	5.23
5.	6.	-6.49
5.	9.	-7.33
5.	12.	1.13
5.	15.	3.39
5.	18.	5.15
5.	21.	-7.09
5.	24.	-4.92
8.	6.	-11.96
8.	9.	-8.00
8.	12.	-5.34
8.	15.	-7.57
8.	18.	-2.81
8.	21.	-6.45
8.	24.	-8.89
8.	26.	-12.03
13.	6.	-11.14
13.	9.	-7.47
13.	12.	-5.51
13.	15.	-4.45
13.	18.	-2.09
13.	21.	-7.43
13.	24.	-4.67
13.	26.	-19.76
16.	6.	-6.30
16.	9.	-3.24
16.	12.	-1.23
16.	15.	1.43
16.	18.	2.54
16.	21.	3.50
16.	24.	1.36
19.	9.	7.55
19.	12.	10.71
19.	15.	13.67
19.	18.	9.13
19.	21.	16.79

RMS DEVIATION FROM A PLANE

8.54

Table A9

EL PASO SAVANNAH TANK #3
 BOTTOM SURVEY, TANK IN SHIP, QUADRANT#1

X	Y	DEV
3.	6.	12.02
3.	9.	10.15
3.	12.	9.00
3.	15.	10.14
3.	18.	11.28
3.	21.	9.22
5.	3.	10.91
5.	6.	-2.35
5.	9.	.79
5.	12.	1.73
5.	15.	2.27
5.	19.	1.01
5.	21.	2.05
5.	24.	-1.81
8.	3.	-8.70
8.	6.	-7.75
8.	9.	-7.71
8.	12.	-5.67
8.	15.	-3.63
8.	18.	-4.29
8.	21.	.05
8.	24.	-10.61
8.	26.	-11.38
13.	3.	-7.47
13.	6.	-10.43
13.	9.	-9.59
13.	12.	-7.75
13.	15.	-6.51
13.	18.	-9.17
13.	21.	-.03
13.	23.	-1.80
13.	26.	-3.56
16.	3.	4.53
16.	5.	-2.85
16.	8.	-6.41
16.	11.	-.97
16.	14.	-.52
16.	17.	-4.18
16.	20.	-.14
16.	23.	-.30
16.	25.	-.28
20.	8.	12.75
20.	11.	10.30
20.	14.	12.84
20.	17.	8.48
20.	20.	7.72
20.	23.	4.76

RMS DEVIATION FROM A PLANE

7.15

Table A10

EL PASO SAVANNAH TANK #3
 BOTTOM SURVEY, TANK IN SHIP, QUADRANT#3

X	Y	DEV
1.	9.	10.40
1.	12.	16.25
1.	15.	10.50
1.	18.	10.64
1.	21.	12.29
5.	6.	-1.67
5.	9.	-1.52
5.	12.	3.22
5.	15.	1.57
5.	18.	3.52
5.	21.	.87
5.	24.	3.71
5.	27.	-6.64
8.	6.	-3.16
8.	9.	-3.92
8.	12.	-5.97
8.	15.	-6.72
8.	18.	-4.77
8.	21.	-3.23
8.	24.	-3.28
8.	27.	-5.83
8.	29.	-1.70
13.	6.	-6.62
13.	9.	-11.57
13.	12.	-6.62
13.	15.	-10.46
13.	18.	-11.02
13.	21.	-8.38
13.	24.	-9.93
13.	27.	-3.89
13.	29.	-1.85
16.	6.	1.19
16.	9.	-3.76
16.	12.	-7.02
16.	15.	-6.27
16.	18.	-4.92
16.	21.	-1.87
16.	24.	-1.93
16.	27.	-1.88
16.	29.	-9.55
20.	9.	6.21
20.	12.	12.36
20.	15.	13.41
20.	18.	14.75
20.	21.	19.60
20.	24.	17.85

RMS DEVIATION FROM A POLY

Table All

EL PASO SAVANNAH, TANK #3
BOTTOM SURVEY, TANK IN SHIP, QUADRANT#3

X	Y	DEV
1.	9.	11.55
1.	12.	11.05
1.	15.	11.75
1.	18.	10.15
1.	21.	13.45
5.	6.	5.19
5.	9.	.79
5.	12.	-1.61
5.	15.	-1.01
5.	18.	-3.41
5.	21.	-2.11
5.	24.	-1.00
5.	27.	-2.40
8.	6.	-6.85
8.	9.	-10.95
8.	12.	-9.55
8.	15.	-13.65
8.	18.	-11.15
8.	21.	-10.75
8.	24.	-4.45
8.	27.	-4.45
13.	6.	3.77
13.	9.	-4.23
13.	12.	-5.03
13.	15.	-3.83
13.	18.	-5.92
13.	21.	-4.32
13.	24.	-2.82
16.	6.	5.43
16.	9.	-4.27
16.	12.	.53
16.	15.	-1.47
16.	18.	.33
16.	21.	-.17
16.	24.	1.53
18.	9.	2.30
18.	12.	7.00
18.	15.	10.10
18.	18.	5.00
18.	21.	9.30
18.	24.	11.00

RMS DEVIATION FROM A PLANE

7.04

Table A12

EL PASO SAVANNAH, TANK #3
 BOTTOM SURVEY, TANK IN CHIP, QUADRANT#4

X	Y	DEV
1.	3.	7.19
1.	6.	11.42
1.	9.	10.24
1.	12.	12.37
1.	15.	7.90
1.	18.	7.13
1.	20.	16.31
5.	1.	2.32
5.	3.	-6.80
5.	6.	-3.87
5.	9.	-4.94
5.	12.	-3.92
5.	15.	-4.79
5.	17.	3.40
5.	20.	1.52
5.	23.	-1.35
8.	1.	2.18
8.	3.	-3.84
8.	6.	-6.01
8.	9.	-10.28
8.	12.	-11.35
8.	15.	-11.13
8.	17.	-1.74
8.	20.	-3.92
8.	23.	-1.79
8.	25.	-2.10
13.	1.	2.14
13.	3.	-2.57
13.	6.	-1.35
13.	9.	-1.22
13.	12.	-3.49
13.	15.	-7.85
13.	17.	-3.23
13.	20.	-2.35
13.	23.	-2.72
13.	25.	-10.14
16.	3.	-1.32
16.	6.	-6.89
16.	9.	-4.86
16.	12.	-3.33
16.	15.	-3.91
16.	17.	-4.32
16.	20.	-3.79
16.	23.	-1.37
16.	25.	-5.33
20.	9.	16.55
20.	12.	15.13
20.	15.	12.31
20.	17.	15.29
20.	20.	10.62

Table A13

EL PASO SAVANNAH, TANK #4
BOTTOM SURVEY, TANK IN SHIP, QUADRANT#1

X	Y	DEV
3.	6.	-6.39
3.	9.	-9.50
3.	12.	-9.10
3.	15.	-12.71
3.	18.	-9.71
5.	3.	2.63
5.	6.	.13
5.	9.	-2.58
5.	12.	-3.89
5.	15.	-5.29
5.	18.	-5.30
5.	21.	-3.30
5.	23.	-1.47
8.	3.	7.15
8.	6.	6.55
8.	9.	3.04
8.	12.	3.24
8.	15.	.23
8.	18.	2.13
8.	21.	2.62
8.	23.	7.65
8.	25.	2.93
13.	3.	7.59
13.	6.	8.39
13.	9.	6.33
13.	12.	5.68
13.	15.	3.87
13.	18.	2.57
13.	21.	6.66
13.	23.	8.89
13.	26.	11.88
16.	3.	1.82
16.	6.	2.21
16.	9.	1.51
16.	12.	-1.90
16.	15.	-1.20
16.	17.	.92
16.	21.	2.78
16.	23.	6.01
16.	25.	8.54
19.	6.	-6.87
20.	9.	-5.76
20.	12.	-11.17
20.	15.	-10.07
20.	18.	-9.28
20.	21.	-7.78
19.	23.	-11.26

RMS DEVIATION FROM A PLANE

6.42

Table A14

EL PASO SAVANNAH, TANK #4
BOTTOM SURVEY, TANK IN SHIP, QUADRANT#2

X	Y	DEV
1.	9.	-10.54
1.	12.	-9.11
1.	15.	-11.48
1.	18.	-6.34
1.	21.	-9.11
1.	23.	-11.09
5.	6.	-.28
5.	9.	-1.73
5.	12.	-1.00
5.	15.	-.66
5.	18.	3.67
5.	21.	3.50
5.	24.	4.63
5.	27.	5.56
8.	5.	1.64
8.	8.	1.37
8.	9.	4.03
8.	12.	3.71
8.	14.	6.34
8.	17.	7.47
8.	20.	7.10
8.	23.	8.53
8.	26.	8.76
8.	29.	8.30
13.	9.	3.37
13.	10.	.71
13.	12.	-.37
13.	15.	.56
13.	18.	.79
13.	21.	3.03
13.	24.	2.96
13.	27.	1.69
13.	29.	2.71
16.	6.	2.47
16.	9.	3.51
16.	12.	2.04
16.	15.	-1.83
16.	18.	.70
16.	21.	.04
16.	24.	-.13
16.	27.	-.30
16.	29.	.62
18.	6.	3.73
20.	9.	.52
20.	12.	-4.85
20.	15.	-7.32
20.	18.	-6.78
20.	21.	-9.85
18.	24.	-5.83
18.	27.	-9.89

H30

Table A15

EL PASO SAVANNAH, TANK#4
BOTTOM SURVEY, TANK IN SHIP, QUADRANT#3

X	Y	LEV
3.	6.	- .40
1.	9.	-10.17
1.	12.	-7.88
1.	15.	-9.29
1.	18.	-10.50
1.	21.	-8.81
1.	24.	-13.42
5.	6.	3.75
5.	9.	4.64
5.	12.	.03
5.	15.	-2.18
5.	18.	-3.38
5.	21.	-1.89
5.	24.	1.60
5.	27.	5.59
8.	4.	2.15
8.	6.	8.64
8.	9.	6.23
8.	12.	3.62
8.	15.	1.51
8.	18.	3.60
8.	21.	4.79
8.	24.	10.93
8.	27.	15.27
13.	4.	3.29
13.	6.	7.28
13.	9.	7.27
13.	12.	2.16
13.	15.	2.15
13.	18.	2.94
13.	21.	5.53
13.	24.	8.12
13.	27.	7.82
16.	6.	-1.73
16.	9.	-1.14
16.	12.	-1.85
16.	15.	-3.06
16.	18.	-3.17
16.	21.	-1.68
16.	24.	2.61
16.	27.	3.30
18.	9.	-5.18
18.	12.	-9.09
18.	15.	-12.10
18.	18.	-9.31
18.	21.	-9.82
18.	24.	-6.53

Table A16

EL PASO SAVANNAH, TANK#4
BOTTOM SURVEY, TANK IN SHIP, QUADRANT#4

X	Y	DEV
3.	3.	-5.59
1.	6.	-14.93
1.	9.	-14.83
1.	12.	-11.33
1.	15.	-11.97
1.	18.	-10.57
1.	20.	-7.81
3.	23.	-.81
5.	1.	5.14
5.	3.	.60
5.	6.	-1.20
5.	9.	-.99
5.	12.	.11
5.	15.	.11
5.	17.	.83
5.	20.	3.03
5.	23.	2.33
5.	25.	4.35
8.	1.	4.82
8.	3.	1.29
8.	6.	3.99
8.	9.	7.89
8.	12.	6.79
8.	15.	3.50
8.	17.	5.16
8.	20.	3.96
8.	23.	3.57
8.	26.	2.97

(Con'd)

Table A16 (continued)

TANK#4, QUADRANT#4, (Con'd)

13.	1.	13.60
13.	3.	6.97
13.	6.	8.07
13.	9.	3.77
13.	12.	6.97
13.	15.	7.27
13.	17.	7.24
13.	20.	7.84
13.	23.	7.94
13.	25.	9.81
16.	3.	3.15
16.	6.	.56
16.	9.	-3.24
16.	12.	-1.94
16.	15.	-2.04
16.	17.	-1.57
16.	20.	.33
16.	23.	3.43
16.	25.	2.00
18.	6.	-10.35
20.	9.	-11.16
20.	12.	-9.56
20.	15.	-14.36
20.	17.	-13.09
20.	20.	-10.89
18.	23.	.52

RMS DEVIATION FROM A PLANE

7.19

Table A17

EL PASO SAVANNAH, TANK #5
BOTTOM SURVEY, TANK IN SHIP, QUADRANT#1

X	Y	DEV
3.	4.	-12.30
1.	7.	-4.87
1.	9.	-5.17
3.	13.	.52
5.	4.	1.29
5.	7.	.99
5.	9.	.59
5.	13.	-.10
5.	15.	-.70
8.	1.	1.06
8.	4.	.86
8.	7.	1.26
8.	9.	.87
8.	13.	-4.03
9.	16.	3.77
12.	1.	-.38
11.	4.	4.43
11.	7.	3.04
11.	9.	5.04
11.	13.	1.44
11.	16.	-.15
15.	1.	3.59
15.	4.	2.80
15.	7.	2.10
15.	9.	3.70
15.	13.	3.91
14.	16.	5.02
16.	1.	7.43
16.	4.	3.09
16.	7.	1.79
16.	9.	1.89
16.	13.	2.20
18.	4.	-14.13
20.	7.	-7.74
20.	9.	-6.64
19.	12.	-9.43

RMS DEVIATION FROM A PLANE

4.85

Table A18

EL PASO SAVANNAH, TANK #5
BOTTOM SURVEY, TANK IN SHIP, QUADRANT#2

X	Y	DEV
3.	6.	.26
2.	9.	.55
1.	12.	-5.06
1.	15.	-12.88
2.	18.	-11.81
5.	5.	-3.81
5.	6.	2.85
5.	9.	.83
5.	12.	-.69
5.	15.	-4.31
5.	18.	-3.03
5.	21.	2.95
8.	4.	5.60
8.	6.	4.32
8.	9.	5.51
8.	12.	2.99
8.	15.	3.77
8.	18.	4.85
8.	21.	7.23
13.	4.	-.64
13.	6.	-2.22
13.	9.	.57
13.	12.	3.85
13.	15.	4.13
13.	18.	4.11
13.	21.	9.69
16.	6.	-.44
16.	9.	-1.26
16.	12.	.62
16.	15.	.90
16.	18.	2.18
16.	21.	1.86
19.	9.	-5.78
19.	12.	-6.20
20.	15.	-9.43
19.	18.	-5.64

RMS DEVIATION FROM A PLANE

5.06

Table A19

EL PASO SAVANNAH, TANK #5
BOTTOM SURVEY, TANK IN SHIP, QUADRANT#3

X.	Y	DEV
3.	7.	-7.83
1.	10.	-6.74
1.	13.	-12.06
1.	16.	-12.08
2.	19.	-18.00
5.	5.	3.54
5.	7.	.36
5.	10.	-.96
5.	13.	2.92
5.	16.	3.40
5.	19.	.78
5.	21.	4.10
8.	4.	4.26
8.	7.	3.14
8.	10.	4.32
8.	13.	9.30
8.	16.	10.53
8.	19.	11.16
8.	22.	13.14
13.	4.	-.58
13.	7.	-.69
13.	10.	-1.01
13.	13.	3.47
13.	16.	3.85
13.	19.	4.83
13.	22.	6.21
16.	7.	-.21
16.	10.	.37
16.	13.	.45
16.	16.	-.77
16.	19.	-2.99
16.	22.	-2.21
18.	10.	-4.45
18.	13.	-7.37
18.	16.	-7.69
18.	19.	-11.50

RMS DEVIATION FROM A PLANE

6.87

Table A20

EL PASO SAVANNAH, TANK #5
BOTTOM SURVEY, TANK IN SHIP, QUADRANT#4

X	Y	DEV
3.	4.	.93
1.	7.	-7.38
1.	10.	-.98
2.	13.	.18
5.	1.	-23.96
5.	4.	3.74
5.	7.	-.16
5.	10.	.24
5.	13.	.84
5.	15.	1.88
8.	1.	3.91
8.	4.	5.91
10.	7.	7.22
8.	10.	1.61
8.	13.	1.11
9.	16.	.01
13.	1.	5.49
13.	4.	6.78
13.	7.	3.59
13.	10.	3.98
13.	13.	.98
12.	16.	2.53
16.	4.	-1.35
16.	7.	-1.45
16.	10.	-.65
16.	14.	-6.49
19.	10.	-12.14

RMS DEVIATION FROM A PLANE

6.26

Table A21

EL PASO COVE POINT, TANK #1
BOTTOM SURVEY, TANK IN SHIP, QUADRANT#1

X	Y	DEV
3.	5.	4.02
3.	8.	4.75
3.	11.	2.09
3.	12.	2.94
3.	17.	6.27
6.	8.	-7.58
6.	11.	-8.34
6.	12.	-7.29
6.	15.	-4.96
6.	18.	-2.52
9.	5.	-2.55
9.	8.	-4.01
9.	11.	-4.87
9.	14.	-1.03
9.	17.	1.10
9.	20.	1.64
11.	3.	3.03
11.	7.	5.92
11.	10.	2.76
11.	13.	1.60
11.	16.	4.44
11.	19.	1.47

RMS DEVIATION FROM A PLANE 4.42

Table A22

EL PASO COVE POINT, TANK #1
BOTTOM SURVEY, TANK IN SHIP, QUADRANT#2

X	Y	DEV
3.	4.	-7.73
3.	7.	-1.38
3.	10.	-1.64
3.	13.	2.21
3.	16.	6.35
6.	4.	-3.04
6.	7.	.50
6.	10.	3.25
6.	13.	.09
6.	16.	-3.16
9.	4.	-1.66
9.	7.	6.68
9.	10.	8.03
9.	13.	-3.13
9.	16.	-9.28

RMS DEVIATION FROM A PLANE 4.77

Table A23

EL PASO COVE POINT, TANK #1
BOTTOM SURVEY, TANK IN SHIP, QUADRANT#3

X	Y	DEV
3.	5.	-1.27
3.	6.	4.46
3.	9.	8.54
3.	12.	-1.27
3.	15.	1.22
6.	3.	-7.30
6.	6.	-1.32
6.	9.	-1.13
6.	12.	-3.64
6.	15.	-5.76
9.	18.	-6.97
9.	3.	-2.03
9.	6.	1.11
9.	9.	2.69
9.	12.	3.88
9.	15.	5.17
9.	18.	2.75

RMS DEVIATION FROM A PLANE 4.26

Table A24

EL PAID COVE POINT, TANK #1
BOTTOM SURVEY, TANK IN SHIP, QUADRANT#4

X	Y	DEV
1.	4.	-1.82
1.	6.	7.24
1.	9.	5.58
1.	12.	5.12
1.	15.	3.06
1.	18.	5.10
5.	4.	-10.41
5.	6.	-6.75
5.	9.	-5.71
5.	12.	-4.37
5.	15.	.37
5.	18.	-1.09
5.	21.	.95
8.	6.	-7.21
8.	9.	-2.67
8.	12.	-4.13
8.	15.	-1.29
8.	18.	-1.85
8.	21.	-8.51
12.	5.	2.22
12.	6.	7.20
12.	9.	5.94
12.	12.	6.78
12.	15.	7.22
12.	18.	-3.04

RMS DEVIATION FROM A PLANE

5.33

Table A25

EL PASO COVE POINT, TANK #2
BOTTOM SURVEY, TANK IN SHIP, QUADRANT#1

X	Y	DEV
1.	9.	4.04
1.	12.	4.56
1.	15.	5.48
1.	18.	5.60
1.	21.	2.92
5.	6.	-3.72
5.	9.	-2.00
5.	12.	-1.98
5.	15.	.14
5.	18.	-.24
5.	21.	-3.21
5.	24.	-1.09
8.	3.	-5.30
8.	6.	-5.28
8.	9.	-2.86
8.	12.	-2.33
8.	15.	-2.51
8.	18.	-2.79
8.	21.	-4.57
13.	3.	2.58
13.	6.	.90
13.	9.	1.22
13.	12.	2.54
13.	15.	2.86
13.	18.	3.29
13.	21.	.41
13.	24.	-1.57
16.	6.	.15
16.	9.	-.53
16.	12.	-.11
16.	15.	.11
16.	18.	-.17
16.	21.	-2.85
16.	24.	-3.92
20.	9.	2.23
20.	12.	2.75
20.	15.	1.87
20.	18.	1.99
20.	21.	1.22

RMS DEVIATION FROM A PLANE

2.90

Table A26

EL PASO COVE POINT, TANK #2
 BOTTOM SURVEY, TANK IN SHIP, QUADRANT#3

X	Y	DEV
1.	9.	1.02
1.	12.	1.90
1.	15.	1.97
1.	18.	2.75
1.	21.	6.23
1.	24.	4.20
5.	6.	4.51
5.	9.	.28
5.	12.	-4.14
5.	15.	-3.56
5.	18.	-1.99
5.	21.	-.01
5.	24.	-.24
5.	27.	5.04
9.	4.	5.46
9.	6.	.13
9.	9.	-3.84
9.	12.	-6.57
9.	15.	-9.29
9.	18.	-9.72
9.	21.	-7.34
9.	24.	-4.96
9.	27.	2.81
9.	29.	6.03
13.	4.	3.52
13.	6.	2.83
13.	9.	.31
13.	12.	-3.81
13.	15.	-6.04
13.	18.	-5.46
13.	21.	-5.68
13.	24.	-2.21
13.	27.	1.67
13.	29.	1.89
16.	6.	7.21
16.	9.	.48
16.	12.	-1.94
16.	15.	-1.26
16.	18.	-2.29
16.	21.	-.31
16.	24.	1.36
16.	27.	3.44
19.	12.	2.54
19.	15.	3.32
19.	18.	3.03
19.	21.	5.27

Table A27

EL PASO COVE POINT, TANK #2
 BOTTOM SURVEY, TANK IN SHIP, QUADRANT#3

X	Y	DEV
1.	9.	1.02
1.	12.	1.90
1.	15.	1.97
1.	18.	2.75
1.	21.	6.23
1.	24.	4.20
5.	6.	4.51
5.	9.	.28
5.	12.	-4.14
5.	15.	-3.56
5.	18.	-1.99
5.	21.	-.01
5.	24.	-.24
5.	27.	5.04
9.	4.	5.46
9.	6.	.13
9.	9.	-2.84
9.	12.	-6.57
9.	15.	-9.29
9.	18.	-9.72
9.	21.	-7.34
9.	24.	-4.36
9.	27.	2.81
9.	29.	6.03
13.	4.	3.52
13.	6.	2.83
13.	9.	.31
13.	12.	-3.81
13.	15.	-6.04
13.	18.	-5.46
13.	21.	-5.83
13.	24.	-2.21
13.	27.	1.67
13.	29.	1.89
16.	6.	7.21
16.	9.	.48
16.	12.	-1.94
16.	15.	-1.26
16.	18.	-2.29
16.	21.	-.31
16.	24.	1.36
16.	27.	3.44
19.	12.	2.54
19.	15.	3.32
19.	18.	3.09
19.	21.	5.27

RMS DEVIATION FROM A PLANE 4.21

Table A28

EL PASO COVE POINT, TANK #2
BOTTOM SURVEY, TANK IN SHIP, QUADRANT#4

X	Y	DEV
3.	9.	9.36
3.	12.	8.41
3.	15.	8.97
3.	18.	7.82
3.	21.	5.18
5.	6.	-2.84
5.	9.	-1.78
5.	12.	-1.12
5.	15.	-2.77
5.	18.	-3.11
5.	21.	-1.86
5.	24.	-3.00
8.	3.	-4.60
8.	6.	-5.04
8.	9.	-4.98
8.	12.	-4.53
8.	15.	-4.97
8.	18.	-3.52
8.	21.	-3.26
8.	24.	-2.80
13.	9.	-3.42
13.	12.	-1.47
13.	15.	-2.31
13.	18.	-1.96
13.	21.	-1.70
13.	24.	-1.05
16.	3.	2.75
16.	6.	-1.29
16.	9.	-1.13
16.	12.	-1.67
16.	15.	-1.92
16.	18.	.74
16.	21.	-1.01
18.	6.	5.18
18.	9.	1.82
18.	12.	2.33
18.	15.	4.65
18.	18.	3.80
18.	21.	3.26

RMS DEVIATION FROM 4 PLANE

4.05

Table A29

EL PASO COVE POINT, TANK #3
 BOTTOM SURVEY, TANK IN SHIP, QUADRANT#1

X	Y	DEV
3.	6.	9.45
3.	9.	7.96
3.	12.	5.77
3.	15.	6.89
3.	18.	3.10
3.	21.	4.31
5.	3.	1.39
5.	6.	-0.90
5.	9.	1.21
5.	12.	.02
5.	15.	-0.46
5.	18.	-1.05
5.	21.	1.86
8.	3.	1.07
8.	6.	-2.12
8.	9.	-0.21
8.	12.	-4.80
8.	15.	-6.49
8.	18.	-4.07
8.	21.	.74
13.	3.	-4.11
13.	6.	-9.79
13.	9.	-10.68
13.	12.	-10.77
13.	15.	-10.96
13.	18.	-8.65
13.	21.	-3.73
13.	24.	-2.22
16.	6.	-3.42
16.	9.	-0.80
16.	12.	-2.79
16.	15.	-2.43
16.	18.	-1.97
16.	21.	-1.46
16.	24.	-4.74
20.	9.	10.60
20.	12.	13.01
20.	15.	12.62
20.	18.	10.83
20.	21.	6.85

RMS DEVIATION FROM A PLANE

6.27

Table A30

EL PAID COVE POINT, TANK #3
 BOTTOM SURVEY, TANK IN SHIP, QUADRANT#2

X	Y	DEV
1.	9.	8.22
1.	12.	12.01
1.	15.	14.41
1.	18.	16.60
1.	21.	13.89
5.	6.	-2.98
5.	9.	-4.79
5.	12.	-3.50
5.	15.	-1.71
5.	18.	-1.01
5.	21.	-1.82
5.	24.	-.43
5.	27.	-.14
8.	6.	-6.49
8.	9.	-8.50
8.	12.	-10.11
8.	15.	-9.92
8.	18.	-9.12
8.	21.	-9.43
8.	24.	-9.24
8.	27.	-4.65
8.	29.	0.64
13.	6.	-2.91
13.	9.	-3.42
13.	12.	-2.92
13.	15.	-4.93
13.	18.	-3.24
13.	21.	-4.25
13.	24.	-6.76
13.	27.	-7.47
13.	29.	1.23
16.	6.	-2.42
16.	9.	-3.23
16.	12.	-.53
16.	15.	1.05
16.	18.	-.55
16.	21.	.04
16.	24.	-3.57
16.	27.	-6.78
16.	29.	-3.79
20.	9.	9.36
20.	12.	8.25
20.	15.	10.94
20.	18.	9.14
20.	21.	14.93
20.	24.	10.02

RMS DEVIATION FROM A PLANE 7.45

Table A31

EL PASO COVE POINT, TANK #3
 BOTTOM SURVEY, TANK IN SHIP, QUADRANT#3

X	Y	DEV
1.	9.	10.17
1.	12.	12.31
1.	15.	14.26
1.	18.	17.41
1.	21.	14.95
5.	6.	-1.16
5.	9.	-3.91
5.	12.	-1.37
5.	15.	-.92
5.	18.	-.37
5.	21.	.57
5.	24.	-.18
8.	6.	-7.32
8.	9.	-8.57
8.	12.	-8.73
8.	15.	-12.48
8.	18.	-11.53
8.	21.	-11.29
8.	24.	-11.64
8.	27.	-13.59
13.	6.	-4.72
13.	9.	-4.53
13.	12.	-6.33
13.	15.	-8.28
13.	18.	-8.34
13.	21.	-7.19
13.	24.	-9.34
13.	27.	-7.00
16.	9.	-.34
16.	12.	-2.29
16.	15.	.36
16.	18.	-.60
16.	21.	2.35
16.	24.	-.80
16.	27.	3.84
18.	9.	6.22
18.	12.	7.67
18.	15.	10.42
18.	18.	13.76
18.	21.	15.51
18.	24.	20.16

RMS DEVIATION: FROM A PLANE

9.15

Table A32

EL PASO COVE POINT, TANK #3
 BOTTOM SURVEY, TANK IN SHIP, QUADRANT#4

X	Y	DEV
1.	6.	21.17
1.	9.	13.48
1.	12.	16.79
1.	15.	13.40
1.	17.	7.64
5.	1.	-2.53
5.	3.	-3.79
5.	6.	-1.08
5.	9.	1.03
5.	12.	-.25
5.	15.	-.14
5.	18.	-1.23
5.	21.	-4.92
5.	24.	-8.21
8.	1.	1.59
8.	3.	-12.77
8.	6.	-7.86
8.	9.	-4.95
8.	12.	-7.24
8.	15.	-4.03
8.	18.	-5.92
8.	21.	-4.21
8.	24.	-5.40
13.	1.	3.03
13.	3.	-16.23
13.	6.	-14.37
13.	9.	-12.46
13.	12.	-14.25
13.	15.	-13.24
13.	17.	-8.40
13.	21.	-6.92
16.	3.	-2.67
16.	6.	-1.46
16.	9.	.35
16.	12.	-.83
16.	15.	-2.22
16.	18.	-.51
16.	21.	3.30
20.	9.	24.21
20.	12.	19.92
20.	15.	17.23
20.	17.	17.57

RMS DEVIATION FROM A PLANE

10.45

Table A33

EL PASO COVE POINT, TANK #4
BOTTOM SURVEY, TANK IN SHIP, QUADRANT #1

X	Y	DEV
3.	6.	9.81
3.	9.	7.75
3.	12.	7.09
3.	15.	3.94
3.	18.	6.88
3.	21.	7.32
3.	23.	4.05
5.	6.	-1.73
5.	9.	-1.09
5.	12.	.85
5.	15.	-1.10
5.	18.	.74
5.	21.	1.38
8.	3.	-4.84
8.	6.	-7.40
8.	9.	-4.85
8.	12.	-5.11
8.	15.	-6.95
8.	18.	-1.72
8.	21.	-.18
8.	23.	2.65
13.	3.	-9.24
13.	6.	-9.50
13.	9.	-7.75
13.	12.	-5.71
13.	15.	-5.77
13.	18.	-3.32
13.	21.	-5.18
13.	23.	-6.95
13.	27.	-3.99
16.	6.	-1.86
16.	9.	-.32
16.	12.	2.73
16.	15.	1.07
16.	18.	-2.69
16.	21.	-6.54
16.	23.	-6.71
20.	6.	9.26
20.	9.	10.90
20.	12.	13.85
20.	15.	11.29
20.	18.	7.43
20.	21.	2.33
20.	23.	-1.69

Table A34

EL PASO COVE POINT, TANK #4
 BOTTOM SURVEY, TANK IN SHIP, QUADRANT#2

X	Y	DEV
1.	9.	11.12
1.	12.	12.39
1.	15.	11.36
1.	18.	10.32
1.	21.	11.39
5.	6.	3.34
5.	9.	1.20
5.	12.	-1.03
5.	15.	1.34
5.	18.	1.51
5.	21.	3.33
5.	24.	-.45
5.	27.	-3.68
9.	3.	-2.19
9.	6.	-2.63
9.	9.	-5.16
9.	12.	-5.19
9.	15.	-7.42
9.	18.	-6.15
9.	21.	-5.83
9.	24.	-6.41
9.	27.	-2.04
9.	29.	-.87
13.	6.	-5.89
13.	9.	-6.43
13.	12.	-8.56
13.	15.	-7.89
13.	18.	-10.72
13.	21.	-11.85
13.	24.	-8.88
13.	27.	-2.01
13.	29.	.07
16.	6.	-3.35
16.	9.	-9.19
16.	12.	-12.42
16.	15.	-11.15
16.	18.	-10.28
16.	21.	-9.01
16.	24.	-9.84
16.	27.	-1.97
16.	29.	2.21
20.	9.	10.30
20.	12.	15.37
20.	15.	17.04
20.	18.	13.01
20.	21.	20.57
20.	24.	23.24

Table A35

EL PASO COVE POINT, TANK #4
BOTTOM SURVEY, TANK IN SHIP, QUADRANT#3

X	Y	DEV
1.	9.	7.87
1.	12.	7.93
1.	15.	13.48
1.	18.	15.34
1.	21.	14.69
5.	6.	1.17
5.	9.	-6.07
5.	12.	-3.52
5.	15.	-3.26
5.	18.	-2.11
5.	21.	-1.65
5.	24.	-2.40
8.	6.	-4.73
8.	9.	-7.58
8.	12.	-10.22
8.	15.	-11.67
8.	18.	-11.91
8.	21.	-10.56
8.	24.	-8.80
8.	27.	-3.75
13.	6.	-1.91
13.	9.	-1.06
13.	12.	.10
13.	15.	-5.23
13.	18.	-6.49
13.	21.	-6.64
13.	24.	-5.99
13.	27.	.37
16.	6.	1.98
16.	9.	-1.06
16.	12.	-1.01
16.	15.	.15
16.	18.	-1.20
16.	21.	-1.14
16.	24.	-1.69
16.	27.	9.67
18.	9.	5.97
18.	12.	8.12
18.	15.	7.33
18.	18.	6.13
18.	21.	7.59
18.	24.	7.64

RMS DEVIATION FROM A PLATE

6.96

Table A36

EL PASO COVE POINT, TANK #4
BOTTOM SURVEY, TANK IN SHIP, QUADRANT#4

X	Y	DEV
1.	9.	13.73
1.	12.	15.49
1.	15.	9.84
1.	18.	10.49
1.	21.	3.05
1.	24.	1.10
5.	3.	1.18
5.	6.	.43
5.	9.	-1.11
5.	12.	1.44
5.	15.	-1.21
5.	18.	-1.25
5.	21.	-6.40
5.	24.	-2.94
8.	1.	3.92
8.	3.	-1.98
8.	6.	-5.53
8.	9.	-4.77
8.	12.	-4.82
8.	15.	-9.37
8.	18.	-6.41
8.	21.	-4.46
8.	24.	-5.90
13.	1.	1.68
13.	3.	-7.51
13.	6.	-10.36
13.	9.	-6.21
13.	12.	-7.35
13.	15.	-9.70
13.	18.	-6.94
13.	21.	-7.59
16.	6.	-4.82
16.	9.	-1.17
16.	12.	-3.41
16.	15.	-6.46
16.	18.	-1.90
16.	21.	1.75
16.	24.	.40
20.	9.	12.29
20.	12.	13.04
20.	15.	11.30
20.	18.	13.45
20.	21.	11.20

RMS DEVIATION FROM A PLANE

7.28

Table A37

EL PASO COVE POINT, TANK #5
 BOTTOM SURVEY, TANK IN SHIP, QUADRANT#1

X	Y	DEV
1.	6.	7.26
1.	9.	3.33
1.	12.	2.59
5.	3.	-3.76
5.	6.	1.11
5.	9.	2.18
5.	12.	1.64
5.	15.	-1.29
8.	1.	5.08
8.	3.	-1.94
8.	6.	-3.08
8.	9.	-1.01
8.	12.	3.45
9.	15.	-4.48
13.	1.	.66
13.	3.	-5.66
13.	6.	-4.09
13.	9.	-5.63
13.	12.	-3.16
13.	15.	-2.49
16.	1.	-1.43
16.	3.	-2.45
16.	6.	-27.63
16.	9.	1.29
16.	12.	-2.25
16.	15.	-3.68
20.	6.	19.87
20.	9.	16.14
20.	12.	4.50

RMS DEVIATION FROM A PLANE

7.72

Table A38

EL PASO COVE POINT, TANK #5
BOTTOM SURVEY, TANK IN SHIP, QUADRANT#2

X	Y	DEV
1.	9.	.26
1.	12.	11.60
1.	15.	13.75
1.	18.	14.69
5.	6.	-.43
5.	9.	-.18
5.	12.	.06
5.	15.	.40
5.	18.	-2.35
5.	21.	.69
8.	6.	-7.58
8.	9.	-5.64
8.	12.	-5.90
8.	15.	-7.05
8.	18.	-9.51
8.	21.	-6.37
13.	6.	-3.71
13.	9.	3.83
13.	12.	-6.02
13.	15.	-6.38
13.	18.	-9.54
13.	21.	-8.79
16.	6.	-3.37
16.	9.	-2.03
16.	12.	-1.88
16.	15.	-2.24
16.	18.	-1.80
16.	21.	-1.35
20.	9.	6.83
20.	12.	11.47
20.	15.	12.52
20.	18.	14.06

RMS DEVIATION FROM A PLANE

7.22

Table A39

EL PASO COVE POINT, TANK #5
BOTTOM SURVEY, TANK IN SHIP, QUADRANT#3

X	Y	DEV
1.	9.	5.65
1.	12.	5.37
1.	15.	6.85
1.	18.	8.40
5.	6.	-1.87
5.	9.	1.75
5.	12.	-1.33
5.	15.	-1.32
5.	18.	-1.40
5.	21.	.32
8.	6.	-5.92
8.	9.	-4.50
8.	12.	-6.28
9.	15.	-6.37
8.	18.	-6.25
9.	21.	-7.53
13.	6.	-1.87
13.	9.	-1.35
13.	12.	1.37
13.	15.	-1.62
13.	18.	-1.30
13.	21.	-1.58
16.	6.	1.13
16.	9.	1.40
16.	12.	.42
16.	15.	-.07
16.	18.	1.65
16.	21.	.87
18.	9.	3.40
18.	12.	3.02
18.	15.	4.13
18.	18.	5.45

RMS DEVIATION FROM A PLANE 4.01

Table A40

EL PASO COVE POINT, TANK #5
BOTTOM SURVEY, TANK IN SHIP, QUADRANT#4

X	Y	DEV
1.	3.	7.80
1.	6.	7.47
1.	9.	7.03
5.	1.	-1.60
5.	3.	-1.62
5.	6.	-3.06
5.	9.	-3.69
5.	12.	-4.73
8.	1.	-1.26
8.	3.	-2.19
8.	6.	-3.92
8.	9.	-1.76
8.	12.	-1.90
8.	15.	-2.83
13.	1.	-2.74
13.	3.	-3.06
13.	6.	-4.60
13.	9.	-3.24
13.	12.	-1.97
16.	6.	3.03
16.	9.	2.60
16.	12.	1.36
16.	15.	1.12
18.	9.	12.68

RMS DEVIATION FROM A PLANE

4.50

7. References

- 1) Haight, W. C., Borchardt, B., Hartsock, R. G., Veale, R. C., and Hocken, R. J., "Lifting Distortion of Free-Standing LNG Cargo Tanks".
- 2) Hocken, R. J., and Haight, W. C., "Multiple Redundancy in the Measurement of Large Structures", Annals of the CIRP (1978).
- 3) Jelffs, P. A., "Calibration of Containers and Gages", J. Inst. Pet., Vol. 58, No. 561, p 117-25 (May 1972).
- 4) Mann, D. B., Editor, 1977, LNG Materials and Fluids. Thermophysical Properties Division, National Bureau of Standards, Boulder, Colorado.
- 5) Haight, W. C., Borchardt, B., Hartsock, R. G., Johnson, C. J., and Hocken, R. J., "Hydrostatic Distortion in Free-Standing LNG Cargo Tanks". Appendix F of this report.

U.S. DEPT. OF COMM. BIBLIOGRAPHIC DATA SHEET (See instructions)		1. PUBLICATION OR REPORT NO. NBSIR 81-1655	2. Performing Organ. Report No.	3. Publication Date January 1982
4. TITLE AND SUBTITLE Estimated Uncertainty of Calibrations of Freestanding Prismatic Liquefied Natural Gas Cargo Tanks				
5. AUTHOR(S) J. D. Siegwarth and J. F. LaBrecque				
6. PERFORMING ORGANIZATION (If joint or other than NBS, see instructions) NATIONAL BUREAU OF STANDARDS DEPARTMENT OF COMMERCE WASHINGTON, D.C. 20234			7. Contract/Grant No.	8. Type of Report & Period Covered
9. SPONSORING ORGANIZATION NAME AND COMPLETE ADDRESS (Street, City, State, ZIP) LNG Custody Transfer Measurements Supervisory Committee, c/o El Paso Marine Co., P.O. Box 1592, Houston, TX 77001; and the Maritime Administration, 14th and E Streets, Washington, DC 20235.				
10. SUPPLEMENTARY NOTES <input type="checkbox"/> Document describes a computer program; SF-185, FIPS Software Summary, is attached.				
11. ABSTRACT (A 200-word or less factual summary of most significant information. If document includes a significant bibliography or literature survey, mention it here) The accuracy of the tank calibrated by the photogrammetric technique was examined during the calibration of fifteen freestanding prismatic LNG transport tanks. This examination indicated that the calibration accuracy of the tanks calibrated in the storage position was better than $\pm 0.1\%$. Additional factors influencing the accuracy of the calibration of the tanks, such as the effects of installing the tanks into the ship and loading the ships with LNG, were examined in the course of this work and the results are reported here. The various measurements used by various NBS personnel to analyze the calibration accuracy are detailed in the eight Appendices included in this report.				
12. KEY WORDS (Six to twelve entries; alphabetical order; capitalize only proper names; and separate key words by semicolons) calibration accuracy; laser calibration; LNG ship tanks; photogrammetry; volume calibration.				
13. AVAILABILITY <input checked="" type="checkbox"/> Unlimited <input type="checkbox"/> For Official Distribution, Do Not Release to NTIS <input type="checkbox"/> Order From Superintendent of Documents, U.S. Government Printing Office, Washington, D.C. 20402. <input checked="" type="checkbox"/> Order From National Technical Information Service (NTIS), Springfield, VA. 22161			14. NO. OF PRINTED PAGES 294	
			15. Price \$21.50	

